Design of control system for ailaunch vehicle

van Cuong Nguyen

UNIVERSITE D'EVRY-VAL-D'ESSONNE
Laboratoire d'Informatique, Biologie Intégrative et Systèmes Complexes

Thèse pour l'obtention du titre de Docteur de l'Université d'Evry-Val-d'Essonne
Spécialité : AUTOMATIQUE

Système de commande embarqué pour le pilotage d'un lanceur aéroporté automatisé

présentée et soutenue publiquement par

Van Cuong NGUYEN

le 20 mars 2013

JURY

Antonio LORIA	: Rapporteur
Anuradha ANNASWAMY	: Rapporteur
Riccardo MARINO	: Examinateur
Naoufel AZOUZ	: Examinateur
Alain GLUMINEAU	: Examinateur
Gilney DAMM	: Directeur de thèse

Contents

List of Figures

List of Tables

Acknowledgements

I would like to thank my advisor, Professor Gilney Damm, for his scientific understanding and for his support during my PhD studies. I have been so lucky to work with him, who was always available and gave me the best research conditions and research opportunities.

I would like to thank Professor Etienne COLLE for being my administrative advisor in the first year of my PhD studies.

I would like to thank Professor Antonio Loria and Professor Anuradha Annaswamy for their time to review my PhD thesis. I would like also to thank Professor Alain Glumineau for participating in my doctoral committee and Professor Naoufel Azouz for participating in this doctoral committee but also annual thesis committees.

I would like to thank Professor Riccardo Marino (University of Rome "Tor Vergata", Rome) for participating in my doctoral committee and, specially, accepting me to joinhis laboratory for three months for a research collaboration. There I had the chance to open my scientific knowledge, in particular, about dynamic feedback linearization control. Besides, I would like also to thank very much, Professor Gianluca Santosuosso and Professor Cristiano Maria Verrelli, for their kindness in helping me with the lodging in Rome and for discussions about interesting subjects.

My sincere thanks go to Thuan, Hung, Duc Anh, Lam,...; to VL9 group for friendship and happy and unforgottable moments in France; and to Toan, Tu, Yen, Phuong, Quy... for their helps during my three months in Rome.

I would like to thank my friends: Bruno, Paul, Antonio, Maxime, Jean-Cl´ement, Wenhao... and all members of the staff of the IBISC laboratory during my Phd studies in the laboratory.

Finally, I would like to address my special thanks to Ba, Ma, chi Ni, Hue, Hien and Hang xinh who have supported during my PhD studies and who always support me.

Abstract

Abstract (in English): This thesis addresses the problem of the stabilization of an (unmanned) airlaunch system. Air launching consists in bringing a satellite and its launcher (rocket) to a certain height using an aircraft, and then launching it from the air (often by dropping the rocket), in a similar way of launching a missile from a fighter. The main difference is that the envisaged mass ratio is much closer to one (heavy rocket compared to aircraft mass). It is then composed of two stages: the first stage called carrier aircraft consists of an <unmanned> aerial vehicle that carries the launcher which constitutes the second stage (rocket). This thesis starts by introducing the problem and objectives, continues by presenting several approaches to model the airlaunch system, and ends by developing different advanced control methods to stabilize it after the launching phase.

In the modeling part we propose a firstly approach called the initial condition model which assumes that the separation phase is instantaneous, and then the airlaunch system is composed of an aircraft model after the launching phase but with large initial conditions on its state variables, caused by a non-perfect split phase. A second approach assumes that the separation phase itself is modeled by a disturbance on aerodynamic forces and moments (from a worst case) during a time interval.

In the control part a modified conditional integrator controller for a class of nonlinear multi-input multi-output systems is first developed starting from the conditional integrator theory developed by Khalil and co-workers. It is then extended to a modified conditional servocompensator control for a class of nonlinear multi-input multi-output systems. Both control strategies were then applied to stabilize the airlaunch system after the separation phase. They have the advantage of being very robust, and they don't depend so much on reliable models. Even if these control strategies gave good results, it was investigated in this thesis another control approach much more dependent on detailed and reliable models. This approach was based on dynamic feedback linearization theory, and the main idea is to obtain better performance in trade off better models.

Finally, all proposed control methods (plus some standard ones) were compared and illustrated by simulations under Matlab/Simulink on a nonlinear F-16 model. These simulations have shown that the results were as expected, and that each control strategy

was well fit for a particular situation.

Keywords: airlaunch system modeling and stabilization, nonlinear control, nonlinear analysis, dynamic feedback linearization, aircraft control.

Abstract (en français): Cette thèse traite du problème de la stabilisation d'un système de lancement aéroporté (éventuellement non habité) pour satellites. Le lancement aéroporté consiste à ramener, à l'aide d'un avion, un satellite et son lanceur (fusée) à une certaine hauteur, et d'exécuter son lancement dans les airs (souvent en larguant la fusée). Ceci est similaire au lancement d'un missile par un avion chasseur. La plus grande différence réside dans le rapport de masse entre l'avion et le lanceur qui est beaucoup plus proche de l'unité (fusée lourde comparée à la masse de l'avion). Le système est composé de deux étages: le premier étage est dit avion porteur qui est un véhicule aérien automatisé. Il porte le lanceur qui constitue le deuxième étage (la fusée).

Dans la première partie, sont proposées des approches de modélisation pour le système de largage pendant et après le largage. La première approche considère que la phase de séparation est instantanée, mais imparfaite. Par conséquent le système est vu comme un modèle d'aéroplane dont les variables d'état sont avec des larges conditions initiales dues à la séparation imparfaite. Une deuxième approche considère la séparation elle-même, représentée par une forte perturbation (un extrême cas) sur les forces et couples aérodynamiques du modèle au cours d'un intervalle de temps.

Dans la deuxième partie, afin de stabiliser le système de largage après la séparation, la commande à intégrateur conditionnel modifié est développée dans un premier temps pour une classe des systèmes non-linéaires multi-entrées multi-sorties, avec comme point de départ la théorie introduite par Khalil et co-auteurs pour des systèmes mono entrée mono sortie. Cette commande a été ensuite étendue pour la commande à servo-compensateur conditionnel modifié pour une classe de systèmes non-linéaires multi-entrées multi-sorties. Les deux stratégies ont été appliquées pour stabiliser le système de largage pendant et après la phase de séparation. Ces techniques ont l'avantage d'être robustes et de pouvoir utiliser des modèles approximatifs. D'un autre côté, il était important d'examiner la possibilité d'obtenir de meilleures performances en utilisant de meilleurs modèles. Pour cette raison, la commande de linéarisation par bouclage dynamique a été étudiée.

Finalement, les performances de toutes ces méthodes de commande (ainsi que certaines commandes de base additionnelles) ont été illustrées par des simulations sous Matlab/Simulink sur un modèle non-linéaire de F-16.

Mots clés: modélisation et commande d'un système aéroporté de lancement de satellites, commande non-linéaire, analyse non-linéaire, linéarisation par bouclage dynamique, commande de véhicules aériens.

Résumé des contributions (in french)

Contexte

Depuis que le premier Spoutnik a été lancé avec succès sur sa trajectoire elliptique autour de la Terre en octobre 1958, une ère spatiale et une course spatiale ont été ouvertes entre les États-Unis et l'Union soviétique. Aujourd'hui, de nombreux satellites ont été lancés sur des orbites autour de la Terre, de la Lune et de Mars pour de différents objectifs tels que la communication, la recherche météorologique, la science de la Terre,etc. La plupart de ces satellites ont été lancés à partir de bases de lancement au sol comme le Center Spatial Kennedy, le Centre Spatial Guyanais, etc. Toutefois, le lancement des satellites depuis le sol nécessite une force de poussée importante pour plusieurs tonnes de matériel et d'êtres humains, comme pour établir des bases satellites autour de la Terre ou de la Lune et Mars. Avec la technologie actuelle, les coûts de lancement sont de l'ordre de \$6000 à \$20000/kg. Un développement des structures de matériaux ultra légères et fiables pour le système de lancement et leurs charges ne peut pas réduire signicativement les coûts de lancement des satellites. Par conséquent, ces coûts de lancement élevés ne permettent pas aux gouvernements des pays à budgets limités de marquer leur présence sur l'orbite terrestre avec leurs satellites. Pour la même raison, ils ne permettent pas aux organisations ayant des restrictions budgétaires de réaliser leurs objectifs de recherche. Une solution possible consiste à utiliser de petits satellites et même de très petits satellites. Malheureusement, ces solutions sont encore chères, car il existe des coûts de lancement fixes indépendants de la taille et du poids des dispositifs lancés. Une solution tout à fait logique dans ce cas serait d'embarquer plusieurs petits appareils et de les lancer en même temps. Malheureusement, cela implique beaucoup de risques supplémentaires dans la phase de séparation et n'est pas envisagé.

Une autre solution à ce problème est le largage. Le largage signifie lancer un étage contenant un satellite, à partir d'un objet volant, vers l'orbite terrestre. Le largage fournit de nombreux avantages par rapport au lancement au sol. Tout d'abord, le système de largage peut voler vers un océan ouvert, évitant les zones peuplées ou les avions de

ligne. Il y a aussi une minimisation des contraintes climatiques, car le système de largage peut voler au dessus ou autour des turbulences météologiques qui gênent le lancement. En conséquence, le retard de lancement est beaucoup plus faible qu'un lancement au sol qui nécessite toujours une météo acceptable ainsi qu'un point de lancement convenable. Le largage produit aussi beaucoup moins d'énergie acoustique à partir du moteur d'un véhicule de lancement, car il n'y a pas de réflexion acoustique vers le sol, et la densité de l'air est plus faible. Le largage réduit également le changement de vitesse (appelée delta V) qu'un véhicule de lancement doit fournir pour atteindre l'orbite avec une vitesse désirée. L'utilisation d'un système de largage réutilisable permet une grande flexibilité pour déployer de petits satellites conçus pour des tâches spécifiques telles que la communication ou la collection de données en temps réel pour les situations d'urgence. Toutefois, le système de largage limite la taille de la charge lancée.

Dans cette thèse, nous considérons un système de largage qui utilise un véhicule aérien sans pilote (UAV) au lieu d'un avion standard avec pilote à bord, et s'intéresse en particulier à la phase de largage. Ce système de largage peut être très difficile, car le deuxième étage (lanceur) peut être aussi lourd que le premier étage. Par conséquence, la tâche de stabilisation du système de largage est complexe pendant et après la phase de largage. Nous développons par la suite une série de systèmes de commande comme la commande à intégrateur conditionnel, la commande à servo-compensateur conditionnel ou la commande de linéarisation par bouclage dynamique. Nous examinons également si elles peuvent stabiliser l'avion porteur après la phase de largage, en évitant toute possibilité de collision entre le porteur d'avion et le lanceur. Même si cette thèse est consacrée à étudier le cas d'un système de largage automatisé, ses résultats sont également valables pour le cas d'un système de largage avec pilote à bord. Dans la suite nous résumons les problèmes liés au système de largage.

Problème de largage

Larguer en l'air un étage à partir d'un avion porteur provoque une modification de paramètres du système de largage telle que la masse, la matrice d'inertie, le centre de gravité et les caractéristiques aérodynamiques du système de largage après la phase de séparation. En conséquence, il change le point d'équilibre du système de largage après cet instant. Plus le lanceur est lourd comparé à l'avion porteur, plus son impact est important que nous avons sur la dynamique de l'avion porteur après la phase de séparation. Un B52 qui porterait de petits missiles air-air, aurait un très petit rapport entre leurs masses, ainsi le largage d'un de ces missiles à partir du B52 n'entraîne quasiment aucun

effet sur la stabilité du B52 après la phase de lancement. Des projets qui utilisent un B52 ou un Boeing 747 qui larguent un petit module de lancement vers l'orbite de la Terre, ont un faible rapport de poids lanceur/avion porteur,et par conséquent, la séparation n'a pas d'impact sur la stabilité du système de largage.

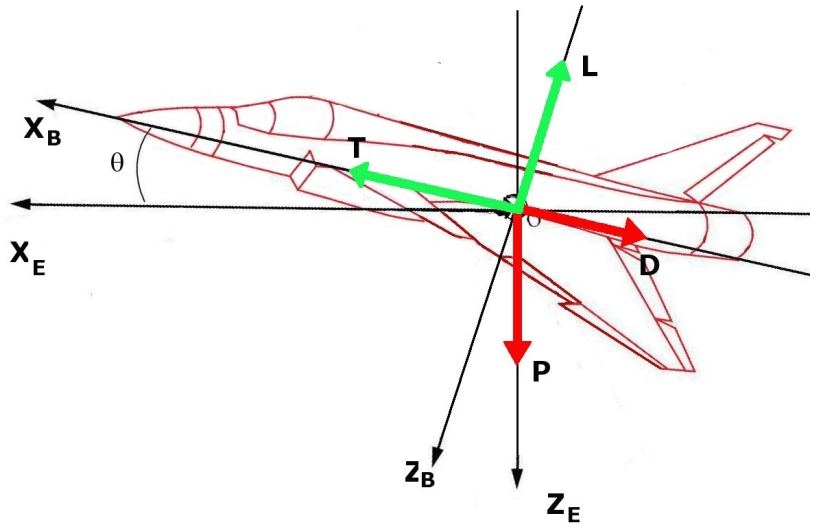

Figure 1: Bilan de forces d'un avion

L'objet de cette thèse est d'étudier un système de largage avec un avion porteur automatisé aussi lourd que le lanceur. Le rapport de masse lanceur/avion porteur est beaucoup plus grand que celle d'un système de largage avec pilote à bord. Il est alors nécessaire d'étudier le problème de la stabilisation du système de largage après la phase de lancement.

Prenons la phase de lancement parfaite (infiniment rapide) à l'instant t_0. A l'instant t_0^-, le système de largage (le porteur + le lanceur) est en équilibre, nous avons donc la force de gravité du (porteur + lanceur) égale à la force de portance, ce qui signifie:

$$\begin{cases} W_- = (m_c + m_l)g\cos\theta = L \\ L = 1/2\rho V^2 S C_l(\cdot) \end{cases}$$

où W_- est la projection de la force de gravité du système de largage sur l'axe OZ_B, m_c est la masse de l'avion porteur, m_l est la masse du lanceur, S est la surface de l'ail, V est la vitesse du système de largage, L est la force de portance, ρ la densité de l'air, et $C_l(\cdot)$ est le coefficient aérodynamique de la force de portance en fonction de la pression et des états du système de largage, et θ est l'angle de tangage.

À l'instant t_0^+, qui suit la phase de lancement, la force de portance sera la même que celle à l'instant t_0^-. Par contre, la force de gravité est maintenant seulement celle

correspondante à la masse de l'avion porteur:

$$\{W_+ = m_c g \cos\theta \neq L \tag{1}$$

En raison de cette réduction de masse, l'avion porteur gagnera en altitude et changera son point d'équilibre (en particulier l'angle d'attaque). L'avion porteur sera peut-être dans une situation dangereuse, et même possiblement instable. De plus l'effet de la phase de séparation peut produire une force et un couple de rotation sur l'avion porteur, ce couple pourrait déstabiliser le porteur avec de nombreux résultats imprévisibles. Enfin, tous ces phénomènes peuvent provoquer une collision entre l'avion porteur et le lanceur.

Méthodes de modélisation

La modélisation du système de largage lors de la séparation des étages est un problème difficile en raison de la complexité du système, les interactions entre deux phases et le manque de disponibilité de données aérodynamiques du système de largage. Puisque le rapport de poids entre le lanceur/porteur est grand, les caractéristiques nonlinéaires du système de largage sont également un point difficile et non négligeable.

Il existe une méthode pour modéliser et simuler la séparation des étages en utilisant l'outil de simulation ConSep appliqué à un véhicule en deux étapes vers l'orbite appelé véhicule jumeau puisque la géométrie de ces deux étapes sont identiques. Cette méthode utilise les coefficients aérodynamiques à partir de données d'essai du véhicule dans une soufflerie avec la technique d'interpolation pendant la phase de séparation (voir dans la série des documents [2] et [3]). La référence [4] utilise un autre outil pour modéliser et simuler la phase de séparation des étages, l'outil Constraint Force Equation/ Optimite Simulated Trajectories II (CFE/POST II). Ces méthodes nécessitent un outil spécifique disponible seulement dans certains laboratoires et centres de recherche tels que la NASA, etc.

Dans l'objectif de modéliser le système de largage et d'étudier la stabilité du système pendant et après la phase de lancement, une autre méthode est proposée dans notre thèse qui consiste en deux modèles avec trois phases pendant la procédure de largage. Le premier modèle correspond au système de largage avant la phase de séparation (c'est à dire que le lanceur reste attachée au l'avion porteur), le second modèle correspond au système de largage, après la phase de séparation(c'est à dire le porteur). Les trois phases correspondent à: des phases avant, pendant et après la séparation. Cette méthode est mise en oeuvre pour des simulations sur un modèle mathématique du système de largage sous Simulink/Matlab avec les données aérodynamiques obtenues à partir des essais dans

une soufflerie. Cette procédure simple procure déjà plusieurs caractéristiques difficiles à évaluer lors du largage, et n'a pas besoin d'un outil spécifique.

Problème de commande

Le problème de commande d'un avion a été traité dans la littérature par beaucoup d'approches au cours des dernières décennies. La première et la plus simple méthode consiste en un régulateur simple PI (proportionnel plus intégrateur). Cette commande est appliquée à un modèle d'avion linéarisé sur plusieurs points de fonctionnement. Cette structure de commande a besoin d'un planning de gains pour chacun des points de fonctionnement de l'avion. Une autre approche étudiée pour améliorer les performances de commande de l'avion utilise la synthèse H_∞/μ (voir [5]), elle est également conçue pour le modèle nominal sur un certain nombre de points de fonctionnement de l'avion. Le paramètre μ améliore la performance de la commande en dépit de la variation des paramètres de l'avion. Ces approches ont contribué à la solution du problème de commande d'avion, mais ont besoin d'une linéarisation du modèle ainsi qu'un planning de gains pour chaque point de fonctionnement. Cela limite les performances du contrôleur, en particulier dans le cas de vol sous des conditions extrêmes telles qu'un angle d'attaque important, etc

Plusieurs autres approches ont été développées pour la commande de l'avion dans des conditions de vol extrêmes tels que Dynamic and Time Scale Separation ([6]), Nonlinear Inverse Dynamics ([7]), Backstepping Control ([8]), Plus récemment, la commande par retour d'état avec le réseau de neurones a également été proposée par [9] pour la commande d'avion.

Cependant, et d'après nos connaissances actuelles, une conception de commande pour le système de largage en se concentrant sur la phase de lancement n'a jamais été étudiée jusqu'à présent. Dans [3], [2] et [4], un simple contrôleur PI est appliqué sur les deux étapes du système de largage, mais les auteurs n'ont pas envisagé l'utilisation de ce contrôleur dans la phase de séparation.

En résumé, les problèmes posés par le système de largage pendant la phase de séparation sont:

- Une stratégie de commande où les non-linéarités du système de largage sont prises en compte

- Des systèmes multi-entrées multi-sorties

- Une stabilisation du système de largage formellement assurée après la phase de séparation
- La contrainte sur la limitation physique des surfaces de commande (aileron, profondeur et gouvernail)

En outre, concernant le point de vue de la stratégie de commande, les conditions suivantes lors de la conception des commandes sont également importantes:

- Caractéristiques des données de l'avion (coefficients des forces et des couples aérodynamiques sous forme de tables)
- Besoin d'une adaptativité pour diverses conditions de vol
- L'évitement de collision entre le lanceur et l'avion porteur

Dans ce qui suit, nous présenterons les approches de commande utilisées dans cette thèse. Les deux premières techniques de commande sont robustes, et donc relativement indépendantes du modèle du système. La troisième est plus fortement basée sur le modèle du système, et nécessite une meilleure connaissance du système, par contre elle permet une meilleure performance de vol. Ces trois théories du contrôle sont les suivantes:

- Commande à intégrateur conditionnel modifié
- Commande à servo-compensateur conditionnel modifié
- Commande de linéarisation par bouclage dynamique

Modèle du système de largage

La phase de largage du système de largage peut être décrite par des variations de la masse, de l'inertie et des coefficients aérodynamiques du système avant et après la phase de lancement. La modélisation de cette phase nécessite une grande disponibilité de données et de connaissances préalables sur le système réel, qui n'existent pas encore dans le cas de cette étude. Cependant, ce système peut être représenté comme un système hybride composé par deux (ou trois) modèles continus qui sont commutés. ces modèles représentent le système avant, (éventuellement pendant) et après la phase de séparation. Dans cette étude, nous adoptons cette stratégie, nous examinerons trois phases:

1. avant la séparation $\Rightarrow$ le premier modèle du système de largage (représentant l'avion porteur et la fusée) est stable à un point de fonctionnement

2. pendant la séparation ⇒ le deuxième modèle du système ne représente que l'avion porteur qui part du point de fonctionnement du modèle de la première phase, et est perturbé par des impulsions sur les forces et les couples aérodynamiques. Ces perturbations durent pendant un intervalle de temps T_{int} et représentent une séparation imparfaite. En outre, les conditions initiales héritées de la première phase ne sont pas un point d'équilibre du second modèle.

3. après la séparation ⇒ l'arrêt des perturbations (l'avion porteur et la fusée n'ont plus aucun contact physique). Nous pouvons montrer que l'effet du largage de la fusée à partir du porteur influence surtout les forces de portance et de traînée, ainsi que les couples de roulis et de tangage seulement.

A partir de ce point de vue nous avons deux approches pour modéliser la phase de largage que nous présentons dans la suite:

Approche des conditions initiales

Comme avec la première approche pour modéliser le système de largage, nous adoptons une technique hybride qui considère que le système de largage est considéré comme un commutateur entre deux modèles continus, un modèle précédant la phase de largage et un modèle suivant celle-ci. La séparation elle-même est considérée comme instantanée, mais imparfaite. Dans ce sens les impulsions sur les forces et les couples affectent le système de largage de manière instantanée, ce qui se traduit par de larges conditions initiales sur le second modèle, qui est un modèle de F-16 dans cette thèse. l'objectif est donc de concevoir une commande pour stabiliser le deuxième modèle (après la commutation) avec éventuellement de larges conditions initiales.

Approche des perturbations sur forces et couples aérodynamiques

Pour la deuxième approche afin de modéliser notre système, nous examinons également le largage comme un commutateur entre deux modèles continus:

1. avant la séparation ⇒ le premier modèle est sur un point de fonctionnement stable

2. pendant la séparation ⇒ la phase de largage déroule pendant un intervalle T_{int} pendant lequel le second modèle est utilisé, mais perturbé par des forces et couples aérodynamiques constants représentant l'imperfection du largage de la fusée à partir du porteur.

3. après la séparation ⇒ arrêt des perturbations, et le porteur continue à être représenté par le second modèle

Afin de rendre notre étude aussi générale que possible, le premier modèle est considéré comme un F-16 avec deux fois sa masse standard, tandis que le second modèle est considéré comme celui d'un F-16.

Il faut noter que l'effet du largage de la fusée à partir de l'avion porteur perturbe surtout les forces de portance et de traînée, ainsi que les couples de tangage et de roulis seulement. Nous supposons que ces forces et ces couples perturbateurs sont constants pendant l'intervalle T_{int}. Nous appelons respectivement F_{w_p}, F_{u_p}, et L_p, M_p les perturbations sur la force de portance, sur la force de traînée, sur le couple de tangage et sur le couple de roulis.

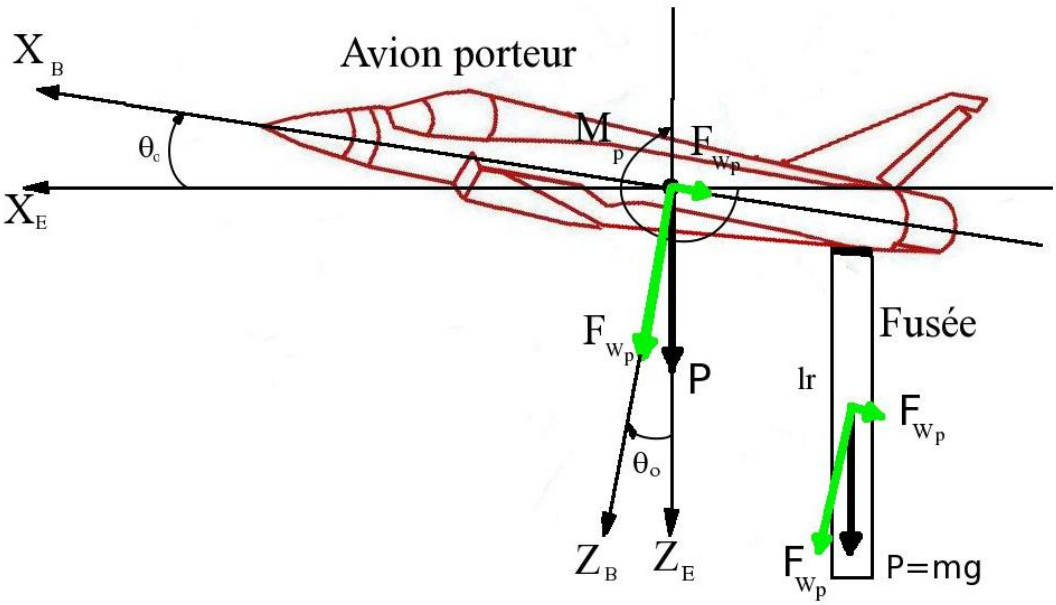

Figure 2: Le lanceur accroché à l'avion porteur dans le défavorable cas

Nous avons pris un "cas extrême" qui correspondrait au cas où le lanceur reste accroché au porteur par une seule accroche pendant un court intervalle de temps:

- la perturbation sur la force de portance pendant un intervalle de temps T_{int} est égale à la force de gravité de la fusée, ce qui signifie $F_{w_p} = mg\cos\theta_0$.

- la perturbation sur la force de traînée est de $F_{u_p} = -P\sin\theta_0 = -mg\sin\theta_0$ où θ_0 est l'angle de tangage initial du premier modèle avant la phase de largage.

- la perturbation sur le couple de tangage pendant T_{int} est le pire cas représenté par la fusée qui reste attaché au porteur sur une extrémité pendant T_{int}, ce qui se traduit par un couple de rotation sur le porteur, dont la valeur est de $M_p = mgl_r \cos\theta_0/2$ où l_r est la longueur de fusée.

- la perturbation sur le moment de roulis pendant T_{int} est faible en raison de la forme de la fusée (longue et mince).

- le modèle après la phase de largage est celui du F-16 dont la condition initiale est l'état sur le point d'équilibre du modèle précédent la phase de largage, qui est le modèle du F-16 avec deux fois sa masse normale.

Modèle du système

La dynamique de l'avion porteur se décrit dans le repère local (voir [10], [11], [12]):

$$
\begin{cases}
\dot{x} = u\cos\psi\cos\theta + v(\cos\psi\sin\theta\sin\phi - \sin\psi\cos\phi) + w(\cos\psi\sin\theta\cos\phi + \sin\psi\sin\phi) & \text{(2a)}\\
\dot{y} = u\sin\psi\cos\theta + v(\sin\psi\sin\theta\sin\phi + \cos\psi\cos\phi) + w(\sin\psi\sin\theta\cos\phi - \cos\psi\sin\phi) & \text{(2b)}\\
\dot{z} = -u\sin\theta + v\cos\theta\sin\phi + w\cos\theta\cos\phi & \text{(2c)}\\
\dot{u} = rv - qw - g\sin\theta + \dfrac{1}{m}(F_u + T) & \text{(2d)}\\
\dot{v} = pw - ru + g\sin\phi\cos\theta + \dfrac{1}{m}F_v & \text{(2e)}\\
\dot{w} = qu - pv + g\cos\phi\cos\theta + \dfrac{1}{m}F_w & \text{(2f)}\\
\dot{\phi} = p + \tan\theta(q\sin\phi + r\cos\phi) & \text{(2g)}\\
\dot{\theta} = q\cos\phi - r\sin\phi & \text{(2h)}\\
\dot{\psi} = \dfrac{q\sin\phi + r\cos\phi}{\cos\theta} & \text{(2i)}\\
\dot{p} = \dfrac{1}{I_{xx}I_{zz} - I_{xz}^2}[(I_{yy}I_{zz} - I_{zz}^2 - I_{xz}^2)rq - I_{xz}(I_{xx} + I_{zz} - I_{yy})pq + I_{zz}L - I_{xz}N] & \text{(2j)}\\
\dot{q} = \dfrac{1}{I_{yy}}[(I_{zz} - I_{xx})pr + I_{xz}(p^2 - r^2) + M] & \text{(2k)}\\
\dot{r} = \dfrac{1}{I_{xx}I_{zz} - I_{xz}^2}[(-I_{xx}I_{yy} + I_{zz}^2 + I_{xz}^2)pq + I_{xz}(I_{xx} + I_{zz} - I_{yy})rq + I_{xx}N - I_{xz}L] & \text{(2l)}
\end{cases}
$$

En outre, nous préférons représenter les variables d'état dans le repère aérodynamique (l'axe OX_W du repère aérodynamique $OX_WY_WZ_W$ dans la Fig. 3 qui s'oriente sur le vecteur de vitesse du système V) au lieu d'utiliser des variables dans le repère local en raison de la mesurabilité de ces variables, nous réécrivons alors la dynamique du système:

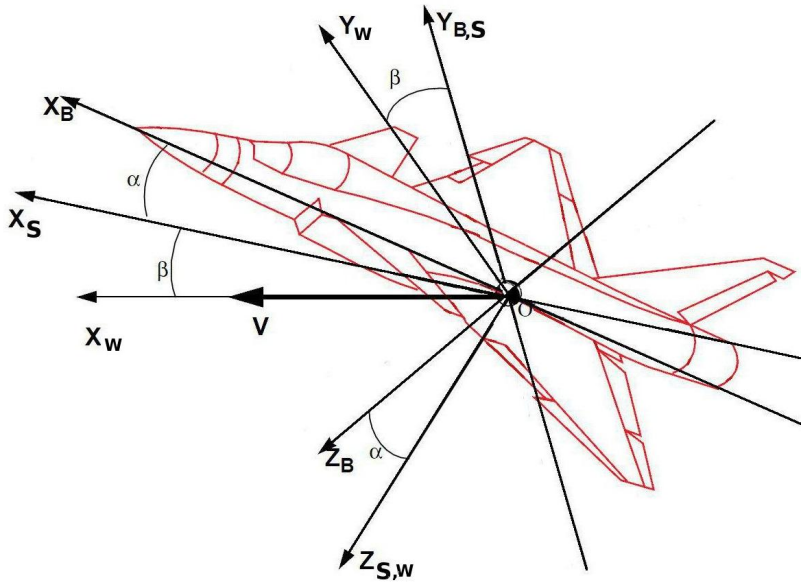

Figure 3: Le repère local et le repère aérodynamque

$$
\begin{cases}
\dot{\alpha} = -\cos\alpha\tan\beta p + q - \sin\alpha\tan\beta r - \frac{\sin\alpha}{mV\cos\beta}(T+F_u) + \frac{\cos\alpha}{mV\cos\beta}F_w \\
+\frac{g}{V\cos\beta}[\sin\alpha\cos\theta + \cos\alpha\cos\phi\cos\theta] \\
\dot{\beta} = \sin\alpha p - \cos\alpha r - \frac{\cos\alpha\sin\beta}{mV}[T+F_u] + \frac{\cos\beta}{mV}F_v - \frac{\sin\alpha\sin\beta}{mV}F_w + \frac{g}{V}[\cos\alpha\sin\beta\sin\theta \\
+\cos\beta\cos\theta\sin\phi - \sin\alpha\sin\beta\cos\phi\cos\theta] \\
\dot{V} = \frac{\cos\alpha\cos\beta}{m}[T+F_u] + \frac{\sin\beta}{m}F_v + \frac{\sin\alpha\cos\beta}{m}F_w + g[\cos\alpha\cos\beta\sin\theta \\
+\sin\beta\sin\phi\cos\theta + \sin\alpha\cos\beta\cos\phi\cos\theta] \\
\dot{p} = \frac{1}{I_{xx}I_{zz}-I_{xz}^2}[(I_{yy}I_{zz} - I_{zz}^2 - I_{xz}^2)rq - I_{xz}(I_{xx}+I_{zz}-I_{yy})pq + I_{zz}L - I_{xz}N] \\
\dot{q} = \frac{1}{I_{yy}}[(I_{zz}-I_{xx})pr + I_{xz}(p^2-r^2) + M] \\
\dot{r} = \frac{1}{I_{xx}I_{zz}-I_{xz}^2}[(-I_{xx}I_{yy} + I_{zz}^2 + I_{xz}^2)pq + I_{xz}(I_{xx}+I_{zz}-I_{yy})rq + I_{xx}N - I_{xz}L] \\
\dot{\phi} = p + \tan\theta(q\sin\phi + r\cos\phi) \\
\dot{\theta} = q\cos\phi - r\sin\phi \\
\dot{\psi} = \frac{q\sin\phi + r\cos\phi}{\cos\theta}
\end{cases}
\tag{3}
$$

où $I_{xx}, I_{yy}, I_{zz}, I_{xz}$ sont les composants de la matrice d'inertie, m est la masse du système (kg) et g la constante de gravité. u, v, w sont les vitesses linéaires du système dans le repère local en m/s. $\alpha, \beta, V, p, q, r, \phi, \theta, \psi$ sont les variables d'état du porteur, c'est à dire l'angle d'attaque, l'angle de dérapage, la vitesse du système, la vitesse angulaire de roulis, la vitesse angulaire de tangage, la vitesse angulaire de lacet, l'angle de roulis, l'angle de tangage et l'angle de lacet, respectivement. $\alpha, \beta, \phi, \theta, \psi$ s'expriment en rad, p, q, r dans rad/s et V dans m/s. F_u, F_v, F_w et L, M, N sont des forces et des couples aérodynamiques

respectivement. Toutes les forces et les couples sont exprimés en N et Nm.

Ces forces et couples aérodynamiques sont fonction de tous les états considérés. Dans ce modèle, les forces et couples aérodynamiques sont sous forme de tableau de valeurs à partir de données mesurées dans une soufflerie. Ces données peuvent être trouvées dans [13]. Enfin, les entrées de commande sont respectivement l'aileron (δ_a), le gouvernail (δ_r) et l'élévateur (δ_e), ainsi que T la force de poussée.

Les contributions de la thèse

Contribution 1: La commande à intégrateur conditionnel modifié pour une classe des systèmes nonlinéaires multi-entrées multi-sorties (MEMS)

La commande à intégrateur conditionnel pour la régulation d'un système nonlinéaire à une entrée-une sortie à phase minimale dans les cas de références asymptotiquement constantes est étudiée dans [14], [15], et a été étendu à une classe de systèmes non-linéaires multi-entrées multi-sorties dans cette thèse, et dans [16]. Cette commande à intégrateur conditionnel fonctionne comme une commande en mode glissant à l'extérieur d'une couche limite, et comme un intégrateur conditionnel à l'intérieur de cette couche limite. Les premiers résultats ont étudié le cas d'un système SISO (single input single output) avec une surface de glissement scalaire, et ont demontré la stabilité asymptotique du système à l'intérieur de la couche limite. Ces résultats ont été étendus dans [17] mais n'étaient pas adaptés au cas étudié dans cette thèse. Notre travail s'est consacré à étendre encore plus ce résultat dans le but de stabiliser le système de largage.

Considérons le système:

$$\begin{cases} \dot{e}_1 &= e_2 \\ \dot{e}_2 &= f(e_1, e_2) + g(e_1, e_2)u \end{cases} \tag{4}$$

où $e_1(t) \in \mathbb{R}^n$ est le vecteur d'erreur, $e_2 = \dot{e}_1$, $u \in \mathbb{R}^n$ est l'entrée de la commande et $f(e_1, e_2) \in \mathbb{R}^n$, $g(e_1, e_2) \in \mathbb{R}^{n\times n}$ sont des fonctions continues.

Nous définissons une mesure des erreurs, semblable à une surface de glissement:

$$s = k_0\sigma + K_1 e_1 + e_2 \tag{5}$$

où $\sigma \in \mathbb{R}^n$ est la sortie de l'intégrateur conditionnel

$$\dot{\sigma} = -k_0\sigma + \mu \text{sat}(s/\mu) \tag{6}$$

dans laquelle μ est la couche limite, k_0 est un paramètre positif, $K_1 \in \mathbb{R}^{n\times n}$ est choisie telle que $K_1 + sI_n$ soit Hurwitzienne.

La fonction de saturation est déterminée:

$$\text{sat}(s/\mu) = \begin{cases} s/\|s\| & \text{si} \quad \|s\| \geq \mu \\ s/\mu & \text{si} \quad \|s\| < \mu \end{cases} \tag{7}$$

Nous définissons $\mathcal{O}_\mu$ comme un voisinage de $(e_1, e_2) = (0, 0)$ avec un rayon R_μ pour que $\|s\| < \mu$

$$\mathcal{O}_\mu \quad = \quad \{e = (e_1, e_2) \in \mathbb{R}^n \times \mathbb{R}^n \mid \|e\| \leq R_\mu\} \tag{8}$$

Avant de présenter le théorème de la commande à intégrateur conditionnel modifié, nous considérons les hypothèses suivantes sur les fonctions $f(e_1, e_2)$ et $g(e_1, e_2)$.

Hypothèse 0.0.1 *$f(e_1, e_2)$ est bornée par une fonction $\gamma(\|e_1\| + \|e_2\|)$ (où $\gamma(\cdot)$ est une fonction de la classe $\mathcal{K}$) plus une constante positive Δ_0 :*

$$\|f(e_1, e_2)\| \leq \gamma(\|e_1\| + \|e_2\|) + \Delta_0$$

et par conséquence,

$$\|f(e_1 = 0, e_2 = 0)\| = \|f(0, 0)\| \leq \Delta_0$$

pour $(e_1, e_2) \in \mathbb{R}^n \times \mathbb{R}^n$.

A l'intérieur de la couche limite, la fonction $f(e_1, e_2)$ doit être Lipschitzienne pour $(e_1, e_2) \in \mathcal{O}_\mu$, par conséquence

$$\|f(e_1, e_2) - f(0, 0)\| \leq L_1\|e_1\| + L_2\|e_2\|$$

$\gamma(\|e_1\| + \|e_2\|)$ doit être Lipschitzienne pour $(e_1, e_2) \in \mathcal{O}_\mu$:

$$\gamma(\|e_1\| + \|e_2\|) \leq \gamma_1\|e_1\| + \gamma_2\|e_2\|$$

Hypothèse 0.0.2 *La fonction $g(e_1, e_2)$ est continue et inversible pour tout $(e_1, e_2) \in \mathbb{R}^n \times \mathbb{R}^n$.*

Nous indiquons le résultat développé sur la commande à intégrateur conditionnel modifié dans cette thèse par le théorème:

Théorème 0.0.1 *Une classe des systèmes non linéaires multi-entrées multi-sorties décrits par (4) qui satisfait les hypothèses 0.0.1 et 0.0.2, peut être globalement stabilisée vers leur référence constante par le contrôleur:*

$$u = -\Pi(e_1, e_2)\text{sat}(s/\mu) \tag{9}$$

dans laquelle nous définissons:

$$\Pi(\cdot) = (\pi_0 + \gamma(\cdot) + k_0\mu + \Delta_0)g^{-1}(\cdot) \tag{10}$$

où π_0 est un paramètre positif, les paramètres à régler π_0, k_0, μ, K_1 et une fonction $\gamma(\cdot)$ convenable.

En outre, la stabilité est exponentielle à l'intérieur d'une région définie en (8).

$\diamond$

La stabilité de la commande (9 et 10) pour le système (4) est démontrée dans la section 3.2. Il est important de remarquer que cette commande n'est pas équivalente à une commande en modes glissants avec une continuité autour de l'origine. En effet la commande n'est pas bornée, voir terme (10).Elle correspond plutôt au produit de deux termes, un saturé et l'autre illimité. Dans une région le premier terme domine la commande alors que dans une autre région c'est le deuxième terme qui domine.

Contribution 2: La commande à servo-compensateur conditionnel modifié pour une classe des systèmes nonlinéaires multi-entrées multi-sorties (MEMS)

La précédente contribution concerne l'étude de la commande à intégrateur conditionnel modifié pour une classe de systèmes nonlinéaires MEMS. La commande définie par les paramètres k_0 et π_0 scalaires. Cette définition simplifie l'étude de la commande au prix de sa généralité et de sa performance. La deuxième contribution vise alors à améliorer la précédente commande en développant une théorie appelée la commande à servo-compensateur conditionnel modifié pour un système nonlinéaire MEMS.

Nous définissons de nouveau la mesure des erreurs:

$$s \;=\; K_0\sigma + K_1 e_1 + e_2 \tag{11}$$

où $\sigma \in \mathbb{R}^n$ est la sortie du servo-compensateur conditionnel

$$\dot{\sigma} \;=\; -K_0\sigma + \mu\text{sat}(s/\mu) \tag{12}$$

où μ est la couche limite, K_0 est une matrice définie positive, $K_1 \in \mathbb{R}^{n\times n}$ est choisie telle que $K_1 + sI_n$ soit Hurwitzienne.

Le précédent travail [16] a montré que le système (4) est exponentiellement stabilisé par la commande appelée intégrateur conditionnel modifié dans le cas où K_0 est un scalaire. Nous développons le résultat pour le cas où K_0 est une matrice, qu'on appelera dans ce cas la commande à servo-compensateur conditionnel modifié et que nous décrivons ci-dessous par le théorème:

Théorème 0.0.2 *Une classe de systèmes nonlinéaires multi-entrées multi-sorties décrits par (4) qui satisfait les hypothèses (0.0.1 et 0.0.2), peut être exponentiellement stabilisée vers une référence constante par le contrôleur:*

$$\begin{cases} u = -\Pi(e_1, e_2)\text{sat}(s/\mu) \\ \Pi(\cdot) = g^{-1}(\cdot)(\Pi_0 + \mu K_0 + (\gamma(\cdot) + \Delta_0)I_n) \end{cases} \tag{13}$$

Π_0 est une matrice définie positive, μ est la couche limite et K_0 est une matrice définie positive. (Π_0, K_0, μ et K_1) sont les paramètres à régler et la fonction $\gamma(\cdot)$ choisi de manière convenable.

En outre, la stabilité est exponentielle à l'intérieur de la couche limite μ.

◇

Il est important de remarquer que, même si le développement de la première commande vers la deuxième semble moins compliqué (l'une étant la version scalaire et l'autre la version matricielle), la différence entre les deux est équivalente à celle entre une commande proportionnelle et une commande par retour d'état.

La démonstration que le système (4) est exponentiellement stabilisé par la commande (13) se trouve dans la section 3.3 du chapitre 3.

Une application de ces commandes pour stabiliser le système de largage est faite ensuite. Dans le premier temps, la commande à intégrateur conditionnel modifié est appliquée au système décomposé en deux modes de mouvement, le longitudinal, et le latéral. Ces deux modes sont transformés sous forme canonique avant une application de la commande à intégrateur conditionnel modifié et ce après avoir démontré au'ils satisfassent les hypothèses mentionnées (voir le chapitre 4). Dans un deuxième temps on présente l'application de la commande à servo-compensateur conditionnel modifié pour le système de largage complet après une transformation similaire de ce système vers la forme canonique. Les résultats de simulation illustrent une bonne stabilisation du système de largage pendant et après le moment de largage sans aucune collision entre les deux étages (voir le chapitre 4).

Contribution 3: La commande de linéarisation par bouclage dynamique

Les travaux ([18]), ([19] et [20]) sur la théorie de la commande de linéarisation par bouclage dynamique ont prouvé que le système composé des neuf premières équations différentielles (2a à 2i) du système (2) peut être dynamiquement linéarisable par les variables de commande (p, q, r), ainsi qu'un premier ordre d'intégration de la force de poussée. Nous cherchons à démontrer la "linéarisabilité" dynamique du système de l'avion complet de 12^e ordre avec le second ordre d'intégration de la force de poussée. Nous développons ensuite un algorithme de la commande de linéarisation par bouclage dynamique pour stabiliser notre système de largage pendant la phase de largage.

Hypothèse 0.0.3 *Les variables de commande ne produisent que des couples aérodynamiques, et pas de forces aérodynamiques. En outre, leur dynamique est supposée suffisamment rapide pour être négligée.*

Les forces aérodynamiques ne dépendent que des vitesses linéaires et pas de vitesses angulaires.

Sachant que les variables (p, q, r) dans (2) peuvent être commandées par $(\delta_a, \delta_e, \delta_r)$ qui interviennent au sein des couples (L, M, N), on peut simplifier le mouvement angulaire de ces trois dernières équations (2):

$$\begin{cases} \dot{p} = \dot{p}_0 \\ \dot{q} = \dot{q}_0 \\ \dot{r} = \dot{r}_0 \end{cases} \tag{14}$$

où $\dot{p}_0, \dot{q}_0, \dot{r}_0$ sont les entrées de commande.

Le système (2) est alors du type:

$$\dot{\xi}_s = f_s(\xi_s) + \dot{p}_0 g_1(\xi_s) + \dot{q}_0 g_2(\xi_s) + \dot{r}_0 g_3(\xi_s) + \eta g_4(\xi_s) \tag{15}$$

où f_s, g_1, g_2, g_3, g_4 sont obtenus à partir de (14) et $\eta = T/m$,

$$\begin{aligned} g_1 &= (0,0,0,0,0,0,0,0,0,1,0,0)^T \\ g_2 &= (0,0,0,0,0,0,0,0,0,0,1,0)^T \\ g_3 &= (0,0,0,0,0,0,0,0,0,0,0,1)^T \\ g_4 &= (0,0,0,1,0,0,0,0,0,0,0,0)^T \end{aligned}$$

Théorème 0.0.3 *Le système (2) avec l'hypothèse 0.0.3 n'est pas statiquement linéarisable par retour d'état, mais il est dynamiquement linéarisable avec un seconde ordre d'intégration de la force de poussée.*

◇

Preuve:

Système non statiquement linéarisable

Afin de démontrer la non linéarisabilité statique du système, nous calculons les crochets de Lie $ad_{g_i}g_j$ pour $1 \leq i, j \leq 4$ et vérifions facilement que:

- span(g_1, g_2, g_3, g_4) est involutive
- span$(g_1, g_2, g_3, g_4, ad_f g_1, ad_f g_2, ad_f g_3, ad_f g_4)$ n'est pas involutive

Ce résultat implique donc que le système (2) n'est pas statiquement linéarisable (voir [21]).

Système dynamiquement linéarisable

Puisque g_4, qui se situe sur la direction de la force de poussée, joue un rôle important dans la dynamique de l'avion, nous choisissons d'appliquer un second ordre d'intégration sur la poussée (η, $\dot{\eta}$ et $\ddot{\eta}$), et de vérifier l'état de la linéarisabilité dynamique du système étendu:

$$\begin{cases} \Delta_0 = span(g_1, g_2, g_3) \\ \Delta_1 = \Delta_0 + ad_{f_s}\Delta_0 + span\{g_4\} \\ \Delta_2 = \Delta_1 + ad_{f_s}\Delta_1 + span\{g_4\} \\ \Delta_3 = \Delta_2 + ad_{f_s}\Delta_2 = \mathbb{R}^{12\times 1} \end{cases} \tag{16}$$

Il est facile de vérifier que le système (16) satisfait à toutes les conditions suffisantes de la théorie présentée dans [20] et [22]. Le système (2) avec les équations simplifiées (14) et le second ordre d'intégration de la poussée est dynamiquement linéarisable. Cela peut physiquement s'expliquer par le fait que la dynamique de la force de poussée est du second ordre comme mentionné dans [7].

Nous définissons d'abord $\zeta_1 = x$, $\zeta_2 = y$, $\zeta_3 = z$, $\sigma_1 = \eta$. Ensuite, un changement de coordonnées de $\tilde{X} = (x, y, z, u, v, w, \phi, \theta, \psi, \eta)$ vers $\tilde{\zeta} = (x, L_{\tilde{f}}x, L^2_{\tilde{f}}x, y, L\ _{tilde f}y, L^2_{\tilde{f}}y, z, L_{\tilde{f}}z, L^2_{\tilde{f}}z, \sigma_1)$ rend les neuf premières équations différentielles du système (2) dynamiquement linéarisable par rapport aux variables de contrôle $(p, q, r, \dot{\eta})$. Ces neuf premières équations différentielles avec $v_4 = \dot{\eta} = \dot{T}/m$ peuvent être réécrites sous la forme $\dot{\tilde{X}} = \tilde{f} + \tilde{g}\tilde{u}$.

D'une manière autre que celle utilisée dans [22], nous définissons σ_1 différemment afin d'éviter une singularité de la matrice $\gamma_1(\cdot)$ que nous allons présenter plus tard. Pour cette raison, les neuf premières équations différentielles et le premier ordre d'intégration sur la poussée peuvent être transformés sous forme:

$$\begin{cases} \dot{\zeta}_1 = \zeta_4 = L_{\tilde{f}} x \\ \dot{\zeta}_2 = \zeta_5 = L_{\tilde{f}} y \\ \dot{\zeta}_3 = \zeta_6 = L_{\tilde{f}} z \\ \dot{\zeta}_4 = \zeta_7 = L^2_{\tilde{f}} x \\ \dot{\zeta}_5 = \zeta_8 = L^2_{\tilde{f}} y \\ \dot{\zeta}_6 = \zeta_9 = L^2_{\tilde{f}} z \\ \dot{\zeta}_7 = D^1_0 + D^1_1 p + D^2_1 q + D^3_1 r + D^4_1 v_4 \\ \dot{\zeta}_8 = D^2_0 + D^1_2 p + D^2_2 q + D^3_2 r + D^4_2 v_4 \\ \dot{\zeta}_9 = D^3_0 + D^1_3 p + D^2_3 q + D^3_3 r + D^4_3 v_4 \\ \dot{\sigma}_1 = D^4_0 + D^1_4 p + D^2_4 q + D^3_4 r + D^4_4 v_4 \end{cases} \tag{17}$$

où $v_4 = \dot{\eta}$ et D^i_j pour $i = 1..4$, $j = 1..3$ sont fonction de $\tilde{X}$ et peuvent être facilement calculés (voir le chapitre 5).

$$\begin{cases} \zeta_4 = uc\theta c\psi + v(c\psi s\theta s\phi - c\phi s\psi) + w(s\theta c\phi c\psi + s\phi s\psi) \\ \zeta_5 = uc\theta s\psi + v(s\psi s\theta s\phi + c\phi c\psi) + w(s\theta c\phi s\psi - s\phi c\psi) \\ \zeta_6 = -s\theta u + vc\theta s\phi + wc\theta c\phi \\ \zeta_7 = c\theta c\psi(-gs\theta + F_u + \eta) + (c\psi s\theta s\phi - c\phi s\psi)(gc\theta s\phi + F_v) \\ \quad + (s\theta c\phi c\psi + s\phi s\psi)(gc\phi c\theta + F_w) \\ \zeta_8 = c\theta s\psi(-gs\theta + F_u + \eta) + (s\psi s\theta s\phi + c\phi c\psi)(gc\theta s\phi + F_v) \\ \quad + (s\theta c\phi s\psi - s\phi c\psi)(gc\phi c\theta + F_w) \\ \zeta_9 = -s\theta(-gs\theta + F_u + \eta) \\ \quad + c\theta s\phi(gc\theta s\phi + F_v) + c\theta c\phi(gc\phi c\theta + F_w) \end{cases} \tag{18}$$

A partir de (17), nous définissons quatre nouvelles variables $\zeta_{10} = \dot{\zeta}_7$, $\zeta_{11} = \dot{\zeta}_8$, $\zeta_{12} = \dot{\zeta}_9$ et $\sigma_2 = \dot{\sigma}_1$.

$$\begin{bmatrix} \zeta_{10} \\ \zeta_{11} \\ \zeta_{12} \\ \sigma_2 \end{bmatrix} = \chi_1(\tilde{X}) + \gamma_1(\tilde{X}) \begin{bmatrix} p \\ q \\ r \\ v_4 \end{bmatrix} \tag{19}$$

où

$$\chi_1(\tilde{X}) = \begin{bmatrix} D^1_0 \\ D^2_0 \\ D^3_0 \\ D^4_0 \end{bmatrix} ; \gamma_1(\cdot) = \begin{bmatrix} D^1_1 & D^2_1 & D^3_1 & D^4_1 \\ D^1_2 & D^2_2 & D^3_2 & D^4_2 \\ D^1_3 & D^2_3 & D^3_3 & D^4_3 \\ D^1_4 & D^2_4 & D^3_4 & D^4_4 \end{bmatrix} \tag{20}$$

D_4^i pour $i = 1..4$ sont fonction de $\tilde{X}$ et dépendent du choix de la variable σ_1 pour éviter la singularité de $\gamma_1(\cdot)$.

La dynamique angulaire dans l'équation (2) peut être réécrite comme:

$$\begin{bmatrix} \dot{p} \\ \dot{q} \\ \dot{r} \end{bmatrix} = \chi_r(u, v, w, p, q, r) + \gamma_r(u, v, w) \begin{bmatrix} \delta_a \\ \delta_e \\ \delta_r \end{bmatrix} \tag{21}$$

où $\chi_r(u, v, w, p, q, r) \in \mathbb{R}^{3\times 1}$, $\gamma_r(u, v, w) \in \mathbb{R}^{3\times 3}$. Il est important de noter que la matrice $\gamma_r(u, v, w)$ est inversible dans l'enveloppe de vol désirée.

Les dérivées de (19) peuvent être trouvées facilement en utilisant (21):

$$\begin{bmatrix} \dot{\zeta}_{10} \\ \dot{\zeta}_{11} \\ \dot{\zeta}_{12} \\ \dot{\sigma}_2 \end{bmatrix} = \chi_T(\tilde{X}, p, q, r, v_4) + \gamma_1(\tilde{X}) \begin{bmatrix} \gamma_r(u, v, w) & 0 \\ 0 & 1 \end{bmatrix} \begin{bmatrix} \delta_a \\ \delta_e \\ \delta_r \\ \dot{v}_4 \end{bmatrix} \tag{22}$$

où

$$\chi_T(\tilde{X}) = \dot{\chi}_1(\tilde{X}) + \dot{\gamma}_1(\tilde{X}) \begin{bmatrix} p \\ q \\ r \\ v_4 \end{bmatrix} + \gamma_1(\tilde{X}) \begin{bmatrix} \chi_r(\cdot) \\ 0 \end{bmatrix} \tag{23}$$

En définissant $v_4 = \tau$ comme une variable d'état, $u_T = \dot{v}_4$ comme l'entrée, nous avons un système dynamiquement linéarisable (17 et 22) avec 14 états par le changement de coordonnées de $(x, y, z, u, v, w, \phi, \theta, \psi, p, q, r, \eta, \tau)$ à $(\zeta_1, \zeta_2, \zeta_3, \zeta_4, \zeta_5, \zeta_6, \zeta_7, \zeta_8, \zeta_9, \zeta_{10}, \zeta_{11}, \zeta_{12}, \sigma_1, \sigma_2)$.

Dans le système (17 et 22), nous avons 12 états physiques de l'avion, et 2 états de l'intégration de la poussée. Nous avons besoin maintenant de la non singularité de la matrice:

$$\gamma_T(\cdot) = \gamma_1(\tilde{X}) \begin{bmatrix} \gamma_r(u, v, w) & 0 \\ 0 & 1 \end{bmatrix} \tag{24}$$

Maintenant, nous définissons $\sigma_1 = \phi$, dont la dynamique est:

$$\dot{\phi} = p + q \tan\theta s\phi + r \tan\theta c\phi$$

La matrice $\gamma_1(\cdot)$ devient

$$\gamma_1(\cdot) = \begin{bmatrix} D_1^1 & D_1^2 & D_1^3 & D_1^4 \\ D_2^1 & D_2^2 & D_2^3 & D_2^4 \\ D_3^1 & D_3^2 & D_3^3 & D_3^4 \\ 1 & \tan\theta s\phi & \tan\theta c\phi & 0 \end{bmatrix} \tag{25}$$

La non singularité de la matrice $\gamma_1(\cdot)$ dans ce cas est garantie pour l'enveloppe de vol désiré. Ceci peut s'expliquer par le fait que trois variables de commande sont utilisées pour commander la trajectoire de l'avion, et la dernière variable de commande est affectée pour le mouvement de roulis. La loi de commande de linéarisation par bouclage dynamique est sous forme:

$$\begin{bmatrix} \delta_a \\ \delta_e \\ \delta_r \\ u_T \end{bmatrix} = \gamma_T^{-1}(\cdot)(-\chi_T(\cdot) + \begin{bmatrix} \dot{\zeta}_{10r} \\ \dot{\zeta}_{11r} \\ \dot{\zeta}_{12r} \\ \dot{\sigma}_{2r} \end{bmatrix} + \begin{bmatrix} -k_{11}(\zeta_1 - \zeta_{1r}) \\ -k_{21}(\zeta_2 - \zeta_{2r}) \\ -k_{31}(\zeta_3 - \zeta_{3r}) \\ 0 \end{bmatrix} \tag{26}$$
$$\begin{bmatrix} -k_{12}(\zeta_4 - \zeta_{4r}) & -k_{13}(\zeta_7 - \zeta_{7r}) & -k_{14}(\zeta_{10} - \zeta_{10r}) \\ -k_{22}(\zeta_5 - \zeta_{5r}) & -k_{23}(\zeta_8 - \zeta_{8r}) & -k_{24}(\zeta_{11} - \zeta_{11r}) \\ -k_{32}(\zeta_6 - \zeta_{6r}) & -k_{33}(\zeta_9 - \zeta_{9r}) & -k_{34}(\zeta_{12} - \zeta_{12r}) \\ 0 & -k_{33}(\sigma_1 - \sigma_{1r}) & -k_{44}(\sigma_2 - \sigma_{2r}) \end{bmatrix})$$

où k_{ij} pour $1 \leq i, j \leq 4$ sont des paramètres positifs à régler, les références de sortie sont définies comme suit:

$$\begin{cases} (x_r, y_r, z_r)^T = (\zeta_{1r}, \zeta_{2r}, \zeta_{3r})^T \\ (\dot{x}_r, \dot{y}_r, \dot{z}_r)^T = (\zeta_{4r}, \zeta_{5r}, \zeta_{6r})^T \\ (\ddot{x}_r, \ddot{y}_r, \ddot{z}_r, \phi_r)^T = (\zeta_{7r}, \zeta_{8r}, \zeta_{9r}, \sigma_{1r})^T \\ (x_r^{(3)}, y_r^{(3)}, z_r^{(3)}, \dot{\phi}_r)^T = (\zeta_{10r}, \zeta_{11r}, \zeta_{12r}, \sigma_{2r})^T \\ (x_r^{(4)}, y_r^{(4)}, z_r^{(4)}, \ddot{\phi}_r)^T = (\dot{\zeta}_{10r}, \dot{\zeta}_{11r}, \dot{\zeta}_{12r}, \dot{\sigma}_{2r})^T \end{cases} \tag{27}$$

L'application de la commande de linéarisation par bouclage dynamique au système de largage dans la phase de séparation est décrite et illustrée par les résultats de simulation dans le chapitre 5. Une bonne stabilisation du système après le largage est montrée pour un large intervalle de temps T_{int} pendant lequel la perturbation se produit sur les forces et les couples aérodynamiques (voir le chapitre 5).

Conclusion et perspectives

Conclusion

Dans cette thèse, nous avons étudié le modèle du système de largage pendant et après la phase de lancement. Nous avons développé la commande de l'intégrateur conditionnel modifié, la commande à servo-compensateur conditionnel modifié et la commande de linéarisation par bouclage dynamique pour stabiliser le système de largage sans aucune collision entre l'avion porteur et le lanceur après le largage.

Les résultats de ce travail sont présentés dans les chapitres 3, 4, 5, et 6 de cette thèse. Pour finir, les principales contributions de cette thèse sont:

En terme de modélisation:

- Une modélisation du système de largage pendant et après la phase de lancement en utilisant deux approches (voir le chapitre 2):
  - l'approche des conditions initiales
  - l'approche de la perturbation sur les forces et les couples aérodynamiques

En terme de méthodologie de commande:

- Une commande simple LQR comme première approche pour stabiliser notre système de largage après la phase de lancement. Le contrôleur nous a permis d'avoir un premier point de vue sur la stabilisation du système.
- Un développement de la commande à intégrateur conditionnel modifié pour une classe de systèmes nonlinéaires multi-entrées multi-sorties (MEMS) à partir de la théorie de la commande à intégrateur conditionnel modifié inventée par Khalil et ses collègues.
- Une commande à servo-compensateur conditionnel modifié étendue par la commande à intégrateur conditionnel modifié développée pour la même classe de systèmes nonlinéaires MEMS. Ces commandes montrent une meilleure performance par rapport à la commande LQR, la commande en modes glissants, ainsi que la commande à intégrateur conditionnel modifié pour le système de largage linéarisé autour de son point d'équilibre.
- La démonstration de la possibilité d'un avion dynamiquement linéarisable (voir le chapitre 5). Une commande de linéarisation par bouclage dynamique est ensuite conçue pour le système de largage. L'intérêt de cette technique est qu'elle est capable de stabiliser un système de largage d'une manière globale.

En terme d'application des résultats

- L'application de la commande LQR est la première approche qui nous a donné une stabilisation du système de largage, mais seulement pour de petites conditions initiales dans la première approche de modélisation du système de largage, et dans la deuxième méthode de modélisation, seulement pour un petit intervalle de temps T_{int}

pendant lequel la perturbation se produit sur la force et le couple aérodynamiques, comme on peut voir dans le chapitre 2 .

- La commande à intégrateur conditionnel modifié, en particulier la commande à servocompensateur conditionnel modifié, a montré une meilleure performance pour stabiliser le système de largage après la phase de séparation, ce qui se traduit par l'obtention d'un intervalle de temps T_{int} supérieur. Parce que la commande à intégrateur conditionnel modifié et la commande à servo-compensateur conditionnel modifié sont développées pour un système nonlinéaire MEMS, elles seront alors non seulement appliquées pour stabiliser le système de largage, mais aussi pour commander une classe de systèmes non linéaires MEMS comme nous l'avons montré dans le chapitre 3.

- La commande de linéarisation par bouclage dynamique est la plus efficace pour stabiliser notre système comme indiqué dans le chapitre 5, elle a stabilisé le système de largage complet à partir d'angles d'Euler, les vitesses linéaires ainsi que les vitesses angulaires.

- Les trois commandes étudiées sont capables d'éviter la collision entre le système de largage et la fusée pendant et après le moment de la séparation.

Perspectives

Bien que de bons résultats ont été obtenus, les résultats de cette thèse pourront être améliorés au cours de futures recherches dans ces quelques directions:

- La modélisation du système de largage pendant et après la phase de lancement est un point clé de la thèse. En raison de l'indisponibilité du modèle réel dans la littérature, nous avons utilisé l'approche où la phase de lancement est perturbée par les effets de la séparation au cours d'un intervalle de temps. En cas de disponibilité du modèle réel, l'approche de deux modèles avec trois phases améliorera la précision du problème. Le passage du premier modèle au second modèle peut être modélisé par une approche linéaire ou non linéaire en fonction des besoins spécifiques.

- La commande à intégrateur conditionnel modifié et la commande à servocompensateur conditionnel modifié ont été développées pour une classe de systèmes non linéaires MEMS. Dans cette thèse, elles ont servi à stabiliser le système de largage après la phase de lancement, mais aussi elles peuvent être utilisées pour commander un système non linéaire MEMS satisfaisant les hypothèses montrées dans la section

3.4 du chapitre 3. Cette classe est en effet assez large, et inclu en particulier les avions.

- Dans la conception de ces commandes, nous avons supposé que la sortie du système et ses dérivées sont mesurables. En fait, nous avons parfois besoin dans la pratique d'un observateur qui construit et fournit ces composants pour la conception du contrôle. La technique d'estimation du type nonlinéaire ou linéaire peut être trouvée dans la littérature, et leur couplage aux systèmes de commande doit être évalué.

- La commande de linéarisation par bouclage dynamique nous a permis d'obtenir un meilleur résultat par rapport à la commande à intégrateur conditionel ou la commande à servocompensateur conditionnel modifié. Elle stabilise complètement le système de largage après la séparation. Toutefois, ce contrôle dépend d'une bonne précision du modèle analytique et des coefficients aérodynamiques qui sont sous la forme de tables obtenues depuis des tests dans une soufflerie. La précision des modèles analytiques et leurs dérivées n'est pas assurée. Par conséquent, une nouvelle technique qui profite de la performance de cette méthode et corrige des points négatifs pourrait être proposée, nous prenons pour exemple la commande de linéarisation par bouclage dynamique avec réseau de neurones. Ce serait une commande adaptative et robuste.

- Pour toutes les commandes, nous avons supposé que toutes les variables d'état du système sont mesurables, mais parfois ce n'est pas le cas. Il nous faut donc un observateur qui permet de construire et de fournir l'estimation de ces variables pour la procédure de la conception des commandes. Le choix des types d'observateur dépend de la performance exigée et peut être trouvé dans la littérature (voir par exemple [23] et [24]).

- L'amélioration des résultats de simulation des chapitres 4 et 5 est nécessaire. Par ailleurs, une comparaison avec d'autres méthodes de commande serait importante pour démontrer la performance des méthodes proposées: la commande à intégrateur conditionnel modifié, la commande à servocompensateur conditionnel modifié et la commande de linéarisation par bouclage dynamique.

- Un test de ces commandes sur le modèle réel reste toutefois nécessaire.

General Introduction

This thesis is devoted to study and design a control system for stabilizing an air launch system which is used to launch small satellites to the low earth orbit. This system is composed of two stages: the first stage called carrier aircraft consists of an <unmanned> aerial vehicle that carries the launcher which constitutes the second stage (rocket). We focus particularly on the stabilization of the air launch system during and after separating the launcher from the unmanned carrier aircraft at the desired drop point. The fact that the carrier aircraft is a kind of unmanned aerial vehicle and that the launcher/carrier weight ratio is large, results in many advantages for the satellites launch industry. However it also causes the problem of instability of the air launch system after the separation phase. The objective of the thesis is to model the air launch system and develop a control system which the proof of stability is demonstrated formally.

The work of this thesis is inspired by the PERSEUS project (Projet Etudiant de Recherche Spatiale Européen Universitaire et Scientifique) initiated by the CNES French Space Agency (Centre National d'Etudes Spatiales) in which it intends to design an air launch system for the purpose of launching small and even very small satellites called nano-satellites to the low earth orbit. This system has a unmanned aerial vehicle as a carrier aircraft to fly a launcher to the desired drop point instead of a standard or modified aircraft with human pilot in board in the existing air launch system. It is clear that the unmanned carrier aircraft is reusable. The proposed air launch system has the advantages of a classical air launch system in respect to the surface for launching, in terms of flexibility, weather constraints and launch costs. It also has advantages of a unmanned aerial vehicle as carrier aircraft in terms of no life supporting kit and no human restrictions as tiredness and safety. The air launch system is then a really ambitious and promising project in the field of small satellites launching. Nevertheless there are still many problems of air launch systems to be solved.

Automatic launching the launcher from the carrier aircraft at the desired drop point requires not only an absolute guarantee of stability of the aircraft after this separation

phase, but also the collision avoidance between two stages when the launcher mounts to the desired orbit and the aircraft stabilizes to return to the base site. Moreover the high weight ratio between airlaunch vehicle/carrier aircraft implies a high variation in mass, inertia matrix and center of gravity beside the change in aerodynamic characteristics of the air launch system after the separation phase. As a consequence a possibility of instability of air launch system after this launching phase is really a big problem.

In the literature many authors have studied and proposed several approaches about the control and stabilization system for the aviation field in general and for flight in particular. As an example, NASA and her partners have worked on air launch system through a number of projects with success. These air launch system projects where the carrier aircraft is a standard or modified aircraft with human pilot in board, have improved the launching technique for a class of small and very small satellites. Even the recent air launch project named Stratolaunch initiated by Paul G. Allen has a new carrier aircraft but with human pilot crew. In fact the air launch system without human pilot in board is an interesting and difficult topic and the object of our work, but still completely open at the moment. As a consequence the work in this thesis has studied firstly how to mathematically model the air launch system during and after the launch phase. Because of non availability of the real model in practice and in literature, we used the approach of splitting the launching phase into three phases: before the separation, during the separation and after the separation, with two models used for before and after phases. An F-16 model is used after the separation because it was already used for air-launch, and for the accessibility of its data and its aerodynamic characteristics (which are under look up table) from wind tunnel test data. The thesis is followed by studying a control system for the modeled air launch system. Since the modeled system is nonlinear and has data under look up table, the first control strategy to be considered is rather robust to the system model and is based on conditional integrator control. This theory was developed by Khalil and co-workers for single input single output nonlinear systems, and is extended for a class of multi-input multi-output nonlinear systems in this thesis. The thesis has also developed the control of a conditional servo-compensator control for a class of multi-input multi-output nonlinear systems. These controllers get knowledge on a saturation (natural or not) on the control signal, and takes advantage on that to behave, under some conditions, as an sliding mode controller (SMC). On other conditions, when not saturated, the controller behaves as a dynamical feedback with an important integral (servo-compensator) term. In this way the control scheme assures the good properties of robustness and performance of sliding mode controllers for large errors, while allowing a smooth behavior given by its continuity what avoids chattering

The thesis has demonstrated formally the proof of stability of the air launch system by these control techniques. Application of these controllers to the studied system results in a good convergence of air launch system's states to their equilibrium point through numerical simulation results.

We continued the work by another control strategy that is based on the system model, called Nonlinear Dynamic Feedback Linearization Control. It is shown that the flight dynamics can be transformed into a linear form by the dynamic feedback linearization with assumptions on the effects of moments and control surfaces on aerodynamic forces and on thrust dynamics. A controller is then designed for the linear system by pole placement. A proof of stability of air launch system's states is realized for the general case considering the effects neglected of moments and control surfaces on aerodynamic forces. Application of this control to the studied system is also done and obtained a convergence of the system through simulation results under Matlab/Simulink environment. The simulation results also show a better results of Dynamic Feedback Linearization Control compared with the results of conditional integrator and servo - compensator controls.

Because of the short duration of this thesis, these controllers which obtained a good results on theory through simulations when applied to the air launch model, have still not been used to practical experimentation in order to check the robustness of controllers under the real environment.

In order to obtain the results previously presented, the thesis is structured and presented as the following.

The first chapter is devoted to present the advantages of air launching compared with surface launching in small and very small satellites launch field. The different kinds of air launch systems under projects of NASA and her partners are also introduced in this chapter. These air launch systems based on carrier aircraft with human pilot crew, are simpler (even if also considered in this thesis) from the air launch system serving as inspiration for this thesis. For example PERSEUS/CNES student project uses an unmanned aerial vehicle as a carrier aircraft and presents, as a consequence, several advantages compared with the formers. However it also introduces several problems caused by the physical changes of the air launch system when air launching. These problems are shown in the end of the chapter.

The second chapter presents the model of air launch system. Several approaches are proposed to model the air launch system in particular at the launching phase. The chapter ends with a simple control technique called LQR control, that is applied to study

the stabilization of the air launch system after the launching phase.

The third chapter develops the theory of conditional integrator control for a class of multi-input multi-output (MIMO) nonlinear systems. The conditional integrator control theory is extended for MIMO nonlinear systems from the existing control theory for single input single output nonlinear systems in literature. In this case the control parameter is considered under scalar form. An extension of the conditional integrator control called servo - compensator is then developed in Chapter four. This control is built for MIMO nonlinear systems with control parameters under matrix forms. These control systems insure the globally exponential stability of a class of MIMO nonlinear systems under several assumptions on system properties through a proof of stability for the case of no saturation on control inputs. These control techniques which, are less based on the system model, are then designed for and applied to our air launch system. Through several simulation results under Matlab/Simulink, they guarantee a convergence of output states of the studied system to their equilibrium values even in the case of saturation existence on control inputs.

The fifth chapter aims to develop a control technique more strongly based on the system model, called Dynamic Feedback Linearization Control. This technique allows to describe the studied system dynamics with standard state vector given by position, linear velocities, Euler's angles and angular rates into a new linear model using a change of variables. The new linear system can then be controlled by standard pole placement techniques. The chapter ends with an illustration of convergence of all states after the launching phase through simulation results.

The sixth chapter is used to compare the control strategies developed in the previous chapters.

The chapter of conclusion resumes the main results of our works and opens perspectives for possible future works.

Chapter 1

Introduction

Contents

Since the first Sputnik was launched successfully to orbit the Earth on its elliptical path on October 1958, it was opened the space age and the U.S and Soviet Union space race. Nowadays many satellites were launched around Earth, Moon and Mars for different purposes such as communication, weather researches, Earth science. Most of these satellites were launched from ground launch bases as Kennedy Space Center, Guiana Space Center,etc. However, launching satellites requires a heavy lift for several tons of propellant and hardware, and even humans to establish bases on Earth orbit or on Moon and Mars. With the present heavy lift technology, launch costs are in the range of $6000 to $20000/kg. A development of reliable ultra light weight structures for launch system and payloads can not reduce much more the launch costs of satellites. These high launch costs don't allow then every country's government with budget limitations to mark their presence on Earth orbit through their satellites. In the same way, it does not allow organizations with budget limitations to realize their purposes of research objectives. A possible solution is to use small and even very small satellites for these purposes. Unfortunately, they are still expensive because of fix launch costs independent on the size and weight of the launched devices. A quite logical solution in this case would be to pack several small devices to be launched together. However this implies in many additional risks in the split phase and is not envisaged.

Another solution for this problem is: Air launch. Air launch means launching a stage containing the satellite from a flying object to orbit Earth. Air launching provides many advantages over ground launching. Firstly, air launch systems can fly to open ocean, avoiding populated areas or ships and airplane paths. There is also a minimization of weather constraints since the air launch systems can fly over or around the launch constraint weather. As a consequence, the launching delay is much shorter than surface launching that requires always a suitable launch weather as well as a suitable orbital meeting. Air launch produces much less acoustic energy from the engine than a surface launch vehicle since there is no reflection from the ground and air density. Air launch reduces also the change of velocity (called delta V) that a launch vehicle must provide to reach the orbit with a desired velocity. Using a reusable air launch system allows a great flexibility and allows to deploy small satellites designed for specific tasks of communication or data gathering in real time for urgent situations. However the air launch system limits the size of air launch effective payloads.

1.1 Categories of air launch systems

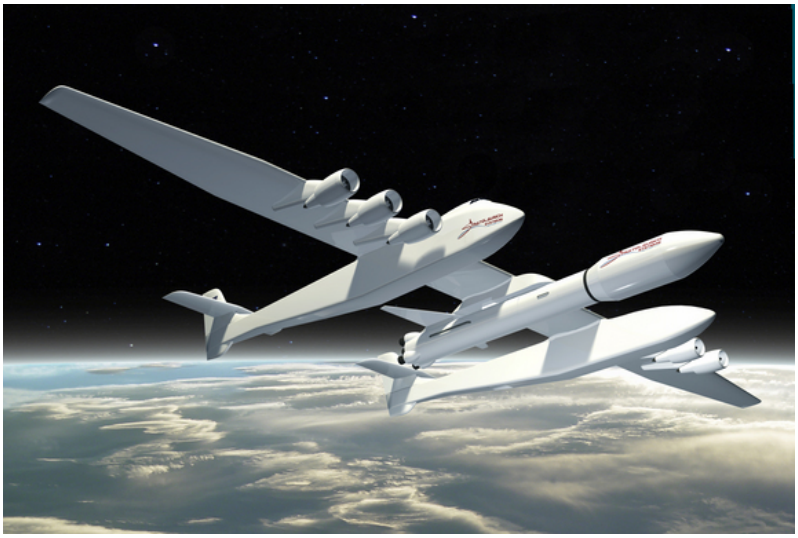

Figure 1.1: Stratolaunch system credited © Stratolaunch Systems, Inc.

An air launch system is a composition of two stages (see Fig. 1.1). The first stage is a (unmanned or manned) carrier aircraft, which carries an air launch vehicle that constitutes the second stage. The second stage may use specific nozzles and propellants for the low outside atmospheric pressure altitude. The first stage is in most current air launch projects taken from a standard or lightly modified airplane. We can classify air launch systems into several categories according to the launch methods (see [25]):

- Captive on top: Spiral project, Saenger II project, Boeing Airlaunch
- Captive on bottom: Pegasus, Yakovlev HAAL, Yakovlev Skylifter
- Towed: Kelly Space's Astroliner
- Aerial Refueled: Pioneer Rocketplane, Andrews Space Alchemist
- Internally Carried: BladeRunner, Vozdushny Start, SwiftLaunch RLV

Captive on top: This launch method has advantages in term of carrying heavy payloads on the top of the carrier aircraft. But it needs a specific release system at separation of the air launch vehicle from the carrier aircraft. We can take for example the Spiral project or Saenger II project which use captive on top method (see [26]). However, these projects are still not possible with our present technology.

Figure 1.2: Spiral Project 50-50 credited © Mark Wade

Figure 1.3: Saenger II project credited © Mark Lindroos

Another project named Boeing Airlaunch project ([27]) is feasible with present technology. It consists of a modified 747 Boeing and a space maneuver vehicle into the low earth orbit or a conventional payload module on it.

Figure 1.4: Boeing Airlaunch project credited © Boeing

Captive on bottom: This launch method has advantages in term of easy separation of launch vehicle from the carrier aircraft. But it limits the size of the air launch vehicle under the carrier aircraft and it needs a high modification to the carrier aircraft. Typical example of this launch method is the Pegasus project with over 40 launches. It consists of a B52 or a L1011 airplane for the carrier aircraft and a launch vehicle with 3 stages.

Other projects like Yakovlev HAAL (High Altitude Aerial Launch) project and Yakovlev Skylifter project are possible concepts with today's technology ([25]).

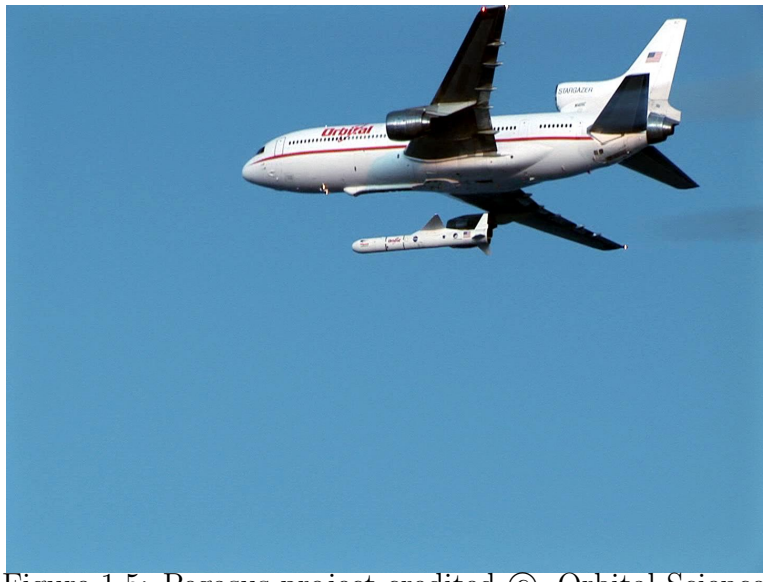

Figure 1.5: Pegasus project credited © Orbital Sciences

Towed: The advantages of this launch method is low modification to the carrier aircraft. However it has a problem of propellant boil-off and the air launch vehicle's wings sizing. An example of towed method is Astroliner project which is conceived by Kelly Space and Technology from Nasa funding (see [28]). The project uses a Boeing 747 as

tow airplane and expect to accelerate the air launch system to Mach 0.8 and then coast to 20000 ft. Although the Astroliner concept's size is not possible with today's technology.

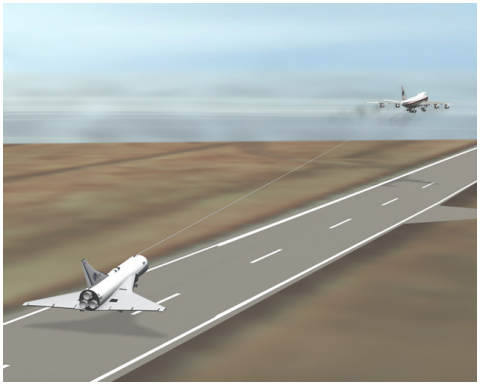

Figure 1.6: Astroliner project credited © Kelly Space

Aerial Refueled: The advantage of this launch method is that it reduces the size of carrier aircraft's wings and landing gear. An example of this method is Pioneer Rocket plane project from NASA funding and another project is Andrews Space Alchemist project also funded by NASA for Andrews Space and Technology Alchemist.

Internally carried: The launch method provides many advantages compared with previous methods. It needs little or no modification to carrier aircrafts since the air launch vehicle is inside the carrier aircraft, failure problems on the air launch vehicle can be detected and resolved directly inside the carrier aircraft. These concepts are able to carry and release the air launch vehicle at higher altitudes compared with other methods. A disadvantage of this method is that the air launch vehicle is sized and fixed inside the carrier aircraft. There are many projects using this launch method in practice. Vozdushny Start and BladeRunner projects are an example. But a typical example of this method is the SwiftLaunch RLV project in which they use U.S Air Force C5 aircraft or a Ukrainian An - 124 aircraft as carrier aircraft with no modification requirement.

In these projects, methods of captive on bottom and internally carried are more studied for now. Other air launch methods can not be realized in the present instant and need an advanced technology to develop the concept.

Recently, a new air launch project named Stratolaunch has developed by Paul Allen and his colleagues (see Fig. 1.1 and [29]). This project aims to launch a payloads of 45360 kg to the low earth orbit. The project is ran in partnership with Scaled Composites for carrier aircraft part, with Space X for the multi-stages booster part and with Dynetics

for the mating and integration system part. The project started in 2010 and will do flight tests in 2016.

It is important to remark that the carrier aircraft used in the previously presented projects is an airplane with human pilot in board. Airplanes use the wing's lift force to fly. For this reason, higher (low altitude) air density benefit the flight while the aircraft uses standard fuel to keep flying. A first stage (air launch vehicle) would use a much more complex, dangerous and expensive fuel while in this higher air density. From a certain altitude, air density is too low to be useful for an airplane, while not representing anymore a drawback for air launch vehicle.

For all these reasons, some projects intend to use an unmanned aerial vehicle as a carrier aircraft to carry the launch vehicle to a desired drop point. There are many advantages in doing so. In the first place, safety of the pilot crew is assured because there is no human lives involved during the delicate launching phase. In addition, since there is no need for life supporting devices, weight of carrier aircraft is restricted to the strict minimum or the carrier aircraft of the same weight can carries a heavier launch vehicle. Finally, mission may take as long as necessary without human restriction as tiredness and without human constraints required in other air launch system.

In this thesis, we consider an air launch system that uses an unmanned aerial vehicle (UAV) instead of a standard aircraft with human pilot in board, and addresses in particular the launch phase. This air launch system may be very challenging since the second stage (launch vehicle) may be almost as heavy as the first stage (UAV). As a consequence, the stabilization task of the air launch system is complex during and after the launching phase. So we develop a series of control systems like a Conditional Integrator Control, a Conditional Servo-compensator control or a Dynamic Feedback Linearization Control and investigate if they can globally stabilize the carrier aircraft after the launching phase without any collision between the carrier aircraft (UAV) and the launch vehicle. Even if this thesis is dedicated to the unmanned case, its results are also valid to the manned case, where it will behave as a pilot assistance system. We will further introduce the problem in the following section.

1.2 Air launch Problem

To air launch a stage from the carrier aircraft causes a modification to parameters of the air launch system such as mass, inertia matrix, center of gravity and aerodynamic characteristics after the separation phase. As a consequence it changes the equilibrium point of air launch system. The larger the air launch vehicle's mass compared with the

carrier aircraft, the larger its impact on the carrier aircraft dynamics after the separation phase. B52 aircraft and missiles on it have a small ratio between their masses, then the release of missiles from B52 aircraft does not result in any effect on the stability of B52 aircraft after the launching phase. The previously mentioned projects using B52 and Boeing 747 which release a conventional launch module to orbit, and have a small weight ratio air launch vehicle/carrier aircraft, the separation phase does not have impacts on the stability of air launch system after the separation phase.

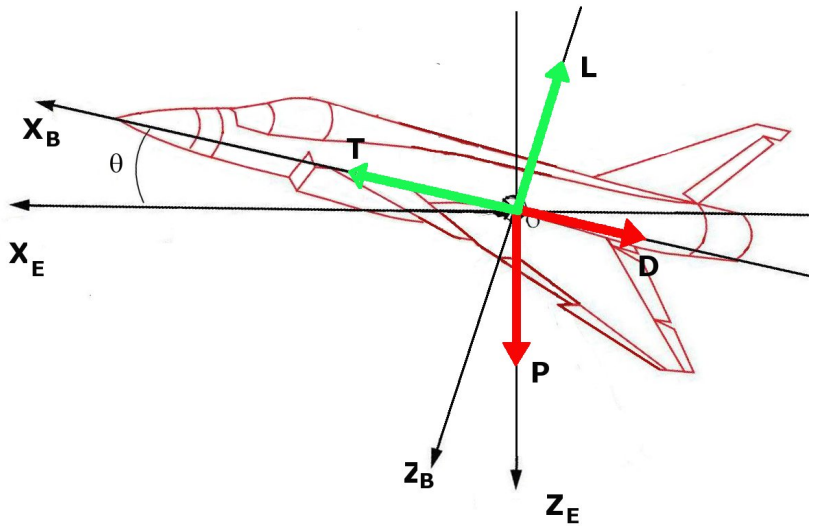

Figure 1.7: Equilibrium of forces on an Aircraft

The object of the work in this thesis is an air launch system which has a unmanned carrier aircraft (an UAV) as heavy as launcher. The ratio launch vehicle/UAV is much larger than that of current air launch system with human pilot. It is then necessary to study the stabilization problem of the UAV after the launching phase.

Let us consider a perfect air launch phase at instant t_0. At instant t_0^- the air launch system (UAV + launch vehicle) is in equilibrium, so we have gravity of (UAV + launch vehicle) equal to the lift force, that means:

$$\begin{cases} W_- = (m_c + m_l)g\cos\theta = L \\ L = 1/2\rho V^2 S C_L(\cdot) \end{cases} \tag{1.1}$$

where W_- the weight force of air launch system, m_c is the UAV's mass, m_l is the launch vehicle's mass, S the wing area, V the airspeed of the air launch system, L the lift force, ρ the air density, and $C_L(\cdot)$ is the aerodynamic coefficient of the lift force depending on pressure and states of air launch system. θ is the pitch angle.

At instant t_0^+, that follows the launching phase, the lift force will be the same as instant t_0^-. The weight is now only that of UAV:

$$\{W_- = m_c g \cos\theta \neq L \tag{1.2}$$

Because of this reduction of mass, the carrier aircraft will gain altitude and will change its equilibrium point (in particular the angle of attack). The carrier aircraft will possibly be in a dangerous situation, and even be unstable. Moreover the impact of the separation phase may produce a force and then a torque on the carrier aircraft, this torque could destabilize the carrier aircraft with many unpredictable results. Finally, all these phenomena may cause a collision between the carrier and the launcher.

1.3 Modeling methods

Modeling an air launch system during the stage separation is a challenging difficult problem because of the complexity of the system, the interactions between two stages and the availability of aerodynamic data of air launch system. Since the ratio air launch vehicle/carrier aircraft is large, the nonlinear air launch characteristics of air launch system are also a difficult point.

There is a method to model and simulate the stage separation using ConSep simulation tool applied to a Two Stages to Orbit (TSTO) vehicle called a bimese vehicle since the geometry of both stages are identical. This method uses the aerodynamic coefficients from wind tunnel test data of two stages with interpolation technique during the separation phase (see in a series of papers [2] and [3]). Reference [4] uses other tool to model and simulate the stage separation, which is Constraint Force Equation/ Optimite Simulated Trajectories II (CFE/POST II) tool. These methods require a specific tool that is available in certain specific laboratories and centers such as NASA, etc.

For the purpose of stability study and modeling of air launch system during the launch phase, another method is proposed in my thesis that consists of two models for three phases of launching procedure. The first model corresponding to the air launch system before the launching phase (i.e. the carrier aircraft with the launcher still attached to it), the second model corresponding to air launch system after the launching phase. The three phases correspond to the system before, during and after the split. This method is implemented for simulations on a mathematic model under Simulink/Matlab with aerodynamic data from wind tunnel tests. This procedure is simpler and does not require a specific tool anymore.

1.4 Control Problem

The flight control problem has been tackled with many approaches during the last decades. The first and simplest approach consists of a simple PI controller. This type of controller is applied to a linearized model of flight at several operating points. This control structure needs then a gain schedule for the whole operating points of the aircraft. Another approach is studied to improve the flight control performance using H_∞/μ synthesis (see [5]), it is also designed for the nominal model on a number of operating points of the flight. Parameter μ improves the performance of controller against parameter variations of aircraft. These approaches have contributed solution of the the flight control problem, but they need a linearization of flight model as long as a gain schedule for every operating point. That limits the performance of the controller in particular for the case of flight with extreme flight condition such as hight angle of attack, etc.

Several other approaches have been developed for the flight control in the extreme flight conditions such as Dynamic and Time Scale Separation [6], Nonlinear Inverse Dynamics [7], Backstepping Control [8], More recently, neural network mixed with backstepping was also proposed by [9] for the flight control.

However to our best knowledges, a control design for air launch system focusing on the launching phase was not studied until now. In [3], [2] and [4], a simple PI controller is applied to the two stages of the air launch system but the authors did not investigate the use of this control for the launch phase.

As a summary, the challenges raised by the air launch system during the separation phase are:

- A control design where the nonlinearility of the air launch must be taken into account
- A multi-input multi-output system
- Stabilization of the air launch system after the separation phase must be assured
- Constrained Control because of physic limitations of control surfaces (aileron, elevator and rudder surface)

Besides, concerning the point of view of control design, the following requirements, when designing the control strategy, are important as well:

- Characteristics of the flight's data (data of aerodynamic coefficients of force and moment in tabular form)
- Adaptivity for various flight conditions

- Collision avoidance between the air launch vehicle and carrier aircraft

In the following, we present the control approaches used in this thesis. The first two control techniques are very robust, and as a consequence are rather independent of system's model. The third one is more model based, and requires better knowledge of the system, in exchange it allows better flight performance. These three control theories are:

- MIMO Conditional Integrator
- MIMO Conditional Servo-compensator
- Nonlinear Dynamic Feedback Linearization

Conclusion

The objective of this chapter was to present the existing categories of air launch systems found in literature. An air launch system with unmanned carrier aircraft, that is the object of this thesis, is introduced in this chapter. This air launch system has several advantages compared with current air launch systems. However it results in linked specific problems that are also detailed in this chapter. The problem of modeling the air launch system is the object of Chapter 2. The air launch problems ask us to study and design a new control system for this system in Chapter 3, Chapter 4 and Chapter 5. Chapter 6 is for control comparisons and Chapter 7 for the conclusion and perspectives.

Chapter 2

System's dynamics and Modeling

Contents

2.1 Introduction

Satellites launching is a strategical activity today. Launchers are able to carry from micro-satellites of some tens of kilograms up to 10 tons in the case of French Ariane 5 launcher.

Recently new applications have called upon very small satellites mostly used in groups (see [30]). These very small satellites need a new class of launchers to put them on orbit since launching implies in many fixed costs that are independent of the size and weight of the launched device.

A more efficient solution in this case is to use the procedure of airlaunch (see [31], [32]). It consists of using a two stages launching system. The first stage is composed of an air vehicle (manned or unmanned) that carries (inside, beneath or above) a launcher which constitutes the second stage (see in Fig. 1.1 as an example). There are many advantages in air launch as presented in Chapter 1, mainly because there is no need for specific large non populated launching areas and it provides a great flexibility since instead of waiting for specific launch windows (to attain desired orbits), the vehicle may be flown to a better suited launch point, with a better alignment with the desired orbit. There have been tests using a C-17 airplane in QuickReach project (see [33], [34], [35] and [36]), a F15 airplane in Rascal project (see [37]), a B52 airplane in Proteus project and L-1011 in Pegasus project (see [25]) as manned carrier aircraft without or little modification. Unlike them, some others like the PERSEUS project are interested in an air launch system using a unmanned carrier aircraft to fly the air launch vehicle to a drop point for example. This idea presents several advantage compared to a classical air launch system in terms of safety, and also because there is no need for life supporting kit and because there is no human restrictions as tiredness in a long flight.

The present chapter considers an air launch system that uses an Unmanned Aerial Vehicle (UAV) instead of a standard aircraft with a human pilot inboard, and addresses the launching phase. It intends to introduce modeling and a robust controller for this delicate procedure. In fact, air launch may be very challenging since the air launch vehicle may be almost as heavy as the UAV. This means that the aircraft will instantaneously lose almost half of its mass. Current air launch systems present a much smaller ratio launcher/aircraft and rely on human pilot to stabilize the aircraft during and immediately after the launching instant. Unlike those systems, this air launch uses an UAV, and as consequence, the stabilization task is much more complex during and after the launching phase with a much more adverse mass ratio. To the best of our knowledge, it does not exist an equivalent research line, and then there is no results in the literature considering this problem (modeling and control).

Chapter 2 is organized as follows: in section 2.2, the necessary mathematical tools are presented. In section 2.3, we describe the nonlinear mathematical system model, two approaches of air launch phase are also presented in this section. An LQR control design is discussed in section 2.4, and its application to the full system model. The chapter is

completed by computer simulations and conclusions.

2.2 Mathematical Tools

In this section the nonlinear dynamical model of an aerial vehicle is described. This description is based on [10], [11], [12].

2.2.1 Reference frames

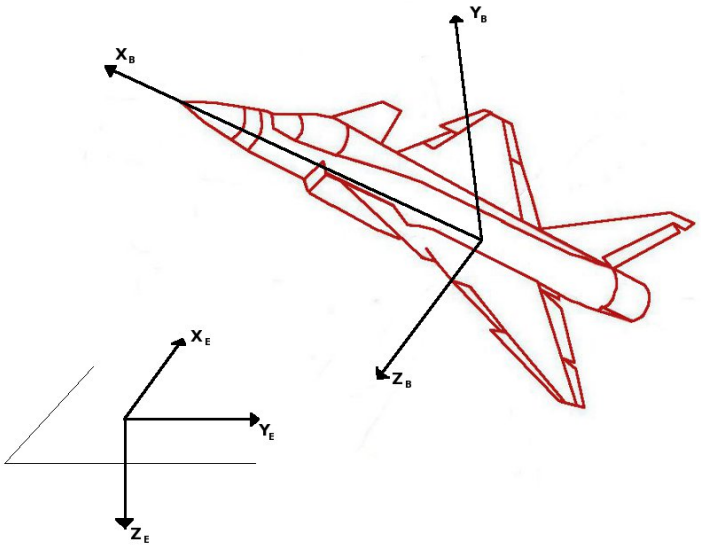

Figure 2.1: Reference frames on a flight

In order to describe the equations of an aerial vehicle's motion, it is necessary to define some reference frames on which the motion is described. The most commonly used reference frame is Earth fixed reference frame R_E, see Fig. 2.1. In the Earth fixed reference frame R_E, the Z_E axis points to the center of Earth. The X_E axis is in an arbitrary direction (to the north for example) and Y_E axis is perpendicular to the X_E axis. This reference frame is used to describe the position and orientation of the flight.

Another reference frame is the body fixed reference frame R_B, the origin of this reference frame is at the flight's center of gravity, the X_B axis points forward through the aircraft nose, the Y_B axis through the right wing and the Z_B axis downwards.

The coordinate transformation to the body fixed reference frame from the Earth fixed reference frame is a matrix which is composed of three transformations, by the so called

Euler's angles: yaw(ψ), pitch(θ) and roll(ϕ) angles. Two intermediate systems are needed to complete this transformation (see Fig. 2.2).

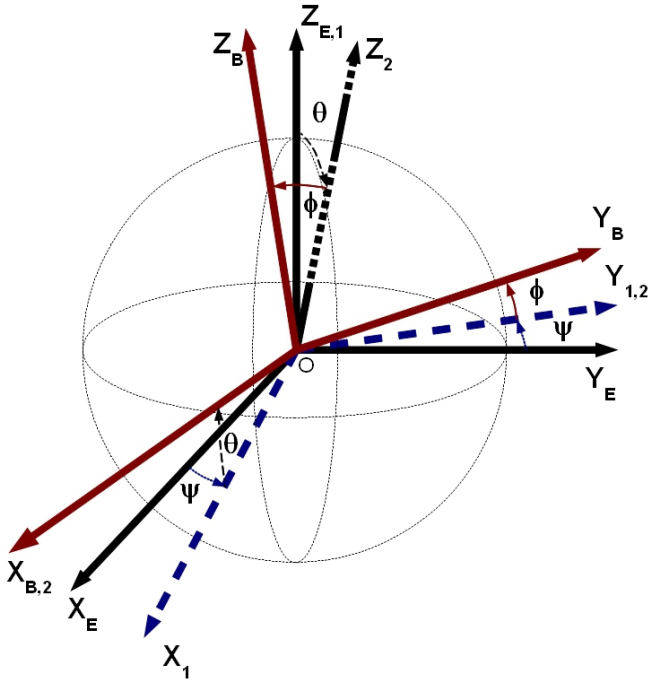

Figure 2.2: Body fixed reference frame to Earth fixed reference frame transformation

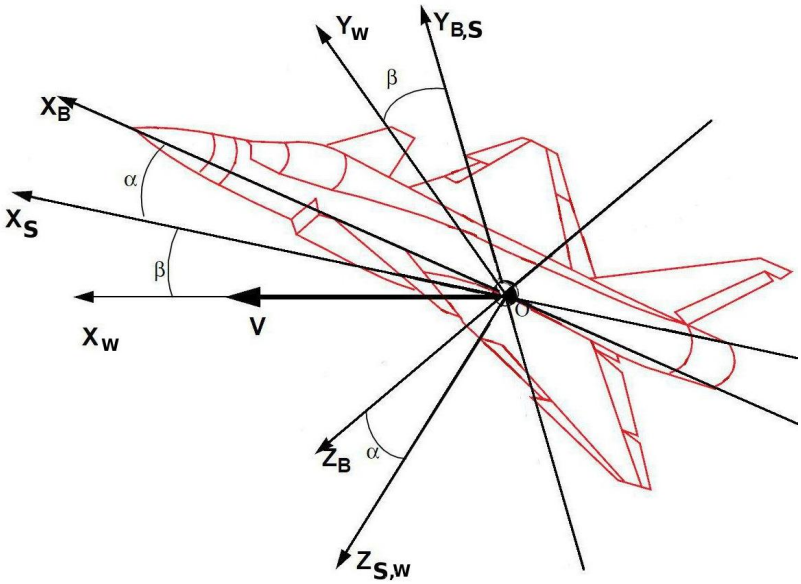

Figure 2.3: Body fixed reference frame and Wind axes reference frame

$$R_{X_E Y_E Z_E} \overset{T^{1E}(\psi)}{\rightarrow} R_{X_1 Y_1 Z_E} \overset{T^{21}(\theta)}{\rightarrow} R_{X_2 Y_1 Z_2} \overset{T^{B2}(\phi)}{\rightarrow} R_{X_B Y_B Z_B} \tag{2.1}$$

The first coordinate transformation from the R_E reference frame to the intermediate frame R_1 is through the yaw angle ψ around Z_E axis.

The second coordinate transformation is around Y_1 axis through the pitch angle θ to the second immediate reference frame.

And the last transformation to the body fixed reference frame through the roll angle ϕ around X_2 axis.

Multiplying the three matrices it is obtained the Euler transformation matrix from Earth fixed reference frame to the body fixed reference frame.

Two other reference frames are useful for describing the flight dynamics, the stability axis reference frame R_S and the wind axis reference frame R_W (see Fig. 2.1).

The stability axes reference frame: X_S axis is parallel and in the direction of the projection of velocity vector $\vec{V}$ on the symmetric plane $X_B Y_B$ of the flight. The Y_S axis stays with Y_B axis. The transformation from $X_B Y_B Z_B$ frame to $X_S Y_S Z_S$ frame is by a rotation around Y_B axis through the angle of attack α.

The wind axes reference frame: X_W axis is parallel and in the direction of velocity vector $\vec{V}$ of the flight. It is a transformation from stability axes reference frame $X_S Y_S Z_S$ to wind axes reference frame $X_W Y_W Z_W$ by a rotation around Z_S axis through the sideslip angle β.

2.2.1.1 Flight variables

In order to study the flight dynamic we determine some assumptions for the flight:

Assumption 2.2.1 *The flight is a rigid body that means the distance of any two points is fixed during the time interval over which the motion is considered.*

Assumption 2.2.2 *The Earth is flat and non rotating.*

Assumption 2.2.3 *The mass is constant and the mass distribution is symmetric to the $X_B O Z_B$ plane of the flight (i.e. left and right sides of the aircraft are identical). It implies that inertia on $O X_B Y_B$ plane $O Y_B Z_B$ planes of the flight are zero. This assumption is necessary to apply Newton's and Euler's motion laws.*

Under these assumptions, the flight is a solid body with 6 degrees of freedom. The flight dynamics can be described by its position through position vector η_1 and velocity

vector ν_1 and by its orientation through the orientation vector η_1 and the angular velocity ν_2.

$\eta_1 = \begin{bmatrix} x \\ y \\ z \end{bmatrix}$ is the position vector expressed in the Earth fixed reference frame R_E.

$\nu_1 = \begin{bmatrix} u \\ v \\ w \end{bmatrix}$ is the velocity vector expressed in the body fixed reference frame R_B where u is the longitudinal velocity, v the lateral velocity and w the normal velocity.

$\eta_2 = \begin{bmatrix} \phi \\ \theta \\ \psi \end{bmatrix}$ is the orientation vector where ϕ is the roll angle, θ the pitch angle and ψ the yaw angle.

$\nu_2 = \begin{bmatrix} p \\ q \\ r \end{bmatrix}$ is the angular rates vector where p, q and r are the roll, pitch and yaw angular velocities.

$\begin{bmatrix} V \\ \alpha \\ \beta \end{bmatrix}$ is the airspeed vector in wind reference frame where V, α and β are the airspeed, angle of attack and sideslip angle respectively.

These vectors can be illustrated in the Fig. 2.4.

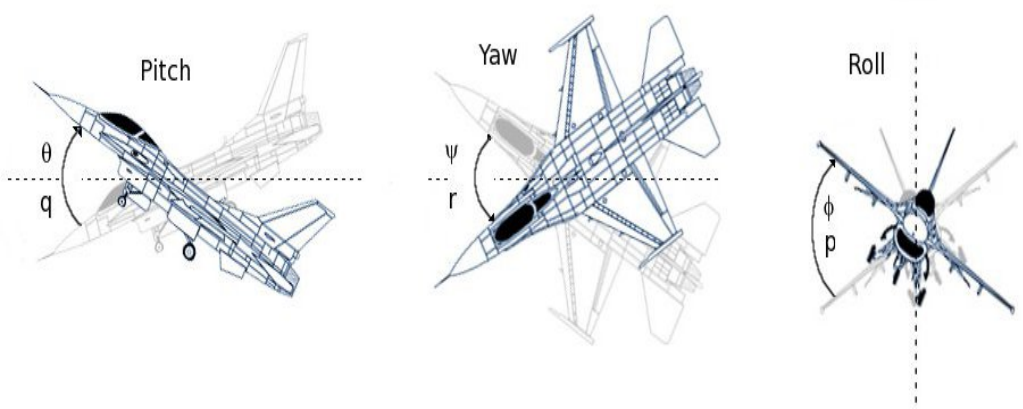

Figure 2.4: Orientation and rotation vectors

The change of velocity expressed in R_E to that expressed in R_B is obtained through the transformation:

$$\dot{\eta_1} = T_{E/B}\nu_1$$

where

$$T_{B/E} = \begin{pmatrix} \cos\psi\cos\theta & \cos\psi\sin\theta\sin\phi - \sin\psi\cos\phi & \cos\psi sin\theta\cos\phi + \sin\psi\sin\phi \\ \sin\psi\cos\theta & \sin\psi\sin\theta\sin\phi - \cos\psi\cos\phi & \sin\psi sin\theta\cos\phi + \cos\psi\sin\phi \\ \sin\theta & \cos\theta\sin\phi & \cos\theta\cos\phi \end{pmatrix} \tag{2.2}$$

In the same way, the change of velocity expressed in body fixed coordinate system R_B to the wind axes coordinate system R_W is obtained through matrix:

$$T_{B/W} = \begin{pmatrix} \cos\alpha\cos\beta & \sin\beta & \sin\alpha\cos\beta \\ -\cos\alpha\sin\beta & \cos\beta & -\sin\alpha\sin\beta \\ -\sin\alpha & 0 & \cos\alpha \end{pmatrix} \tag{2.3}$$

We remind that the coordinate transformation of reference frame R_E with respect to the reference frame R_B is consists of three rotations (see Fig. 2.2):

- Rotation of R_E reference frame to the intermediate frame R_1 through the yaw angle ψ around Z_E axis.
- Rotation around Y_1 axis through the pitch angle θ to the second intermediate reference frame R_2.
- Rotation to the body fixed reference frame through the roll angle ϕ around X_2 axis.

This can be expressed as:

$$\vec{\omega} = R_B/R_E = R_1/R_E + R_2/R_1 + R_B/R_2$$

This rotation vector of body fixed reference frame R_B with respect to Earth fixed reference frame R_E can be stated:

$$\vec{\omega} = \dot{\psi}\vec{Z_E} + \dot{\theta}\vec{Y_1} + \dot{\phi}\vec{X_B} \tag{2.4}$$

and expressing the vector in body fixed coordinate system $\omega = (p, q, r)^T = \nu_2$, that means:

$$\begin{bmatrix} p \\ q \\ r \end{bmatrix} = \begin{bmatrix} 1 & 0 & -\sin\theta \\ 0 & \cos\phi & \sin\phi\cos\theta \\ 0 & -\sin\phi & \cos\phi\cos\theta \end{bmatrix} \begin{bmatrix} \dot{\phi} \\ \dot{\theta} \\ \dot{\psi} \end{bmatrix}$$

It implies that by inversing the matrix, obtain the Euler's angles dynamics through the following differential equations:

$$\begin{bmatrix} \dot{\phi} \\ \dot{\theta} \\ \dot{\psi} \end{bmatrix} = \begin{bmatrix} 1 & \sin\phi\tan\theta & \cos\phi\tan\theta \\ 0 & \cos\phi & -\sin\phi \\ 0 & \sin\phi/\cos\theta & \cos\phi/\cos\theta \end{bmatrix} \begin{bmatrix} p \\ q \\ r \end{bmatrix} \tag{2.5}$$

Remark 1 *The nonlinear differential equations need the nonsingularity of matrix in (2.5), which implies that θ is different from $\pi/2 + k\pi$ where k is an integer.*

2.2.1.2 Equations of motion of flight

In this section we will state the Newton's second law and Euler's law for a rigid body. At first we introduce the external forces and external moments.

Definitions:

$\tau_1 = [\tau_{1x}, \tau_{1y}, \tau_{1z}]^T$ is the external force acting on the body of the aircraft in the body fixed reference frame.

$\tau_2 = [\tau_{2x}, \tau_{2y}, \tau_{2z}]^T$ is the external moment acting on the body of the aircraft in the body fixed reference frame.

Force Equation: The Newton's second law states that the sum of all external forces acting on a body is equal to the time rate of change of its momentum, that means in Earth fixed reference frame, we have:

$$\tau_1 = \left[\frac{d(m\vec{\nu}_1)}{dt}\right]_E \tag{2.6}$$

It is interesting to study the velocity ν_1 in body fixed reference, a change of reference frame from R_E to R_B is done as (see []):

$$\left[\frac{d(\vec{\nu}_1)}{dt}\right]_E = \left[\frac{d(m\vec{\nu}_1)}{dt}\right]_B + \vec{\omega} \times \vec{\nu}_1 = \left[\frac{d(m\nu_1)}{dt}\right]_B + \Omega(m\nu_1) \tag{2.7}$$

where ω is the rotation vector and Ω is defined as:

$$\Omega = \begin{pmatrix} 0 & -r & q \\ r & 0 & -p \\ -q & p & 0 \end{pmatrix}$$

Expressing the previous equation on each axis of the body fixed reference frame, we obtain:

$$\begin{cases} \tau_{1x} &= m(\dot{u} - vr + wq) \\ \tau_{1y} &= m(\dot{v} - wp + ur) \\ \tau_{1z} &= m(\dot{w} - uq + vp) \end{cases}$$

where τ_{1x}, τ_{1y} and τ_{1z} depend on weight force W, aerodynamic force R and thrust force E.

Thrust is assumed to be through the X_B axis, then

$$\begin{cases} E_x &= T \\ E_y &= 0 \\ E_z &= 0 \end{cases} \tag{2.8}$$

The weight force W can be expressed in the R_B frame with g the gravity constant:

$$\begin{cases} W_x &= -mg\sin\theta \\ W_y &= mg\sin\phi\cos\theta \\ W_z &= mg\cos\phi\cos\theta \end{cases} \tag{2.9}$$

and the aerodynamic force vector is $E = (F_u, F_v, F_w)^T$ in which F_u, F_v and F_w are function of aircraft's states:

- total velocity (airspeed) of the vehicle (V)
- geometry of the vehicle: wing area S, wing span $\bar{b}$ and mean aerodynamic chord $\bar{c}$
- orientation of the flight angle of attack α and sideslip angle β, angular rates p, q and r
- control surfaces δ of the aircraft: aileron δ_a, elevator δ_e and rudder δ_r

The standard aerodynamic forces can be expressed under the form:

$$\begin{cases} F_u &= \bar{q}SC_x(\alpha, \beta, p, q, r, \delta, \cdots) \\ F_v &= \bar{q}SC_y(\alpha, \beta, p, q, r, \delta, \cdots) \\ F_w &= \bar{q}SC_z(\alpha, \beta, p, q, r, \delta, \cdots) \end{cases} \tag{2.10}$$

where $\bar{q} = 1/2\rho V^2$ is the aerodynamic pressure. C_x, C_x and C_x are aerodynamic coefficients obtained from wind tunnel data tests.

From these definitions, we have the complete force equations:

$$\begin{cases} F_u + T - mg\sin\theta &= m(\dot{u} - vr + wq) \\ F_v + mg\sin\phi\cos\theta &= m(\dot{v} - wp + ur) \\ F_w + mg\cos\phi\cos\theta &= m(\dot{w} - uq + vp) \end{cases} \tag{2.11}$$

Moment Equation: The Euler's law states that the summation of all external moments acting on the body is equal to the time rate of change of its angular momentum, so that in Earth fixed reference frame it is expressed as:

$$\tau_2 = \left[\frac{d(I\vec{\nu}_2)}{dt}\right]_E \tag{2.12}$$

In body fixed reference frame, it can be rewritten:

$$\tau_2 = \left[\frac{d(I\vec{\nu}_2)}{dt}\right]_B + \vec{\omega} \times (I\vec{\nu}_2) = \left[\frac{d(I\nu_2)}{dt}\right]_B + \Omega(I\nu_2) \tag{2.13}$$

Because of the symmetry of the vehicle with respect to OX_BZ_B plane, inertia matrix has the form:

$$I = \begin{pmatrix} I_{xx} & 0 & -I_{xz} \\ 0 & I_{yy} & 0 \\ -I_{xz} & 0 & I_{zz} \end{pmatrix}$$

The external moments are those due to aerodynamic and thrust forces. In this case we suppose that the moment due to thrust force can be neglected. The aerodynamic moments are expressed as:

$$\begin{cases} L &= \bar{q}S\bar{b}C_l(\alpha, \beta, p, q, r, \delta, \cdots) \\ M &= \bar{q}S\bar{c}C_m(\alpha, \beta, p, q, r, \delta, \cdots) \\ N &= \bar{q}S\bar{b}C_n(\alpha, \beta, p, q, r, \delta, \cdots) \end{cases} \tag{2.14}$$

Expanding the previous equation on each axis of R_B reference frame, results in the complete axis moment equation:

$$\begin{cases} \dot{p} &= \frac{1}{I_{xx}I_{zz}-I_{xz}^2}[(I_{yy}I_{zz} - I_{zz}^2 - I_{xz}^2)rq - I_{xz}(I_{xx} + I_{zz} - I_{yy})pq + I_{zz}L - I_{xz}N] \\ \dot{q} &= \frac{1}{I_{yy}}[(I_{zz} - I_{xx})pr + I_{xz}(p^2 - r^2) + M] \\ \dot{r} &= \frac{1}{I_{xx}I_{zz}-I_{xz}^2}[(-I_{xx}I_{yy} + I_{zz}^2 + I_{xz}^2)pq + I_{xz}(I_{xx} + I_{zz} - I_{yy})rq + I_{xx}N - I_{xz}L] \end{cases} \tag{2.15}$$

2.2.1.3 Summary of flight's dynamics

The equations of motion presented in the previous sections can be rewritten as a system of 12 equations to describe the flight dynamics.

Force Equations of motion:

$$\begin{cases} \dot{u} = rv - qw - g\sin\theta + \dfrac{1}{m}(F_u + T) & (2.16a) \\ \dot{v} = pw - ru + g\sin\phi\cos\theta + \dfrac{1}{m}F_v & (2.16b) \\ \dot{w} = qu - pv + g\cos\phi\cos\theta + \dfrac{1}{m}F_w & (2.16c) \end{cases}$$

Equations of motion:

$$\begin{cases} \dot{p} = \dfrac{1}{I_{xx}I_{zz} - I_{xz}^2}[(I_{yy}I_{zz} - I_{zz}^2 - I_{xz}^2)rq - I_{xz}(I_{xx} + I_{zz} - I_{yy})pq + I_{zz}L & (2.17a) \\ \quad - I_{xz}N] \\ \dot{q} = \dfrac{1}{I_{yy}}[(I_{zz} - I_{xx})pr + I_{xz}(p^2 - r^2) + M] & (2.17b) \\ \dot{r} = \dfrac{1}{I_{xx}I_{zz} - I_{xz}^2}[(-I_{xx}I_{yy} + I_{zz}^2 + I_{xz}^2)pq + I_{xz}(I_{xx} + I_{zz} - I_{yy})rq + I_{xx}N & (2.17c) \\ \quad - I_{xz}L] \end{cases}$$

Euler's angles dynamics:

$$\begin{cases} \dot{\phi} = p + \tan\theta(q\sin\phi + r\cos\phi) & (2.18a) \\ \dot{\theta} = q\cos\phi - r\sin\phi & (2.18b) \\ \dot{\psi} = \dfrac{q\sin\phi + r\cos\phi}{\cos\theta} & (2.18c) \end{cases}$$

Aircraft's position dynamics:

$$\begin{cases} \dot{x_E} = u\cos\psi\cos\theta + v(\cos\psi\sin\theta\sin\phi - \sin\psi\cos\phi) & (2.19a) \\ \qquad + w(\cos\psi sin\theta\cos\phi + \sin\psi\sin\phi) \\ \dot{y_E} = u\sin\psi\cos\theta + v(\sin\psi\sin\theta\sin\phi - \cos\psi\cos\phi) & (2.19b) \\ \qquad + w(\sin\psi sin\theta\cos\phi + \cos\psi\sin\phi) \\ \dot{z_E} = u\sin\theta + v\cos\theta\sin\phi + w\cos\theta\cos\phi & (2.19c) \end{cases}$$

It may be more convenient to express the force equations in wind axes reference frame, it means the transformation (see Fig. 2.3):

$$\begin{array}{lcl} u = V\cos\alpha\cos\beta & & V = \sqrt{u^2 + v^2 + w^2} \\ v = V\sin\beta & \Leftrightarrow & \alpha = \arctan(w/u) \\ w = V\sin\alpha\cos\beta & & \beta = \arcsin(v/V) \end{array} \quad (2.20)$$

The force equation of motion can be expressed in wind axes reference frame as:

$$\begin{aligned} \dot{V}_a &= \tfrac{u\dot{u}+v\dot{v}+w\dot{w}}{V_a} \\ \dot{\alpha} &= \tfrac{u\dot{w}-w\dot{u}}{u^2+w^2} \\ \dot{\beta} &= \tfrac{\dot{v}V_a-\dot{V}_a v}{V_a^2\cos\beta} \end{aligned} \tag{2.21}$$

Substituting $(\dot{u}, \dot{v}, \dot{w})$ gives another form as follows:

$$\begin{cases} \dot{V} = \dfrac{\cos\alpha\cos\beta}{m}[T+F_u] + \dfrac{\sin\beta}{m}F_v + \dfrac{\sin\alpha\cos\beta}{m}F_w & \text{(2.22a)} \\ \quad + g[-\cos\alpha\cos\beta\sin\theta + \sin\beta\sin\phi\cos\theta + \sin\alpha\cos\beta\cos\phi\cos\theta] \\ \dot{\alpha} = -\cos\alpha\tan\beta p + q - \sin\alpha\tan\beta r - \dfrac{\sin\alpha}{mV\cos\beta}(T+F_u) + \dfrac{\cos\alpha}{mV\cos\beta}F_w & \text{(2.22b)} \\ \quad + \dfrac{g}{V\cos\beta}[\sin\alpha\cos\theta + \cos\alpha\cos\phi\cos\theta] \\ \dot{\beta} = \sin\alpha p - \cos\alpha r - \dfrac{\cos\alpha\sin\beta}{mV}[T+F_u] + \dfrac{\cos\beta}{mV}F_v - \dfrac{\sin\alpha\sin\beta}{mV}F_w & \text{(2.22c)} \\ \quad + \dfrac{g}{V}[\cos\alpha\sin\beta\sin\theta + \cos\beta\cos\theta\sin\phi - \sin\alpha\sin\beta\cos\phi\cos\theta] \end{cases}$$

2.3 Modeling

The air launch phase can be described by the variations in mass, inertia and aerodynamic coefficients of air launch system before and after launch phase. Modeling this phase requires a large amount of data and previous knowledge about the real system, which is actually not available in the case of study. However, it can also be represented as a hybrid system composed by two (or three) continuous models that are switched. These models represents the system before, (possible during) and after the separation phase. In the present work we have adopted this strategy, we have considered three phases.

1. before the separation ⇒ a first aircraft model (representing the UAV and the rocket) is in a stable operating condition

2. during the separation ⇒ a second aircraft model representing only the UAV, starting on the previous operating condition is disturbed by impulses on forces and moments. These disturbances are inside a time interval T_{int} and represent a not perfect separation. Furthermore the initial conditions, inherited from the first phase, are not an equilibrium point for the second aircraft model.

3. after the separation ⇒ the disturbances stop (UAV and rocket are not in physical contact anymore). It can be shown that the effect of launching the rocket from the UAV impacts most the lift force, and the roll and pitch moments.

From this strategy, we have two approaches to model the air launch phase that we present in the following section.

2.3.1 Initial Condition Approach

As a first approach to model the system, we adopt a hybrid technique that considers the air launch as a switch between two continuous models, one previous the launch phase and one following it. The switch itself is considered as instantaneous, but imperfect. In this way impulses on the forces and moments affect the aircraft, resulting in possibly large initial conditions for the second model, which is taken as an F-16. The resulting control task may be stated as to design an stabilizing controller for this second system (after the switch) with possible large initial conditions.

2.3.2 Perturbation on aerodynamic force and moment approach

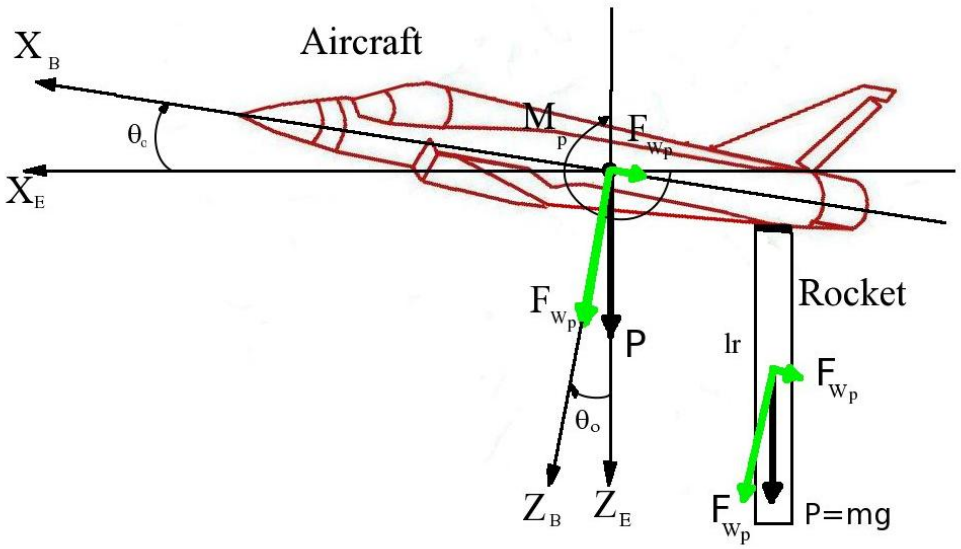

Figure 2.5: The launcher attached to the aircraft carrier in the worst case

In a second approach to model our system, we have also considered the air launch as a switch between two continuous models:

1. before the separation ⇒ the first model is considered at a stable operating condition

2. during the separation ⇒ the launch phase itself happens during an interval T_{int}. During this interval the second model is used, but disturbed by constant aerodynamic force and moment representing an imperfect launch of the rocket from the aircraft

3. after the separation ⇒ the disturbances stop, and the second model continues to be used

In order to make our study as much general as possible, the first model is taken as an F-16 with twice its normal mass, while the second model is taken as the complete F-16 model. It is important to remark that the first model, in practice, is only used to compute the initial conditions. for the separation phase.

It can be shown that the effect of launching the rocket from the carrier aircraft disturb mostly lift force, drag force and pitch and roll moments. We suppose that these disturbing forces and moments are constant during the interval T_{int} (see Fig. 2.6). We call F_{w_p}, F_{u_p}, L_p and M_p the disturbances on the lift force, on the roll moment and pitch moment respectively (see Fig. 2.6).

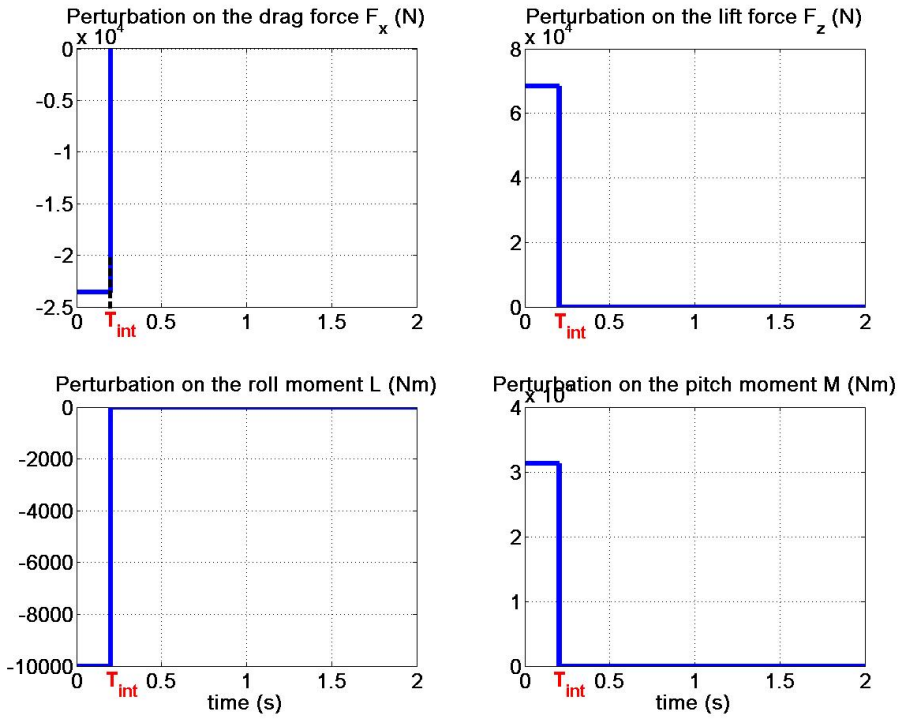

Figure 2.6: Perturbation on aerodynamic forces and moments

We suppose that:

- the perturbation on lift force during T_{int} is equal to the air launch vehicle's mass, that means $F_{w_p} = mg\cos\theta_0$.

- the perturbation on drag force is $F_{u_p} = -P\sin\theta_0 = -mg\sin\theta_0$ where θ_0 is the initial pitch angle of the first model at the launching phase.

- the perturbation on pitch moment during T_{int} is an worst case that is represented by the rocket that remains attached to the aircraft by only one end during T_{int}, applying a rotational movement to the aircraft, so a moment with value $M_p = mgl_r\cos\theta_0/2$ where l_r is the rocket length.

- the perturbation on roll moment during T_{int} is small because of the rocket shape (long and thin).

- the model following the launch phase is the F-16 model. Its initial condition is the state at an equilibrium point of the model previous the launch phase that is the F-16 model but with twice its standard mass.

2.3.3 System Model

Following this strategy, the F-16 aircraft in the instant following the launching phase has dynamics of a flying object as in (2.16), (2.5) (2.18) presented in the previous section. We are interested in motion of velocity vector, Euler's angles and angular rates only. The carrier aircraft after the separation phase can be summarized as:

$$\begin{cases} \dot{u} = rv - qw - g\sin\theta + \frac{1}{m}(F_u + T) \\ \dot{v} = pw - ru + g\sin\phi\cos\theta + \frac{1}{m}F_v \\ \dot{w} = qu - pv + g\cos\phi\cos\theta + \frac{1}{m}F_w \\ \dot{p} = \frac{1}{I_{xx}I_{zz} - I_{xz}^2}[(I_{yy}I_{zz} - I_{zz}^2 - I_{xz}^2)rq - I_{xz}(I_{xx} + I_{zz} - I_{yy})pq + I_{zz}L - I_{xz}N] \\ \dot{q} = \frac{1}{I_{yy}}[(I_{zz} - I_{xx})pr + I_{xz}(p^2 - r^2) + M] \\ \dot{r} = \frac{1}{I_{xx}I_{zz} - I_{xz}^2}[(-I_{xx}I_{yy} + I_{zz}^2 + I_{xz}^2)pq + I_{xz}(I_{xx} + I_{zz} - I_{yy})rq + I_{xx}N - I_{xz}L] \\ \dot{\phi} = p + \tan\theta(q\sin\phi + r\cos\phi) \\ \dot{\theta} = q\cos\phi - r\sin\phi \\ \dot{\psi} = \frac{q\sin\phi + r\cos\phi}{\cos\theta} \end{cases}$$

In the present case, it is better to represent the state variables in the wind axes reference frame $OX_WY_WZ_W$ because of the measurability of these state variables. We write again

the dynamics of this carrier aircraft:

$$
\begin{cases}
\dot{\alpha} = -\cos\alpha\tan\beta p + q - \sin\alpha\tan\beta r - \dfrac{\sin\alpha}{mV\cos\beta}(T+F_u) + \dfrac{\cos\alpha}{mV\cos\beta}F_w & (2.23a)\\
\quad + \dfrac{g}{V\cos\beta}[\sin\alpha\cos\theta + \cos\alpha\cos\phi\cos\theta] & \\
\dot{\beta} = \sin\alpha p - \cos\alpha r - \dfrac{\cos\alpha\sin\beta}{mV}[T+F_u] + \dfrac{\cos\beta}{mV}F_v - \dfrac{\sin\alpha\sin\beta}{mV}F_w & (2.23b)\\
\quad + \dfrac{g}{V}[\cos\alpha\sin\beta\sin\theta + \cos\beta\cos\theta\sin\phi - \sin\alpha\sin\beta\cos\phi\cos\theta] & \\
\dot{V} = \dfrac{\cos\alpha\cos\beta}{m}[T+F_u] + \dfrac{\sin\beta}{m}F_v + \dfrac{\sin\alpha\cos\beta}{m}F_w & (2.23c)\\
\quad + g[\cos\alpha\cos\beta\sin\theta + \sin\beta\sin\phi\cos\theta + \sin\alpha\cos\beta\cos\phi\cos\theta] & \\
\dot{p} = \dfrac{1}{I_{xx}I_{zz} - I_{xz}^2}[(I_{yy}I_{zz} - I_{zz}^2 - I_{xz}^2)rq - I_{xz}(I_{xx} + I_{zz} - I_{yy})pq + I_{zz}L - I_{xz}N] & (2.23d)\\
\dot{q} = \dfrac{1}{I_{yy}}[(I_{zz} - I_{xx})pr + I_{xz}(p^2 - r^2) + M] & (2.23e)\\
\dot{r} = \dfrac{1}{I_{xx}I_{zz} - I_{xz}^2}[(-I_{xx}I_{yy} + I_{zz}^2 + I_{xz}^2)pq + I_{xz}(I_{xx} + I_{zz} - I_{yy})rq + I_{xx}N - I_{xz}L] & (2.23f)\\
\dot{\phi} = p + \tan\theta(q\sin\phi + r\cos\phi) & (2.23g)\\
\dot{\theta} = q\cos\phi - r\sin\phi & (2.23h)\\
\dot{\psi} = \dfrac{q\sin\phi + r\cos\phi}{\cos\theta} & (2.23i)
\end{cases}
$$

The aerodynamic forces (F_u, F_v, F_w) and moments (L,M,N) are function of all the considered states. In this model, these aerodynamic forces and moments are under look-up table from wind tunnel data measurements as may be found in [13]. Finally, the control inputs are respectively the aileron (δ_a), rudder (δ_r) and elevator (δ_e) angles, in addition to thrust (T).

In particular, we use the low quality mode of the F-16 model, and the aerodynamic data is interpolated and extrapolated linearly in simulation from tables found in [13].

2.4 LQR control

A consequence of the considered model is that the control design for the air launch phase becomes quite difficult because this is a nonlinear model and its aerodynamic coefficients are under tabular form.

In order to simplify our study, we start our thesis with a control strategy that is robust and simple to implement, and will be used as a first approach to control and stabilize the air launch system, which is a simple LQR controller.

2.4.1 LQR control design

Consider a linear system under state space form:

$$\begin{cases} \dot{x} = Ax + Bu \quad x \in R^n,\ u \in R^m \\ y = Cx \quad y \in R^m \end{cases} \tag{2.24}$$

where x is the system state, y the system output and u the input. $A \in \mathbb{R}^{n\times n}$, $B \in \mathbb{R}^{n\times m}$ and $C \in \mathbb{R}^{m\times n}$.

If (A, B) is stabilizable and for $Q \in \mathbb{R}^{n\times n}$ positive semidefinite matrix, $R \in \mathbb{R}^{m\times m}$ positive definite matrix, the LQR control law has the from (see [38],[39]):

$$u = -Kx \tag{2.25}$$

where $K = R^{-1}BP$ with P the positive semidefinite solution of the Riccati equation:

$$A^TP + PA + Q - PBR^{-1}B^TP = 0 \tag{2.26}$$

2.4.2 Application to Air launch system

We will linearize the air launch system defined in (2.23) at an equilibrium point. Note that the dynamics of airspeed (V) is much slower than any other state variables and it is controlled by thrust force, we then assume that airspeed of the flight and the thrust are constant.

The linearization of (2.23) except the airspeed's equation (2.23) was done through its variables:

- angle of attack (α) and sideslip angle (β)
- Euler's angles $(\phi, \theta, \psi)^T$
- angular rates $(p, q, r)^T$

The equilibrium point of the second model, a F - 16 in our case, is $(V, h) = (154m/s, 5000m)$ which corresponds to the trimmed angle of attack $\bar{\alpha} = 4.6°$, pitch angle $\bar{\theta} = 4.6°$ sideslip $\bar{\beta} = 0°$ and $\bar{\phi} = 0°$ and to trimmed control surface states: aileron $\bar{\delta}_a = 0°$, elevator $\bar{\delta}_e = -2.5°$, rudder $\bar{\delta}_r = 0°$ and all angular rates $\bar{p}, \bar{q}, \bar{r}$ are zero.

A linearization of the second model at this equilibrium point gives us the linearized system:

$$\begin{cases} \begin{bmatrix} \dot{\tilde{\alpha}} \\ \dot{\tilde{\beta}} \\ \dot{\tilde{p}} \\ \dot{\tilde{q}} \\ \dot{\tilde{r}} \\ \dot{\tilde{\phi}} \\ \dot{\tilde{\theta}} \\ \dot{\tilde{\psi}} \end{bmatrix} = A \begin{bmatrix} \tilde{\alpha} \\ \tilde{\beta} \\ \tilde{p} \\ \tilde{q} \\ \tilde{r} \\ \tilde{\phi} \\ \tilde{\theta} \\ \tilde{\psi} \end{bmatrix} + B \begin{bmatrix} \tilde{\delta}_a \\ \tilde{\delta}_e \\ \tilde{\delta}_r \end{bmatrix} \\ \tilde{y} = C \begin{bmatrix} \tilde{\alpha}, \tilde{\beta}, \tilde{p}, \tilde{q}, \tilde{r}, \tilde{\phi}, \tilde{\theta}, \tilde{\psi} \end{bmatrix}^T \end{cases}$$

where we define:

$$\tilde{x} = \begin{bmatrix} \tilde{\alpha} \\ \tilde{\beta} \\ \tilde{p} \\ \tilde{q} \\ \tilde{r} \\ \tilde{\phi} \\ \tilde{\theta} \\ \tilde{\psi} \end{bmatrix} = \begin{bmatrix} \alpha - \bar{\alpha} \\ \beta - \bar{\beta} \\ p - \bar{p} \\ q - \bar{q} \\ r - \bar{r} \\ \phi - \bar{\phi} \\ \theta - \bar{\theta} \\ \psi - \bar{\psi} \end{bmatrix}; \tilde{u} = \begin{bmatrix} \tilde{\delta}_a \\ \tilde{\delta}_e \\ \tilde{\delta}_r \end{bmatrix} = \begin{bmatrix} \delta_a - \bar{\delta}_a \\ \delta_e - \bar{\delta}_e \\ \delta_r - \bar{\delta}_r \end{bmatrix}; \tilde{y} = \begin{bmatrix} \tilde{\alpha} \\ \tilde{\beta} \\ \tilde{p} \\ \tilde{q} \\ \tilde{r} \\ \tilde{\phi} \\ \tilde{\theta} \\ \tilde{\psi} \end{bmatrix} = \begin{bmatrix} \alpha - \bar{\alpha} \\ \beta - \bar{\beta} \\ p - \bar{p} \\ q - \bar{q} \\ r - \bar{r} \\ \phi - \bar{\phi} \\ \theta - \bar{\theta} \\ \psi - \bar{\psi} \end{bmatrix} \quad (2.27)$$

and

$$A = \begin{bmatrix} -0.5360 & 0.0019 & 0 & 0.9514 & 0 & 0 & -0.0000 \\ -0.0072 & -0.1521 & 0.0493 & 0 & -0.9948 & 0.0643 & 0 \\ 0.0047 & -15.9601 & -1.8407 & 0 & 0.3955 & 0 & 0 \\ -0.2637 & -0.0167 & 0 & -0.6989 & 0 & 0 & 0 \\ 0.0453 & 4.0567 & -0.0166 & 0 & -0.2507 & 0 & 0 \\ 0 & 0 & 1.0000 & 0 & 0.0494 & 0 & 0 \\ 0 & 0 & 0 & 1.0000 & 0 & 0 & 0 \end{bmatrix};$$

$$B = \begin{bmatrix} 0 & -0.0014 & 0 \\ 0.0001 & 0 & 0.0004 \\ -0.3473 & 0.0025 & 0.0659 \\ 0 & -0.1001 & 0 \\ -0.0145 & 0.0007 & -0.0326 \\ 0 & 0 & 0 \\ 0 & 0 & 0 \end{bmatrix}; C = \begin{bmatrix} 1 & 0 & 0 & 0 & 0 & 0 & 0 \\ 0 & 1 & 0 & 0 & 0 & 0 & 0 \\ 0 & 0 & 1 & 0 & 0 & 0 & 0 \\ 0 & 0 & 0 & 1 & 0 & 0 & 0 \\ 0 & 0 & 0 & 0 & 1 & 0 & 0 \\ 0 & 0 & 0 & 0 & 0 & 1 & 0 \\ 0 & 0 & 0 & 0 & 0 & 0 & 1 \end{bmatrix}$$

This system can be rewritten symbolically as:

$$\begin{cases} \dot{\tilde{x}} = A\tilde{x} + B\tilde{u} \\ \tilde{y} = C\tilde{x} \end{cases} \tag{2.28}$$

It is easy to check that (A, B) is stabilizable, then an application of LQR control to this system gives:

$$u = -Kx \tag{2.29}$$

$$\tag{2.30}$$

where K is calculated under Matlab for given R and Q.

$$K = \begin{bmatrix} -0.2 & 29.4 & -11.2 & -0.2 & -7.7 & -13.7 & -0.0 & -0.4 \\ 0.7 & -1.9 & 0.3 & -38.3 & 0.0 & 0.3 & -1.0 & 0.0 \\ -0.2 & 0.6 & 1.9 & -0.1 & -12.4 & 1.4 & -0.0 & -0.1 \end{bmatrix} \tag{2.31}$$

and

$$Q = \begin{bmatrix} 100 & 0 & 0 & 0 & 0 & 0 & 0 \\ 0 & 500 & 0 & 0 & 0 & 0 & 0 \\ 0 & 0 & 1000 & 0 & 0 & 0 & 0 \\ 0 & 0 & 0 & 2000 & 0 & 0 & 0 \\ 0 & 0 & 0 & 0 & 1000 & 0 & 0 \\ 0 & 0 & 0 & 0 & 0 & 1000 & 0 \\ 0 & 0 & 0 & 0 & 0 & 0 & 1 \end{bmatrix}; R = \begin{bmatrix} 5 & 0 & 0 \\ 0 & 1 & 0 \\ 0 & 0 & 5 \end{bmatrix}$$

2.5 Simulation and Results

In the following simulations, we have applied the LQR control for stabilizing studied states of the second model to its equilibrium point from several initial conditions in the first modeling approach and from impulses on aerodynamic forces and moments for the second modeling approach. This illustrates the performance of the LQR control face to several launch conditions. Our control task is to:

- stabilize the states of the second model to its equilibrium point, which is is considered on the operating point ($V = 154m/s, h = 5000m$) corresponding to the trimmed angle of attack $\alpha_r = 4.6°$, sideslip $\beta_r = 0°$, roll angle $\phi_r = 0°$ and to trimmed control surface states: aileron $\delta_a = 0°$, elevator $\delta_e = -2.5°$ and rudder $\delta_r = 0°$.

- guarantee the physical limitations of the actuators ($|\delta_a| < 21.5°$, $|\delta_e| < 25°$ and $|\delta_r| < 30°$).
- assure the flighting envelop of the F-16 model:
  - limit of rates $60°/s$ for pitch and yaw rates, and $90°/s$ for roll rate.
  - limit angles $|360°|$ for roll and yaw angles and $|90°|$ for pitch angle.

The parameter of the controller $\tilde{u} = -K\tilde{x}$ is:

$$K = \begin{bmatrix} -0.2 & 29.4 & -11.2 & -0.2 & -7.7 & -13.7 & -0.0 & -0.4 \\ 0.7 & -1.9 & 0.3 & -38.3 & 0.0 & 0.3 & -1.0 & 0.0 \\ -0.2 & 0.6 & 1.9 & -0.1 & -12.4 & 1.4 & -0.0 & -0.1 \end{bmatrix} \tag{2.32}$$

In order to control airspeed, we design a simple PI controller for the thrust to regulate the airspeed of the system. Its form is:

$$T = -k_P(V - V_{ref}) - k_I(\dot{V} - \dot{V}_{ref})$$

where V_{ref} is the airspeed reference, $k_P = 711.0$ and $k_I = 6.2$.

In the control cases, we suppose that there are measurement errors on the state variable of the the system. These errors are defined as white noises perturbing the state variables as seen in the Fig. 2.7.

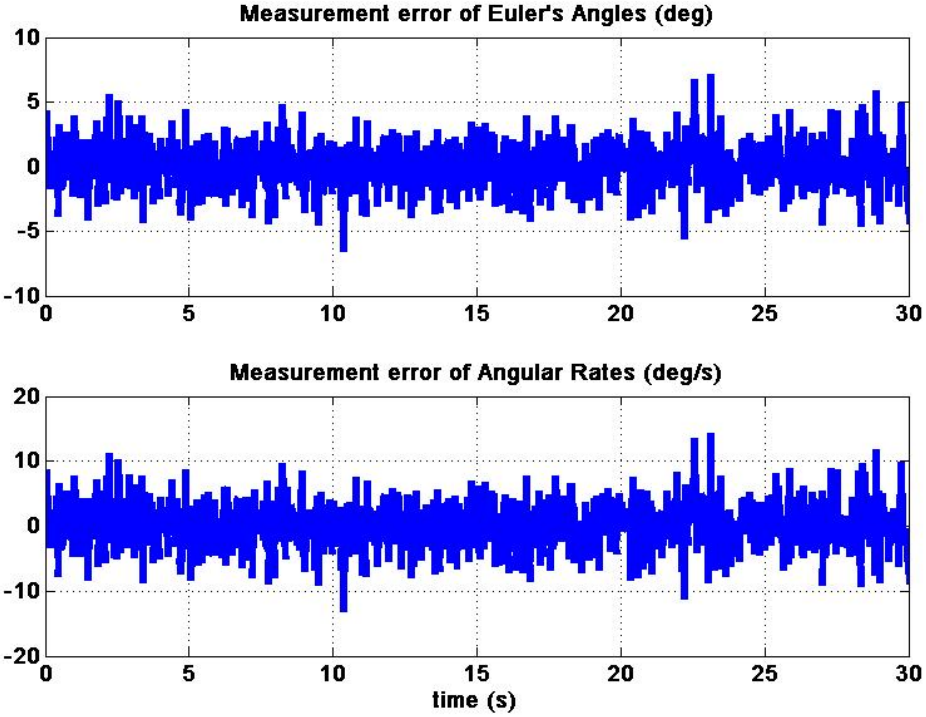

Figure 2.7: Measurement errors of the state variables

In the following section we will present the simulation results for two modeling approaches for the launch phase. First is the resulting initial condition, and second is impulses during a T_{int} time interval.

2.5.1 Initial Condition Approach

As explained in section (2.3.1), this approach only uses the second model. The separation phase results in large initial conditions in respect to the equilibrium point (angle of attack $\alpha = 4.6°$, sideslip angle $\beta = 0°$ and roll angle $\phi = 0°$) on the second model, which is an F-16.

For our study, we consider three sets of initial conditions:

First case corresponds to a small initial condition error from the trimmed ones of the aircraft after the phase of drop, with an angle of attack $\alpha = 8.0°$, sideslip $\beta = 5°$ and roll angle $\phi = 10°$.

The second case is a medium error between the initial and trimmed conditions with $\alpha = 18.0°$, sideslip $\beta = 10°$ and $\phi = 20°$. The last case corresponds to a large initial condition with $\alpha = 33.0°$, sideslip $\beta = 20°$ and $\phi = 40°$. In the following, one may see how the system responds to these three cases.

Fig. 2.8 shows the convergence of the controlled outputs with the LQR controller for different initial conditions, in the three cases distinct from the equilibrium point. The dashed black line indicates the controlled outputs of system in the first case, the continuous line is the controlled outputs for an medium error case, and the large error situation corresponds to the dash dotted line.

Fig. 2.9 represents the behavior of other states of the system. In the left side, one can see that the angular rates return to the origin. In the right side, it is shown how Euler's angles converge. The yaw angle that illustrates the lateral motion, is left free (the airplane can go in any direction), but in this case it is converged. In Fig. 2.10 it illustrated the input controls for the three studied cases.

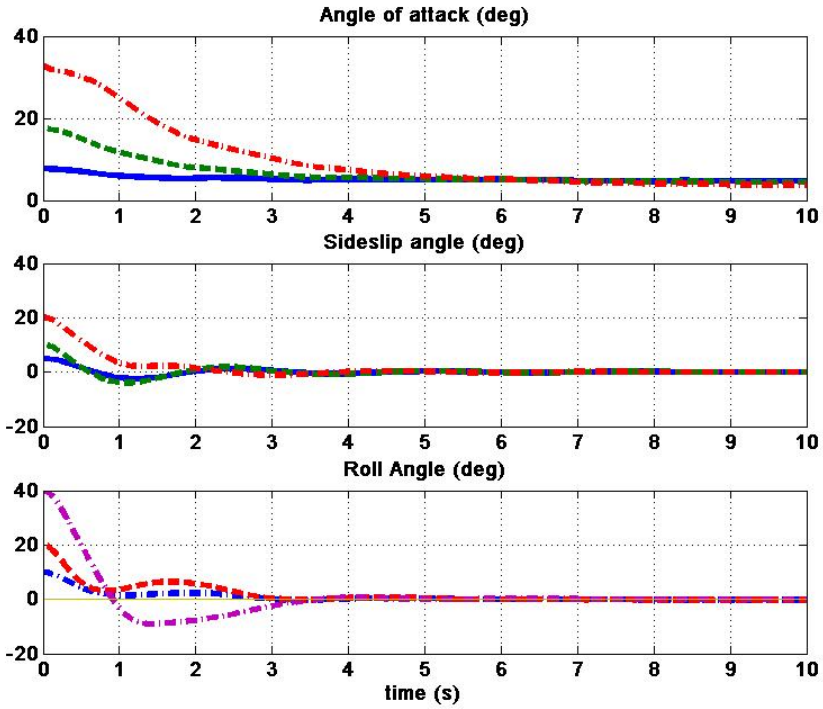

Figure 2.8: Angle of attack α, sideslip β and roll angle ϕ stabilized by LQR controller

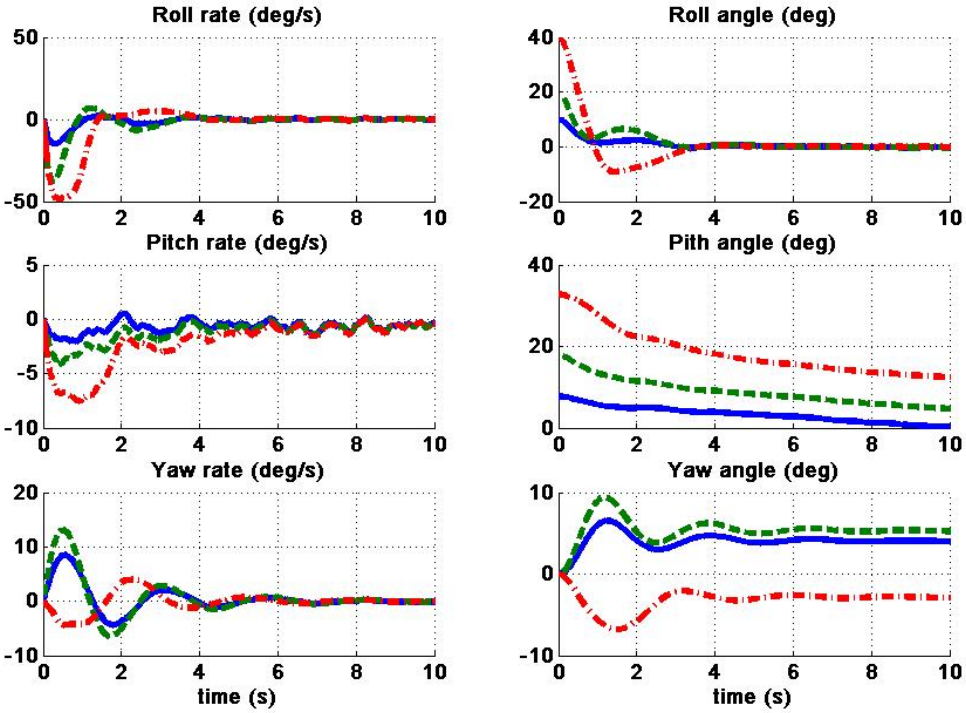

Figure 2.9: Angular rates and Euler's angles by LQR controller

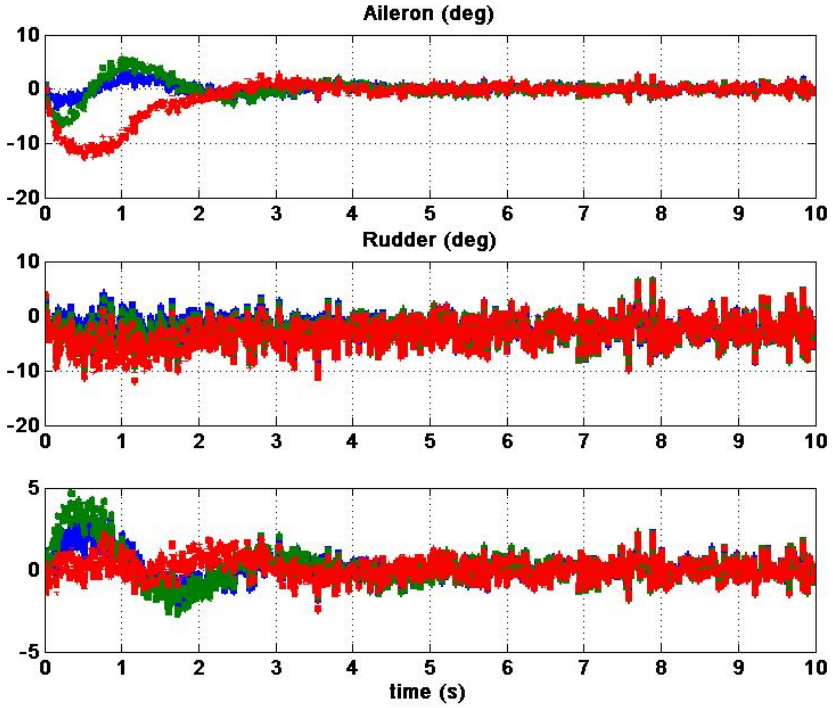

Figure 2.10: Aileron δ_a, elevator δ_e and rudder δ_a of LQR controller

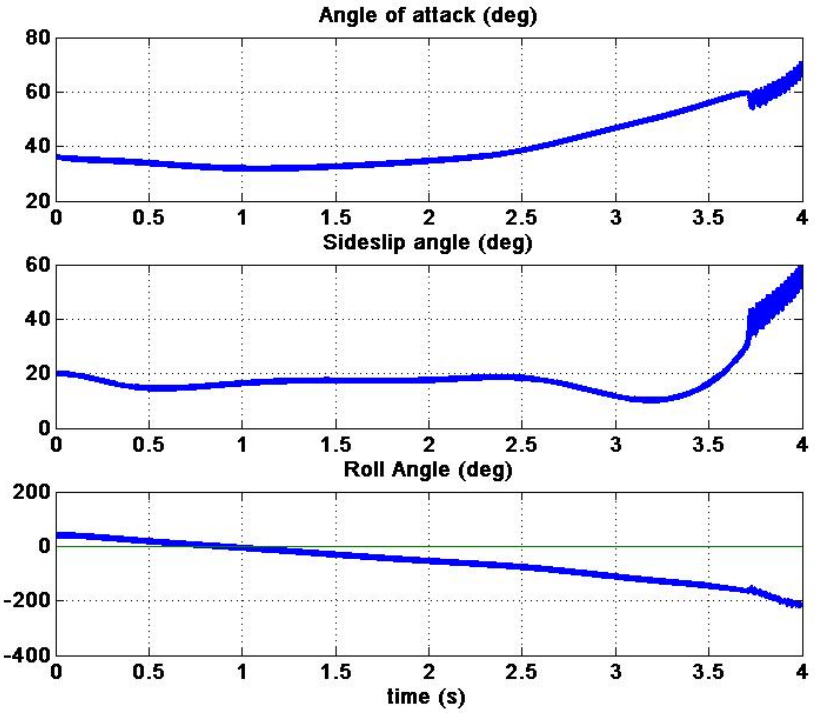

Figure 2.11: Angle of attack α, sideslip β and roll angle ϕ unstable by LQR controller

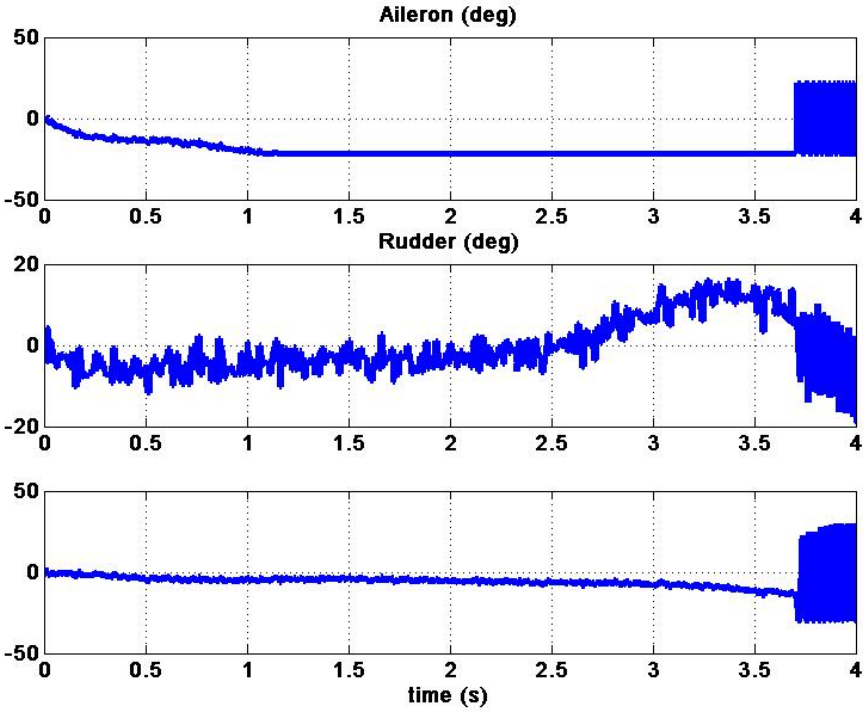

Figure 2.12: Aileron δ_a, elevator δ_e and rudder δ_a saturated with LQR controller

In these three cases of study, the outputs are stabilized to the operating point values. This illustrates the good performance of the LQR controller. It can be easily seen that the outputs return quickly to the operating point in $5s$. This is compatible to the desired specification. In terms of control inputs in Fig. 2.10, all actuators are inside their bounds for the three cases, i.e. inside the limits of 21.5° for ailerons δ_a, 25° for elevators δ_e and of 30° for rudders δ_r. It's interesting to remark that the control input continues to react to the very large measurement noise we have considered (see Fig. 2.7)

To verify the impact of very large errors on the initial conditions in the drop phase, we increase them to: angle of attack $\alpha = 35°$, sideslip $\beta = 20°$ and $\phi = 40°$. The simulation result is demonstrated in Fig. 2.11 for the controlled outputs and in Fig. 2.12 for the control surfaces.

Fig. 2.11 shows that the state outputs become unstable, the roll angle is out of the flighting range of the F-16 model. In Fig. 2.12 it is shown that the demanded surface controls are very high compared to their physical limitations. The response of the system in this case is not compatible to the required specification and flighting range of the F-16 model. It is possible that, since control inputs are saturated, this illustrates the physical limits of stabilizability of this kind of aircraft, independently of the applied control strategy.

2.5.2 Modeling approach of perturbation on aerodynamic force and moment

We consider now the modeling approach of the airlaunch phase studied in subsection 2.3.2. In a first step, the airlaunch system is taken with constant control inputs. We can then find a maximum time interval T_{Max} beyond which the disturbances affecting aerodynamic force and moment bring the system unstable. In a second step, we show that the LQR controller designed in section 2.4 will stabilize the airlaunch system for several intervals T_{int} greater than T_{Max}.

We take, as the initial condition of the second model, an equilibrium point of the first model, which is $(V, h) = (154m/s, 5000m)$, that corresponds to the trimmed angle of attack $\alpha_0 = 12.5°$, pitch angle $\theta_0 = 12.5°$ sideslip $\beta_0 = 0°$, $\phi_0 = 0°$ and to control surface states: aileron $\delta_a = 0°$, elevator $\delta_e = -4.0°$ and rudder $\delta_r = 0°$.

The second model following the launch phase will be stabilized to its equilibrium point $(V, h) = (154m/s, 5000m)$, that means angle of attack α_0 to 4.6°, sideslip β to 0°, and roll angle ϕ to 0°.

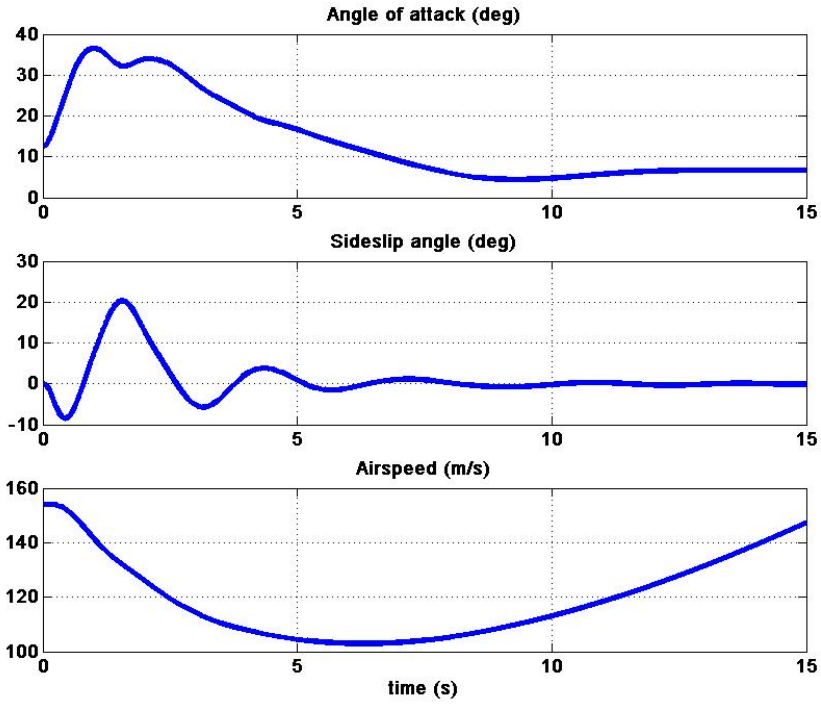

Figure 2.13: Angle of attack α, Sideslip β and Airspeed V stabilized by constant inputs

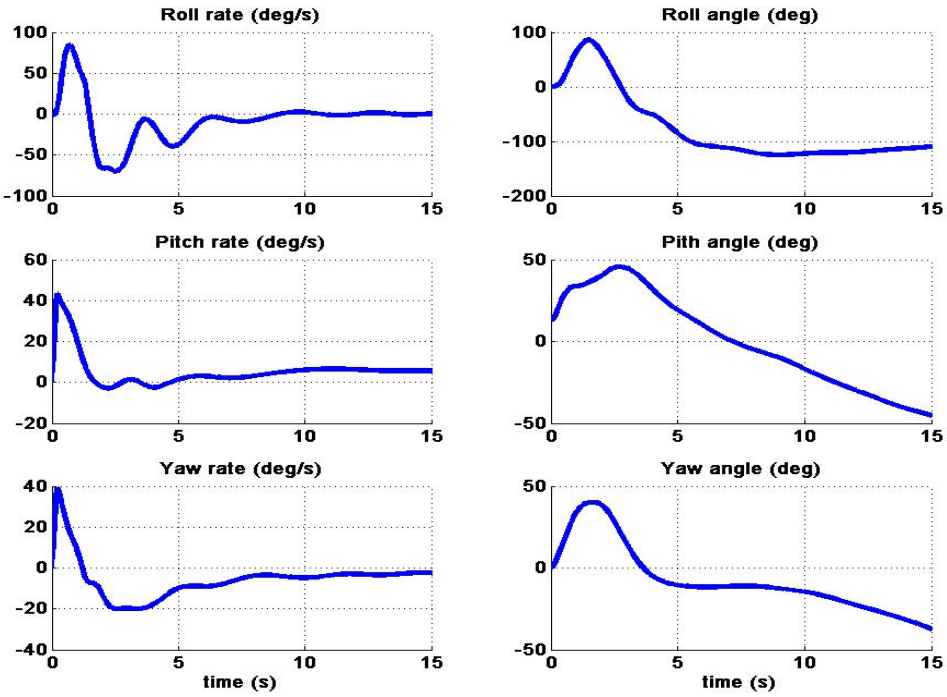

Figure 2.14: Angular Rates and Euler's Angles stabilized by constant inputs

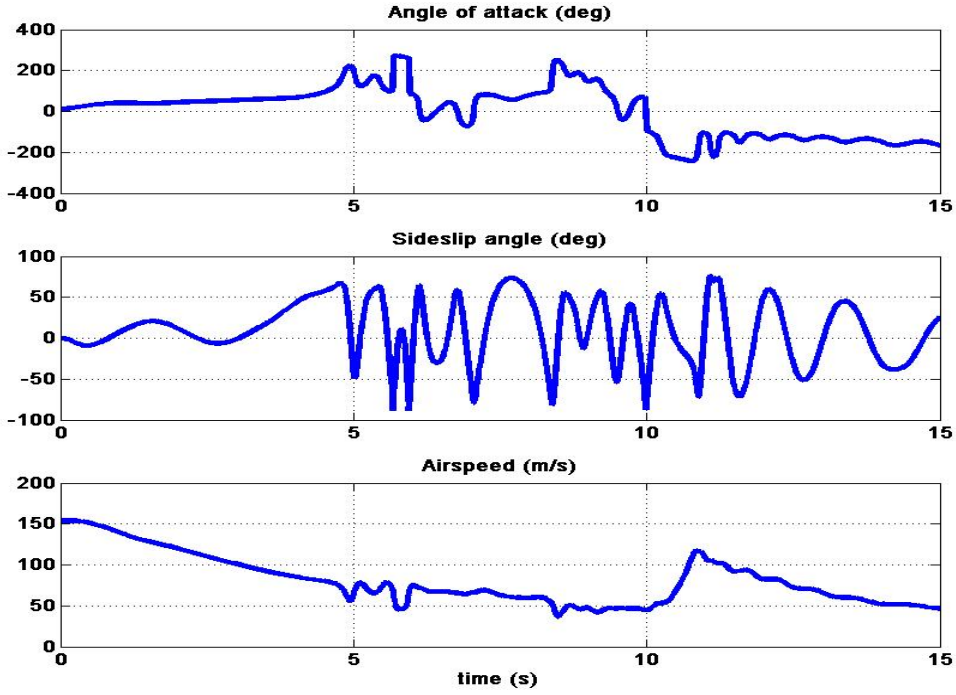

Figure 2.15: Instability of Angle of attack, Sideslip and Airspeed by constant inputs

2.5.2.1 Airlaunch system with constant inputs

At first, we take an interval of perturbation $T_{int} = 0.2s$, the simulation can be seen in Fig. 2.13. The angle of attack and the sideslip seem to be stabilized in spite of the perturbation on aerodynamic force and moment. However, Fig. 2.14 shows that roll angle and pitch angle are not converged. The system becomes then unstable for a perturbation that lasts $T_{int} = 0.2s$.

In order to see more clearly the instability of the second model affected by the perturbation, we increase T_{int} to $0.227s$, the system will be completely unstable as shown in Fig. 2.15. The value of T_{Max} is then $0.227s$.

2.5.2.2 Airlaunch system with LQR Controller

The LQR designed in section 2.4 is applied to the airlaunch system in order to stabilize the system states after the launch phase. To this purpose, we are interested in the stability of angle of attack, sideslip, roll angle, pitch angle, roll rate, pitch rate and yaw rate. The yaw angle, that illustrates the lateral motion, can be neglected in this study (the aircraft may be heading in any direction east-west-north-south).

We make the simulations using two disturbance durations, $T_{int} = 0.227s$ that made the airlaunch with constant control inputs unstable, and $T_{int} = 0.3s$ that will show the limits of the proposed control scheme. For the simulation procedure, we take the worst case perturbation described in subsection 2.3.2.

Figs. 2.16 to 2.18 show the simulation of airlaunch system controlled by LQR control with perturbation during $T_{int} = 0.227s$. The desired system outputs are the angle of attack, sideslip and roll angle which are stabilized by LQR control to the equilibrium point of the model following the launch phase (see Fig. 2.16 and Fig. 2.17).

Fig. 2.17 also shows the convergence to zero of angular rates of the system after launch phase. Control surfaces seen in Fig. 2.18 are always in their physical limitations (plus the result of the measurement noise). The result from Fig. 2.16 to Fig. 2.18 shows that the airlaunch system is stabilized by the LQR controller.

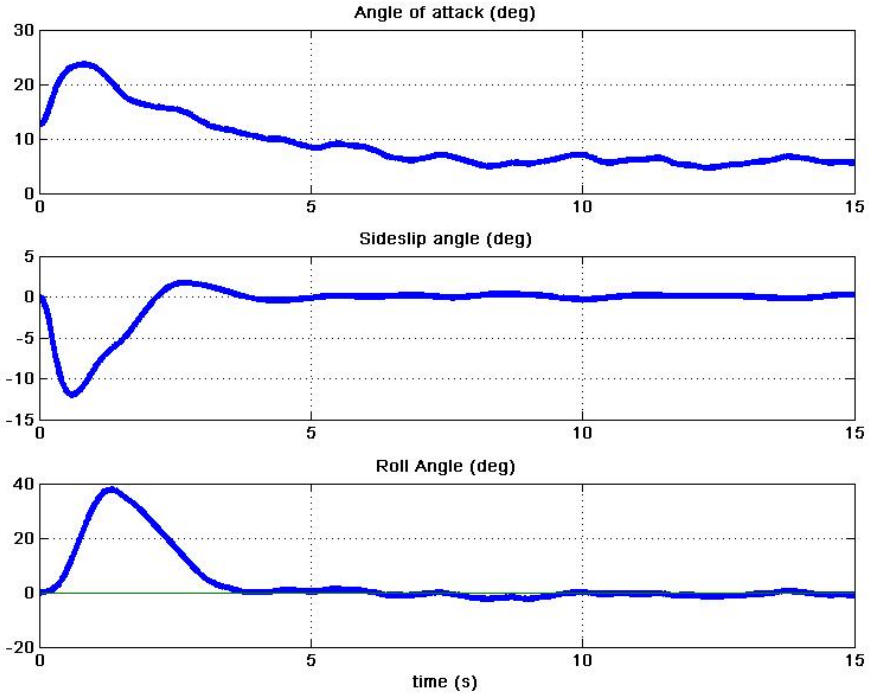

Figure 2.16: Angle of attack α, sideslip β stabilized by LQR controller

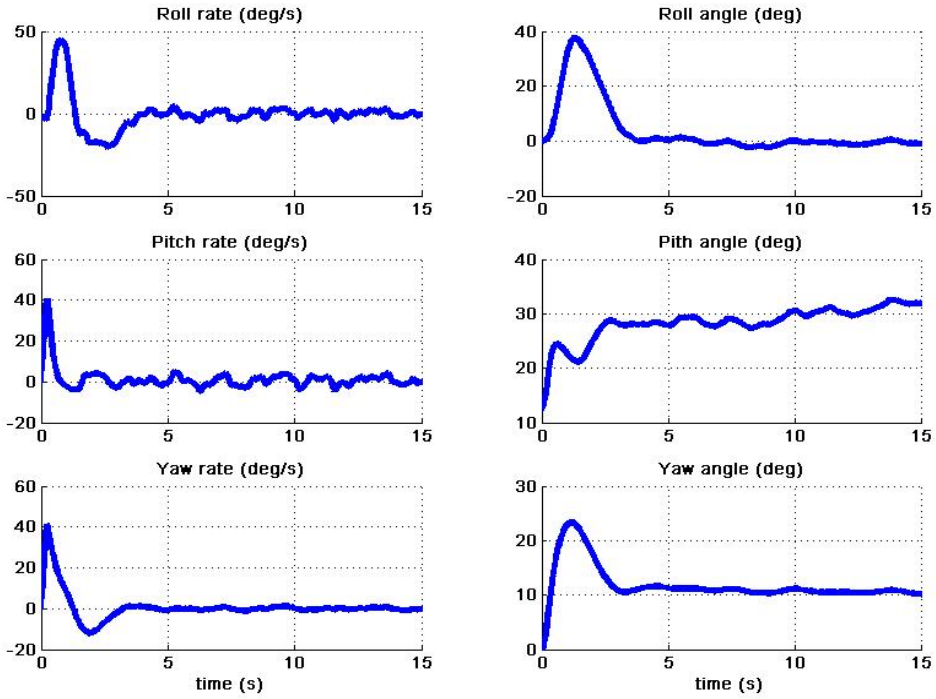

Figure 2.17: Angular rates and Euler's angles stabilized by LQR controller

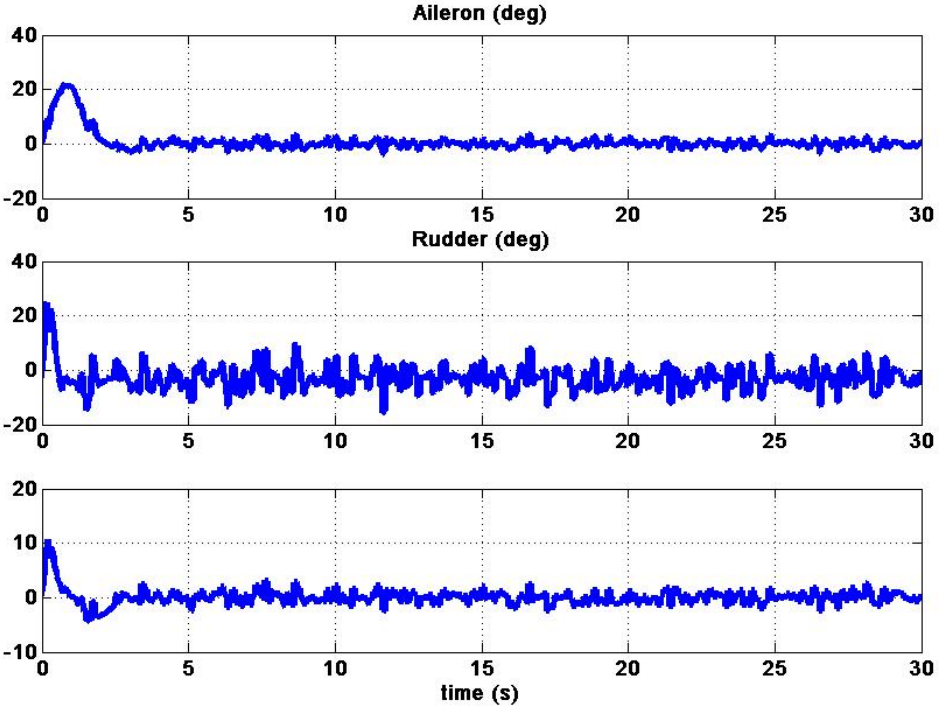

Figure 2.18: Aileron δ_a, Elevator δ_e and Rudder δ_a of LQR controller

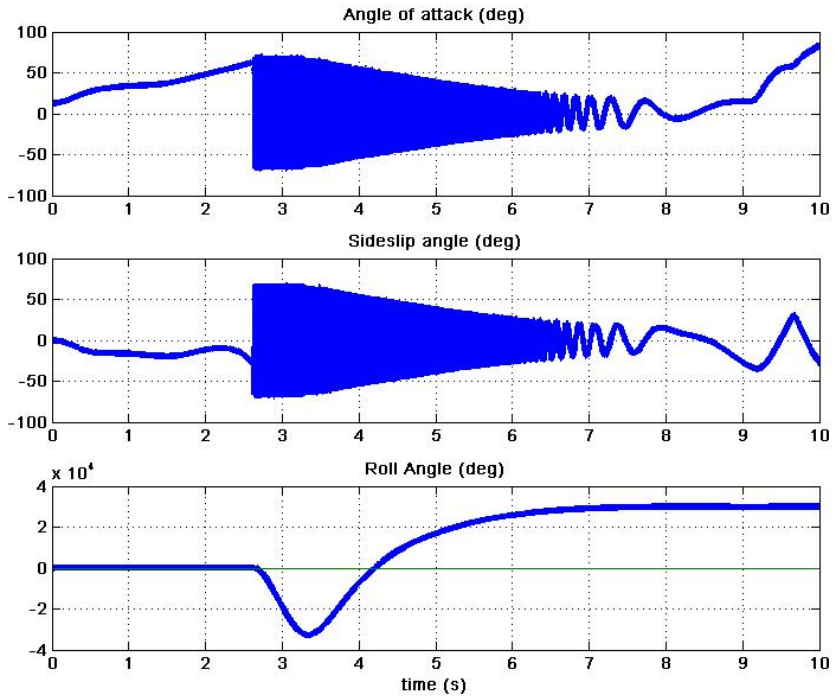

Figure 2.19: Angle of attack α, Sideslip β unstable by LQR controller

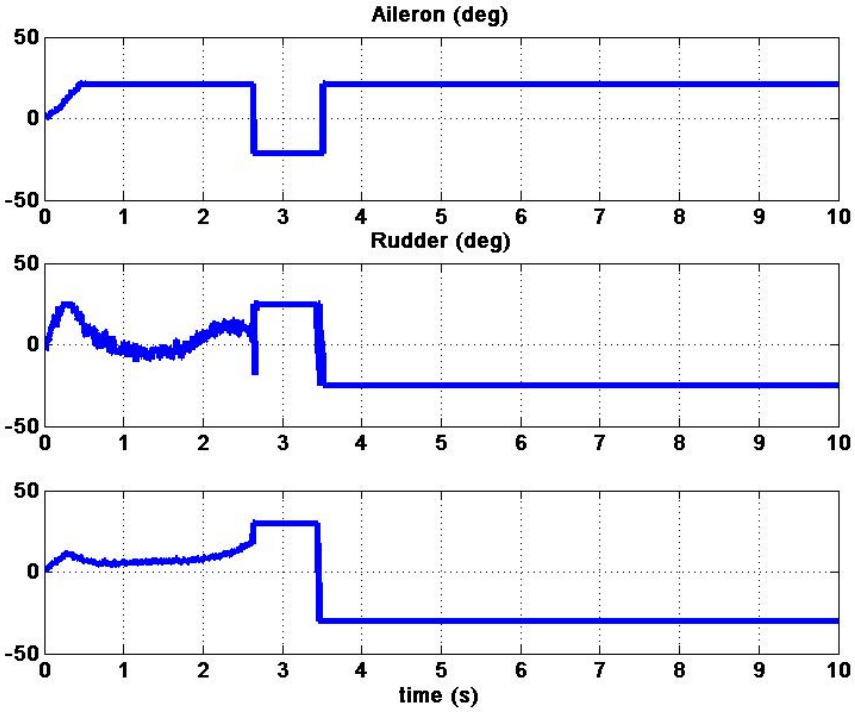

Figure 2.20: Aileron δ_a, Elevator δ_e and Rudder δ_a saturated with LQR controller

When the perturbation T_{int} becomes too long, the airlaunch system can not remain stable even with the LQR controller. Fig. 2.19 shows the system becomes unstable because of long perturbation time on aerodynamic force and moment. The control surfaces in this case are saturated by their physical limitations (see in Fig. 2.20).

We see in all figures from Fig. 2.8 to Fig. 2.11 and from Fig. 2.16 to Fig. 2.19, the oscillation of state variables due to the measurement errors that we put during the simulation.

Conclusion

We have introduced the modeling and simulation of an air launch system at the stage phase between a reusable air launch vehicle and the down stage. This section allows to illustrate the effects of the variations in mass, inertia, and aerodynamic coefficients at the staging phase in the stability of the air launch system. Because our air launch system have a down stage mass close to the launch vehicle's one, the separation phase produces large changes in the angle of attack, sideslip and other states of the system in a first modeling approach and large changes in aerodynamic force and moment for a second modeling approach of air launch phase, as demonstrated in section 2.3, which may bring

the system unstable.

The first approach to model the air launch phase based on initial conditions is simpler, but less complete, mainly because we can not study all initial conditions of system's states in the required flight envelop. The second approach based on perturbation on aerodynamic force and moment of the air launch system represents the continuity of the effect of air launch on the second model and is a better choice for modeling the air launch phase. It has also the advantage of allowing simulation of proposed controllers during the disturbance itself, such as to evaluate the ability of the controller to attenuate the effects of these disturbances.

To stabilize the air launch system after this stage separation phase, an LQR control is designed using optimal robust control theory. This controller is made using an F-16 model representing the aircraft just after dropping the second stage.

In the modeling approach based on an initial condition different from the equilibrium point, the effects of the proposed controller are illustrated in computer simulations with several initial conditions distinct from the equilibrium. In the case of small error on initial conditions, the stability of the system after the drop stage is assured. When the error becomes large, the state outputs are poorly stabilized causing bad transients. This can either illustrate the limitations of the proposed controller or the limitations of the aircraft itself.

In the second modeling approach applying disturbances on aerodynamic force and moment, the stability of the system after the drop stage is assured even in an worst case when the disturbance does not last too long. When the disturbance lasts longer, the state outputs become unstable. Since inputs saturate, this could also happen for other control schemes and would represent physical limitations.

The chapter presents our contribution in modeling and simulation of air launch system during launching phase through two approaches. The chapter finished by a simple and robust LQR control technique as our first control approach to illustrate the purpose of the works in this thesis.

A more study on control techniques to stabilize the air launch system after the launching phase will be presented the next chapters concerning conditional integrator control and its extension which is servo-compensator control. Another control strategy will be also mentioned, that is nonlinear feedback linearization control.

Chapter 3

Modified Conditional Integrator and Modified Conditional Servocompensator

Contents

3.1 Introduction

In Chapter 1, we introduced the problem of air launch system using an unmanned carrier aircraft during and after the launching phase. We then introduced in Chapter 2, two

methods for modeling and simulating the air launch system during the separation phase. A simple LQR control was applied to stabilize the air launch system after the stage phase. It is designed taking into account a linearized system, so it is not a good solution in the considered case where the launching phase results in large variation of states and parameters and as a consequence, the nonlinear behaviors will dominate. Moreover, the aerodynamic parameters of air launch are obtained by wind tunnel experiments and are presented in tabular form. They are then smoothed through interpolation and extrapolation. These characteristics can be efficiently dealt with by a robust control that does not rely too much on extremely detailed models and parameter's values. For these reasons, we choose to investigate the possibility of applying a more robust nonlinear control which in my thesis takes the form, in a first step, of a modified Conditional Integrator control. This control will be then further generalized into a conditional servocompensator control.

The control theory known as Conditional Integrator (CI) for single input single output systems was developed in a series of papers from Khalil and co-workers ([14], [15], [17] and [40]). This controller acknowledges a saturation (natural or not) on the control signal, and takes advantage on that to behave, under some conditions, similar to a sliding mode controller (SMC). On other conditions, when not saturated, the controller behaves as a dynamical feedback with an important integral term. This approach has some interesting features. For example well known drawbacks of integrators like performance degradation and in particular the problem of integrator wind-up are avoided by the conditional nature of such control scheme. The integral action is then only present inside a boundary given by the saturations. In this way the control scheme assures the good properties of robustness and performance of sliding mode controllers for large errors, while allowing a smooth behavior given by its continuity what avoids chattering. Furthermore, the robustness of the SMC-like nature of the system while saturated is combined with the "adaptive" characteristic of the integral term when closer to equilibrium. In this way, such technique is very interesting in the cases of poorly known systems or with large parameters's uncertainties.

More recently ([41] and [42]), efforts were consecrated to extend these results for the Multi-Input Multi-Output (MIMO) case, with good results for some classes of MIMO nonlinear systems.

This chapter presents our work of [16] and [43], which can be seen as an extension of those. This present work was motivated by airspace applications, that have poorly known models and parameters. For these applications CI is an interesting control strategy, but unfortunately they are also an example of a class of nonlinear systems not addressed by previous results. On the other hand, in our work we have introduced important changes to the CI and CS controllers, such that the SMC nature is much weaker. The main change

is that the control algorithms we have developed are composed of two parts, one that saturates and another that can grow unbounded. In this way, the comparison with SMC is not valid anymore. In some sense, our proposed controller is more.

In this chapter, Section 3.2 will present the main results that develop a modified CI controller for a class of nonlinear systems, mostly based on the nonlinear theory found in [44], [45] and [46]. The modified conditional servocompensator control is then described in Section 3.3, it is considered as an extension of Conditional Integrator control. These results are applied in Section 3.4 to the lateral mode of a F-16 aircraft model, which is a MIMO nonlinear system. This work should be seen in the optics of the recent papers ([47] and [1]) that have applied the Conditional Integrator controller to airspace, but in a SISO framework for the first and a MIMO framework for a linearized case on the second.

3.2 Modified Conditional Integrator control design

The Conditional Integrator (CI) controller designed for the output regulation of a class of minimum-phase nonlinear systems in case of asymptotically constant references is studied in [17] and [40]. The works of these papers concerns an integrator performing as a sliding mode controller outside a boundary layer, and performing as a conditional one that provides the integration only inside the boundary layer; achieving asymptotic output regulation.

However, these works have addressed the case of single input single output systems or linearized systems. The main objective of this section is to present a modified Conditional Integrator(mCI) controller design for the output regulation of a class of MIMO nonlinear systems, in the case of asymptotically constant references, providing the proof of the exponential stability of the system under some assumptions.

Consider the nonlinear MIMO system in canonical form:

$$\begin{cases} \dot{x}_1 = x_2 & \text{(3.1a)} \\ \dot{x}_2 = f(x_1, x_2) + g(x_1, x_2)u & \text{(3.1b)} \\ y = x_1 & \text{(3.1c)} \end{cases}$$

where $x_1 \in \mathbb{R}^n$ and $x_2 \in \mathbb{R}^n$ are the state vector, $y \in \mathbb{R}^n$ the output vector, $u \in \mathbb{R}^n$ the control input and $f(x_1, x_2) \in \mathbb{R}^n$, $g(x_1, x_2) \in \mathbb{R}^{n \times n}$ are continuous functions.

Let $y_{ref} = x_{1ref}$ be a prescribed reference output function considered as constant such that their derivatives are null.

Define the tracking error vector $e_1(t)$ as the difference between the actual system output $y(t) = x_1(t)$ and the reference output x_{1ref}: $e_1 = x_1 - x_{1ref}$, $e_2 = \dot{e}_1 = x_2 - \dot{x}_{1ref} =$

x_2 such that (3.1) can be expressed as:

$$\begin{cases} \dot{e}_1 = e_2 \\ \dot{e}_2 = f(e_1, e_2, x_{ref}, \dot{x}_{ref}) + g(e_1, e_2, x_{ref}, \dot{x}_{ref})u \end{cases}$$

Since x_{ref} is constant, for a simpler notation we can skip $x_{ref}, \dot{x}_{ref}$ inside the functions $f(\cdot)$ and $g(\cdot)$, and then the previous system can be rewritten as:

$$\begin{cases} \dot{e}_1 = e_2 & \text{(3.3a)} \\ \dot{e}_2 = f(e_1, e_2) + g(e_1, e_2)u & \text{(3.3b)} \end{cases}$$

Saturation function

The saturation function of a vector v in $\mathbb{R}^n$ is determined as:

$$\text{sat}(v) = \begin{cases} v/\|v\| & \text{if } \|v\| \geq 1 \\ v & \text{if } \|v\| < 1 \end{cases} \tag{3.4}$$

where $\|\cdot\|$ is a 2 - norm.

Integral error measurement and conditional integrator

The integral error measurement surface is a vector in $\mathbb{R}^n$ defined as:

$$s = k_0\sigma + K_1 e_1 + e_2 \tag{3.5}$$

where $\sigma \in \mathbb{R}^n$ is the output of the conditional integrator

$$\dot{\sigma} = -k_0\sigma + \mu\text{sat}(s/\mu) \tag{3.6}$$

in which μ is the boundary layer, k_0 is a positive parameter, $K_1 \in \mathbb{R}^{n\times n}$ is a positive definite matrix chosen such a way that $K_1 + sI_n$ is Hurwitz, and I_n is the $n \times n$ identity matrix.

The derivative of the integral error measurement surface can be then expressed as:

$$\dot{s} = k_0\dot{\sigma} + K_1\dot{e_1} + \dot{e_2} \tag{3.7}$$

From (3.3a), (3.3b) and (3.5), the previous equation may be written again :

$$\begin{aligned} \dot{s} &= k_0(-k_0\sigma + \mu sat(s/\mu)) + K_1 e_2 + \dot{e}_2 \\ &= k_0(-(s - (K_1 e_1 + e_2)) + \mu sat(s/\mu)) + K_1 e_2 + \dot{e}_2 \\ &= -k_0 s + k_0\mu sat(s/\mu) + k_0(K_1 e_1 + e_2) + K_1 e_2 + f(e_1, e_2) + g(e_1, e_2)u \end{aligned} \tag{3.8}$$

Now by letting

$$\Delta(e_1, e_2) = k_0(K_1 e_1 + e_2) + K_1 e_2 + f(e_1, e_2)$$

The derivative of the integral error measurement surface becomes:

$$\dot{s}{=}-k_0 s + k_0 \mu sat(s/\mu) + \Delta(e_1, e_2) + g(e_1, e_2)u \tag{3.9}$$

We will present now in a constructive way the control design in order to stabilize the class of nonlinear MIMO systems defined in (3.2). This control design is done in two parts representing the internal and external regions of the boundary layer. It will then be summarized in the form of a theorem.

In the following we denote $\mathcal{O}_\mu$ the region in the neighborhood of $(0, 0)$ with a radius R_μ.

$$\mathcal{O}_\mu{=}\{e = (e_1, e_2) \in \mathbb{R}^n \times \mathbb{R}^n \ \mid \ \|e\| \leq R_\mu\} \tag{3.10}$$

3.2.1 In the region $\|s\| \geq \mu$, $sat(s/\mu) = s/\|s\|$.

In this part, the controller is designed to bring the integral error measurement surface inside the boundary layer. Before proceeding further, we introduce the following assumptions.

Assumption 3.2.1 *$\Delta(e_1, e_2)$ defined in equation (3.9) is bounded by a class $\mathcal{K}$ function $\gamma(\|e_1\| + \|e_2\|)$ and a positive constant Δ_0 :*

$$\|\Delta(e_1, e_2)\| \leq \gamma(\|e_1\| + \|e_2\|) + \Delta_0 \tag{3.11}$$

and as a consequence,

$$\|\Delta(e_1 = 0, e_2 = 0)\| = \|f(0, 0)\| \leq \Delta_0$$

for $(e_1, e_2) \in \mathbb{R}^n \times \mathbb{R}^n$.

Function $f(e_1, e_2)$ is required to be Lipschitz for $(e_1, e_2) \in \mathcal{O}_\mu$, as a consequence

$$\|f(e_1, e_2) - f(0, 0)\| \leq L_1\|K_1 e_1\| + L_2\|e_2\|$$

$\gamma(\|e_1\| + \|e_2\|)$ is also required to be Lipschitz for $(e_1, e_2) \in \mathcal{O}_\mu$:

$$\gamma(\|e_1\| + \|e_2\|) \leq \gamma_1\|K_1 e_1\| + \gamma_2\|e_2\|$$

∘

Assumption 3.2.2 *Function $g(e_1, e_2)$ is continuous and invertible for all $(e_1, e_2) \in \mathbb{R}^n \times \mathbb{R}^n$.*

∘

Theorem 3.2.1 *Consider the nonlinear system in (3.3) where function $f(e_1, e_2)$ satisfies Assumption 3.2.1, function $g(e_1, e_2)$ satisfies Assumption 3.2.2, and integral error measurement surface is defined as (3.7), then control law*

$$u = -\Pi(e_1, e_2) sat(s/\mu) \tag{3.12}$$

where we define:

$$\Pi(\cdot) = (\pi_0 + \gamma(\cdot) + k_0\mu + \Delta_0)g^{-1}(\cdot) \tag{3.13}$$

and π_0 is a positive constant.

will bring the surface s into the boundary layer μ in finite time.

◇

Remark 2 *It is important to remark that the proposed control law differs from the standard CI. In fact, the control can even grow unbounded since the term (3.13) is not necessarily bounded. Functions $\gamma(\cdot)$ and $g^{-1}(\cdot)$ can grow continuously. For this reason we call this controller a modified Conditional Integrator, composed of two terms (see (3.12-3.13)) one saturated and one not. The later will dominate for small errors, and as a consequence the controller will behave as an integrator. In the case of large errors, it is the first that dominates, and the controller acts as a robust controller.*

Proof: Let's consider the product $s^T\dot{s}$

$$s^T\dot{s} \;=\; -s^T k_0 s + k_0\mu s^T sat(s/\mu) + s^T\Delta(e_1, e_2) + s^T g(e_1, e_2)u$$

This product $s^T\dot{s}$ can be developed with the previous assumptions and the definition of saturation function (3.4):

$$\begin{aligned}
s^T\dot{s} =& -s^T k_0 s + \mu s^T k_0 s/\|s\| + s^T\Delta(\cdot) - s^T g(\cdot)\Pi(\cdot)s/\|s\| \\
\leq& -s^T k_0 s + \mu s^T k_0 s/\|s\| + \|\Delta(\cdot)\|\|s\| - s^T g(\cdot)\Pi(\cdot)s/\|s\| \\
\leq& -s^T k_0 s + \mu s^T k_0 s/\|s\| + (\gamma(\cdot) + \Delta_0)\|s\| - s^T g(\cdot)\Pi(\cdot)s/\|s\| \\
\leq& -s^T k_0 s - s^T(g(\cdot)\Pi(\cdot) - (\mu k_0 + \gamma(\cdot) + \Delta_0)I_n)s/\|s\|
\end{aligned}$$

Replacing the control law in (3.12) and (3.13), the term $s^T\dot{s}$ can be expressed as:

$$\begin{aligned}
s^T\dot{s} \leq& -s^T k_0 s - s^T(g(\cdot)\Pi(\cdot) - (\mu k_0 + \gamma(\cdot) + \Delta_0)I_n)s/\|s\| \\
\leq& -s^T k_0 s - s^T\pi_0 s/\|s\| \\
\leq& -k_0\|s\|^2 - \pi_0\|s\|
\end{aligned}$$

The product $s^T\dot{s}$ is then not positive and we have also

$$\begin{aligned}
\tfrac{d(\|s\|^2)}{dt} &= 2\|s\|\tfrac{d(\|s\|)}{dt} = 2\tfrac{s^T\dot{s}}{dt} \leq 2(-\pi_0\|s\| - k_0\|s\|^2) \\
\therefore\ \tfrac{d(\|s\|)}{dt} &\leq -\pi_0 - k_0\|s\| \\
\therefore\ \|s(t)\| &\leq \|s(0)\| - \pi_0 t - \|s(0)\|(e^{-k_0 t} - 1)
\end{aligned}$$

Then the integral error measurement surface $s(t)$ reaches the boundary layer μ in finite time. Moreover, σ and e_1 reach the region $\mathcal{O}_\mu$ previously defined.

□

3.2.2 In the region $\|s\| \leq \mu$, $sat(s/\mu) = s/\mu$.

Consider again (3.3a), (3.5) and (3.9), which inside the boundary layer may be rewritten as:

$$\begin{cases}
\dot{\sigma} = -k_0\sigma + s & \text{(3.14a)} \\
\dot{e}_1 = -K_1 e_1 + s - k_0\sigma & \text{(3.14b)} \\
\dot{s} = \Delta(\cdot) - g(\cdot)\Pi(\cdot)s/\mu & \text{(3.14c)}
\end{cases}$$

It can be shown that system (3.14) has an equilibrium point:

$$\begin{cases}
\bar{e}_1 = \bar{e}_2 = 0 \\
s = \bar{s}, \sigma = \bar{\sigma} \\
\bar{s} = k_0\bar{\sigma} = \mu\Pi^{-1}(0,0)g^{-1}(0,0)f(0,0) = \frac{1}{\pi_0 + k_0\mu + \Delta_0}f(0,0)
\end{cases} \tag{3.15}$$

The previous system may be rewritten with respect to $\bar{s}$ and $\bar{\sigma}$:

$$\begin{cases}
\dot{\tilde{\sigma}} = -k_0\tilde{\sigma} + \tilde{s} & \text{(3.16a)} \\
\dot{e}_1 = -K_1 e_1 + \tilde{s} - k_0\tilde{\sigma} & \text{(3.16b)} \\
\dot{\tilde{s}} = \Delta(\cdot) - g(\cdot)\Pi(\cdot)\tilde{s}/\mu - g(\cdot)\Pi(\cdot)\bar{s}/\mu & \text{(3.16c)}
\end{cases}$$

where $\tilde{\sigma} = \sigma - \bar{\sigma}$, $\tilde{s} = s - \bar{s}$.

Theorem 3.2.2 *Consider system (3.14) that has an equilibrium point ($\bar{e}_1$, $\bar{e}_2$, $\bar{s}$, $\bar{\sigma}$), function $f(e_1, e_2)$ satisfying Assumption 3.2.1 inside the boundary layer, then the control law design in (3.12-3.13) guarantees*

- *that the equilibrium point of integral error measurement surface s is inside the boundary layer, that means $\|\bar{s}\| \leq \mu$.*
- *the exponential stability of system (3.16) to the equilibrium point.*

◇

Proof:

The integral error measurement surface is in the boundary layer, $\|\bar{s}\| \leq \mu$.

In order that this is true, it is sufficient that:

$$\|\bar{s}\| \leq \mu \Rightarrow \|\Pi^{-1}(0,0)g^{-1}(0,0)f(0,0)\| \leq 1 \tag{3.17}$$

where $\Pi(0,0) = \Pi(e_1 = 0, e_2 = 0)$, $g(0,0) = g(e_1 = 0, e_2 = 0)$ and $f(0,0) = f(e_1 = 0, e_2 = 0)$.

In Assumption 3.2.1, we have:

$$\begin{aligned} \|\Delta(e_1,e_2)\| &\leq \gamma(e_1,e_2) + \Delta_0 \\ \therefore \|f(0,0)\| &= \|\Delta(0,0)\| \leq \Delta_0 \end{aligned} \tag{3.18}$$

Applied into (3.13) leads to:

$$\begin{aligned} &\Pi(0,0) = (\pi_0 + k_0\mu + \Delta_0)g^{-1}(0,0) \\ &\therefore \|\Pi^{-1}(0,0)g^{-1}(0,0)f(0,0)\| = \|((\pi_0 + k_0\mu + \Delta_0)g^{-1}(0,0))^{-1}g^{-1}(0,0)f(0,0)\| \\ &\therefore \|\Pi^{-1}(0,0)g^{-1}(0,0)f(0,0)\| = \tfrac{1}{\pi_0+k_0\mu+\Delta_0}\|f(0,0)\| \leq \tfrac{1}{\Delta_0}\|f(0,0)\| \\ &\therefore \|\Pi^{-1}(0,0)g^{-1}(0,0)f(0,0)\| \leq \tfrac{\Delta_0}{\Delta_0} \leq 1 \end{aligned} \tag{3.19}$$

The integral error measurement surface s is then inside the boundary layer.

▪

Exponential stability of the system (3.16) to the equilibrium point

We would like to demonstrate that every trajectory starting inside the boundary layer, will approach the equilibrium point as time tends to infinity when the control law (3.12) is applied. Toward that end, we take

$$W = \frac{\lambda_1}{2}k_0\tilde{\sigma}^T\tilde{\sigma} + \frac{\lambda_2}{2}e_1^TK_1e_1 + \frac{\lambda_3}{2}\tilde{s}^T\tilde{s}$$

as a Lyapunov candidate, where λ_1, λ_2 and λ_3 are positive constants.

Its derivative can be easily calculated as:

$$\begin{aligned} \dot{W} =& \lambda_1k_0\tilde{\sigma}^T\dot{\tilde{\sigma}} + \lambda_2e_1^TK_1\dot{e_1} + \lambda_3\tilde{s}^T\dot{\tilde{s}} \\ =& \lambda_1k_0\tilde{\sigma}^T(-k_0\tilde{\sigma} + \tilde{s}) + \lambda_2e_1^TK_1(-K_1e_1 + \tilde{s} - k_0\tilde{\sigma}) \\ &+\lambda_3\tilde{s}^T(\Delta(\cdot) - g(\cdot)\Pi(\cdot)\tilde{s}/\mu - g(\cdot)\Pi(\cdot)\bar{s}/\mu) \end{aligned} \tag{3.20}$$

Since $(e_1, e_2) \in \mathcal{O}_\mu$ which means that $\|s\| \leq \mu$, $\Delta(\cdot)$ can be expressed as:

$$\begin{aligned}\Delta(\cdot)=&k_0(s-k_0\sigma)+K_1(-K_1e_1+s-k_0\sigma)+f(\cdot)\\ =&k_0\tilde{s}-k_0^2\tilde{\sigma}-K_1^2e_1+K_1\tilde{s}-k_0K_1\tilde{\sigma}+f(\cdot)\end{aligned}$$

Replacing system (3.16) and $\Delta(\cdot)$ into the derivative of the Lyapunov function, we have then (reminding that $\bar{s} = \mu\Pi^{-1}(0,0)g^{-1}(0,0)f(0,0)$ and $\Pi(0,0) = (\pi_0 + k_0\mu + \Delta_0)g^{-1}(0,0)$):

$$\begin{aligned}\dot{W}=&\lambda_1k_0\tilde{\sigma}^T(-k_0\tilde{\sigma}+\tilde{s})+\lambda_2e_1^TK_1(-K_1e_1+\tilde{s}-k_0\tilde{\sigma})\\ &+\lambda_3\tilde{s}^T(k_0\tilde{s}-k_0^2\tilde{\sigma}-K_1^2e_1+K_1\tilde{s}-k_0K_1\tilde{\sigma}-g(\cdot)\Pi(\cdot)\tilde{s}/\mu)\\ &+\lambda_3\tilde{s}^T(f(\cdot)-g(\cdot)\Pi(\cdot)\bar{s}/\mu)\\ =&-\lambda_1k_0^2\tilde{\sigma}^T\tilde{\sigma}+\lambda_1k_0\tilde{\sigma}^T\tilde{s}-\lambda_2e_1^TK_1^2e_1+\lambda_2e_1^TK_1(\tilde{s}-k_0\tilde{\sigma})\\ &+\lambda_3(\tilde{s}^T(k_0I_n+K_1)\tilde{s}+\tilde{s}^T(k_0+K_1)k_0\tilde{\sigma}-\tilde{s}^TK_1^2e_1-\tilde{s}^Tg(\cdot)\Pi(\cdot)\tilde{s}/\mu)\\ &+\lambda_3\tilde{s}^T(f(\cdot)-f(0,0)-\tfrac{\gamma(\cdot)}{\pi_0+k_0\mu+\Delta_0}f(0,0))\end{aligned} \tag{3.21}$$

Using equations (3.3a), (3.16b) and Assumption 3.2.1, we can have:

$$\begin{aligned}&\tilde{s}^T(f(\cdot)-f(0,0)-\tfrac{\gamma(\cdot)}{\pi_0+k_0\mu+\Delta_0}f(0,0))\\ &\leq\|\tilde{s}\|(l_1\|K_1e_1\|+l_2\|e_2\|)+\tfrac{\gamma(\cdot)}{\pi_0+k_0\mu+\Delta_0}\|\tilde{s}\|\|f(0,0)\|\\ &\leq\|\tilde{s}\|(l_1\|K_1e_1\|+l_2\|e_2\|)+\tfrac{\Delta_0}{\pi_0+k_0\mu+\Delta_0}\|\tilde{s}\|(\gamma_1\|K_1e_1\|+\gamma_2\|e_2\|)\\ &\leq\|\tilde{s}\|(l_1\|K_1e_1\|+l_2\|e_2\|)+\|\tilde{s}\|(\gamma_1\|K_1e_1\|+\gamma_2\|e_2\|)\\ &\leq(l_1+\gamma_1)\|\tilde{s}\|\|K_1e_1\|+(l_2+\gamma_2)\|\tilde{s}\|\|e_2\|\\ &\leq\tfrac{(l_1+\gamma_1)}{2}(\tilde{s}^T\tilde{s}+e_1^TK_1^2e_1)+\tfrac{(l_2+\gamma_2)}{2}(\tilde{s}^T\tilde{s}+e_2^Te_2)\\ &\leq\tfrac{(l_1+\gamma_1)}{2}(\tilde{s}^T\tilde{s}+e_1^TK_1^2e_1)+\tfrac{(l_2+\gamma_2)}{2}(\tilde{s}^T\tilde{s}+(\tilde{s}-k_0\tilde{\sigma}-K_1e_1)^T(\tilde{s}-k_0\tilde{\sigma}-K_1e_1))\\ &\leq\tfrac{(l_1+\gamma_1)}{2}(\tilde{s}^T\tilde{s}+e_1^TK_1^2e_1)+\tfrac{(l_2+\gamma_2)}{2}(\tilde{s}^T\tilde{s}+3(\tilde{s}^T\tilde{s}+k_0^2\tilde{\sigma}^T\tilde{\sigma}+e_1K_1^2e_1))\\ &\leq\tfrac{3(l_2+\gamma_2)}{2}k_0^2\tilde{\sigma}^T\tilde{\sigma}+\tfrac{(l_1+\gamma_1)+3(l_2+\gamma_2)}{2}(e_1^TK_1^2e_1)+\tfrac{(l_1+\gamma_1)+4(l_2+\gamma_2)}{2}(\tilde{s}^T\tilde{s})\\ &\leq c_1k_0^2\tilde{\sigma}^T\tilde{\sigma}+c_2\tilde{s}^T\tilde{s}+c_3e_1^TK_1^2e_1\end{aligned} \tag{3.22}$$

where $c_1 = \frac{3(l_2+\gamma_2)}{2}$ and $c_2 = \frac{(l_1+\gamma_1)+3(l_2+\gamma_2)}{2}$ and $c_3 = \frac{(l_1+\gamma_1)+4(l_2+\gamma_2)}{2}$.

The derivative of the Lyapunov function is then:

$$
\begin{aligned}
\dot{W}=&-\lambda_1 k_0^2\tilde{\sigma}^T\tilde{\sigma}+\lambda_1\tilde{\sigma}^T k_0\tilde{s}-\lambda_2 e_1^T K_1^2 e_1+\lambda_2 e_1^T K_1(\tilde{s}-k_0\tilde{\sigma})+\lambda_3(\tilde{s}^T(k_0 I_n+K_1)\tilde{s}\\
&-\tilde{s}^T(k_0+K_1)k_0\tilde{\sigma}-\tilde{s}^T K_1^2 e_1-\tilde{s}^T g(\cdot)\Pi(\cdot)\tilde{s}/\mu+\tilde{s}^T(f(\cdot)-g(\cdot)\Pi(\cdot)\bar{s}/\mu))\\
\leq&-\lambda_1 k_0^2\tilde{\sigma}^T\tilde{\sigma}+\lambda_1/2(\tilde{s}^T\tilde{s}+k_0^2\tilde{\sigma}^T\tilde{\sigma})-\lambda_2 e_1^T K_1^2 e_1+\lambda_2/2(e_1^T K_1^2 e_1\\
&+(\tilde{s}-k_0\tilde{\sigma})^T(\tilde{s}-k_0\tilde{\sigma}))+\lambda_3(\tilde{s}^T(k_0 I_n+K_1)\tilde{s}+1/2(\tilde{s}^T(k_0 I_n+K_1)^2\tilde{s}+\lambda_1 k_0^2\tilde{\sigma}^T\tilde{\sigma})\\
&+1/2(\tilde{s}^T K_1^2\tilde{s}+e_1^T K_1^2 e_1)-\tilde{s}^T g(\cdot)\Pi(\cdot)\tilde{s}/\mu+c_1 k_0^2\tilde{\sigma}^T\tilde{\sigma}+c_2 e_1^T K_1^2 e_1+c_3\tilde{s}^T\tilde{s})\\
\leq&-\lambda_1 k_0^2\tilde{\sigma}^T\tilde{\sigma}+\lambda_1/2(\tilde{s}^T\tilde{s}+k_0^2\tilde{\sigma}^T\tilde{\sigma})-\lambda_2 e_1^T K_1^2 e_1+\lambda_2/2(e_1^T K_1^2 e_1+2(\tilde{s}^T\tilde{s}+k_0^2\tilde{\sigma}^T\tilde{\sigma}))\\
&+\lambda_3(\tilde{s}^T(k_0 I_n+K_1)\tilde{s}+1/2(\tilde{s}^T(k_0 I_n+K_1)^2\tilde{s}+k_0^2\tilde{\sigma}^T\tilde{\sigma})+1/2(\tilde{s}^T K_1^2\tilde{s}+e_1^T K_1^2 e_1)\\
&-\tilde{s}^T g(\cdot)\Pi(\cdot)\tilde{s}/\mu+c_1 k_0^2\tilde{\sigma}^T\tilde{\sigma}+c_2 e_1^T K_1^2 e_1+c_3\tilde{s}^T\tilde{s})\\
\leq&-(\lambda_1 k_0^2-\lambda_1/2k_0^2-\lambda_2 k_0^2-\lambda_3/2k_0^2-\lambda_3 c_1 k_0^2)\tilde{\sigma}^T\tilde{\sigma}\\
&-e_1^T(\lambda_2 K_1^2-\lambda_2/2K_1^2-\lambda_3/2K_1^2-\lambda_3 c_2 K_1^2)e_1\\
&-\tilde{s}^T(\lambda_3(g(\cdot)\Pi(\cdot)/\mu-(k_0 I_n+K_1)-\lambda_1/2I_n-\lambda_2 I_n\\
&-1/2(k_0 I_n+K_1)^2-1/2K_1^2-c_3 I_n))\tilde{s}\\
\leq&-(\lambda_1/2-\lambda_2-\lambda_3/2-\lambda_3 c_1)k_0^2\tilde{\sigma}^T\tilde{\sigma}-(\lambda_2/2-\lambda_3/2-\lambda_3 c_2)e_1^T K_1^2 e_1\\
&-\tilde{s}^T(\lambda_3((\pi_0+k_0\mu+\gamma(\cdot)+\Delta_0)/\mu-(k_0 I_n+K_1)-1/2(k_0 I_n+K_1)^2-1/2K_1^2)\\
&-(\lambda_1/2+\lambda_2+\lambda_3 c_3)I_n)\tilde{s}
\end{aligned}
\tag{3.23}
$$

It can be verified that by taking λ_1, λ_2, λ_3 and $\Pi(\cdot)$ large enough and μ small enough, the following conditions are satisfied. The derivative of the Lyapunov function is then not positive for all $\tilde{\sigma}$, e_1 and $\tilde{s}$.

$$
\begin{cases}
\lambda_1/2-\lambda_2-\lambda_3/2 & >\lambda_3 c_1\\
\lambda_2/2-\lambda_3/2 & >\lambda_3 c_2\\
\lambda_3(\frac{(\pi_0+k_0\mu+\gamma(\cdot)+\Delta_0)}{\mu})I_n & >\lambda_3((k_0 I_n+K_1)-1/2(k_0 I_n+K_1)^2-1/2K_1^2)\\
 & \quad +(\lambda_1/2+\lambda_2+\lambda_3 c_3)I_n
\end{cases}
\tag{3.24}
$$

The previous inequality implies that the design condition of parameter π_0 must satisfy:

$$
\begin{cases}
\frac{\lambda_1}{\lambda_3}-2\frac{\lambda_2}{\lambda_3} & >1+2c_1\\
\frac{\lambda_2}{\lambda_3} & >1+2c_2\\
\frac{(\pi_0+\Delta_0)}{\mu}I_n-K_1-1/2(k_0 I_n+K_1)^2-1/2K_1^2 & >(\frac{\lambda_1}{2\lambda_3}+\frac{\lambda_2}{\lambda_3}+c_3)I_n
\end{cases}
$$

In this way it is easy to check that $W(t)$ satisfies $W(t)>0$ and $\dot{W}<0$ for all $\sigma\neq\bar{\sigma}$, $e_1\neq 0$ and $s\neq\bar{s}$. Then $W(t)$ reaches zero when time tends to infinite. As consequence, the output error $e_1(t)$ tends to zero, σ and s tend to their equilibrium values as time tends to infinite. We may assure the stability of the system in the region of $\|s\|\leq\mu$.

□

We can then state the results developed above in the form of the theorem:

Theorem 3.2.3 *A class of Multi-Input Multi-Output nonlinear systems described by (3.3), and satisfying Assumptions (3.2.1 and 3.2.2) can be stabilized globally to their constant reference by the controller (3.12-3.13) with tunning parameters (π_0, k_0, μ and K_1 defined in the previous section) and function $\gamma(\cdot)$ conveniently set.*

$\diamond$

In modified Conditional Integrator control theory, the fact that π_0 and in particular k_0 are a scalar, restricts the control performance to the nonlinear system where each state has its proper dynamic. In order to improve the control performance, we will study the control theory assuming the matrix of those parameters in the next section. The control is then called Conditional Servocompensator (CS). Because CS control can be seen as a generalization of CI, we will apply this control for an example of MIMO nonlinear system and to our air launch system, while the modified Conditional Integrator is neglected.

3.3 Modified Conditional Servo-Compensator control design

In Section 3.2 we have introduced the modified Conditional Integrator (mCI) control theory for a class of MIMO nonlinear systems with application to the air launch system. In this study the CI term is defined through k_0 and π_0 parameters which are scalar. This definition simplifies the study, however it loses generality for nonlinear system which different dynamics affect different outputs. This section aims to develop mCI theory towards a theory called (modified) Conditional Servo-Compensator (mCS) control for a MIMO nonlinear system (see [42]).

Consider again the nonlinear MIMO system in (3.3):

$$\begin{cases} \dot{e}_1 &= e_2 \\ \dot{e}_2 &= f(e_1, e_2) + g(e_1, e_2)u \end{cases}$$

We define the integral error measurement surface as:

$$s = K_0\sigma + K_1 e_1 + e_2 \tag{3.25}$$

where $\sigma \in \mathbb{R}^n$ is the output of the Conditional Servo-Compensator

$$\dot{\sigma} = -K_0\sigma + \mu sat(s/\mu) \tag{3.26}$$

in which μ is the boundary layer, $K_1 \in \mathbb{R}^{n\times n}$ is chosen such a way that $K_1 + sI_n$ is Hurwitz, I_n is the $n \times n$ identity matrix. Unlike the previous case in (3.6) where k_0 is a positive scalar, K_0 in this case is a positive definite matrix.

Its derivative can be expressed as:

$$\dot{s} \quad = \quad K_0\dot{\sigma} + K_1\dot{e_1} + \dot{e_2} \tag{3.27}$$

Equation (3.27) may be written again from (3.26) and (3.3)

$$\begin{aligned}\dot{s}=&K_0(-K_0\sigma + \mu sat(s/\mu)) + K_1e_2 + \dot{e}_2\\ =&-K_0s + \mu K_0 sat(s/\mu) + K_1e_2 + \dot{e}_2 + K_0(K_1e_1 + e_2)\end{aligned} \tag{3.28}$$

We define an intermediate variable:

$$\Delta(e_1, e_2) = K_0(K_1e_1 + e_2) + K_1e_2 + f(e_1, e_2) \tag{3.29}$$

Equation (3.28) becomes

$$\dot{s}=-K_0s + \mu K_0 sat(s/\mu) + \Delta(e_1, e_2) + g(e_1, e_2)u \tag{3.30}$$

We can then define the controller:

$$u = -\Pi(e_1, e_2)\text{sat}(s/\mu) \tag{3.31}$$

where we define:

$$\Pi(\cdot) = g^{-1}(\cdot)(\Pi_0 + \mu K_0 + (\gamma(\cdot) + \Delta_0)I_n) \tag{3.32}$$

and Π_0 is a positive definite matrix.

We will show that the control law defined in (3.31) and (3.32) can stabilize the class of nonlinear MIMO systems defined in (3.3). This demonstration is also decomposed in two parts representing the internal and external regions of the boundary layer and will be later formally stated in the form of a theorem. It's also important to remark that, like in the previous section, the control law is composed of two terms where the first may grows unbounded, while the second is saturated.

3.3.1 In the region $\|s\| \geq \mu$, $sat(s/\mu) = s/\|s\|$.

This part demonstrate that the proposed controller is able to bring the integral error measurement surface inside the boundary layer under some assumptions (3.2.1 and 3.2.2) in Section 3.2. We remind these assumptions in the following paragraph:

Definition 1 *λ_i is an eigenvalue of the $n \times n$ positive definite matrix A, then $\lambda_i \geq 0$.*

- $\lambda_{min}(A)$ *is the smallest eigenvalue of* A.
- $\lambda_{MAX}(A)$ *is the greatest eigenvalue of* A.
- $\forall\lambda_i, \lambda_{min}(A)$ *and* $\lambda_{MAX}(A)$ *satisfy:*

$$\begin{cases} \lambda_{min}(A) \leq \lambda_i \leq \lambda_{MAX}(A) & \text{(3.33a)} \\ \lambda_{min}(A)x^T x \leq x^T Ax \leq \lambda_{MAX}(A)x^T x & \text{(3.33b)} \end{cases}$$

Assumption 3.2.1: $f(e_1, e_2)$ is bounded by a class $\mathcal{K}$ function and a positive constant. As a consequence, $\Delta(e_1, e_2)$ function of $f(e_1, e_2)$ is bounded by a function of $\gamma(\|e_1\|+\|e_2\|)$ (where $\gamma(\cdot)$ is a class $\mathcal{K}$ function) and a positive constant Δ_0 :

$$\|\Delta(e_1, e_2)\| \leq \gamma(\|e_1\| + \|e_2\|) + \Delta_0$$

and as a consequence,

$$\|\Delta(e_1 = 0, e_2 = 0)\| = \|f(0, 0)\| \leq \Delta_0$$

for $(e_1, e_2) \in \mathbb{R}^n \times \mathbb{R}^n$. Inside the boundary layer, the function $f(e_1, e_2)$ is required to be Lipschitz for $(e_1, e_2) \in \mathcal{O}_\mu$, as a consequence

$$\|f(e_1, e_2) - f(0, 0)\| \leq l_1\|K_1 e_1\| + l_2\|e_2\|$$

$\gamma(\|e_1\| + \|e_2\|)$ is also required to be Lipschitz for $(e_1, e_2) \in \mathcal{O}_\mu$:

$$\gamma(\|e_1\| + \|e_2\|) \leq \gamma_1\|K_1 e_1\| + \gamma_2\|e_2\|$$

in which, l_1, l_2, γ_1 and γ_2 are positive constants.

∘

Assumption 3.2.2: Function $g(e_1, e_2)$ is continuous and invertible for all $(e_1, e_2) \in \mathbb{R}^n \times \mathbb{R}^n$.

∘

Theorem 3.3.1 *Consider the nonlinear system in (3.3) where function* $f(e_1, e_2)$ *satisfies Assumption 3.2.1, function* $g(e_1, e_2)$ *satisfies Assumption 3.2.2, and integral error measurement surface is defined as (3.25), then control law defined in (3.31) and (3.32) will bring surface* s *into the boundary layer* μ *in finite time.*

◇

Proof: Let's consider the product $s^T\dot{s}$

$$s^T\dot{s} \;=\; -s^TK_0s + \mu s^TK_0sat(s/\mu) + s^T\Delta(e_1,e_2) + s^Tg(e_1,e_2)u \tag{3.34}$$

This product $s^T\dot{s}$ can be developed with the previous Assumption 3.2.1 and the definition of saturation function (3.4):

$$\begin{aligned}
s^T\dot{s} =& -s^TK_0s + \mu s^TK_0s/\|s\| + s^T\Delta(\cdot) - s^Tg(\cdot)\Pi(\cdot)s/\|s\| \\
\leq& -s^TK_0s + \mu s^TK_0s/\|s\| + \|\Delta(\cdot)\|\|s\| - s^Tg(\cdot)\Pi(\cdot)s/\|s\| \\
\leq& -s^TK_0s - s^T(g(\cdot)\Pi(\cdot) - \mu K_0 - (\gamma(\cdot) + \Delta_0)I_n)s/\|s\| \\
\leq& -\lambda_{min}(K_0)s^Ts - \lambda_{min}(\Pi_0)s^Ts/\|s\| \\
\leq& \lambda_{min}(K_0)\|s\|^2 - \lambda_{min}(\Pi_0)\|s\|
\end{aligned}$$

The product $s^T\dot{s}$ is then not positive and

$$\begin{cases}
s^T\dot{s} \leq -\lambda_{min}(K_0)\|s\|^2 - \lambda_{min}(\Pi_0)\|s\| \leq -\lambda_{min}(\Pi_0)\|s\| \\
\frac{d\|s\|^2}{dt} = 2\|s\|\frac{d(\|s\|)}{dt} = 2s^T\dot{s} \leq 2(-\lambda_{min}(\Pi_0)\|s\|) \\
\therefore\ \frac{d(\|s\|)}{dt} \leq -\lambda_{min}(\Pi_0) \\
\therefore\ \|s(t)\| \leq \|s(0)\| - \lambda_{min}(\Pi_0)t
\end{cases}$$

Then $s(t)$ reaches the set $\|s(t)\| \leq \mu$ in finite time. σ and e_1 reach the region called $\mathcal{O}_\mu$ previously defined.

3.3.2 In the region $\|s\| \leq \mu$, $sat(s/\mu) = s/\mu$.

Consider again (3.25), (3.3), (3.26) and control law (3.31) and (3.32), which inside the boundary layer may be rewritten as (remind that $\dot{e}_1 = e_2$):

$$\begin{cases}
\dot{\sigma} = -K_0\sigma + s \\
\dot{e}_1 = -K_1e_1 + s - K_0\sigma \\
\dot{s} = \Delta(\cdot) - g(\cdot)\Pi(\cdot)s/\mu
\end{cases} \tag{3.35}$$

It can be shown that this system has an equilibrium point:

$$\begin{cases}
\bar{e}_1 = \bar{e}_2 = 0 \\
s = \bar{s}, \sigma = \bar{\sigma} \\
\bar{s} = K_0\bar{\sigma} = \mu\Pi^{-1}(0,0)g^{-1}(0,0)f(0,0) = (\Pi_0 + \mu K_0 + \Delta_0 I_n)^{-1}f(0,0)
\end{cases} \tag{3.36}$$

We can then conclude the design condition:

$$\|\bar{s}\| \leq \mu \tag{3.37}$$

where $\Pi(0,0) = \Pi(e_1, e_2)|_{e_1=0, e_2=0}$

System (3.35) may be rewritten with respect to $\bar{s}$ and $\bar{\sigma}$:

$$\begin{cases} \dot{\tilde{\sigma}} = -K_0\tilde{\sigma} + \tilde{s} \\ \dot{e}_1 = -K_1 e_1 + \tilde{s} - K_0\tilde{\sigma} \\ \dot{\tilde{s}} = \Delta(\cdot) - \Pi(\cdot)g(\cdot)\tilde{s}/\mu - \Pi(\cdot)g(\cdot)\bar{s}/\mu \end{cases} \tag{3.38}$$

where $\tilde{\sigma} = \sigma - \bar{\sigma}$, $\tilde{s} = s - \bar{s}$.

Theorem 3.3.2 *Consider system (3.35) that has an equilibrium point ($\bar{e}_1$, $\bar{e}_2$, $\bar{s}$, $\bar{\sigma}$), function $f(e_1, e_2)$ satisfying Assumption 3.2.1 inside the boundary layer, then the control law (3.31) and (3.32) guarantees*

- *that the equilibrium point of surface s is inside the boundary layer, that means $\|\bar{s}\| \leq \mu$.*
- *exponential stability of (3.35) to its equilibrium point.*

◇

Proof:

Surface s is in the boundary layer, $\|\bar{s}\| \leq \mu$.

The design condition in 3.37 means:

$$\|\bar{s}\| \leq \mu \Rightarrow \|\Pi^{-1}(0,0)g^{-1}(0,0)f(0,0)\| \leq 1 \tag{3.39}$$

where $\Pi(0,0) = \Pi(e_1 = 0, e_2 = 0)$, $g(0,0) = g(e_1 = 0, e_2 = 0)$ and $f(0,0) = f(e_1 = 0, e_2 = 0)$.

We have (see (3.18)):

$$\|f(0,0)\| \leq \Delta_0 \tag{3.40}$$

As in (3.32)

$$\begin{aligned} &\Pi(0,0) = g^{-1}(0,0)(\Pi_0 + K_0\mu + \Delta_0 I_n) \\ &\therefore \|\Pi^{-1}(0,0)g^{-1}(0,0)f(0,0)\| = \|(\Pi_0 + K_0\mu + \Delta_0 I_n)^{-1}f(0,0)\| \\ &\therefore \|\Pi^{-1}(0,0)g^{-1}(0,0)f(0,0)\| \leq \|(\Delta_0 I_n)^{-1}\|\|f(0,0)\| = \tfrac{1}{\Delta_0}\|f(0,0)\| \\ &\therefore \|\Pi^{-1}(0,0)g^{-1}(0,0)f(0,0)\| \leq 1 \end{aligned} \tag{3.41}$$

Condition $\|\bar{s}\| \leq \mu$ is satisfied, the equilibrium point of (3.14) is then inside its boundary layer.

Exponential stability of (3.35) to its equilibrium point.

We would like to demonstrate that every trajectory starting inside the boundary layer, will approach the equilibrium point as time tends to infinity. Toward that end, we take again

$$W = \frac{\lambda_1}{2}\tilde{\sigma}^T K_0 \tilde{\sigma} + \frac{\lambda_2}{2} e_1^T K_1 e_1 + \frac{\lambda_3}{2}\tilde{s}^T\tilde{s} \tag{3.42}$$

as a Lyapunov candidate, where λ_1, λ_2 and λ_3 are positive constants.

Its derivative can be easily calculated as:

$$\begin{aligned}\dot{W}=&\lambda_1\tilde{\sigma}^T K_0\dot{\tilde{\sigma}} + \lambda_2 e_1^T K_1 \dot{e_1} + \lambda_3\tilde{s}^T\dot{\tilde{s}}\\ =&\lambda_1\tilde{\sigma}^T K_0(-K_0\tilde{\sigma}+\tilde{s}) + \lambda_2 e_1^T K_1(-K_1 e_1 + \tilde{s} - K_0\tilde{\sigma})\\ &+\lambda_3\tilde{s}^T(\Delta(\cdot) - g(\cdot)\Pi(\cdot)\tilde{s}/\mu - g(\cdot)\Pi(\cdot)\bar{s}/\mu)\end{aligned} \tag{3.43}$$

Since $(e_1, e_2) \in \mathcal{O}_\mu$, $\Delta(\cdot)$ can be rewritten as:

$$\begin{aligned}\Delta(\cdot)=&K_0(s-K_0\sigma) + K_1(-K_1 e_1 + s - K_0\sigma) + f(\cdot)\\ =&(K_0+K_1)\tilde{s} - (K_0+K_1)K_0\tilde{\sigma} - K_1^2 e_1 + f(\cdot)\end{aligned} \tag{3.44}$$

then,

$$\begin{aligned}\dot{W}=&-\lambda_1\tilde{\sigma}^T K_0^2\tilde{\sigma} + \lambda_1\tilde{\sigma}^T K_0\tilde{s} - \lambda_2 e_1^T K_1^2 e_1 + \lambda_2 e_1^T K_1(\tilde{s} - K_0\tilde{\sigma})\\ &+\lambda_3\tilde{s}^T((K_0+K_1)\tilde{s} - (K_0+K_1)K_0\tilde{\sigma} - K_1^2 e_1 - g(\cdot)\Pi(\cdot)\tilde{s}/\mu)\\ &+\lambda_3\tilde{s}^T(f(\cdot) - g(\cdot)\Pi(\cdot)\bar{s}/\mu)\end{aligned} \tag{3.45}$$

We denote $f(0) = f(0,0)$, $g(0) = g(0,0)$ and $\Pi(0) = \Pi(0,0)$. In order to express the derivative of the Lyapunov function candidate more clearly, we firstly consider the term:

$$\begin{aligned}&\|f(\cdot) - g(\cdot)\Pi(\cdot)\bar{s}/\mu\| = \|f(\cdot) - g(\cdot)\Pi(\cdot)\Pi^{-1}(0)g^{-1}(0)f(0)\|\\ &= \|f(\cdot) - (\Pi_0 + K_0\mu + (\gamma(\cdot)+\Delta_0)I_n)(\Pi_0 + K_0\mu + \Delta_0 I_n)^{-1}f(0)\|\\ &= \|f(\cdot) - f(0) - \gamma(\cdot)(\Pi_0 + K_0\mu + \Delta_0 I_n)^{-1}f(0)\|\\ &\le \|f(\cdot) - f(0)\| + \|\gamma(\cdot)(\Pi_0 + K_0\mu + \Delta_0 I_n)^{-1}f(0)\|\\ &\le \|f(\cdot) - f(0)\| + \gamma(\cdot) \le (l_1+\gamma_1)\|K_1 e_1\| + (l_2+\gamma_2)\|e_2\|\end{aligned} \tag{3.46}$$

Term $\tilde{s}^T(f(\cdot) - g(\cdot)\Pi(\cdot)\bar{s}/\mu)$ may be written using Assumption 3.2.1 and the relation in (3.3a):

$$\begin{aligned}&\tilde{s}^T(f(\cdot) - g(\cdot)\Pi(\cdot)\bar{s}/\mu) \le \|\tilde{s}\|\|f(\cdot) - g(\cdot)\Pi(\cdot)\bar{s}/\mu\|\\ &\le (l_1+\gamma_1)\|\tilde{s}\|\|K_1 e_1\| + (l_2+\gamma_2)\|\tilde{s}\|\|e_2\|\\ &\le \tfrac{(l_1+\gamma_1)}{2}(\tilde{s}^T\tilde{s} + e_1 K_1^2 e_1) + \tfrac{(l_2+\gamma_2)}{2}(\tilde{s}^T\tilde{s} + e_2^T e_2)\\ &\le \tfrac{(l_1+\gamma_1)}{2}(\tilde{s}^T\tilde{s} + e_1 K_1^2 e_1) + \tfrac{(l_2+\gamma_2)}{2}(\tilde{s}^T\tilde{s} + (\tilde{s} - K_0\tilde{\sigma} - K_1 e_1)^T(\tilde{s} - K_0\tilde{\sigma} - K_1 e_1))\\ &\le \tfrac{(l_1+\gamma_1)}{2}(\tilde{s}^T\tilde{s} + e_1 K_1^2 e_1) + \tfrac{(l_2+\gamma_2)}{2}(\tilde{s}^T\tilde{s} + 3(\tilde{s}^T\tilde{s} + \tilde{\sigma}^T K_0^2\tilde{\sigma} + e_1^T K_1^2 e_1))\\ &\le \tfrac{(l_1+\gamma_1)+4(l_2+\gamma_2)}{2}\tilde{s}^T\tilde{s} + \tfrac{3(l_2+\gamma_2)}{2}\tilde{\sigma}^T K_0^2\tilde{\sigma} + \tfrac{(l_1+\gamma_1)+3(l_2+\gamma_2)}{2}e_1^T K_1^2 e_1\\ &\le c_1\tilde{\sigma}^T\tilde{\sigma} + c_2 e_1^T e_1 + c_3\tilde{s}^T\tilde{s}\end{aligned} \tag{3.47}$$

where we define $c_1 = 3/2(l_2+\gamma_2)$, $c_2 = 1/2(l_1+\gamma_1)+3/2(l_2+\gamma_2)$ and $c_3 = 1/2((l_1+\gamma_1)+4(l_2+\gamma_2))$.

From (3.35) and (3.47) the derivative of W can be developed:

$$\begin{aligned}
\dot{W}=&-\lambda_1\tilde{\sigma}^T K_0^2\tilde{\sigma}+\lambda_1\tilde{\sigma}^T K_0\tilde{s}-\lambda_2 e_1^T K_1^2 e_1+\lambda_2 e_1^T K_1(\tilde{s}-K_0\tilde{\sigma})+\lambda_3(\tilde{s}^T(K_0+K_1)\tilde{s}\\
&-\tilde{s}^T(K_0+K_1)K_0\tilde{\sigma}-\tilde{s}^T K_1^2 e_1-\tilde{s}^T g(\cdot)\Pi(\cdot)\tilde{s}/\mu+\tilde{s}^T(f(\cdot)-g(\cdot)\Pi(\cdot)\bar{s}/\mu))\\
\leq&-\lambda_1\tilde{\sigma}^T K_0^2\tilde{\sigma}+\lambda_1/2(\tilde{s}^T\tilde{s}+\tilde{\sigma}^T K_0^2\tilde{\sigma})-\lambda_2 e_1^T K_1^2 e_1+\lambda_2/2(e_1^T K_1^2 e_1\\
&+(\tilde{s}-K_0\tilde{\sigma})^T(\tilde{s}-K_0\tilde{\sigma}))+\lambda_3(\tilde{s}^T(K_0+K_1)\tilde{s}+1/2(\tilde{s}^T(K_0+K_1)^2\tilde{s}+\lambda_1\tilde{\sigma}^T K_0^2\tilde{\sigma})\\
&+1/2(\tilde{s}^T K_1^2\tilde{s}+e_1^T K_1^2 e_1)-\tilde{s}^T g(\cdot)\Pi(\cdot)\tilde{s}/\mu+c_1\tilde{\sigma}^T K_0^2\tilde{\sigma}+c_2 e_1^T K_1^2 e_1+c_3\tilde{s}^T\tilde{s})\\
\leq&-\lambda_1\tilde{\sigma}^T K_0^2\tilde{\sigma}+\lambda_1/2(\tilde{s}^T\tilde{s}+\tilde{\sigma}^T K_0^2\tilde{\sigma})-\lambda_2 e_1^T K_1^2 e_1+\lambda_2/2(e_1^T K_1^2 e_1+2(\tilde{s}^T\tilde{s}+\tilde{\sigma}^T K_0^2\tilde{\sigma}))\\
&+\lambda_3(\tilde{s}^T(K_0+K_1)\tilde{s}+1/2(\tilde{s}^T(K_0+K_1)^2\tilde{s}+\tilde{\sigma}^T K_0^2\tilde{\sigma})+1/2(\tilde{s}^T K_1^2\tilde{s}+e_1^T K_1^2 e_1)\\
&-\tilde{s}^T g(\cdot)\Pi(\cdot)\tilde{s}/\mu+c_1\tilde{\sigma}^T K_0^2\tilde{\sigma}+c_2 e_1^T K_1^2 e_1+c_3\tilde{s}^T\tilde{s})\\
\leq&-\tilde{\sigma}^T(\lambda_1 K_0^2-\lambda_1/2K_0^2-\lambda_2 K_0^2-\lambda_3/2K_0^2-\lambda_3 c_1 K_0^2)\tilde{\sigma}\\
&-e_1^T(\lambda_2 K_1^2-\lambda_2/2K_1^2-\lambda_3/2K_1^2-\lambda_3 c_2 K_1^2)e_1\\
&-\tilde{s}^T(\lambda_3(g(\cdot)\Pi(\cdot)/\mu-(K_0+K_1)-1/2(K_0+K_1)^2-1/2K_1^2-c_3 I_n)-\lambda_1/2I_n-\lambda_2 I_n)\tilde{s}\\
\leq&-(\lambda_1/2-\lambda_2-\lambda_3/2-\lambda_3 c_1)\tilde{\sigma}^T K_0^2\tilde{\sigma}-(\lambda_2/2-\lambda_3/2-\lambda_3 c_2)e_1^T K_1^2 e_1\\
&-\tilde{s}^T(\lambda_3(g(\cdot)\Pi(\cdot)/\mu-(K_0+K_1)-1/2(K_0+K_1)^2-1/2K_1^2)-(\lambda_1/2+\lambda_2+\lambda_3 c_3)I_n)\tilde{s}
\end{aligned} \tag{3.48}$$

This inequality implies that λ_1, λ_2, λ_3 and $\Pi(\cdot)$ must be taken large enough and μ small enough in order to $\dot{W}$ negative for all $\tilde{s}$, $\tilde{\sigma}$ and e_1:

$$\begin{cases}
\lambda_1/2-\lambda_2-\lambda_3/2-\lambda_3 c_1 & >0\\
\lambda_2/2-\lambda_3/2-\lambda_3 c_2 & >0\\
\lambda_3(g(\cdot)\Pi(\cdot)/\mu-(K_0+K_1)-1/2(K_0+K_1)^2-1/2K_1^2) & >(\lambda_1/2+\lambda_2+\lambda_3 c_3)I_n
\end{cases} \tag{3.49}$$

and if we consider that c_1, c_2 and c_3 are significantly small then the design conditions must satisfy:

$$\begin{cases}
\lambda_1 > 2\lambda_2+\lambda_3 > 3\lambda_3\\
\lambda_2 > \lambda_3\\
g(\cdot)\Pi(\cdot)/\mu-(K_0+K_1)-1/2(K_0+K_1)^2-1/2K_1^2 > (\frac{\lambda_1}{2\lambda_3}+\frac{\lambda_2}{\lambda_3})I_n > \frac{5}{2}I_n
\end{cases}$$

or,

$$\begin{cases}
\lambda_1 > 2\lambda_2+\lambda_3 > 3\lambda_3\\
\lambda_2 > \lambda_3\\
(\Pi_0+\Delta_0 I_n)/\mu-K_1-1/2(K_0+K_1)^2-1/2K_1^2 > \frac{5}{2}I_n
\end{cases}$$

It can be verified that by taking λ_1, λ_2 large enough, $\|\Pi_0\|$ large enough with respect to control dynamics or μ small enough. In this way, $W(t)$ satisfies $W(t) > 0$ and $\dot{W} < -w_0 W$

(where w_0 is a positive constant) for all $\sigma \neq \bar{\sigma}$, $e_1 \neq 0$ and $s \neq \bar{s}$. Then $W(t)$ reaches exponentially zero when time tends to infinite. As consequence, the output error $e_1(t)$ tends to zero and σ and s tend to their equilibrium values as time tends to infinite. We may assure the exponential stability of the system in the region of $\|s\| \leq \mu$.

▪

We can then state the results developed above in the form of the theorem:

Theorem 3.3.3 *A class of Multi-Input Multi-Output nonlinear systems described by (3.3), and satisfying assumptions (3.2.1 and 3.2.2) can be stabilized globally to their constant reference by the controller (3.25-3.26-3.31-3.32) with tunning parameters (Π_0, K_0, μ and K_1 defined in the previous section) and function $\gamma(\cdot)$ conveniently set. Furthermore, the stability is exponential inside an error region defined in (3.10).*

■

Remark 3 *The modified Conditional Integrator and modifier conditional servo-compensator previously designed are applied to a class of systems defined in (3.3). These controllers are interesting in the case where the system has a $f(\cdot)$ uncertain but $g(\cdot)$ known. A study in the case where the system has $f(\cdot)$ and $g(\cdot)$ unknown, can be seen in Appendix A.1.*

In the following section we will apply this result to a nonlinear MIMO aircraft control problem. The linearized version of this problem is already addressed in [1].

3.4 Example: F-16 aircraft's lateral mode control design

In this section, we address the control of a nonlinear MIMO system applying the results obtained in the previous section. The considered system is the nonlinear MIMO model of an F-16 aircraft lateral mode. The work [1] has addressed this case designing a standard Conditional Integrator based on the linearization of the system around an operating point. In the present case, we extend those results and those of [42] addressing the nonlinear MIMO system without linearization.

3.4.1 Lateral control design

The F-16 aircraft lateral mode has two inputs (aileron and rudder) and two outputs (sideslip angle and roll angle). In this way, only lateral state variables are time varying. Others longitudinal state variables (like height, pitch, angle of attack, etc) are considered as constant or null. Moreover it is assumed that the airspeed's response is much slower than other states, and that the control surface deflection has no effects on the aerodynamic force components (lift and drag) but only on moments. Aerodynamic force F_v and moments L, N are calculated by their aerodynamic coefficients (see more in [12] and [11]).

$$F_v = (C_y(\beta) + (C_{y_p}(\alpha)p + + C_{y_r}(\alpha)r)\bar{b}/(2V))\bar{q}S$$

$$L = (C_l(\beta) + C_{l_p}(\alpha,\beta)p\bar{b}/(2V) + C_{l_r}(\alpha,\beta)r\bar{b}/(2V) + C_{l_{\delta_a}}(\alpha)\delta_a + C_{l_{\delta_r}}(\alpha)\delta_r)\bar{q}S\bar{b}$$

$$N = (C_n(\beta) + C_{n_p}(\alpha,\beta)p\bar{b}/(2V) + C_{n_r}(\alpha,\beta)r\bar{b}/(2V) + C_{n_{\delta_a}}(\alpha)\delta_a + C_{n_{\delta_r}}(\alpha)\delta_r)\bar{q}S\bar{b}$$

By replacing F_v, moments L, N and $\alpha = \alpha_0$, $\theta = \theta_0$ in (2.23b, 2.23g, 2.23d and 2.23f), the lateral nonlinear dynamic model used for the control design procedure is consequently reduced as:

$$\begin{cases}
\dot{\beta} = \frac{1}{mV}(-\cos(\alpha_0)\sin(\beta)(T + C_x(\alpha_0)\bar{q}S) + \cos(\beta)C_y(\beta)\bar{q}S - \sin(\alpha_0)\sin(\beta)C_z(\alpha_0,\beta)\bar{q}S) \\
\quad + \sin(\alpha_0)p - \cos(\alpha_0)r + \frac{\rho S}{4m}(\cos(\beta)C_{y_p}(\alpha_0)\bar{b}p + \cos(\beta)C_{y_r}(\alpha_0)\bar{b}r) \\
\quad + \frac{g}{V}(\cos(\alpha_0)\sin(\beta)\sin(\theta_0) + \cos(\beta)\cos(\theta_0)\sin(\phi) - \sin(\alpha_0)\sin(\beta)\cos(\phi)\cos(\theta_0)) \\
\dot{\phi} = p + \cos(\phi)\tan(\theta_0)r \\
\dot{p} = I_3 C_l(\alpha_0,\beta)\bar{q}S\bar{b} + I_4 C_n(\alpha_0,\beta)\bar{q}S\bar{b} + \frac{\rho V S\bar{b}}{4}[(I_3 C_{l_p}(\alpha_0) \\
\quad + I_4 C_{n_p}(\alpha_0))p + (I_3 C_{l_r}(\alpha_0) + I_4 C_{n_r}(\alpha_0))r] \\
\quad + \bar{q}S[(I_3 C_{l_{\delta_a}}(\alpha_0) + I_4 C_{n_{\delta_a}}(\alpha_0))\delta_a + (I_3 C_{l_{\delta_r}}(\alpha_0) + I_4 C_{n_{\delta_r}}(\alpha_0))\delta_r] \\
\dot{r} = I_4 C_l(\alpha_0,\beta)\bar{q}S\bar{b} + I_9 C_n(\alpha_0,\beta)\bar{q}S\bar{b} + \frac{\rho V S\bar{b}}{4}[(I_4 C_{l_p}(\alpha_0) \\
\quad + I_9 C_{n_p}(\alpha_0))p + (I_4 C_{l_r}(\alpha_0) + I_9 C_{n_r}(\alpha_0))r] \\
\quad + \bar{q}S[(I_4 C_{l_{\delta_a}}(\alpha_0) + I_9 C_{n_{\delta_a}}(\alpha_0))\delta_a + (I_4 C_{l_{\delta_r}}(\alpha_0) + I_9 C_{n_{\delta_r}}(\alpha_0))\delta_r]
\end{cases} \tag{3.50}$$

in which S is the wing area, $\bar{q}$ dynamic pressure, $\bar{b}$ is reference wing span, $I_3 = \frac{I_{zz}}{(I_{xx}I_{zz} - I_{xz}^2)}$, $I_4 = \frac{I_{xz}}{(I_{xx}I_{zz} - I_{xz}^2)}$, $I_9 = \frac{I_{xx}}{(I_{xx}I_{zz} - I_{xz}^2)}$. α_0, θ_0 and V are angle of attack, pitch angle and airspeed considered as constant in the studied case, T, the thrust force is also constant. The state variables of the system are β, ϕ, p, r which represent the sideslip angle, roll angle, roll rate, yaw rate, respectively. $C_y(\alpha, \delta_e)$, $C_{y_p}(\alpha_0)$, $C_{y_r}(\alpha_0)$, $C_l(\alpha_0,\beta)$, $C_n(\alpha_0,\beta)$, $C_{l_p}(\alpha_0)$, $C_{n_p}(\alpha_0)$, $C_{l_r}(\alpha_0)$, $C_{n_r}(\alpha_0)$, $C_{l_{\delta_a}}(\alpha_0)$, $C_{n_{\delta_a}}(\alpha_0)$, $C_{l_{\delta_r}}(\alpha_0)$, $C_{n_{\delta_r}}(\alpha_0)$ are lateral aerodynamic coefficients taken from [48].

The previous equation can be rearranged as:

$$\begin{cases} \begin{bmatrix} \dot{\beta} \\ \dot{\phi} \end{bmatrix} = f_{11}^{\beta}(\beta,\phi) + f_{12}^{\beta}(\beta,\phi) \begin{bmatrix} p \\ r \end{bmatrix} \\ \begin{bmatrix} \dot{p} \\ \dot{r} \end{bmatrix} = f_{21}^{\beta}(\beta,\phi) + f_{22}^{\beta}(\beta,\phi) \begin{bmatrix} p \\ r \end{bmatrix} + g_2^{\beta}(\beta,\phi) \begin{bmatrix} \delta_a \\ \delta_r \end{bmatrix} \end{cases} \tag{3.51}$$

where $f_{11}^{\beta}(\cdot)$, $f_{12}^{\beta}(\cdot)$, $f_{13}^{\beta}(\cdot)$, $f_{21}^{\beta}(\cdot)$, $f_{22}^{\beta}(\cdot)$, and $g_2^{\beta}(\cdot)$ represent the terms of (3.50) respectively (see Appendix A.2).

Let us define $x_1^{\beta} = [\beta, \phi]^T$, $x_2^{\beta} = \dot{x}_1^{\beta} = [\dot{\beta}, \dot{\phi}]^T$ and $u^{\beta} = (\delta_a, \delta_r)^T$, then:

$$x_2^{\beta} = f_{11}^{\beta}(\cdot) + f_{12}^{\beta}(\cdot) \begin{bmatrix} p \\ r \end{bmatrix} \Leftrightarrow \begin{bmatrix} p \\ r \end{bmatrix} = (f_{12}^{\beta}(\cdot))^{-1}(\cdot)(x_2^{\beta} - f_{11}^{\beta}(\cdot)) \tag{3.52}$$

$$\begin{aligned} \dot{x}_2^{\beta} =& \frac{\partial f_{11}^{\beta}(\cdot)}{\partial x_1^{\beta}} x_2^{\beta} + \frac{\partial (f_{12}^{\beta}(\cdot) \begin{bmatrix} p \\ r \end{bmatrix})}{\partial x_1^{\beta}} x_2^{\beta} + f_{12}^{\beta}(\cdot) \begin{bmatrix} \dot{p} \\ \dot{r} \end{bmatrix} \\ =& \frac{\partial f_{11}^{\beta}(\cdot)}{\partial x_1^{\beta}} x_2^{\beta} + f^{\beta}(\cdot) \begin{bmatrix} p \\ r \end{bmatrix} + f_{12}^{\beta}(\cdot)(f_{21}^{\beta}(\cdot) + f_{22}^{\beta} \begin{bmatrix} p \\ r \end{bmatrix} + g_2^{\beta}(\cdot)u^{\beta}) \\ =& \frac{\partial f_{11}^{\beta}(\cdot)}{\partial x_1^{\beta}} x_2^{\beta} + (f^{\beta}(\cdot) + f_{12}^{\beta}(\cdot) f_{22}^{\beta}(\cdot))(f_{12}^{\beta}(\cdot))^{-1}(\cdot)(x_2^{\beta} - f_{11}^{\beta}(\cdot)) + f_{12}^{\beta}(\cdot) f_{21}^{\beta}(\cdot) + f_{12}^{\beta}(\cdot) g_2^{\beta}(\cdot) u^{\beta} \end{aligned}$$

where we note that the term $\frac{\partial (f_{12}^{\beta}(\cdot) \begin{bmatrix} p \\ r \end{bmatrix})}{\partial x_1^{\beta}} x_2^{\beta}$ can be transformed into $f^{\beta}(\cdot) \begin{bmatrix} p \\ r \end{bmatrix}$ by a simple calculation, in which $f(\cdot)$ is function of x_1^{β} and x_2^{β}.

It allows us to rewrite equation (3.51) into:

$$\begin{cases} \dot{x}_1^{\beta} &= x_2^{\beta} \\ \dot{x}_2^{\beta} &= F^{\beta'}(x_1^{\beta}, x_2^{\beta}) + G^{\beta'}(x_1^{\beta}, x_2^{\beta}) u^{\beta} \end{cases} \tag{3.53}$$

where

$$\begin{cases} F^{\beta'}(\cdot) = \frac{\partial f_{11}^{\beta}(\cdot)}{\partial x_1} x_2^{\beta} + (f(\cdot) + f_{12}^{\beta}(\cdot) f_{22}^{\beta}(\cdot))(f_{12}^{\beta}(\cdot))^{-1}(\cdot)(x_2^{\beta} - f_{11}^{\beta}(\cdot)) + f_{12}^{\beta}(\cdot) f_{21}^{\beta}(\cdot) \\ G^{\beta'}(\cdot) = f_{12}^{\beta}(\cdot) g_2^{\beta}(\cdot) \\ f^{\beta}(\cdot) \begin{bmatrix} p \\ r \end{bmatrix} = \frac{\partial (f_{12}^{\beta}(\cdot) \begin{bmatrix} p \\ r \end{bmatrix})}{\partial x_1^{\beta}} \end{cases} \tag{3.54}$$

We define an output error vector $e_1^\beta = x_1^\beta - x_{1ref}^\beta$ and $e_2^\beta = \dot{e}_1^\beta$ where $x_{1ref}^\beta = (\beta_{ref}, \phi_{ref})^T$ is the output reference considered as constant. Equation (3.54) can be transformed into (3.55) with two new state variables e_1^β and e_2^β.

$$\begin{cases} \dot{e}_1^\beta = e_2^\beta & \text{(3.55a)} \\ \dot{e}_2^\beta = F^\beta(e_1^\beta, e_2^\beta) + G^\beta(e_1^\beta, e_2^\beta)u^\beta & \text{(3.55b)} \end{cases}$$

Remark 4 *It is worth noting that:*

- f_{11}^β, f_{12}^β, f_{21}^β *and* f_{22}^β *are function of aerodynamic coefficients under analytical forms by interpolation from wind tunnel test data.* $F^\beta(\cdot)$*, formed from these functions, can be then bounded by a class* $\mathcal{K}$ *function and be a Lipschitz function in a flighting envelop.*
- $G^\beta(x_1^\beta, x_2^\beta)$ *is invertible in the flight domain, that means* $\beta \in (-30°, 30°)$ *and* $\phi \in (-180°, 180°)$.

  As a consequence, they fulfill Assumptions 3.2.1 and 3.2.2.

An application of modified conditional servocompensator control law designed in previous section to (3.31) leads to the controller form:

$$u^\beta = -\Pi^\beta(e_1^\beta, e_2^\beta)\text{sat}(s^\beta/\mu^\beta) \tag{3.56}$$

where we define:

$$\Pi^\beta(\cdot) = (G^\beta)^{-1}(\cdot)(\Pi_0^\beta + \mu^\beta K_0^\beta + (\gamma^\beta(\cdot) + \Delta_0^\beta)I_2) \tag{3.57}$$

with

$$\begin{cases} s^\beta &= K_0^\beta \sigma^\beta + K_1^\beta e_1^\beta + e_2^\beta \\ \dot{\sigma} &= -K_0^\beta \sigma^\beta + \mu^\beta \text{sat}(s^\beta/\mu^\beta) \end{cases} \tag{3.58}$$

where Π_0^β is a positive definite matrix, K_0^β is a positive definite matrix, μ^β is the boundary layer and K_1^β is a positive definite matrix chosen such a way that $K_1^\beta + sI_2$ is Hurwitz.

◇

Theorem 3.4.1 *System (3.55) with* $F^\beta(\cdot)$ *satisfying Assumption 3.2.1,* $G^\beta(\cdot)$ *satisfying Assumption 3.2.2, and applying the control law (3.56- 3.58), will globally reach an arbitrary error region in finite time, and there on will be exponentially stabilized towards its equilibrium point.*

□

Proof: As in Section 3.3 of Chapter 3, we will demonstrate the exponential stability of designed controller (3.56) and (3.58) for the lateral mode in (3.55). We will also consider two regions: outside the boundary layer ($\|s^\beta\| \geq \mu^\beta$) where the integral error measurement surface will reaches the boundary layer and inside the boundary layer ($\|s^\beta\| \leq \mu^\beta$) where the system is exponentially stabilized to the its equilibrium point.

3.4.1.1 *In the region* $\|s^\beta\| \geq \mu^\beta$, $sat(s^\beta/\mu^\beta) = s^\beta/\|s^\beta\|$.

We differentiate the surface expressed in (3.58):

$$\begin{aligned} \dot{s}^\beta &= K_0^\beta \dot{\sigma}^\beta + K_1^\beta \dot{e}_1^\beta + \dot{e}_2^\beta \\ &= -K_0^\beta s^\beta + \mu^\beta K_0^\beta \text{sat}(s^\beta/\mu^\beta) + K_0^\beta (K_1^\beta e_1^\beta + e_2^\beta) + K_1^\beta e_2^\beta + F^\beta(\cdot) + G^\beta(\cdot)u^\beta \end{aligned}$$

We define then Δ^β

$$\Delta^\beta(\cdot) = K_0^\beta (K_1^\beta e_1^\beta + e_2^\beta) + K_1^\beta e_2^\beta + F^\beta(\cdot)$$

The previous derivative becomes:

$$\dot{s}^\beta = -K_0^\beta s^\beta + \mu^\beta K_0^\beta \text{sat}(s^\beta/\mu^\beta) + \Delta^\beta(\cdot) + G^\beta(\cdot)u^\beta \tag{3.59}$$

Using remark 4, $\Delta^\beta(\cdot)$ function of $F^\beta(\cdot)$ is then bounded by:

$$\|\Delta^\beta(e_1^\beta, e_2^\beta)\| \leq \gamma^\beta(\|e_1^\beta\| + \|e_2^\beta\|) + \Delta_0^\beta \tag{3.60}$$

and

$$\|\Delta^\beta(e_1^\beta = 0, e_2^\beta = 0)\| = \|F^\beta(0,0)\| \leq \Delta_0^\beta$$

for $(e_1^\beta, e_2^\beta) \in \mathbb{R}^n \times \mathbb{R}^n$.

Consider product $(s^\beta)^T \dot{s}^\beta$ outside the boundary layer.

$$\begin{aligned} (s^\beta)^T \dot{s^\beta} &= -(s^\beta)^T K_0 s^\beta + \mu^\beta (s^\beta)^T K_0^\beta \text{sat}(s^\beta/\mu^\beta) + (s^\beta)^T \Delta^\beta(e_1^\beta, e_2^\beta) + (s^\beta)^T g^\beta(e_1^\beta, e_2^\beta)u^\beta \\ &= -(s^\beta)^T K_0^\beta s^\beta + \mu^\beta (s^\beta)^T K_0^\beta s^\beta/\|s^\beta\| + (s^\beta)^T \Delta^\beta(\cdot) - (s^\beta)^T G^\beta(\cdot)\Pi^\beta(\cdot)s^\beta/\|s^\beta\| \\ &\leq -(s^\beta)^T K_0^\beta s^\beta + \mu^\beta (s^\beta)^T K_0^\beta s^\beta/\|s^\beta\| + \|\Delta^\beta(\cdot)\|\|s^\beta\| - (s^\beta)^T G^\beta(\cdot)\Pi^\beta(\cdot)s^\beta/\|s^\beta\| \\ &\leq -(s^\beta)^T K_0^\beta s^\beta - (s^\beta)^T (G^\beta(\cdot)\Pi^\beta(\cdot) - \mu^\beta K_0^\beta - (\gamma^\beta(\cdot) + \Delta_0^\beta) I_2) s^\beta/\|s^\beta\| \end{aligned}$$

Using the control law in (3.57), the term $(s^\beta)^T \dot{s}^\beta$ can be developed as:

$$
\begin{aligned}
(s^\beta)^T \dot{s^\beta} \leq & -(s^\beta)^T K_0^\beta s^\beta - (s^\beta)^T (g^\beta(\cdot)\Pi^\beta(\cdot) - \mu^\beta K_0^\beta - (\gamma^\beta(\cdot) + \Delta_0^\beta) I_2) s^\beta / \|s^\beta\| \\
\leq & -(s^\beta)^T K_0^\beta s^\beta - (s^\beta)^T \Pi_0^\beta s^\beta / \|s^\beta\| \\
\leq & -\lambda_{min}(K_0^\beta)(s^\beta)^T s^\beta - \lambda_{min}(\Pi_0^\beta)(s^\beta)^T s^\beta / \|s^\beta\| \\
\leq & -\lambda_{min}(K_0^\beta)\|s^\beta\|^2 - \lambda_{min}(\Pi_0^\beta)\|s^\beta\|
\end{aligned}
$$

$(s^\beta)^T \dot{s}^\beta$ is then not positive and we also obtain

$$
\begin{aligned}
& (s^\beta)^T \dot{s^\beta} \leq -\lambda_{min}(K_0^\beta)\|s^\beta\|^2 - \lambda_{min}(\Pi_0^\beta)\|s^\beta\| \leq -\lambda_{min}(\Pi_0^\beta)\|s^\beta\| \\
\therefore \quad & \tfrac{d\|s^\beta\|^2}{dt} = 2\|s^\beta\| \tfrac{d(\|s^\beta\|)}{dt} = 2(s^\beta)^T \dot{s^\beta} \leq 2(-\lambda_{min}(\Pi_0^\beta)\|s^\beta\|) \\
\therefore \quad & \tfrac{d(\|s^\beta\|)}{dt} \leq -\lambda_{min}(\Pi_0^\beta) \\
\therefore \quad & \|s^\beta(t)\| \leq \|s^\beta(0)\| - \lambda_{min}(\Pi_0^\beta) t
\end{aligned}
$$

Then surface $s^\beta(t)$ reaches the boundary layer μ^β in finite time.

.

3.4.1.2 *In the region* $\|s^\beta\| \leq \mu^\beta$, $sat(s^\beta/\mu^\beta) = s^\beta/\mu^\beta$.

In this region the system enters the boundary layer, the controller then behaves continuously. We consider again (3.50), (3.58) and (3.59), but the saturation disappears in this case.

$$
\begin{cases}
\dot{\sigma}^\beta = -K_0^\beta \sigma^\beta + s^\beta & \text{(3.61a)} \\
\dot{e}_1^\beta = -K_1^\beta e_1^\beta + s - K_0^\beta \sigma^\beta & \text{(3.61b)} \\
\dot{s}^\beta = \Delta^\beta(\cdot) - G^\beta(\cdot)\Pi^\beta(\cdot) s^\beta / \mu^\beta & \text{(3.61c)}
\end{cases}
$$

When $\dot{e}_1 = 0$, $\dot{\sigma} = 0$ and $\dot{s} = 0$ this system has an equilibrium point: $e_1^\beta = e_2^\beta = 0$, $s^\beta = \bar{s}^\beta$, $\sigma^\beta = \bar{\sigma}^\beta$ with $\bar{s}^\beta = K_0^\beta \bar{\sigma}^\beta = \mu^\beta (\Pi^\beta)^{-1}(0)(G^\beta)^{-1}(0) F^\beta(0)$, where $F^\beta(0) = F^\beta(0,0)$, $G^\beta(0) = G^\beta(0,0)$ and $\Pi^\beta(0) = \Pi^\beta(0,0)$. $\Pi^\beta(0,0) = \Pi^\beta(e_1^\beta = 0, e_2^\beta = 0)$, $G^\beta(0,0) = G^\beta(e_1^\beta = 0, e_2^\beta = 0)$ and $F^\beta(0,0) = F^\beta(e_1^\beta = 0, e_2^\beta = 0)$.

It may be rewritten with respect to $\bar{s}^\beta$ and $\bar{\sigma}^\beta$:

$$
\begin{cases}
\dot{\tilde{\sigma}}^\beta = -K_0^\beta \tilde{\sigma}^\beta + \tilde{s}^\beta \\
\dot{e}_1^\beta = -K_1^\beta e_1^\beta + \tilde{s}^\beta - K_0^\beta \tilde{\sigma}^\beta \\
\dot{\tilde{s}}^\beta = \Delta^\beta(\cdot) - \Pi^\beta(\cdot) G^\beta(\cdot) \tilde{s}^\beta / \mu^\beta - \Pi^\beta(\cdot) G^\beta(\cdot) \bar{s}^\beta / \mu^\beta
\end{cases}
\tag{3.62}
$$

where $\tilde{\sigma}^\beta = \sigma^\beta - \bar{\sigma}^\beta$, $\tilde{s}^\beta = s^\beta - \bar{s}^\beta$.

Because of remark 4, $F^\beta(x_1^\beta, x_2^\beta)$ is a Lipschitz function inside the boundary region e.g. $\|s^\beta\| \leq \mu^\beta$, such that:

$$\|F^\beta(e_1^\beta, e_2^\beta) - F^\beta(0,0)\| \leq l_1^\beta \|K_1^\beta e_1^\beta\| + l_2^\beta \|e_2^\beta\| \tag{3.63}$$

where l_1^β and $l_2^\beta \in \mathbb{R}^+$.

Since $\gamma(\cdot)$ is assumed as a Lipschitz function:

$$\gamma^\beta(\cdot) \leq \gamma_1^\beta \|K_1^\beta e_1^\beta\| + \gamma_2^\beta \|e_2^\beta\| \tag{3.64}$$

where γ_1^β and $\gamma_2^\beta \in \mathbb{R}^+$.

We propose again a Lyapunov candidate:

$$W^\beta = \frac{\lambda_1^\beta}{2}(\tilde{\sigma}^\beta)^T K_0^\beta \tilde{\sigma}^\beta + \frac{\lambda_2^\beta}{2}(e_1^\beta)^T K_1^\beta e_1^\beta + \frac{(\tilde{s}^\beta)^T \tilde{s}^\beta}{2}$$

where λ_1^β and λ_2^β are positive constants.

Its derivative can be easily developed as:

$$\begin{aligned}\dot{W}^\beta =& \lambda_1^\beta (\tilde{\sigma}^\beta)^T K_0^\beta \dot{\tilde{\sigma}}^\beta + \lambda_2^\beta (e_1^\beta)^T K_1^\beta \dot{e}_1^\beta + (\tilde{s}^\beta)^T \dot{\tilde{s}}^\beta \\ =& \lambda_1^\beta (\tilde{\sigma}^\beta)^T K_0^\beta (-K_0^\beta \tilde{\sigma}^\beta + \tilde{s}^\beta) + \lambda_2^\beta (e_1^\beta)^T K_1^\beta (-K_1^\beta e_1^\beta + \tilde{s}^\beta - K_0^\beta \tilde{\sigma}^\beta) \\ &+ (\tilde{s}^\beta)^T (\Delta^\beta(\cdot) - G^\beta(\cdot)\Pi^\beta(\cdot)\tilde{s}^\beta/\mu^\beta - G^\beta(\cdot)\Pi^\beta(\cdot)\bar{s}^\beta/\mu^\beta)\end{aligned} \tag{3.65}$$

Since $\|s^\beta\| \leq \mu^\beta$, $\Delta^\beta(\cdot)$ can be expressed as:

$$\begin{aligned}\Delta^\beta(\cdot) =& K_0^\beta(s^\beta - K_0^\beta \sigma^\beta) + K_1^\beta(-K_1^\beta e_1^\beta + s^\beta - K_0^\beta \sigma^\beta) + F^\beta(\cdot) \\ =& (K_0^\beta + K_1^\beta)\tilde{s}^\beta - (K_0^\beta + K_1^\beta)K_0^\beta \tilde{\sigma}^\beta - (K_1^\beta)^2 e_1^\beta + F^\beta(\cdot)\end{aligned}$$

In order to develop the derivative of the Lyapunov function candidate more clearly, we firstly consider the term:

$$\begin{aligned}&\|F^\beta(\cdot) - G^\beta(\cdot)\Pi^\beta(\cdot)\bar{s}^\beta/\mu^\beta\| = \|F^\beta(\cdot) - G^\beta(\cdot)\Pi^\beta(\cdot)(\Pi^\beta)^{-1}(0)(G^\beta)^{-1}(0)F^\beta(0)\| \\ &= \|F^\beta(\cdot) - (\Pi_0^\beta + \mu^\beta K_0^\beta + (\gamma^\beta(\cdot) + \Delta_0^\beta)I_2)(\Pi_0^\beta + \mu^\beta K_0^\beta + \Delta_0^\beta I_2)^{-1}F^\beta(0)\| \\ &= \|F^\beta(\cdot) - F^\beta(0) - \gamma^\beta(\cdot)(\Pi_0^\beta + \mu^\beta K_0^\beta + \Delta_0^\beta I_2)^{-1}F^\beta(0)\| \\ &\leq \|F^\beta(\cdot) - F^\beta(0)\| + \|\gamma^\beta(\cdot)(\Pi_0^\beta + \mu^\beta K_0^\beta + \Delta_0^\beta I_2)^{-1}F^\beta(0)\| \\ &\leq \|F^\beta(\cdot) - F^\beta(0)\| + \gamma^\beta(\cdot)\frac{\|F^\beta(0)\|}{\Delta_0^\beta} \\ &\leq \|F^\beta(\cdot) - F^\beta(0)\| + \gamma^\beta(\cdot) \\ &\leq (l_1^\beta + \gamma_1^\beta)\|K_1^\beta e_1^\beta\| + (l_2^\beta + \gamma_2^\beta)\|e_2^\beta\|\end{aligned} \tag{3.66}$$

Term $(\tilde{s}^\beta)^T(F^\beta(\cdot) - G^\beta(\cdot)\Pi^\beta(\cdot)\bar{s}^\beta/\mu^\beta)$ may be written using using (3.63) and (3.64) and the relation in (3.25):

$$
\begin{aligned}
&(\tilde{s}^\beta)^T(F^\beta(\cdot)-G^\beta(\cdot)\Pi^\beta(\cdot)\bar{s}^\beta/\mu^\beta) \le \|\tilde{s}^\beta\|\|F^\beta(\cdot)-G^\beta(\cdot)\Pi^\beta(\cdot)\bar{s}^\beta/\mu^\beta\| \\
&\le (l_1^\beta+\gamma_1^\beta)\|\tilde{s}^\beta\|\|K_1^\beta e_1^\beta\| + (l_2^\beta+\gamma_2^\beta)\|\tilde{s}^\beta\|\|e_2^\beta\| \\
&\le \tfrac{1}{2}(l_1^\beta+\gamma_1^\beta)((\tilde{s}^\beta)^T\tilde{s}^\beta + (e_1^\beta)^T(K_1^\beta)^2e_1^\beta) + \le \tfrac{1}{2}(l_2^\beta+\gamma_2^\beta)((\tilde{s}^\beta)^T\tilde{s}^\beta + (e_2^\beta)^Te_2^\beta) \\
&\le (\tfrac{1}{2}(l_1^\beta+\gamma_1^\beta)+\tfrac{4}{2}(l_2^\beta+\gamma_2^\beta))\tilde{s}^\beta)^T\tilde{s}^\beta + (\tfrac{1}{2}(l_1^\beta+\gamma_1^\beta)+\tfrac{3}{2}(l_2^\beta+\gamma_2^\beta))(e_1^\beta)^T(K_1^\beta)^2e_1^\beta \\
&+\tfrac{3}{2}(l_2^\beta+\gamma_2^\beta)(\tilde{\sigma}^\beta)^T(K_0^\beta)^2(\tilde{\sigma}^\beta) \\
&\le c_1^\beta(\tilde{\sigma}^\beta)^T(K_0^\beta)^2(\tilde{\sigma}^\beta) + c_2^\beta(e_1^\beta)^T(K_1^\beta)^2e_1^\beta + c_3^\beta(\tilde{s}^\beta)^T\tilde{s}^\beta
\end{aligned}
\tag{3.67}
$$

where we define $c_1^\beta = \frac{3}{2}(l_2^\beta+\gamma_2^\beta)$, $c_2^\beta = \frac{1}{2}(l_1^\beta+\gamma_1^\beta)+\frac{3}{2}(l_2^\beta+\gamma_2^\beta)$ and $c_3^\beta = \frac{1}{2}(l_1^\beta+\gamma_1^\beta)+\frac{4}{2}(l_2^\beta+\gamma_2^\beta)$.

The derivative of the Lyapunov function can be developed as:

$$
\begin{aligned}
\dot{W}^\beta =& -\lambda_1^\beta(\tilde{\sigma}^\beta)^T(K_0^\beta)^2\tilde{\sigma}^\beta + \lambda_1^\beta(\tilde{\sigma}^\beta)^TK_0^\beta\tilde{s}^\beta - \lambda_2^\beta(e_1^\beta)^T(K_1^\beta)^2e_1^\beta + \lambda_2^\beta(e_1^\beta)^TK_1^\beta(\tilde{s}^\beta - K_0^\beta\tilde{\sigma}^\beta) \\
&+(\tilde{s}^\beta)^T(K_0^\beta+K_1^\beta)\tilde{s}^\beta - (\tilde{s}^\beta)^T(K_0^\beta+K_1^\beta)K_0^\beta\tilde{\sigma}^\beta - (\tilde{s}^\beta)^T(K_1^\beta)^2e_1^\beta \\
&-(\tilde{s}^\beta)^TG^\beta(\cdot)\Pi^\beta(\cdot)\tilde{s}^\beta/\mu^\beta + (\tilde{s}^\beta)^T(F^\beta(\cdot)-G^\beta(\cdot)\Pi^\beta(\cdot)\bar{s}^\beta/\mu^\beta) \\
\le& -\lambda_1^\beta(\tilde{\sigma}^\beta)^T(K_0^\beta)^2\tilde{\sigma}^\beta + 1/2\lambda_1^\beta((\tilde{\sigma}^\beta)^T(K_0^\beta)^2\tilde{\sigma}^\beta + (\tilde{s}^\beta)^T\tilde{s}^\beta) - \lambda_2^\beta(e_1^\beta)^TK_1^\beta e_1^\beta \\
&+1/2\lambda_2^\beta((e_1^\beta)^T(K_1^\beta)^2e_1^\beta + 2((\tilde{s}^\beta)^T\tilde{s}^\beta + (\tilde{\sigma}^\beta)^T(K_0^\beta)^2\tilde{\sigma}^\beta)) + (\tilde{s}^\beta)^T(K_0^\beta+K_1^\beta)\tilde{s}^\beta \\
&+1/2((\tilde{s}^\beta)^T(K_0^\beta+K_1^\beta)^2\tilde{s}^\beta + (\tilde{\sigma}^\beta)^T(K_0^\beta)^2\tilde{\sigma}^\beta) + 1/2((\tilde{s}^\beta)^T(K_1^\beta)^2\tilde{s}^\beta + (e_1^\beta)^T(K_1^\beta)^2e_1^\beta) \\
&-(\tilde{s}^\beta)^TG^\beta(\cdot)\Pi^\beta(\cdot)\tilde{s}^\beta/\mu^\beta + c_1^\beta(\tilde{\sigma}^\beta)^T(K_0^\beta)^2(\tilde{\sigma}^\beta) + c_2^\beta(e_1^\beta)^T(K_1^\beta)^2e_1^\beta + c_3^\beta(\tilde{s}^\beta)^T\tilde{s}^\beta \\
\le& -(\tfrac{1}{2}\lambda_1^\beta - \lambda_2^\beta - \tfrac{1}{2} - c_1^\beta)(\tilde{\sigma}^\beta)^T(K_0^\beta)^2\tilde{\sigma}^\beta - (1/2\lambda_2^\beta - 1/2 - c_2^\beta)(e_1^\beta)^T(K_1^\beta)^2e_1^\beta \\
&-(\tilde{s}^\beta)^T(G^\beta(\cdot)\Pi^\beta(\cdot)/\mu^\beta - 1/2\lambda_1^\beta I_2 - \lambda_2^\beta I_2 - (K_0^\beta+K_1^\beta) - 1/2(K_0^\beta+K_1^\beta)^2 \\
&-1/2(K_1^\beta)^2 - c_3^\beta I_2)\tilde{s}^\beta
\end{aligned}
\tag{3.68}
$$

We obtain the same result on the derivative of the Lyapunov function found in the theoretic part (see Section 3.3), but in this case it is applied for the lateral mode. This inequality implies that the design condition matrices λ_1^β, λ_2^β and Π_0 must satisfy:

$$
\begin{cases}
\frac{1}{2}\lambda_1^\beta - \lambda_2^\beta & > \frac{1}{2} + c_1^\beta \\
\frac{1}{2}\lambda_2^\beta & > 1/2 + c_2^\beta \\
(\Pi_0^\beta + \mu^\beta K_0^\beta + (\gamma^\beta(\cdot)+\Delta_0^\beta)I_2)/\mu^\beta & > (K_0^\beta+K_1^\beta) + 1/2(K_0^\beta+K_1^\beta)^2 + 1/2(K_1^\beta)^2 \\
& \quad +(1/2\lambda_1^\beta + \lambda_2^\beta + c_3^\beta)I_2
\end{cases}
$$

Now we will show that the Lyapunov function will reach zero exponentially. From (3.68), we have

$$
\begin{aligned}
\dot{W}^\beta \leq & -(\tfrac{1}{2}\lambda_1^\beta - \lambda_2^\beta - \tfrac{1}{2} - c_1^\beta)(\tilde{\sigma}^\beta)^T (K_0^\beta)^2 \tilde{\sigma}^\beta - (\tfrac{1}{2}\lambda_2^\beta - \tfrac{1}{2} - c_2^\beta)(e_1^\beta)^T (K_1^\beta)^2 e_1^\beta \\
& -(\tilde{s}^\beta)^T (G^\beta(\cdot)\Pi^\beta(\cdot)/\mu^\beta - \tfrac{1}{2}\lambda_1^\beta I_2 - \lambda_2^\beta I_2 - (K_0^\beta + K_1^\beta) - \tfrac{1}{2}(K_0^\beta + K_1^\beta)^2 \\
& -\tfrac{1}{2}(K_1^\beta)^2 - c_3^\beta I_2)\tilde{s}^\beta \\
\leq & -\lambda_{\frac{1}{2}}^\beta (\tilde{\sigma}^\beta)^T W_1^\beta K_0^\beta \tilde{\sigma}^\beta - \lambda_2^\beta/2 (e^\beta)_1^T W_2^\beta K_1^\beta e_1^\beta - \tfrac{1}{2}(\tilde{s}^\beta)^T W_3^\beta \tilde{s}^\beta \\
\leq & -\lambda_1^\beta \lambda_{min}(W_1)/2 (\tilde{\sigma}^\beta)^T K_0^\beta \tilde{\sigma}^\beta - \lambda_2^\beta \lambda_{min}(W_2^\beta)/2 (e^\beta)_1^T K_1^\beta e_1^\beta - \lambda_{min}(W_3^\beta)/2 (\tilde{s}^\beta)^T \tilde{s}^\beta \\
\leq & w_0 (-\tfrac{\lambda_1^\beta \lambda_{min}(W_1^\beta)}{2w_0}(\tilde{\sigma}^\beta)^T K_0^\beta \tilde{\sigma}^\beta - \tfrac{\lambda_2^\beta \lambda_{min}(W_2^\beta)}{2w_0}(e^\beta)_1^T K_1^\beta e_1^\beta - \tfrac{\lambda_{min}(W_3^\beta)}{2w_0}(\tilde{s}^\beta)^T \tilde{s}^\beta) \\
\leq & w_0 (-\tfrac{\lambda_1^\beta}{2}(\tilde{\sigma}^\beta)^T K_0^\beta \tilde{\sigma}^\beta - \tfrac{\lambda_2^\beta}{2}(e_1^\beta)^T K_1^\beta e_1^\beta - \tfrac{1}{2}(\tilde{s}^\beta)^T \tilde{s}^\beta) \\
\leq & -w_0 W
\end{aligned}
$$

where

$$
\begin{cases}
W_1 = (1 - \frac{2\lambda_2^\beta + 1 + 2c_1^\beta}{\lambda_1^\beta}) K_0^\beta \\
W_2 = (1 - \frac{1 + 2c_2^\beta}{\lambda_2^\beta}) K_1^\beta \\
W_3 = 2((\Pi_0 + \mu K_0^\beta + \Delta_0 I_2)/\mu^\beta - \frac{1}{2}\lambda_1^\beta I_2 - \lambda_2^\beta I_2 - (K_0^\beta + K_1^\beta) - \frac{1}{2}(K_0^\beta + K_1^\beta)^2 \\
\qquad -\frac{1}{2}(K_1^\beta)^2 - c_3^\beta I_2) \\
w_0 = min(\lambda_{min}(W_1), \lambda_{min}(W_2), \lambda_{min}(W_3))
\end{cases}
$$

First we take $\lambda_1^\beta, \lambda_2^\beta$ large enough, $\Pi^\beta(\cdot)$ large enough with respect to control dynamics or μ^β small enough. In this way, $W^\beta(t)$ satisfies $W^\beta(t) > 0$ and $\dot{W}^\beta < -w_0 W^\beta$ (where w_0 is a positive constant) for all $\sigma^\beta \neq \bar{\sigma}^\beta$, $e_1^\beta \neq 0$ and $s \neq \bar{s}^\beta$. Then $W^\beta(t)$ reaches exponentially zero when time tends to infinite. As a consequence, the system is then stabilized exponentially to the equilibrium point in the region of $\|s^\beta\| \leq \mu^\beta$.

.

3.4.2 Simulation Results

In the following simulations, we will apply the MIMO modified conditional servocompensator controller for controlling the sideslip and roll angle of the lateral mode of the F-16 aircraft model at the same operating point that we have studied in Chapter 3. That means $(V, h) = (154m/s, 1500m)$ corresponding to the trimmed angle of attack $\alpha_0 = 2.7°$, pitch angle $\theta_0 = 2.7°$, sideslip $\beta_0 = 0°$, $\phi_0 = 0°$ and to trimmed control surface values: aileron $\delta_a = 0°$ and rudder $\delta_r = 0°$. We remind that the control inputs are always limited by $|\delta_a| < 21.5°$ and $|\delta_r| < 30°$, which represent the physical limitations of these actuators.

The control law in (3.56) and (3.58) whose $\Pi(\cdot)$ can be written in a more simple form as below:

$$\begin{cases} u^{\beta} = -\Pi(\cdot)\text{sat}(s^{\beta}/\mu^{\beta}) \\ \Pi^{\beta}(\cdot) = (G^{\beta}(\cdot))^{-1}(\Pi_0^{\beta} + \gamma^{\beta}(\cdot)I_n) \end{cases}$$

in which, $\gamma(\cdot) = \gamma_1\|e_1\| + \gamma_2\|e_2\|$, γ_1 and γ_2 are positive constant, $G^{\beta}(\cdot)$ can be seen in Appendix A.2.

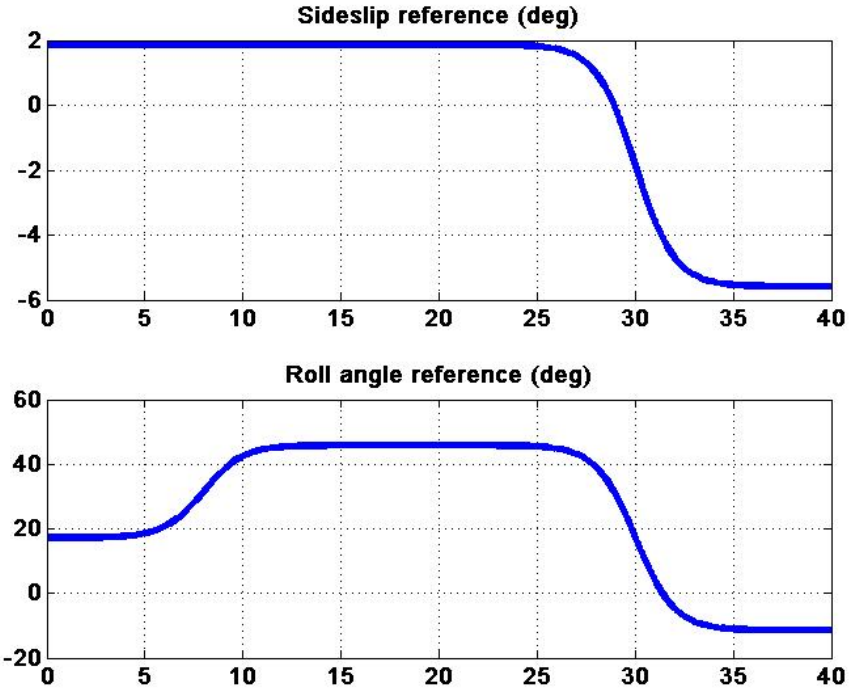

Figure 3.1: Reference input of sideslip and roll angle

Π_0	μ	γ_1 and γ_2	K_0	K_1
$\begin{bmatrix} 12 & 0.0 \\ 0.0 & 13 \end{bmatrix}$	1.0	0.1 and 0.1	$\begin{bmatrix} 1.0 & 0.0 \\ 0.0 & 1.50 \end{bmatrix}$	$\begin{bmatrix} 2.0 & 0.0 \\ 0.0 & 2.1 \end{bmatrix}$

Table 3.1: Parameters of the conditional servo-compensator controller

The reference input Fig. 3.1 is taken as in [1] and [49] with a small change in its amplitude. It consists of a step change in roll angle at $t = 8s$ and of a step change in sideslip and roll angles at $t = 30s$ as:

$$\begin{bmatrix} \beta_{ref}(t) \\ \phi_{ref}(t) \end{bmatrix} = \begin{bmatrix} 0.13(-0.25 + \frac{1}{1+e^{t-30}} - 0.5) \\ 1.0(-\frac{0.5}{1+e^{t-8}} + \frac{1}{1+e^{t-30}} - 0.2) \end{bmatrix} \tag{3.69}$$

Two initial conditions of sideslip and roll angle are studied:

- $\beta_0 = 0°$, $\phi_0 = 5°$, the first corresponds to a small initial condition of sideslip and roll angle from the equilibrium point of the system.

- $\beta_0 = -10°, \phi_0 = 20°$, the second corresponds to a large one.

The simulation results of mCS Control will be compared with the results of Sliding mode control where the integral term in (3.58) is removed, that means $K_0 = 0$. The comparison with this controller allows us to demonstrate the important effects of servocompensator term inside the boundary layer which makes the system stabilize more smoothly. The simulation results is also compared with the results of another control [1] in the literature. These controllers will be described more clearly in the following.

3.4.2.1 Comparison of Conditional Servo-compensator Controller vs Sliding Mode Controller

Sliding mode control

This controller was developed in a close manner compared to the modified Conditional Servocompensator. The controller's two terms become a saturated term (without integral term) times a constant:

$$\begin{cases} u^\beta = -\Pi^\beta(e_1^\beta, e_2^\beta)\text{sat}(s^\beta/\mu^\beta) \\ \Pi^\beta(\cdot) = (G_0^\beta)^{-1}(\Pi_0^\beta + \mu^\beta K_0^\beta + (\Delta_0^\beta)I_n) \end{cases} \tag{3.70}$$

where G_0^β is the transformation matrix at the equilibrium point and the integral error measurement surface is defined as:

$$\left\{ \; s^\beta \;\; = \;\; K_1^\beta e_1^\beta + e_2^\beta \right. \tag{3.71}$$

Assuming a small variation of 3.50 around its equilibrium point, $(G^\beta(\cdot))^{-1} = (G_0^\beta)^{-1}$ and $\gamma^\beta(\cdot) = 0$, and by removing the servocompensator term σ^β from (3.58), the controller has the effects of a sliding mode control outside the boundary layer, which allows the controller to bring the system into the boundary layer. But it can not stabilize smoothly the system to the system's equilibrium point inside the boundary layer. The control quality depends then on the boundary layer value.

Comparison of Simulation Results

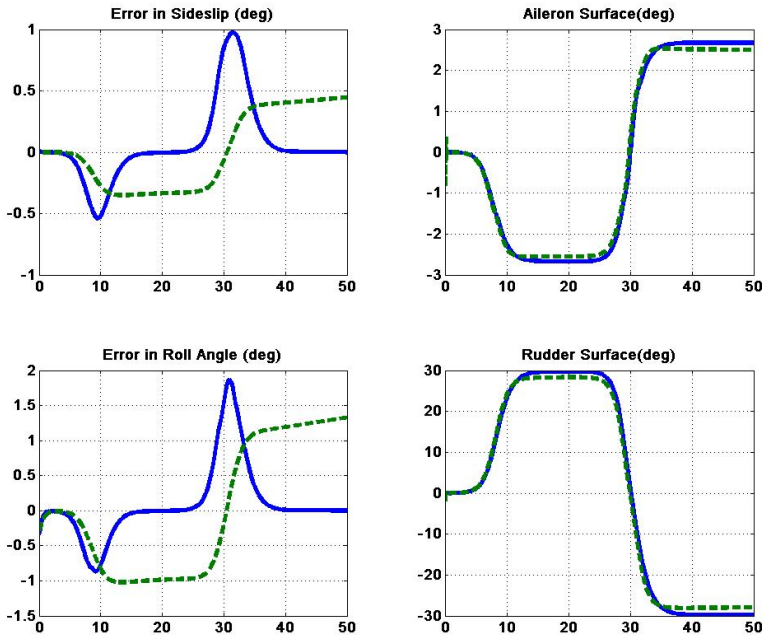

Figure 3.2: Output Errors and Control Surfaces for a small initial condition. CS (solid) - SMC (dashed)

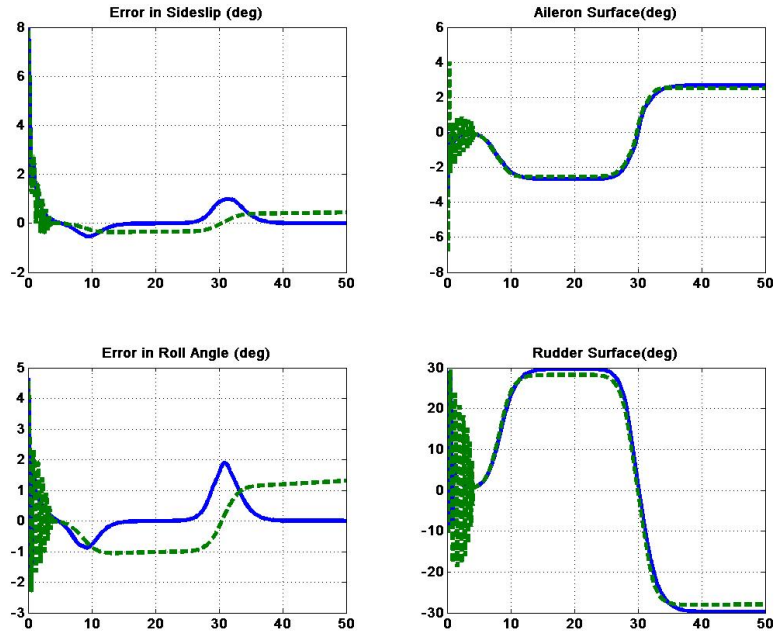

Figure 3.3: Output Errors and Control Surfaces for a high initial condition. CS (solid) - SMC (dashed)

The plots in Fig. 3.2 and Fig. 3.3 are obtained with the controller structure described in Section 3.3 (solid lines) which is compared to a sliding mode controller (dashed lines) where the sign function is replaced by a saturation function to avoid chattering. This controller is used to regulate sideslip angle and roll angle errors. Fig. 3.2 represents the system output errors in respect to the references. The mCS controller provides a convergence to zero of the output error (solid lines) for both sideslip and roll angle in the two cases of initial conditions. In contrast, the sliding mode controller (SMC) produces an output error (dash lines) with non-zero steady state error. This well illustrate the positive contribution of integral term to recover steady state information.

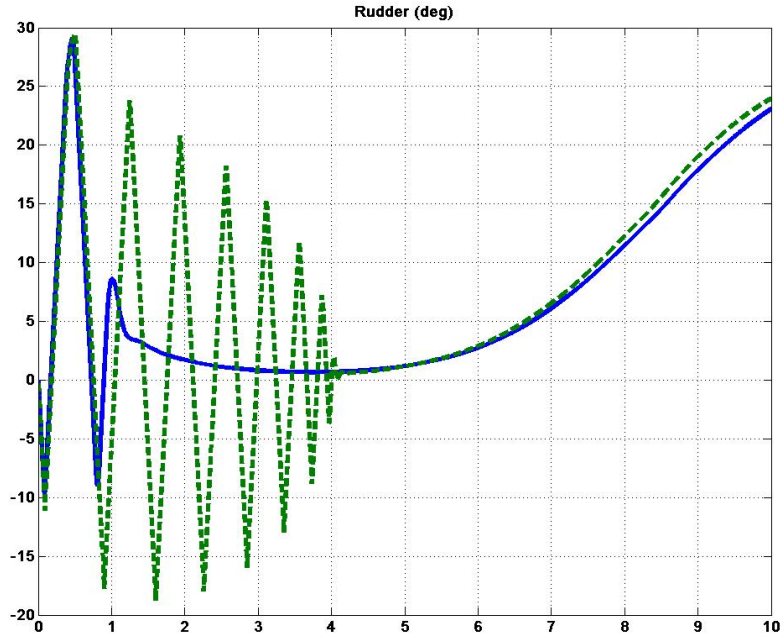

Figure 3.4: Detail on Control Surface (Rudder) for a high initial condition. CS (solid) - SMC (dashed)

The benefit of the proposed controller is even more clear in the case of high initial conditions where the SMC bring the system to a not constant behavior, even if still stable.

Fig. 3.3 shows the control surfaces of the system for both controllers. The solid lines correspond to control surfaces (aileron and rudder) of the controller. The dash lines represent control surfaces of sliding mode controller.

We present a detail of Fig. 3.3 in Fig. 3.4. There it is quite clear the mechanism of the modified conditional servocompensator. One may observe that for large initial conditions, the system is driven to the boundary layer where it is captured by the exponential convergence property of the controller. From there on, the controller behaves in a very

smooth way.

3.4.2.2 Comparison of modified Conditional Servocompensator and the Standard Conditional Integrator

Standard Conditional Integrator Controller

The standard Conditional Integrator controller applied to the F-16 aircraft's lateral mode in [1] used the Conditional Integrator method for a MIMO linearized system. This control is based on the simplified model of lateral mode assuming a small variation of the system around its equilibrium points. The simplified system is then transformed into a normal form, and the standard Conditional Integrator controller is used for each variable of the normal form in such a way that it is used for a single input single output system. In the following we introduce the standard Conditional Integrator for the lateral mode.

The lateral mode is studied in the stability reference frame where the stability roll rate and stability yaw rate are defined:

$$\begin{cases} p_s &= p\cos\alpha_0 + r\sin\alpha_0 \\ r_s &= -p\sin\alpha_0 + r\cos\alpha_0 \end{cases}$$

Substituting this expression into (3.50), we obtain the lateral mode dynamics in the stability axis:

$$\begin{cases}
\dot{\beta} = \frac{1}{mV}(-\cos\alpha_0\sin\beta(T + C_x(\alpha_0)\bar{q}S) + \cos\beta C_y(\beta)\bar{q}S - \sin\alpha_0\sin\beta C_z(\alpha_0,\beta)\bar{q}S) \\
\quad -r_s + \frac{\rho S}{4m}(\cos(\beta)\bar{b}(C_{y_p}(\alpha_0)\cos\alpha_0 + C_{y_r}(\alpha_0)\sin\alpha_0)p_s) \\
\quad +\frac{\rho S}{4m}(\cos\beta\bar{b}(-C_{y_p}(\alpha_0)\sin\alpha_0 + C_{y_r}(\alpha_0)\cos\alpha_0)r_s) \\
\quad +\frac{g}{V}(\cos\alpha_0\sin\beta\sin\theta_0 + \cos\beta\cos\theta_0\sin\phi - \sin\alpha_0\sin\beta\cos\phi\cos\theta_0) \\
\dot{\phi} = \frac{\cos\gamma_0}{\cos\theta_0}p_s + \frac{\sin\gamma_0}{\cos\theta_0}r_s \\
\dot{p_s} = \bar{q}S\bar{b}[(I_3C_l(\alpha_0,\beta) + I_4C_n(\alpha_0,\beta))\cos\alpha_0 + (I_4C_l(\alpha_0,\beta) + I_9C_n(\alpha_0,\beta))\sin\alpha_0] \\
\quad +\frac{\rho VS\bar{b}}{4}[(I_3C_{l_p}(\alpha_0) + I_4C_{n_p}(\alpha_0))\cos^2\alpha_0 + (I_3C_{l_r}(\alpha_0) + I_4C_{n_r}(\alpha_0))\cos\alpha_0\sin\alpha_0 \\
\quad +(I_4C_{l_p}(\alpha_0) + I_9C_{n_p}(\alpha_0))\cos\alpha_0\sin\alpha_0 + (I_4C_{l_r}(\alpha_0) + I_9C_{n_r}(\alpha_0))\sin^2\alpha_0]p_s \\
\quad +\frac{\rho VS\bar{b}}{4}[-(I_3C_{l_p}(\alpha_0) + I_4C_{n_p}(\alpha_0))\cos\alpha_0\sin\alpha_0 - (I_3C_{l_r}(\alpha_0) + I_4C_{n_r}(\alpha_0))\cos^2\alpha_0 \\
\quad -(I_4C_{l_p}(\alpha_0) + I_9C_{n_p}(\alpha_0))\sin^2\alpha_0 + (I_4C_{l_r}(\alpha_0) + I_9C_{n_r}(\alpha_0))\cos\alpha_0\sin\alpha_0]r_s \\
\quad +\bar{q}S[(I_3C_{l_{\delta_a}}(\alpha_0) + I_4C_{n_{\delta_a}}(\alpha_0))\cos\alpha_0 + (I_4C_{l_{\delta_a}}(\alpha_0) + I_9C_{n_{\delta_a}}(\alpha_0))\sin\alpha_0]\delta_a \\
\quad +\bar{q}S[(I_3C_{l_{\delta_r}}(\alpha_0) + I_4C_{n_{\delta_r}}(\alpha_0))\cos\alpha_0 + (I_4C_{l_{\delta_r}}(\alpha_0) + I_9C_{n_{\delta_r}}(\alpha_0))\sin\alpha_0]\delta_r \\
\dot{r_s} = \bar{q}\bar{b}S[-(I_3C_l(\alpha_0,\beta) + I_4C_n(\alpha_0,\beta))\sin\alpha_0 + (I_4C_l(\alpha_0,\beta) + I_9C_n(\alpha_0,\beta))\cos\alpha_0] \\
\quad +\frac{\rho VS\bar{b}}{4}[-(I_3C_{l_p}(\alpha_0) + I_4C_{n_p}(\alpha_0))\cos\alpha_0\sin\alpha_0 - (I_3C_{l_r}(\alpha_0) + I_4C_{n_r}(\alpha_0))\sin^2\alpha_0 \\
\quad +(I_4C_{l_p}(\alpha_0) + I_9C_{n_p}(\alpha_0))\cos^2\alpha_0 + (I_4C_{l_r}(\alpha_0) + I_9C_{n_r}(\alpha_0))\cos\alpha_0\sin\alpha_0]p_s \\
\quad +\frac{\rho VS\bar{b}}{4}[(I_3C_{l_p}(\alpha_0) + I_4C_{n_p}(\alpha_0))\sin^2\alpha_0 - (I_3C_{l_r}(\alpha_0) + I_4C_{n_r}(\alpha_0))\cos\alpha_0\sin\alpha_0 \\
\quad -(I_4C_{l_p}(\alpha_0) + I_9C_{n_p}(\alpha_0))\cos\alpha_0\sin\alpha_0 + (I_4C_{l_r}(\alpha_0) + I_9C_{n_r}(\alpha_0))\cos^2\alpha_0]r_s \\
\quad +\bar{q}S[-(I_3C_{l_{\delta_a}}(\alpha_0) + I_4C_{n_{\delta_a}}(\alpha_0))\sin\alpha_0 + (I_4C_{l_{\delta_a}}(\alpha_0) + I_9C_{n_{\delta_a}}(\alpha_0))\cos\alpha_0]\delta_a \\
\quad +\bar{q}S[-(I_3C_{l_{\delta_r}}(\alpha_0) + I_4C_{n_{\delta_r}}(\alpha_0))\sin\alpha_0 + (I_4C_{l_{\delta_r}}(\alpha_0) + I_9C_{n_{\delta_r}}(\alpha_0))\cos\alpha_0]\delta_r
\end{cases} \tag{3.72}$$

Consider a small variation of the system around its equilibrium point which is $\beta = 0$, $\phi = 0$, $p_s = 0$ and $r_s = 0$ in this case, the previous equation can be rewritten:

$$\begin{cases} \dot{\beta} &= \frac{Y_\beta}{V}\beta + \frac{g\cos\theta_0}{V}\phi + p\cos\alpha_0 + \frac{Y_p}{V}p_s + \frac{Y_r}{V}r_s - r_s \\ \dot{\phi} &= \frac{\cos\gamma_0}{\cos\theta_0}p_s + \frac{\sin\gamma_0}{\cos\theta_0}r_s \\ \dot{p}_s &= L_\beta\beta + L_p p_s + L_r r_s + \delta_l(p_s, r_s) + L_{\delta_a}(\beta, \delta_a) + L_{\delta_r}(\beta, \delta_r) \\ \dot{r}_s &= N_\beta\beta + N_p p_s + N_r r_s + \delta_n(p_s, r_s) + N_{\delta_a}(\beta, \delta_a) + N_{\delta_r}(\beta, \delta_r) \end{cases} \tag{3.73}$$

where we note that $\sin\beta \approx \beta$, $\sin\phi \approx \phi$ around zero, and Y_β,Y_p,Y_r, L_β, L_r, δ_l, L_{δ_a}, L_{δ_r} and N_β, N_r, δ_n, N_{δ_a}, N_{δ_r} are determined in Appendix A.3.

Additionally, the nonlinear expressions $\delta_l(p_s, r_s)+L_{\delta_a}(\beta, \delta_a)+L_{\delta_r}(\beta, \delta_r)$ and $\delta_n(p_s, r_s)+N_{\delta_a}(\beta, \delta_a) + N_{\delta_r}(\beta, \delta_r)$ can be expressed as linear combinations of two unknown functions of β, ϕ, p_s, r_s, δ_a and δ_r.

$$\begin{cases} \delta_l(p_s, r_s) + L_{\delta_a}(\beta, \delta_a) + L_{\delta_r}(\beta, \delta_r) &= L_{\delta_a}(\delta_a + f_1(\cdot)) + L_{\delta_r}(\delta_r + f_2(\cdot)) \\ \delta_n(p_s, r_s) + N_{\delta_a}(\beta, \delta_a) + N_{\delta_r}(\beta, \delta_r) &= N_{\delta_a}(\delta_a + f_1(\cdot)) + N_{\delta_r}(\delta_r + f_2(\cdot)) \end{cases}$$

Substituting this expression into (3.73), we obtain the lateral mode's dynamics in state space form:

$$\begin{bmatrix} \dot{\beta} \\ \dot{\phi} \\ \dot{p}_s \\ \dot{r}_s \end{bmatrix} = A \begin{bmatrix} \beta \\ \phi \\ p_s \\ r_s \end{bmatrix} + B \begin{bmatrix} \delta_a + f_1(\cdot) \\ \delta_r + f_2(\cdot) \end{bmatrix} \tag{3.74}$$

where

$$A = \begin{bmatrix} \frac{Y_\beta}{V} & \frac{g\cos\theta_0}{V} & \frac{Y_p}{V} & \frac{Y_r}{V} - 1 \\ 0 & 0 & \frac{\cos\gamma_0}{\cos\theta_0} & \frac{\sin\gamma_0}{\cos\theta_0} \\ L_\beta & 0 & L_p & L_r \\ N_\beta & 0 & N_p & N_r \end{bmatrix}; B = \begin{bmatrix} 0 & 0 \\ 0 & 0 \\ L_{\delta_a} & L_{\delta_r} \\ N_{\delta_a} & N_{\delta_r} \end{bmatrix}; C = \begin{bmatrix} 1 & 0 & 0 & 0 \\ 0 & 1 & 0 & 0 \end{bmatrix}$$

Or

$$\dot{x} = Ax + B(u + f(\beta, \phi, p_s, r_s, \delta_a, \delta_r)) \tag{3.75}$$

The paper [1] has studied the case $f(\cdot)$ independent on δ_a and δ_r. It is easy to check that (3.75) with $f(\beta, \phi, p_s, r_s, \delta_a = 0, \delta_r = 0)$ has a vector relative degree $\rho = 2, 2$. The change of variables $e_{1\beta} = \beta - \beta_{ref}$, $e_{2\beta} = \dot{e}_{1\beta}$, $e_{1\phi} = \phi - \phi_{ref}$ and $e_{2\phi} = \dot{e}_{1\phi}$, will transform

(3.75) into a normal form where each variable is controllable by a control input. The application of continuous sliding mode control for each new variable is produced as done in the SISO case (see [50] and [40]). We define then:

$$\begin{cases} s_z &= k_{z0}e_{z1} + e_{z2} \\ \dot{\sigma}_z &= -k_{z0}\sigma_z + \mu_z \text{sat}(\frac{s_z}{\mu_z}) \end{cases} \tag{3.76}$$

The control for each new variable of the transformed system is expressed for every $z = \{\beta, \phi\}$:

$$\begin{cases} v_z = -\gamma \text{sat}(\frac{s_z}{\mu_z}) \\ \gamma \quad \text{is a constant} \end{cases} \tag{3.77}$$

The control of (3.75) is then obtained by a transformation matrix:

$$u = \begin{bmatrix} \delta_a \\ \delta_r \end{bmatrix} = T^{-1} \begin{bmatrix} v_\beta \\ v_\phi \end{bmatrix} \tag{3.78}$$

where $T = BAC$.

We can find numerical parameters for this control in [1].

Comparison of modified Conditional Servocompensator Controller and Controller in the literature [1]

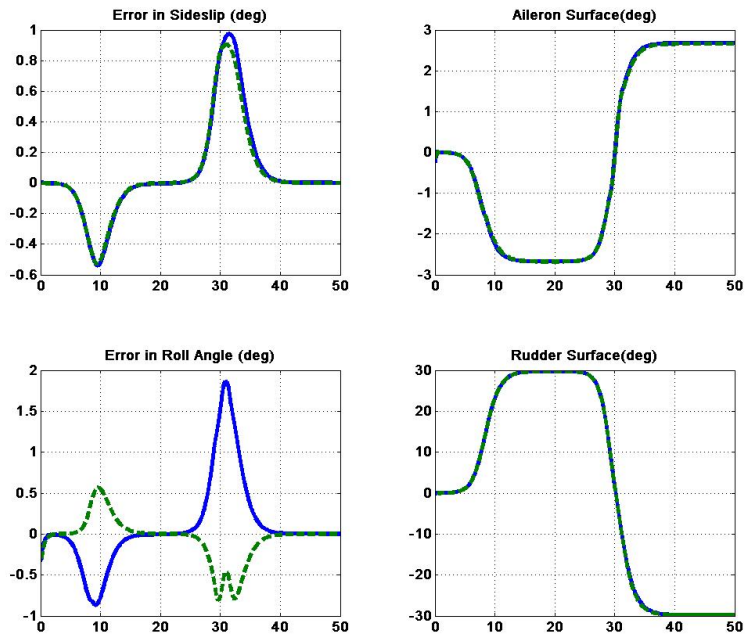

Figure 3.5: Output Errors and Control Surfaces for a small initial condition. CS (solid) - Controller in [1] (dashed)

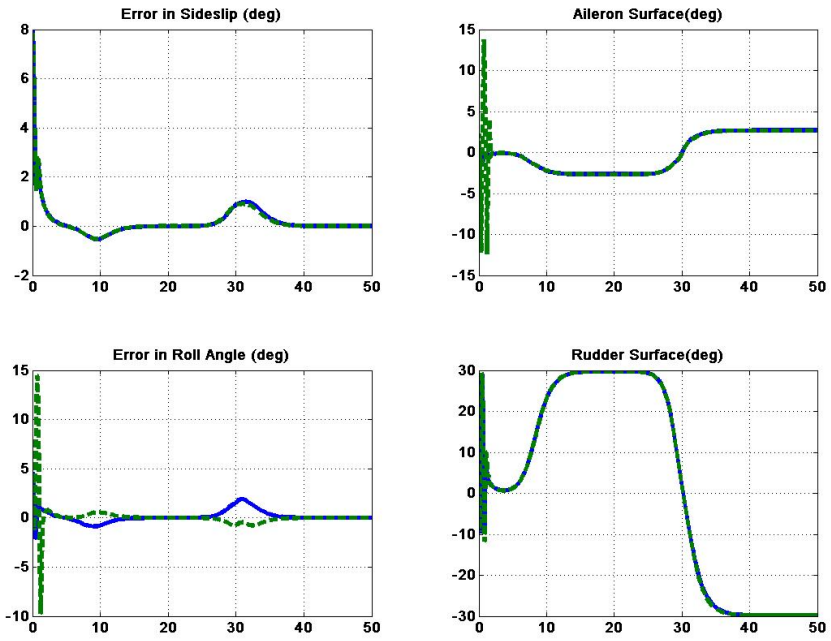

Figure 3.6: Output Errors and Control Surfaces for a high initial condition. CS (solid) - Controller in [1] (dashed)

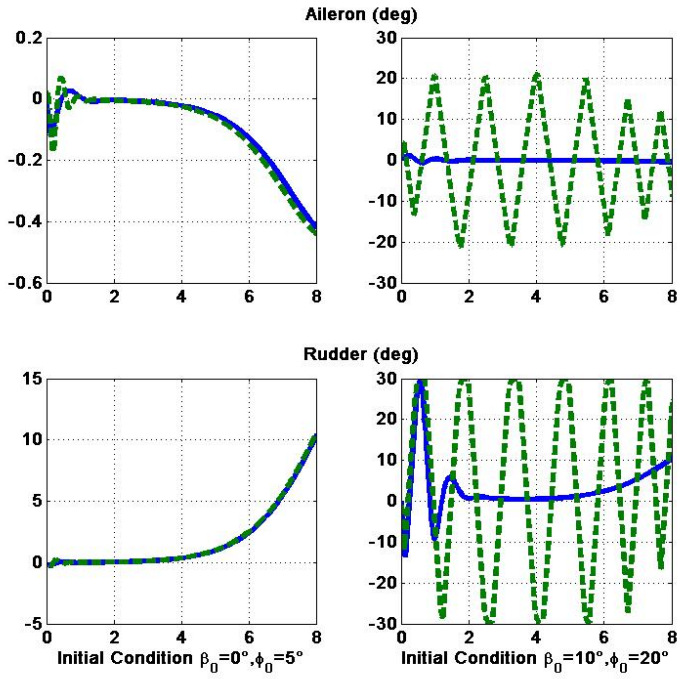

Figure 3.7: Detail on Control surfaces : Aileron (deg) and Rudder (deg)

The plots in Fig. 3.5 to Fig. 3.6 are obtained with the controller structure described

in Section 3.3 and the standard Conditional Integrator for the F-16 aircraft lateral mode, linearized at the equilibrium point ($V = 154m/s, \alpha = 2.7°$) used to regulate sideslip angle and roll angle errors. All parameters are obtained from control design in [1].

The two controllers give the same output error and control surfaces for the case of small initial conditions (Fig. 3.5). That demonstrate the good performance of both controllers. For high initial conditions, the standard Conditional Integrator controller based on linearizations may have very large oscillations (up to 16° in Fig. 3.6). Moreover, Figs 3.7 that presents a closer view of Fig. 3.6 well illustrate the behavior of the controller, with an exponential convergence since entering a residual region, obtaining a better transitory for large initial conditions.

Chapter 4

Application to the Airlaunch System

Contents

4.1 Introduction

The previous chapter has introduced the theory of modified Conditional Integrator(mCI) and modified Conditional Servocompensator(mCS) to a new class of MIMO nonlinear systems. To avoid to much repetition in this thesis, it was only presented an example of mCS control applied to a MIMO nonlinear system. The simulation results in section 3.4 show its performance compared to the other controllers.

In this chapter, we would like to apply these control strategies to the object of this thesis: the air launch during and after the launch phase. A standard method to flight control design is to separate the flight motion in two: longitudinal motion which is in the OX_BZ_B plane which is the symmetrical plane of the object and lateral motion which is the motion in other directions. Another method consists of designing a controller for a complete flying object, which is more difficult and more complex. In general the coupling of the two dynamics is sufficient small what justify this procedure.

In section 4.2 we will design two controllers, using the results developed in the previous chapter. First it will be designed two modified Conditional Integrator controllers, one for each flight mode, which will be evaluated by simulations in the full model. In the following, we'll design a controller using modified Conditional Servocompensator theory for the full airlaunch system. The chapter ends with some conclusion.

Objectives and Assumptions

Following the discussion in Chapter 1, we set up the following objectives for the controller:

- the controller should stabilize the airlaunch system, after the launching phase, to its equilibrium point, i.e. an equilibrium point for the second model after the launching phase.

- the airlaunch system must not collide with the rocket after the separation phase, whose trajectory is represented by a free drop under earth gravity with the same initial speed of the airlaunch system before the separation phase.

In order that the modified Conditional Integrator and modified conditional servocompensator to be applicable to our airlaunch system, we need the following assumptions:

Assumption 4.1.1 *The control surface deflections only produce aerodynamic moments, not aerodynamic forces. Moreover, their dynamics are assumed to be fast enough to be disregarded.*

Assumption 4.1.2 *The airspeed of the airlaunch system varies slowly compared to the controlled variables and is controlled by the thrust force T. Therefore, their time derivatives can be neglected. The thrust is also considered constant.*

The yaw angle which orientates the airlaunch system to right and left directions, has less interest in our objective. Its dynamic is therefore neglected.

4.2 Application of Modified Conditional Integrator to the Airlaunch System

As said before, a very common method for flight control design is to separate the flight into two motions: longitudinal motion which is in the OX_BZ_B plane which is the symmetrical plane of the object and lateral motion which is the motion in other directions. A controller will be designed to regulate the angle of attack in the longitudinal motion. This system is a single input single output nonlinear system. Another controller is designed to control the lateral motion represented by the sideslip angle β and the roll motion represented by the roll angle ϕ.

For the modified Conditional Integrator control to be applicable to our airlaunch system, we therefore need the assumptions 4.1.1 and 4.1.2. Moreover, we also need another assumption:

Assumption 4.2.1 *The longitudinal and lateral modes are assumed to be decoupled. Hence, when the angle of attack is controlled, the sideslip and roll angles are considered constant. Conversely, when sideslip and roll angles are controlled the angle of attack is considered constant.*

Assumption 4.2.1 is not real in practice, but it is quite close to reality (the coupling is usually very small), and it allows us to design two controllers for two motion modes separately. The numerical simulations will show a good performance considering the with coupling between the two motions of the airlaunch system. Under these assumptions, we can now design the controllers for our airlaunch system after the launching phase.

4.2.1 Lateral control design

Nonlinear control problem

We presented in section 3.4 the definition of an output error vector $e_1^\beta = x_1^\beta - x_{1ref}^\beta$ and $e_2^\beta = \dot{e}_1^\beta$ where $x_{1ref}^\beta = (\beta_{ref}, \phi_{ref})^T$ is the output reference considered as constant. The lateral mode's dynamics in (3.50) can be transformed into:

$$\begin{cases} \dot{e}_1^\beta = e_2^\beta & \text{(4.1a)} \\ \dot{e}_2^\beta = F^\beta(e_1^\beta, e_2^\beta) + G^\beta(e_1^\beta, e_2^\beta)u^\beta & \text{(4.1b)} \end{cases}$$

As mentioned in Section 3.4, $F^\beta(\cdot)$ satisfies the Assumption 3.2.1, then bounded and Lipschitz. $G^\beta(x_1^\beta, x_2^\beta)$ is invertible in the considered domain of $x_1^\beta = [\beta, \phi]^T$, $\dot{x}_1^\beta = x_2^\beta$ with $\beta \in (-30°, 30°)$ and $\phi \in (-180°, 180°)$.

Control law

An application of the Modified Conditional Integrator Controller to the lateral motion gives then the controller form (see section 3.3):

$$\begin{cases} u^\beta & = & -\Pi^\beta(e_1^\beta, e_2^\beta) sat(s^\beta/\mu^\beta) \\ \Pi^\beta(\cdot) & = & (\pi_0^\beta + \gamma^\beta(\cdot) + k_0^\beta \mu^\beta + \Delta_0^\beta)(G^\beta(\cdot))^{-1} \end{cases} \tag{4.2}$$

with

$$\begin{cases} s^\beta = k_0^\beta \sigma^\beta + K_1^\beta e_1^\beta + e_2^\beta \\ \dot{\sigma}^\beta = -k_0^\beta \sigma^\beta + \mu^\beta sat(s^\beta/\mu^\beta) \end{cases} \tag{4.3}$$

where π_0^β is a constant, k_0^β is a positive parameter, μ^β is the boundary layer and K_1^β is a positive definite matrix chosen such a way that $K_1^\beta + sI_2$ is Hurwitz.

Remark 5 *We can state that with π_0^β a constant large enough, k_0^β a positive parameter, μ^β the boundary layer small enough, the lateral system will be exponentially stabilized to its equilibrium point inside the boundary layer e.g. $\|s^\beta\| \leq \mu^\beta$. The demonstration is the same as in case of mCS control for the lateral mode of the airlaunch system (see Appendix A.2).*

4.2.2 Longitudinal control design

As in the case of lateral control design, in the longitudinal case it is considered that only longitudinal state variables are time varying. It is a single input single output system where angle of attack is the output and elevator is the input.

Nonlinear control problem

Aerodynamic forces F_u, F_w and moment M can be calculated by its aerodynamic coefficients (see more in [9]).

$$F_u = (C_x(\alpha) + \bar{c} C_{x_q}(\alpha) q/(2V))\bar{q}S$$

$$F_w = (C_z(\alpha, \beta) + \bar{c} C_{z_q}(\alpha) q/(2V))\bar{q}S$$

$$M = (C_m(\alpha) + C_{m_q}(\alpha) q\bar{c}/(2V) + C_{m_{\delta_e}}(\alpha)\delta_e)\bar{q}S\bar{c}$$

By replacing F_u, F_w, moment M and $\beta = 0$, $\phi = 0$, $p = 0$, $r = 0$ in (2.23), the model for longitudinal dynamic can be written as:

$$\begin{cases} \dot{\alpha} = \frac{1}{mV}[-\sin\alpha(T + C_x(\alpha)\bar{q}S) + \cos\alpha C_z(\alpha)\bar{q}S] + q + \frac{\rho S}{4m}(-\sin\alpha C_{x_q}(\alpha)\bar{c} \\ \qquad + \cos\alpha C_{z_q}(\alpha)\bar{c})q + \frac{g}{V}\cos(\theta - \alpha) \\ \dot{q} = I_7 \bar{q}S(C_m(\alpha)\bar{c} + C_{m_q}(\alpha)\bar{c}q + C_{m_{\delta_e}}(\alpha)\bar{c}\delta_e) \\ \dot{\theta} = q \end{cases} \tag{4.4}$$

in which $\bar{c}$ mean aerodynamic chord, $I_7 = 1/I_{yy}$, $C_x(\alpha)$, $C_{x_q}(\alpha)$, $C_z(\alpha)$, $C_{z_q}(\alpha)$, $C_m(\alpha)$, $C_{m_q}(\alpha)$ $C_{m_{\delta_e}}(\alpha)$ are aerodynamic coefficients taken from [48].

Equation (4.4) can be rearranged as:

$$\begin{cases} \dot{\theta} &= q \\ \dot{\alpha} &= f_{11}^{\alpha}(\alpha) + (1 + f_{12}^{\alpha}(\alpha))q + f_{13}^{\alpha}(\alpha, \theta) \\ \dot{q} &= f_{21}^{\alpha}(\alpha) + f_{22}^{\alpha}(\alpha)q + g_2^{\alpha}(\alpha)\delta_e \end{cases} \tag{4.5}$$

where $f_{11}^{\alpha}(\alpha)$, $f_{12}^{\alpha}(\alpha)$, $f_{13}^{\alpha}(\alpha, \theta)$, $f_{21}^{\alpha}(\alpha)$, $f_{22}^{\alpha}(\alpha)$ and $g_2^{\alpha}(\alpha)$ represent the terms of (4.4) respectively (see Appendix A.2).

Let us define $x_1^{\alpha} = \alpha$, $x_2^{\alpha} = \dot{x}_1^{\alpha} = \dot{\alpha}$ and $u^{\alpha} = \delta_e$, which allow us to have the relationship:

$$x_2^{\alpha} = f_{11}^{\alpha}(x_1) + f_{13}^{\alpha}(x_1, \theta) + [1 + f_{12}^{\alpha}(x_1)]\, q \;\Leftrightarrow\; q = \frac{(x_2 - f_{11}^{\alpha}(x_1^{\alpha}) - f_{13}^{\alpha}(x_1, \theta))}{[1 + f_{12}^{\alpha}(x_1)]} \tag{4.6}$$

and

$$\begin{aligned}
\dot{x}_2^{\alpha} =& \frac{\partial f_{11}^{\alpha}(x_1^{\alpha})}{\partial x_1^{\alpha}} x_2^{\alpha} + \frac{\partial f_{13}^{\alpha}(x_1^{\alpha}, \theta)}{\partial x_1^{\alpha}} x_2^{\alpha} + \frac{\partial f_{13}^{\alpha}(x_1^{\alpha}, \theta)}{\partial \theta}\dot{\theta} + \frac{\partial([1 + f_{12}^{\alpha}(x_1)]q)}{\partial x_1^{\alpha}} x_2^{\alpha} + [1 + f_{12}^{\alpha}(x_1)]\,\dot{q} \\
=& \frac{\partial f_{11}^{\alpha}(x_1^{\alpha})}{\partial x_1^{\alpha}} x_2^{\alpha} + \frac{\partial f_{13}^{\alpha}(x_1^{\alpha}, \theta)}{\partial x_1^{\alpha}} x_2^{\alpha} + \frac{\partial f_{13}^{\alpha}(x_1^{\alpha}, \theta)}{\partial \theta}\dot{\theta} + \frac{\partial f_{12}^{\alpha}(x_1^{\alpha})}{\partial x_1^{\alpha}} q + [1 + f_{12}^{\alpha}(x_1)]\,(f_{21}^{\alpha}(x_1^{\alpha}) \\
&+ f_{22}^{\alpha} q + g_2^{\alpha}(x_1^{\alpha})\delta_e) \\
=& \frac{\partial f_{11}^{\alpha}(x_1^{\alpha})}{\partial x_1^{\alpha}} x_2^{\alpha} + \frac{\partial f_{13}^{\alpha}(x_1^{\alpha}, \theta)}{\partial x_1^{\alpha}} x_2^{\alpha} + \frac{\partial f_{13}^{\alpha}(x_1^{\alpha}, \theta)}{\partial \theta}\dot{\theta} + [1 + f_{12}^{\alpha}(x_1)]\, f_{21}^{\alpha}(x_1^{\alpha}) \\
&+ \left[\frac{\partial f_{12}^{\alpha}(x_1^{\alpha})}{\partial x_1^{\alpha}} + [1 + f_{12}^{\alpha}(x_1)]\, f_{22}^{\alpha}(x_1^{\alpha})\right] \frac{(x_2^{\alpha} - f_{11}^{\alpha}(x_1^{\alpha}) - f_{13}^{\alpha}(x_1^{\alpha}, \theta))}{[1 + f_{12}^{\alpha}(x_1)]} + [1 + f_{12}^{\alpha}(x_1)]\, g_2^{\alpha}(x_1^{\alpha})\delta_e \\
=& \frac{\partial f_{11}^{\alpha}(x_1^{\alpha})}{\partial x_1^{\alpha}} x_2^{\alpha} + \left[\frac{\partial f_{12}^{\alpha}(x_1^{\alpha})}{\partial x_1^{\alpha}} / [1 + f_{12}^{\alpha}(x_1)] + f_{22}^{\alpha}(x_1^{\alpha})\right](x_2^{\alpha} - f_{11}^{\alpha}(x_1^{\alpha})) + [1 + f_{12}^{\alpha}(x_1)]\, f_{21}^{\alpha}(x_1^{\alpha}) \\
&+ \frac{\partial f_{13}^{\alpha}(x_1^{\alpha}, \theta)}{\partial x_1^{\alpha}} x_2^{\alpha} + \frac{\partial f_{13}^{\alpha}(x_1^{\alpha}, \theta)}{\partial \theta}\dot{\theta} - \left[\frac{\partial f_{12}^{\alpha}(x_1^{\alpha})}{\partial x_1^{\alpha}} / [1 + f_{12}^{\alpha}(x_1)] + f_{22}^{\alpha}(x_1^{\alpha})\right] f_{13}^{\alpha}(x_1^{\alpha}, \theta) \\
&+ [1 + f_{12}^{\alpha}(x_1)]\, g_2^{\alpha}(x_1^{\alpha})\delta_e
\end{aligned}$$

System (4.5) can be rewritten into:

$$\dot{\theta} = \eta^{\alpha}(x_1^{\alpha}, x_2^{\alpha}, \theta) \tag{4.7a}$$

$$\begin{aligned} \dot{x}_1^{\alpha} &= x_2^{\alpha} \\ \dot{x}_2^{\alpha} &= f^{\alpha\prime}(x_1^{\alpha}, x_2^{\alpha}) + h^{'}(x_1^{\alpha}, x_2^{\alpha}, \theta) + g^{\alpha\prime}(x_1^{\alpha}, x_2^{\alpha})u^{\alpha} \end{aligned} \tag{4.7b}$$

where

$$\begin{cases} \eta^{\alpha} =& (x_2^{\alpha} - f_{11}^{\alpha}(x_1^{\alpha}) - f_{13}^{\alpha}(x_1^{\alpha}, \theta))/(1 + f_{12}^{\alpha}(x_1^{\alpha})) \\ f^{\alpha^{'}} =& \frac{\partial f_{11}^{\alpha}(x_1^{\alpha})}{\partial x_1^{\alpha}} x_2^{\alpha} + \left[\frac{\partial f_{12}^{\alpha}(x_1^{\alpha})}{\partial x_1^{\alpha}} / [1 + f_{12}^{\alpha}(x_1)] + f_{22}^{\alpha}(x_1^{\alpha})\right](x_2^{\alpha} - f_{11}^{\alpha}(x_1^{\alpha})) + [1 + f_{12}^{\alpha}(x_1)]\, f_{21}^{\alpha}(x_1^{\alpha}) \\ h^{'} =& \frac{\partial f_{13}^{\alpha}(x_1^{\alpha}, \theta)}{\partial x_1^{\alpha}} x_2^{\alpha} + \frac{\partial f_{13}^{\alpha}(x_1^{\alpha}, \theta)}{\partial \theta}\eta^{\alpha} - \left[\frac{\partial f_{12}^{\alpha}(x_1^{\alpha})}{\partial x_1^{\alpha}} / [1 + f_{12}^{\alpha}(x_1)] + f_{22}^{\alpha}(x_1^{\alpha})\right] f_{13}^{\alpha}(x_1^{\alpha}, \theta) \\ g^{\alpha^{'}} =& [1 + f_{12}^{\alpha}(x_1)]\, g_2^{\alpha}(x_1^{\alpha}) \end{cases} \tag{4.8}$$

In (4.7b), $f^{\alpha'}(\cdot)$ is function of x_1^α and x_2^α. Function $h'(\cdot)$ is function of x_1^α, x_2^α and θ, it can be expressed as:

$$\begin{aligned} h'(\cdot) &= -\frac{g}{V}\frac{\cos(\theta-\alpha)}{(1+f_{12}^\alpha(x_1^\alpha))}\frac{\partial f_{12}^\alpha(x_1^\alpha)}{\partial x_1^\alpha}x_2^\alpha - \frac{g}{V}\cos(\theta-\alpha)f_{22}^\alpha(x_1^\alpha) + \frac{g}{V}\sin(\theta-\alpha)x_2^\alpha\frac{f_{12}^\alpha(x_1^\alpha)}{(1+f_{12}^\alpha(x_1^\alpha))} \\ &\quad +(\frac{g}{V})^2\frac{\sin(\theta-\alpha)\cos(\theta-\alpha)}{(1+f_{12}^\alpha(x_1^\alpha))} + \frac{g}{V}\frac{\sin(\theta-\alpha)f_{11}^\alpha(x_1^\alpha)}{(1+f_{12}^\alpha(x_1^\alpha))} \end{aligned} \tag{4.9}$$

Remark 6 *We have some remarks:*

- *f_{11}^α, f_{12}^α, f_{13}^α, f_{21}^α, f_{22}^α and g_2^α are function of aerodynamic coefficients under analytical forms by interpolation from wind tunnel test data. $F^{\alpha'}$ and h', formed from these functions, can be then bounded by a class $\mathcal{K}$ function and be a Lipschitz function in a flighting envelop.*
- *$G^{\alpha'}$ is invertible in the flight domain, that means $\alpha \in (-10°, 45°)$ and $\theta \in (-90°, 90°)$. As a consequence, they fulfill Assumptions 3.2.1 and 3.2.2.*

We define now the reference for the angle of attack α_{ref} considered as constant in this study, and the error vector of angle of attack $e_1^\alpha = x_1^\alpha - x_{1ref}^\alpha = \alpha - \alpha_{ref}$ and the variable $e_2^\alpha = \dot{e}_1^\alpha$. Equation (4.7b) can be transformed into:

$$\begin{cases} \dot{e}_1^\alpha = e_2^\alpha & \text{(4.10a)} \\ \dot{e}_2^\alpha = f^\alpha(e_1^\alpha, e_2^\alpha) + h(e_1^\alpha, e_2^\alpha, \theta) + g^\alpha(e_1^\alpha, e_2^\alpha)u^\alpha & \text{(4.10b)} \end{cases}$$

Since function $h(\cdot)$ depends on θ under cosines and sinus functions, it is easy to show that $h(\cdot)$ is bounded by a function of class $\mathcal{K}$ function $\gamma_1^\alpha(\cdot)$ and a constant h_0.

$$|h(e_1^\alpha, e_2^\alpha, \theta)| \leq \gamma_1^\alpha(|e_1^\alpha| + |e_2^\alpha|) + h_0 \tag{4.11}$$

Control law

We will apply the control algorithm presented in (3.12) for system (4.10) which in this case is a nonlinear single input single output system, gives the controller:

$$\begin{cases} u^\alpha &= -\pi^\alpha(e_1^\alpha, e_2^\alpha)sat(s^\alpha/\mu^\alpha) \\ \pi^\alpha(\cdot) &= (\pi_0^\alpha + \gamma^\alpha(\cdot) + k_0^\alpha\mu^\alpha + \delta_0^\alpha)(g^\alpha(\cdot))^{-1} \end{cases} \tag{4.12}$$

with

$$\begin{cases} s^\alpha = k_0^\alpha\sigma^\alpha + k_1^\alpha e_1^\alpha + e_2^\alpha \\ \dot{\sigma^\alpha} = -k_0^\alpha\sigma^\alpha + \mu^\alpha sat(s^\alpha/\mu^\alpha) \end{cases} \tag{4.13}$$

where π_0^α, μ^α, K_1^α and k_0^α are positive constants.

◇

Stability Analysis

Theorem 4.2.1 *System (4.10) with $f^\alpha(\cdot)$ satisfying Assumption 3.2.1, $g^\alpha(\cdot)$ satisfying Assumption 3.2.2, and the control law (4.12-4.13), will globally reach an arbitrary error region in finite time, and there on will be exponentially stabilized towards its equilibrium point.*

□

Proof: In order to demonstrate the exponential stability of designed controller (4.12) and (4.13) for the longitudinal mode in (4.10), we will consider the two regions, outside the boundary layer ($|s^\alpha| \geq \mu^\alpha$) and inside the boundary layer ($|s^\alpha| \leq \mu^\alpha$). The longitudinal mode in this study is a single input single output system.

4.2.2.1 *In the region* $|s^\alpha| \geq \mu^\alpha$, $sat(s^\alpha/\mu^\alpha) = s^\alpha/|s^\alpha|$.

The derivative of the integral error measurement surface can be then expressed as:

$$\dot{s}^\alpha \quad = \quad k_0^\alpha \dot{\sigma}^\alpha + k_1^\alpha \dot{e}_1^\alpha + \dot{e}_2^\alpha \tag{4.14}$$

From (4.10) and (4.13), the previous equation may be written again :

$$\begin{aligned}\dot{s}^\alpha =& k_0^\alpha(-k_0^\alpha\sigma^\alpha + \mu^\alpha sat(s^\alpha/\mu^\alpha)) + k_1^\alpha e_2^\alpha + \dot{e^\alpha}_2\\ =& k_0^\alpha(-(s^\alpha - (k_1^\alpha e_1^\alpha + e_2^\alpha)) + \mu^\alpha sat(s^\alpha/\mu^\alpha)) + k_1^\alpha e_2^\alpha + \dot{e^\alpha}_2\\ =& -k_0^\alpha s^\alpha + k_0^\alpha\mu^\alpha sat(s^\alpha/\mu^\alpha) + k_0^\alpha(k_1^\alpha e_1^\alpha + e_2^\alpha) + k_1^\alpha e_2^\alpha + f^\alpha(\cdot) + g^\alpha(\cdot)u^\alpha\end{aligned}$$

Now by letting

$$\delta^\alpha(\cdot) = k_0^\alpha(k_1^\alpha e_1^\alpha + e_2^\alpha) + k_1^\alpha e_2^\alpha + f^\alpha(\cdot) + h(\cdot) \tag{4.15}$$

The derivative of the integral error measurement surface becomes:

$$\dot{s}^\alpha = -k_0^\alpha s^\alpha + k_0^\alpha\mu^\alpha sat(s^\alpha/\mu^\alpha) + \delta^\alpha(\cdot) + g^\alpha(\cdot)u^\alpha \tag{4.16}$$

The term $f^\alpha(x_1^\alpha, x_2^\alpha)$ is bounded by a function $\gamma_2^\alpha(|e_1^\alpha| + |e_2^\alpha|)$ outside the boundary region e.g. $|s^\alpha| \geq \mu^\alpha$ and a positive constant f_0^α, where $\gamma_2^\alpha(\cdot)$ is a class $\mathcal{K}$ function.

$$|f^\alpha(e_1^\alpha, e_2^\alpha)| \leq \gamma_2^\alpha(|e_1^\alpha| + |e_2^\alpha|) + f_0^\alpha \tag{4.17}$$

Function $h(\cdot)$ is also bounded in the same way (see (4.11)). Then $\delta^\alpha(\cdot)$ is bounded by a $\gamma^\alpha(\cdot)$ class $\mathcal{K}$ function and a positive constant δ_0^α:

$$\begin{array}{rcl} |\delta^\alpha(e_1^\alpha, e_2^\alpha)| & \leq & \gamma_1^\alpha(|e_1^\alpha| + |e_2^\alpha|) + h_0 + \gamma_2^\alpha(|e_1^\alpha| + |e_2^\alpha|) + f_0^\alpha \\ |\delta^\alpha(e_1^\alpha, e_2^\alpha)| & \leq & \gamma^\alpha(|e_1^\alpha| + |e_2^\alpha|) + \delta_0^\alpha \end{array} \tag{4.18}$$

where $\gamma^\alpha(\cdot) = \gamma_1^\alpha(\cdot) + \gamma_2^\alpha(\cdot)$ and $\delta_0^\alpha = h_0 + f_0^\alpha$
and as a consequence,

$$|\delta^\alpha(e_1^\alpha = 0, e_2^\alpha = 0)| = |f^\alpha(0,0)| \leq \delta_0^\alpha \tag{4.19}$$

for $(e_1^\alpha, e_2^\alpha) \in \mathbb{R}^n \times \mathbb{R}^n$.

Let's consider the product $s^\alpha \dot{s}^\alpha$ (since s is a scalar)

$$s^\alpha \dot{s}^\alpha \quad = \quad -k_0^\alpha (s^\alpha)^2 + k_0^\alpha \mu^\alpha s^\alpha sat(s^\alpha/\mu^\alpha) + s^\alpha \delta^\alpha(e_1^\alpha, e_2^\alpha) + s^\alpha g^\alpha(e_1^\alpha, e_2^\alpha) u^\alpha \tag{4.20}$$

This product $(s^\alpha)^T \dot{s}^\alpha$ can be developed with the definition of saturation function (3.4):

$$\begin{array}{rl} s^\alpha \dot{s}^\alpha = & -k_0^\alpha (s^\alpha)^2 + \mu^\alpha k_0^\alpha (s^\alpha)^2/|s^\alpha| + s^\alpha \delta^\alpha(\cdot) - s^\alpha g^\alpha(\cdot)\pi^\alpha(\cdot)s^\alpha/|s^\alpha| \\ \leq & -k_0^\alpha (s^\alpha)^2 + \mu^\alpha k_0^\alpha (s^\alpha)^2/|s^\alpha| + |\delta^\alpha(\cdot)||s^\alpha| - s^\alpha g^\alpha(\cdot)\pi^\alpha(\cdot)s^\alpha/|s^\alpha| \\ \leq & -k_0^\alpha (s^\alpha)^2 + \mu^\alpha k_0^\alpha (s^\alpha)^2/|s^\alpha| + (\gamma^\alpha(\cdot) + \delta_0^\alpha)|s^\alpha| - s^\alpha g^\alpha(\cdot)\pi^\alpha(\cdot)s^\alpha/|s^\alpha| \\ \leq & -k_0^\alpha (s^\alpha)^2 - s^\alpha(g^\alpha(\cdot)\pi^\alpha(\cdot) - (\mu^\alpha k_0^\alpha + \gamma^\alpha(\cdot) + \delta_0^\alpha))s^\alpha/|s^\alpha| \end{array} \tag{4.21}$$

Replacing the control law in (4.12) and (4.13), the term $s^\alpha \dot{s}^\alpha$ can be expressed as:

$$\begin{array}{rl} s^\alpha \dot{s}^\alpha \leq & -k_0^\alpha (s^\alpha)^2 - s^\alpha(g^\alpha(\cdot)\pi^\alpha(\cdot) - (\mu^\alpha k_0^\alpha + \gamma^\alpha(\cdot) + \delta_0^\alpha))s^\alpha/|s^\alpha| \\ \leq & -k_0^\alpha (s^\alpha)^2 - \pi_0^\alpha (s^\alpha)^2/|s^\alpha| \\ \leq & -k_0^\alpha (s^\alpha)^2 - \pi_0^\alpha |s^\alpha| \end{array} \tag{4.22}$$

The product $s^\alpha \dot{s}^\alpha$ is then not positive and we have also

$$\begin{array}{ll} \frac{d((s^\alpha)^2)}{dt} = 2|s^\alpha|\frac{d(|s^\alpha|)}{dt} = 2\frac{s^\alpha \dot{s}^\alpha}{dt} \leq 2(-\pi_0^\alpha |s^\alpha| - k_0^\alpha (s^\alpha)^2) \\ \therefore \ \frac{d(|s^\alpha|)}{dt} \leq -\pi_0^\alpha - k_0^\alpha |s^\alpha| \\ \therefore \ |s^\alpha(t)| \leq |s^\alpha(0)| - \pi_0^\alpha t - |s^\alpha(0)|(e^\alpha)^{-k_0^\alpha t} - 1) \end{array} \tag{4.23}$$

Then the integral error measurement surface $s^\alpha(t)$ reaches the boundary layer μ^α in finite time.

▪

4.2.2.2 *In the region* $|s| \leq \mu^\alpha$, $sat(s/\mu^\alpha) = s/\mu^\alpha$.

Consider again (4.13) and (4.16), which inside the boundary layer may be rewritten as:

$$\begin{cases} \dot{\sigma}^\alpha = -k_0^\alpha \sigma^\alpha + s^\alpha & \text{(4.24a)} \\ \dot{e}_1^\alpha = -k_1^\alpha e_1^\alpha + s^\alpha - k_0^\alpha \sigma^\alpha & \text{(4.24b)} \\ \dot{s}^\alpha = \delta^\alpha(\cdot) - g^\alpha(\cdot)\pi^\alpha(\cdot)s^\alpha/\mu^\alpha & \text{(4.24c)} \end{cases}$$

It can be shown that this system has an equilibrium point: $\bar{e}_1^\alpha = \bar{e}_2^\alpha = 0$, $s^\alpha = \bar{s}^\alpha$, $\sigma^\alpha = \bar{\sigma}^\alpha$ with $\bar{s} = k_0^\alpha \bar{\sigma}^\alpha = \mu^\alpha(\pi^\alpha(0,0))^{-1}(g^\alpha(0,0))^{-1}(f^\alpha(0,0) + h(0,0,\theta)) = (f^\alpha(0,0) + h(0,0,\theta))/(\pi_0^\alpha + k_0^\alpha \mu^\alpha + \delta_0^\alpha)$.

System (4.24) may be rewritten with respect to $\bar{s}^\alpha$ and $\bar{\sigma}^\alpha$:

$$\begin{cases} \dot{\tilde{\sigma}}^\alpha = -k_0^\alpha \tilde{\sigma}^\alpha + \tilde{s}^\alpha & \text{(4.25a)} \\ \dot{e}_1^\alpha = -k_1^\alpha e_1^\alpha + \tilde{s}^\alpha - k_0^\alpha \tilde{\sigma}^\alpha & \text{(4.25b)} \\ \dot{\tilde{s}}^\alpha = \delta^\alpha(\cdot) - g^\alpha(\cdot)\pi^\alpha(\cdot)\tilde{s}^\alpha/\mu^\alpha - g^\alpha(\cdot)\pi^\alpha(\cdot)\bar{s}^\alpha/\mu^\alpha & \text{(4.25c)} \end{cases}$$

where $\tilde{\sigma}^\alpha = \sigma^\alpha - \bar{\sigma}^\alpha$, $\tilde{s}^\alpha = s^\alpha - \bar{s}^\alpha$.

Function $f^\alpha(x_1^\alpha, x_2^\alpha)$ is Lipschitz inside the boundary region e.g. $|s^\alpha| \leq \mu^\alpha$ (see remark 6), such that:

$$|f^\alpha(e_1^\alpha, e_2^\alpha) - f^\alpha(0,0)| \leq l_1^\alpha |k_1^\alpha e_1^\alpha| + l_2^\alpha |e_2^\alpha| \tag{4.26}$$

where l_1^α and $l_2^\alpha \in \mathbb{R}^+$.

$\gamma_2^\alpha(\cdot)$ and $\gamma_1^\alpha(\cdot)$ is are chosen so that are differentiable, then Lipschitz. As a consequence, function $\gamma^\alpha(\cdot)$ is then Lipschitz.

$$\gamma^\alpha(\cdot) \leq d_1^\alpha |k_1^\alpha e_1^\alpha| + d_2^\alpha |e_2^\alpha| \tag{4.27}$$

where d_1^α and $d_2^\alpha \in \mathbb{R}^+$.

We would like to demonstrate that every trajectory of system (4.25) starting inside the boundary layer, will approach the equilibrium point as time tends to infinity when the control law (4.12) is applied. Toward that end, we take:

$$W^\alpha = \frac{\lambda_1^\alpha}{2} k_0^\alpha (\tilde{\sigma}^\alpha)^2 + \frac{\lambda_2^\alpha}{2} k_1^\alpha (e_1^\alpha)^2 + \frac{(\tilde{s}^\alpha)^2}{2} \tag{4.28}$$

as a Lyapunov candidate, where λ_1^α and λ_2^α are positive constants.

Since $|s^\alpha| \leq \mu^\alpha$, $\delta^\alpha(\cdot)$ can be expressed as:

$$\delta^\alpha(\cdot) = (k_0^\alpha + k_1^\alpha)\tilde{s}^\alpha - (k_0^\alpha + k_1^\alpha)k_0^\alpha \tilde{\sigma}^\alpha - (k_1^\alpha)^2 e_1^\alpha + f^\alpha(\cdot) + h(\cdot) \tag{4.29}$$

From (4.25) and reminding that $\bar{s} = (f^\alpha(0,0) + h(0,0,\theta))/(\pi_0^\alpha + k_0^\alpha\mu^\alpha + \delta_0^\alpha)$ and $g^\alpha(\cdot)\pi^\alpha(\cdot) = (\pi_0^\alpha + k_0^\alpha\mu^\alpha + \gamma^\alpha(\cdot) + \delta_0^\alpha)$, the derivative of the Lyapunov function is developed:

$$\begin{aligned}
\dot{W}^\alpha =& \lambda_1^\alpha k_0^\alpha \tilde{\sigma}^\alpha \dot{\tilde{\sigma}}^\alpha + \lambda_2^\alpha k_1^\alpha e_1^\alpha \dot{e_1^\alpha} + \tilde{s}^\alpha \dot{\tilde{s}}^\alpha \\
=& \lambda_1^\alpha \tilde{\sigma}^\alpha k_0^\alpha(-k_0^\alpha\tilde{\sigma}^\alpha + \tilde{s}^\alpha) + \lambda_2^\alpha k_1^\alpha e_1^\alpha(-k_1^\alpha e_1^\alpha + \tilde{s}^\alpha - k_0^\alpha\tilde{\sigma}^\alpha) \\
&+\tilde{s}^\alpha(\delta^\alpha(\cdot) - g^\alpha(\cdot)\pi^\alpha(\cdot)\tilde{s}^\alpha/\mu^\alpha - g^\alpha(\cdot)\pi^\alpha(\cdot)\bar{s}^\alpha/\mu^\alpha) \\
=& -\lambda_1^\alpha(k_0^\alpha\tilde{\sigma}^\alpha)^2 + \lambda_1^\alpha k_0^\alpha\tilde{\sigma}^\alpha\tilde{s}^\alpha - \lambda_2^\alpha(k_1^\alpha e_1^\alpha)^2 + \lambda_2^\alpha k_1^\alpha e_1^\alpha(\tilde{s}^\alpha - k_0^\alpha\tilde{\sigma}^\alpha) \\
&+(k_0^\alpha + k_1^\alpha)(\tilde{s}^\alpha)^2 - (k_0^\alpha + k_1^\alpha)k_0^\alpha\tilde{s}^\alpha\tilde{\sigma}^\alpha - (k_1^\alpha)^2 e_1^\alpha\tilde{s}^\alpha - g^\alpha(\cdot)\pi^\alpha(\cdot)/\mu^\alpha(\tilde{s}^\alpha)^2 \\
&+\tilde{s}^\alpha(f^\alpha(\cdot) + h(\cdot) - g^\alpha(\cdot)\pi^\alpha(\cdot)\bar{s}^\alpha/\mu^\alpha) \\
=& -\lambda_1^\alpha(k_0^\alpha\tilde{\sigma}^\alpha)^2 + \lambda_1^\alpha k_0^\alpha\tilde{\sigma}^\alpha\tilde{s}^\alpha - \lambda_2^\alpha(k_1^\alpha e_1^\alpha)^2 + \lambda_2^\alpha k_1^\alpha e_1^\alpha(\tilde{s}^\alpha - k_0^\alpha\tilde{\sigma}^\alpha) \\
&+(k_0^\alpha + k_1^\alpha)(\tilde{s}^\alpha)^2 - (k_0^\alpha + k_1^\alpha)k_0^\alpha\tilde{s}^\alpha\tilde{\sigma}^\alpha - (k_1^\alpha)^2 e_1^\alpha\tilde{s}^\alpha - g^\alpha(\cdot)\pi^\alpha(\cdot)/\mu^\alpha(\tilde{s}^\alpha)^2 \\
&+\tilde{s}^\alpha(f^\alpha(\cdot) + h(\cdot) - \tfrac{\pi_0^\alpha + k_0^\alpha\mu^\alpha + \gamma(\cdot) + \delta_0^\alpha}{(\pi_0^\alpha + k_0^\alpha\mu^\alpha + \delta_0^\alpha)}(f^\alpha(0,0) + h(0,0,\theta))) \\
=& -\lambda_1^\alpha(k_0^\alpha\tilde{\sigma}^\alpha)^2 + \lambda_1^\alpha k_0^\alpha\tilde{\sigma}^\alpha\tilde{s}^\alpha - \lambda_2^\alpha(k_1^\alpha e_1^\alpha)^2 + \lambda_2^\alpha k_1^\alpha e_1^\alpha(\tilde{s}^\alpha - k_0^\alpha\tilde{\sigma}^\alpha) \\
&+(k_0^\alpha + k_1^\alpha)(\tilde{s}^\alpha)^2 - (k_0^\alpha + k_1^\alpha)k_0^\alpha\tilde{s}^\alpha\tilde{\sigma}^\alpha - (k_1^\alpha)^2 e_1^\alpha\tilde{s}^\alpha - g^\alpha(\cdot)\pi^\alpha(\cdot)/\mu^\alpha(\tilde{s}^\alpha)^2 \\
&+\tilde{s}^\alpha(f^\alpha(\cdot) - f^\alpha(0,0) - \tfrac{\gamma^\alpha(\cdot)}{(\pi_0^\alpha + k_0^\alpha\mu^\alpha + \delta_0^\alpha)}f^\alpha(0,0)) \\
&+\tilde{s}^\alpha(h^\alpha(\cdot) - h^\alpha(0,0,\theta) - \tfrac{\gamma^\alpha(\cdot)}{(\pi_0^\alpha + k_0^\alpha\mu^\alpha + \delta_0^\alpha)}h^\alpha(0,0,\theta))
\end{aligned} \tag{4.30}$$

Using equations (4.10a) and (4.25b), the relation in (4.26) and in (4.27) can be expressed as:

$$\begin{aligned}
&\tilde{s}^\alpha(f^\alpha(e_1^\alpha, e_2^\alpha) - f^\alpha(0,0) - \tfrac{\gamma^\alpha(\cdot)}{(\pi_0^\alpha + k_0^\alpha\mu^\alpha + \delta_0^\alpha)}f^\alpha(0,0)) \\
&\leq |\tilde{s}^\alpha|(|f^\alpha(e_1^\alpha, e_2^\alpha) - f^\alpha(0,0)| + |\tfrac{\gamma^\alpha(\cdot)}{(\pi_0^\alpha + k_0^\alpha\mu^\alpha + \delta_0^\alpha)}f^\alpha(0,0)|) \\
&\leq |\tilde{s}^\alpha|(l_1^\alpha|k_1^\alpha e_1^\alpha| + l_2^\alpha|e_2^\alpha| + d_1^\alpha|k_1^\alpha e_1^\alpha| + d_2^\alpha|e_2^\alpha|) \\
&\leq (d_1^\alpha + l_1^\alpha)|e_1^\alpha||\tilde{s}^\alpha| + (d_2^\alpha + l_2^\alpha)|e_2^\alpha||\tilde{s}^\alpha| \\
&\leq 1/2(d_1^\alpha + l_1^\alpha)((k_1^\alpha e_1^\alpha)^2 + (\tilde{s}^\alpha)^2) + 1/2(d_2^\alpha + l_2^\alpha)((\tilde{s}^\alpha)^2 \\
&+3((\tilde{s}^\alpha)^2 + ((k_1^\alpha e_1^\alpha)^2 + (k_0^\alpha\tilde{\sigma}^\alpha)^2)) \\
&\leq c_1(k_0^\alpha\tilde{\sigma}^\alpha)^2 + c_2(k_1^\alpha e_1^\alpha)^2 + c_3(\tilde{s}^\alpha)^2
\end{aligned} \tag{4.31}$$

where $c_1 = 3/2(d_2^\alpha + l_2^\alpha)$, $c_2 = 1/2(d_1^\alpha + l_1^\alpha) + 3/2(d_2^\alpha + l_2^\alpha)$ and $c_3 = 1/2(d_1^\alpha + l_1^\alpha) + 2(d_2^\alpha + l_2^\alpha)$. and then,

$$\begin{aligned}
\dot{W}^\alpha \leq& -\lambda_1^\alpha(k_0^\alpha\tilde{\sigma}^\alpha)^2 + 1/2\lambda_1^\alpha((k_0^\alpha\tilde{\sigma}^\alpha)^2 + (\tilde{s}^\alpha)^2) - \lambda_2^\alpha(k_1^\alpha e_1^\alpha)^2 \\
&+1/2\lambda_2^\alpha((k_1^\alpha e_1^\alpha)^2 + 2((\tilde{s}^\alpha)^2 + (k_0^\alpha\tilde{\sigma}^\alpha)^2)) + (k_0^\alpha + k_1^\alpha)(\tilde{s}^\alpha)^2 \\
&+1/2((k_0^\alpha\tilde{\sigma}^\alpha)^2 + ((k_0^\alpha + k_1^\alpha)\tilde{s}^\alpha)^2) + 1/2((k_1^\alpha e_1^\alpha)^2 + (k_1^\alpha\tilde{s}^\alpha)^2) - g^\alpha(\cdot)\pi^\alpha(\cdot)/\mu^\alpha(\tilde{s}^\alpha)^2 \\
&+c_1(k_0^\alpha\tilde{\sigma}^\alpha)^2 + c_2(k_1^\alpha e_1^\alpha)^2 + c_3(\tilde{s}^\alpha)^2 + |h^\alpha(\cdot) - h^\alpha(0,0,\theta) - \tfrac{\gamma^\alpha(\cdot)}{(\pi_0^\alpha + k_0^\alpha\mu^\alpha + \delta_0^\alpha)}h^\alpha(0,0,\theta)||\tilde{s}^\alpha| \\
\leq& -(1/2\lambda_1^\alpha - \lambda_2^\alpha - 1/2 - c_1)(k_0^\alpha\tilde{\sigma}^\alpha)^2 - (1/2\lambda_2^\alpha - 1/2 - c_2)(k_1^\alpha e_1^\alpha)^2 \\
&-(g^\alpha(\cdot)\pi^\alpha(\cdot)/\mu^\alpha - 1/2\lambda_1^\alpha - \lambda_2^\alpha - (k_0^\alpha + k_1^\alpha) - 1/2(k_0^\alpha + k_1^\alpha)^2 - 1/2(k_1^\alpha)^2 - c_3)(\tilde{s}^\alpha)^2 \\
&+|h^\alpha(\cdot) - h^\alpha(0,0,\theta) - \tfrac{\gamma^\alpha(\cdot)}{(\pi_0^\alpha + k_0^\alpha\mu^\alpha + \delta_0^\alpha)}h^\alpha(0,0,\theta)||\tilde{s}^\alpha|
\end{aligned} \tag{4.32}$$

Because inside the boundary region e.g. $|s^\alpha| \leq \mu^\alpha$, functions $h(\cdot)$ and $\gamma^\alpha(\cdot)$ are bounded, the following term is bounded by a positive constant $C\mu$:

$$|h^\alpha(\cdot) - h^\alpha(0,0,\theta) - \frac{\gamma^\alpha(\cdot)}{(\pi_0^\alpha + k_0^\alpha \mu^\alpha + \delta_0^\alpha)} h^\alpha(0,0,\theta)||\tilde{s}^\alpha| \leq C\mu \tag{4.33}$$

For any value of θ, it is very important to remark that this variable was not included in this analysis, even if its derivative is. We will discuss this point again later, but the main reason is that the airlaunch may be performed under any pitch angle θ, and even under a looping-like trajectory. From (4.32), the derivative of the Lyapunov function can be further developed:

$$\begin{aligned}
\dot{W}^\alpha \leq & -(1/2\lambda_1^\alpha - \lambda_2^\alpha - 1/2 - c_1)(k_0^\alpha \tilde{\sigma}^\alpha)^2 - (1/2\lambda_2^\alpha - 1/2 - c_2)(k_1^\alpha e_1^\alpha)^2 \\
& -(g^\alpha(\cdot)\pi^\alpha(\cdot)/\mu^\alpha - 1/2\lambda_1^\alpha - \lambda_2^\alpha - (k_0^\alpha + k_1^\alpha) - 1/2(k_0^\alpha + k_1^\alpha)^2 - 1/2(k_1^\alpha)^2 - c_3)(\tilde{s}^\alpha)^2 \\
& +C\mu \\
\leq & -\tfrac{\lambda_1^\alpha w_1}{2} k_0^\alpha (\tilde{\sigma}^\alpha)^2 - \tfrac{\lambda_2^\alpha w_2}{2} k_1^\alpha (e_1^\alpha)^2 - \tfrac{w_3}{2}(\tilde{s}^\alpha)^2 + C\mu \\
\leq & w_0(-\tfrac{\lambda_1^\alpha w_1}{2w_0}(\tilde{\sigma}^\alpha)^2 - \tfrac{\lambda_2^\alpha w_2}{2w_0}(e_1^\alpha)^2 - \tfrac{w_3}{2w_0}(\tilde{s}^\alpha)^2) + C\mu \\
\leq & w_0(-\tfrac{\lambda_1^\alpha}{2}(\tilde{\sigma}^\alpha)^2 - \tfrac{\lambda_2^\alpha}{2}(e_1^\alpha)^2 - \tfrac{1}{2}(\tilde{s}^\alpha)^2) + C\mu \\
\leq & -w_0 W^\alpha + C\mu
\end{aligned} \tag{4.34}$$

where

$$\begin{cases}
w_1 = (1 - \frac{2\lambda_2^\alpha + 1/2 + 2c_1}{\lambda_1^\alpha}) k_0^\alpha \\
w_2 = (1 - \frac{1 + 2c_2}{\lambda_2^\alpha}) k_1^\alpha \\
w_3 = 2((\pi_0^\alpha + k_0^\alpha \mu^\alpha + \delta_0^\alpha)/\mu^\alpha - 1/2\lambda_1^\alpha - \lambda_2^\alpha - (k_0^\alpha + k_1^\alpha) - 1/2(k_0^\alpha + k_1^\alpha)^2 - 1/2(k_1^\alpha)^2 - c_3) \\
w_0 = min(w_1, w_2, w_3)
\end{cases} \tag{4.35}$$

The derivative of Lyapunov function negative implies that $\lambda_1^\alpha, \lambda_2^\alpha$ and π_0^α large enough and μ^α small enough, to satisfy:

$$\begin{cases}
1 > \frac{2\lambda_2^\alpha + 1/2 + 2c_1}{\lambda_1^\alpha} \\
1 > \frac{1 + 2c_2}{\lambda_2^\alpha} \\
(\pi_0^\alpha + \delta_0^\alpha)/\mu^\alpha - k_1^\alpha - 1/2(k_0^\alpha + k_1^\alpha)^2 - 1/2(k_1^\alpha)^2 > 1/2\lambda_1^\alpha + \lambda_2^\alpha + c_3
\end{cases} \tag{4.36}$$

In this way, $W^\alpha(t)$ satisfies $W^\alpha(t) > 0$ and $\dot{W}^\alpha < -w_0 W^\alpha + C\mu$ (where w_0 is a positive constant) for all $\sigma^\alpha \neq \bar{\sigma^\alpha}$, $e_1^\alpha \neq 0$ and $s^\alpha \neq \bar{s}^\alpha$. Then $W^\alpha(t)$ is ultimately bounded towards a neighborhood of zero when time tends to infinite, independent of the pitch angle θ. As

consequence, $e_1^\alpha(t)$, σ^α and s^α tend to a region around their equilibrium point as time tends to infinite and for every pitch angle θ. The system is then said to be ultimately bounded to a small region which is function of pitch angle θ. Finally, it is interesting to remark that, as said before, variable θ is left free in order to allow situations as a looping, where θ is continuously varying. Its derivative on the other hand is bounded, and also goes to a residual set. In fact, the best trajectory for airlaunch is still an open problem. There are proposals of launching in horizontal, constant angle (climbing), concave or convex (zero gravity instant) trajectories.

□

Since the airspeed control is only a secondary objective, we design a simple PI controller for the thrust to regulate airspeed. Its form is:

$$T = -k_P(V - V_{ref}) - k_I(\dot{V} - \dot{V}_{ref})$$

where V_{ref} is the airspeed reference, $k_P = 711.0$ and $k_I = 6.2$.

4.2.3 Simulation Results

In section 3.2, the design methodology of the modified Conditional Integrator controller to stabilize the angle of attack, sideslip and roll angle is proposed. This section presents numerical simulation results to demonstrate the performance of the proposed modified Conditional Integrator control laws in the drop phase.

Baselines

As mentioned in section 2.4, we have considered the launch phase as impulses on aerodynamic force and moments during a time interval T_{int}, and that the model following the launch phase is that of an F-16. This model is used since it has already been applied for (manned) airlaunch, and because its nonlinear model, wind tunnel informations and data are widely known and used for control design. It is important to remark that the model used in the following simulations is even more complete than that used in the control design, for example it includes actuator dynamics and their limitations. As a consequence, simulations also illustrate some properties of robustness to unmodeled dynamics.

In the following simulations, we have simultaneously applied the SISO longitudinal controller for angle of attack, and the MIMO lateral one for sideslip and roll angles in the full nonlinear F-16 aircraft model. We may note that the control inputs are limited by their physical bounds introduced in section 3.2.

The objective for the controller after the launching phase are:

- the controller must return the airlaunch system to the equilibrium point of the second model which corresponds to angle of attack $\alpha_r = 4.6°$, sideslip $\beta_r = 0°$, and roll angle $\phi_r = 0°$ and all others variables to zero (at $V = 154m/s, h = 5000m$). The control surfaces at the equilibrium point are $\delta_a = 0°$, $\delta_e = -2.5°$ and $\delta_r = 0°$.
- There is no collision between airlaunch system and the rocket.
- ($\alpha_0 = 17.5°$, $\beta_0 = 4°$ and $\phi_0 = 10°$) are the initial conditions for the second model which represents the airlaunch system after the separation phase, all others variables are zero. This is the final state of the first model plus a small aleatory disturbance on the system output.

Numerical Applications

The control law in (3.12) whose $\Pi(\cdot)$ can be written more simply as:

$$\begin{cases} u & = & -\Pi(e_1, e_2)\text{sat}(s/\mu) \\ \Pi(\cdot) & = & (\Pi_0 + \gamma(\cdot))G(\cdot)^{-1} \end{cases}$$

with $\gamma(\cdot) = \gamma_1\|e_1\|^2 + \gamma_2\|e_2\|^2$, γ_1 and γ_2 positive constants. $G(\cdot)^{-1}$ is $G^\alpha(\cdot)^{-1}$ defined in (4.10) or $G^\beta(\cdot)^{-1}$ in (3.55) depending on longitudinal mode or lateral mode (they can be found in Appendix A.2).

Application of this control law to two motion modes presented in subsections (3.4.1) and (4.2.2) is done by determining the set of parameters Π_0^i, γ_1^i, γ_2^i, μ^i, K_1^i and k_0^i with $i = \alpha, \beta$ corresponding to longitudinal mode and lateral mode respectively. We use the design parameters in Table 4.1 for the longitudinal controller, and the design parameters in Table 4.2 for the lateral controller.

Π_0^α	μ^α	γ_1^α and γ_2^α	k_0^α	K_1^α
25.0	1.0	0.001 and 0.001	2.0	2.0

Table 4.1: Parameters for the longitudinal mode controller

Π_0^β	μ^β	γ_1^β and γ_2^β	k_0^β	K_1^β
$\begin{bmatrix} 10 & 0.0 \\ 0.0 & 10 \end{bmatrix}$	1.0	0.01 and 0.01	$\begin{bmatrix} 0.8 & 0.0 \\ 0.0 & 0.8 \end{bmatrix}$	$\begin{bmatrix} 1.2 & 0.0 \\ 0.0 & 1.2 \end{bmatrix}$

Table 4.2: Parameters for the lateral mode controller

As we have done in Chapter 2, we also include a set of disturbances representing errors in the split phase. These disturbances last for a time interval T_{int}. The considered disturbances are:

- the perturbation $F_{w_p} = mg\cos\theta_0$ on the aerodynamic normal force, the perturbation on drag force is $F_{u_p} = -P\sin\theta_0 = -mg\sin\theta_0$, the perturbation $M_p = mgl_r\cos\theta_0/2$ on the aerodynamic pitch moment and a small perturbation on the aerodynamic roll force during T_{int}, where l_r is the rocket length.
- three sets of time interval are simulated:
  1. $T_{int} = 0.227s$ (corresponding to solid lines in Fig. 4.1 to Fig. 4.3), produces damped oscillations by constant inputs.
  2. $T_{int} = 0.3s$, the system is unstable for a simple LQR controller (corresponding to dashed lines in Fig. 4.1 to Fig. 4.3).
  3. $T_{int} = 0.43s$ (corresponding to dash dotted lines in Fig. 4.1 to Fig. 4.3), is stabilized by the modified conditional servocompensator controller.
  4. $T_{int} = 0.44s$ (corresponding to Fig. 4.4 to Fig. 4.5), the system is unstable for this large time interval.

Results

Fig. 4.1 illustrates the convergence of the system output to the operating point of the aircraft at the end of 5s without static steady error for the three cases of $T_{int} = (0.227s, 0.3s, 0.43s)$. All system outputs are still under their physical limitations.

Figs. 4.3 shows that angular rates converge to zero in all cases. In Fig. 4.2, it can be seen that the control variables are saturated by their physical limitations due to a high perturbation on aerodynamic forces and moments.

Finally we show in Fig. 4.4 and Fig. 4.5 that the system will be unstable for an interval $T_{int} = 0.46s$.

Collision Avoidance

Airlaunch problem does not only require stability of system's states, but also to avoid the possibility of collision between the aircraft and the rocket after the drop phase. Fig. 4.6 shows the altitude of the aircraft from 0 to $1s$ in the three previous cases of study $T_{int} = (0.227s, 0.3s, 0.43s)$. They are compared with the trajectory of the rocket that drop freely with the initial airspeed of the aircraft (the solid plot). It is important to

remark that there is a small distance from the initial height of the rocket and the aircraft, representing the distance between centers of mass of the aircraft and the rocket.

In the three cases (dotted plot, dashed plot and dash dotted plot), the altitude of the aircraft satisfies the specification that requires there is no collision between the aircraft and the rocket in the airlaunch phase.

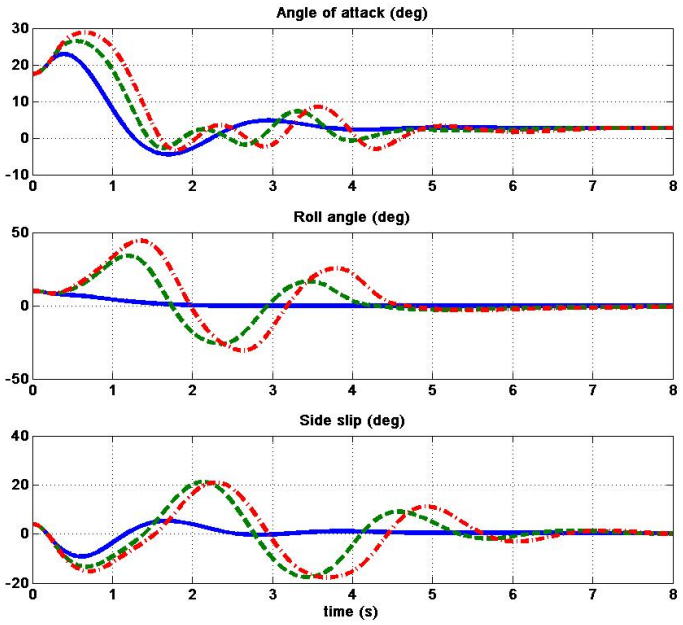

Figure 4.1: Angle of attack, Sideslip Angle and Roll angle stabilized by MCI controller

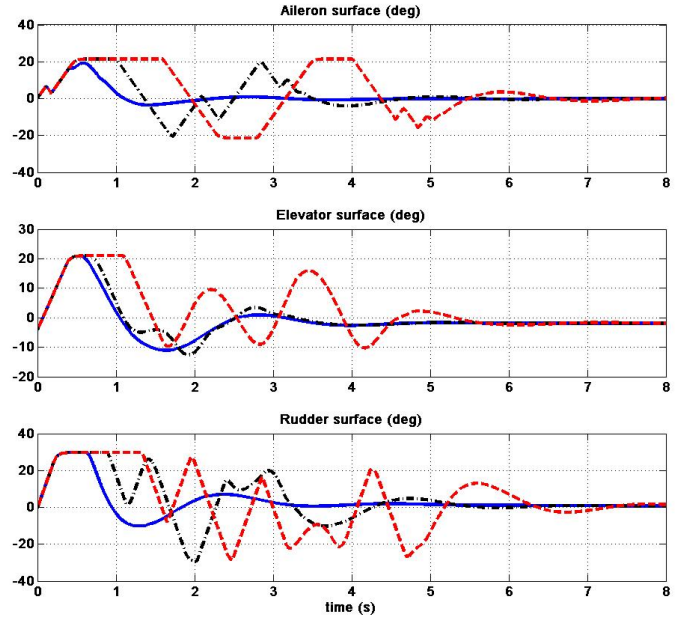

Figure 4.2: Aileron, Elevator and Rudder of MCI controller

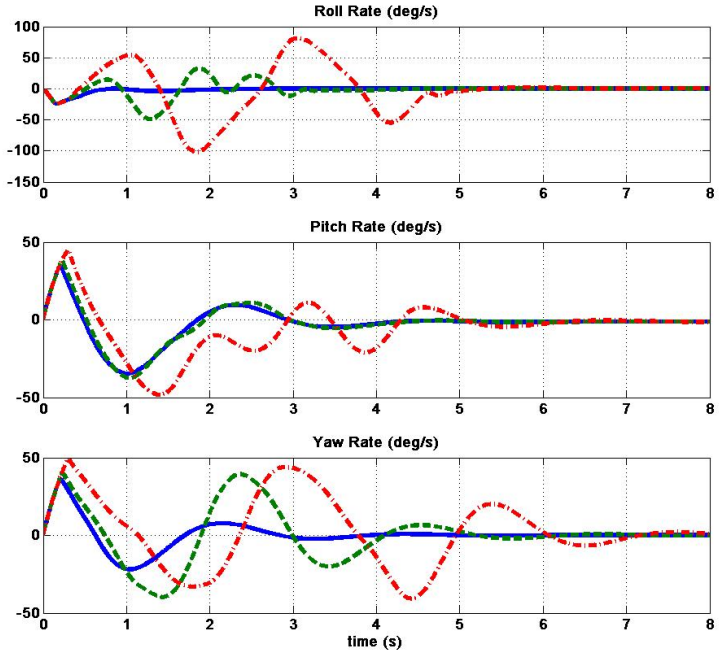

Figure 4.3: Angular rates stabilized by MCI controller

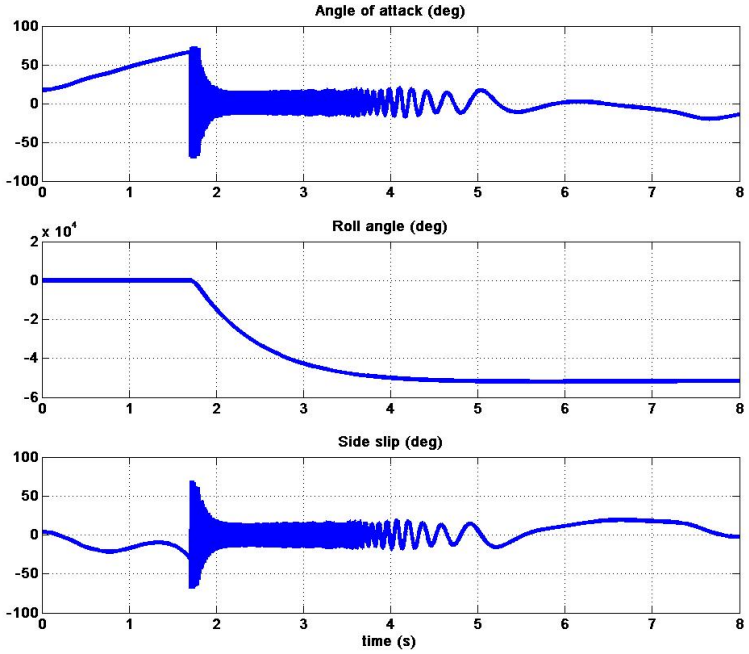

Figure 4.4: Angle of attack, Sideslip Angle and Roll angle unstable by MCI controller

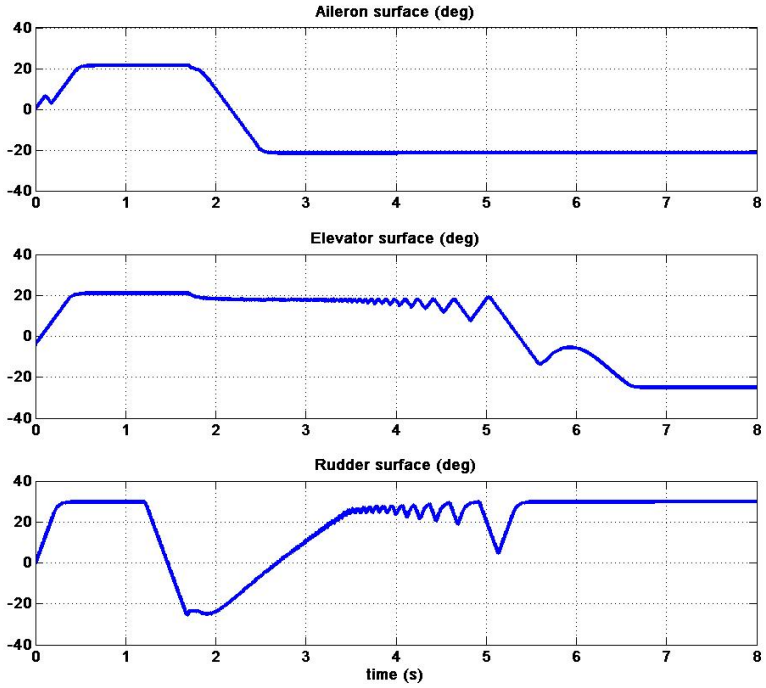

Figure 4.5: Saturation of Aileron, Elevator and Rudder with MCI controller

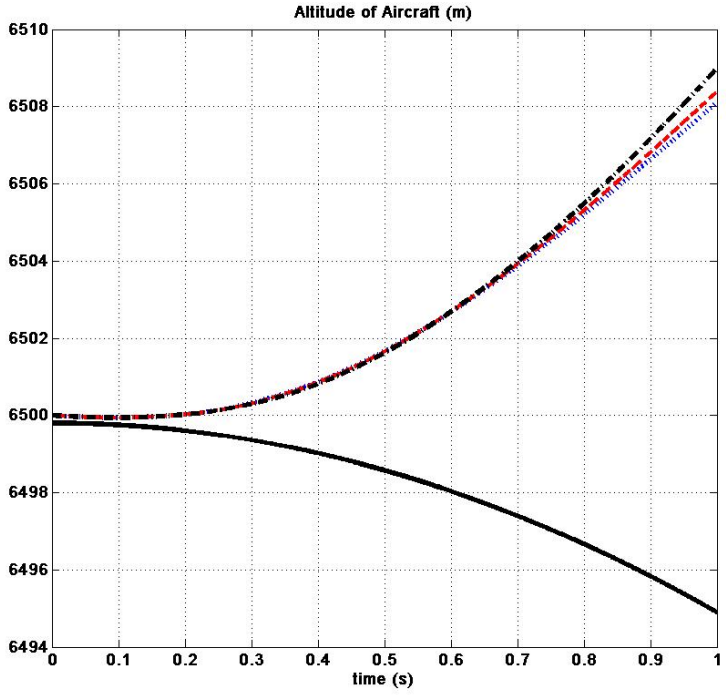

Figure 4.6: Altitude of the aircraft in the case of MCI controller

4.3 Application of modified Conditional Servocompensator Control to the Airlaunch System

In the previous section we have applied the modified Conditional Integrator control to our airlaunch system by separating the complete flight system into two modes: longitudinal mode and lateral mode, and designing then a single input single output controller for the longitudinal mode with angle of attack as the output and a multi-input multi-output lateral controller for the lateral mode with roll and sideslip angles as the output, we obtained a stabilization of our system to its equilibrium point without collision. In the same way, we can apply the modified conditional servocompensator control developed in section 3.3 to two modes of the airlaunch system by designing two controllers: longitudinal controller for angle of attack and lateral controller for roll and sideslip angles, the simulation results can also be found in Appendix A. To avoid repetition this will not be done in this section, we will show that the mCS control can also be applied to the complete airlaunch system without any separation of the system. The simulation results will be presented in the end of the section.

For the modified conditional servocompensator control to be applicable to our airlaunch system, we therefore need two assumptions 4.1.1 and 4.1.2 presented in Section 4.2. In this case, Assumption 4.2.1 is not necessary.

4.3.1 Modifed Conditional Servocompensator Control Design

The mCS control will be designed for the a complete airlaunch system after the launching phase. We define in this case the angle of attack, sideslip angle and roll angle as the system outputs and control surfaces: aileron, elevator and rudder as the control inputs.

Nonlinear control problem

Aerodynamic forces and moments can be calculated from their aerodynamic coefficients (see [13]),

$$
\begin{aligned}
F_u &= (C_x(\alpha) + \bar{c}C_{x_q}(\alpha)q/(2V))\bar{q}S \\
F_w &= (C_z(\alpha,\beta) + \bar{c}C_{z_q}(\alpha)q/(2V))\bar{q}S \\
F_v &= (C_y(\beta) + (C_{y_p}(\alpha)p + +C_{y_r}(\alpha)r)\bar{b}/(2V))\bar{q}S \\
M &= (C_m(\alpha) + C_{m_q}(\alpha)q\bar{c}/(2V) + C_{m_{\delta_e}}(\alpha)\delta_e)\bar{q}S\bar{c} \\
L &= (C_l(\beta) + C_{l_p}(\alpha,\beta)p\bar{b}/(2V) + C_{l_r}(\alpha,\beta)r\bar{b}/(2V) + C_{l_{\delta_a}}(\alpha)\delta_a + C_{l_{\delta_r}}(\alpha)\delta_r)\bar{q}S\bar{b} \\
N &= (C_n(\beta) + C_{n_p}(\alpha,\beta)p\bar{b}/(2V) + C_{n_r}(\alpha,\beta)r\bar{b}/(2V) + C_{n_{\delta_a}}(\alpha)\delta_a + C_{n_{\delta_r}}(\alpha)\delta_r)\bar{q}S\bar{b}
\end{aligned}
$$

By substituting these expressions into 2.23, the airlaunch model can be written as:

$$
\begin{aligned}
\dot{\theta} &= q\cos\phi - r\sin\phi \\
\begin{bmatrix}\dot{\alpha}\\ \dot{\beta}\\ \dot{\phi}\end{bmatrix} &= \tfrac{1}{mV}\begin{bmatrix} -\frac{1}{\cos\beta}((T + C_x\bar{q}S)\sin\alpha + C_z\bar{q}S\cos\alpha) \\ -\sin\beta((T + C_x\bar{q}S)\cos\alpha + C_z\bar{q}S\sin\alpha) + C_y\bar{q}S\cos\beta \\ 0\end{bmatrix} \\
&+ \tfrac{\rho S}{4m}\begin{bmatrix} 0 & \frac{\bar{c}S}{\cos\beta}(C_{z_q}\cos\alpha - C_{x_q}\sin\alpha) & 0 \\ C_{y_p}\bar{b}\cos\beta & -\sin\beta(C_{x_q}\cos\alpha + C_{z_q}\sin\alpha)\bar{c} & C_{y_r}\bar{b}\cos\beta \\ 0 & 0 & 0\end{bmatrix}\begin{bmatrix}p\\q\\r\end{bmatrix} \\
&+ \begin{bmatrix} -\cos\alpha\tan\beta & 1 & -\sin\alpha\tan\beta \\ \sin\alpha & 0 & -\cos\alpha \\ 1 & \sin\phi\tan\theta & \cos\phi\tan\theta\end{bmatrix}\begin{bmatrix}p\\q\\r\end{bmatrix} \\
&+ \tfrac{g}{V}\begin{bmatrix} \frac{1}{\cos\beta}(\sin\alpha\sin\theta + \cos\alpha\cos\phi\cos\theta) \\ \cos\alpha\sin\beta\sin\theta + \cos\beta\cos\theta\sin\phi - \sin\alpha\sin\beta\cos\theta\cos\phi \\ 0\end{bmatrix}
\end{aligned}
\tag{4.37}
$$

$$
\begin{aligned}
\begin{bmatrix}\dot{p}\\ \dot{q}\\ \dot{r}\end{bmatrix} &= \begin{bmatrix} I_2pq + I_1qr \\ I_5pr - I_6(p^2 - r^2) \\ I_2qr + I_8pq\end{bmatrix} + \begin{bmatrix} I_3C_l(\alpha,\beta)\bar{q}S\bar{b} + I_4C_n(\alpha,\beta)\bar{q}S\bar{b} \\ I_7C_m\bar{q}S\bar{c} \\ I_4C_l(\alpha,\beta)\bar{q}S\bar{b} + I_9C_n(\alpha,\beta)\bar{q}S\bar{b}\end{bmatrix} \\
&+ \tfrac{\rho VS}{4}\begin{bmatrix} I_3C_{lp}\bar{b} + I_4C_{np}\bar{b} & 0 & I_3C_{lr}\bar{b} + I_4C_{nr}\bar{b} \\ 0 & I_7C_{mq}\bar{c} & 0 \\ I_4C_{lp}\bar{b} + I_9C_{np}\bar{b} & 0 & I_4C_{lr}\bar{b} + I_9C_{nr}\bar{b}\end{bmatrix}\begin{bmatrix}p\\q\\r\end{bmatrix} \\
&+ \bar{q}S\begin{bmatrix} I_3C_{l\delta_a}(\alpha,\beta)\bar{b} + I_4C_{n\delta_a}(\alpha,\beta)\bar{b} & 0 & I_3C_{l\delta_r}(\alpha,\beta)\bar{b} + I_4C_{n\delta_r}(\alpha,\beta)\bar{b} \\ 0 & I_7C_{mq}\bar{c} & 0 \\ I_4C_{l\delta_a}(\alpha,\beta)\bar{b} + I_9C_{n\delta_a}(\alpha,\beta)\bar{b} & 0 & I_4C_{l\delta_r}(\alpha,\beta)\bar{b} + I_9C_{n\delta_r}(\alpha,\beta)\bar{b}\end{bmatrix}\begin{bmatrix}\delta_a\\ \delta_e\\ \delta_r\end{bmatrix}
\end{aligned}
\tag{4.38}
$$

We note that the control surfaces deflection on the aerodynamic forces are neglected, and the airspeed V is a much slower variable that can be regulated by thrust force T. T in 4.37 is then considered as constant.

Equations (4.37) and (4.38) can be rearranged as:

$$\begin{cases} \dot{\theta} & = & q\cos\phi - r\sin\phi = \eta_0(\cdot)\begin{bmatrix} p \\ q \\ r \end{bmatrix} \\ \begin{bmatrix} \dot{\alpha} \\ \dot{\beta} \\ \dot{\phi} \end{bmatrix} & = & f_{11}(\cdot) + G_1(\cdot)\begin{bmatrix} p \\ q \\ r \end{bmatrix} + f_{13}(\cdot,\theta) \\ \begin{bmatrix} \dot{p} \\ \dot{q} \\ \dot{r} \end{bmatrix} & = & f_{21}(\cdot) + f_{22}(\cdot)\begin{bmatrix} p \\ q \\ r \end{bmatrix} + G_2(\cdot)\begin{bmatrix} \delta_a \\ \delta_e \\ \delta_r \end{bmatrix} \end{cases} \tag{4.39}$$

where $\eta_0(\cdot)$, $f_{11}(\cdot)$, $G_1(\cdot)$, $f_{13}(\cdot,\theta)$, $f_{21}(\cdot)$, $f_{22}(\cdot)$ and $G_2(\cdot)$ represent the terms of (4.37) and (4.38) respectively (see Appendix A.5).

Remark 7 *Functions f_{11}, f_{22} and G_2 are function of (α,β), G_1 function of (α,β,ϕ), $f_{13}(\cdot,\theta)$ function of $(\alpha,\beta,\phi,\theta)$ while f_{21} is function of (α,β,p,q,r) and η_0 function of ϕ.*

Let us define $x_1 = \begin{bmatrix} \alpha \\ \beta \\ \phi \end{bmatrix}$, $x_2 = \dot{x}_1 = \begin{bmatrix} \dot{\alpha} \\ \dot{\beta} \\ \dot{\phi} \end{bmatrix}$ and $u = \begin{bmatrix} \delta_a \\ \delta_e \\ \delta_r \end{bmatrix}$, which allow us to write down the relationship between x_2 and ν_2, where we remind that $\nu_2 = (p,q,r)^T$.

$$x_2 = f_{11}(\cdot) + f_{13}(\cdot,\theta) + G_1(\cdot)\nu_2 \;\Leftrightarrow\; \nu_2 = G_1^{-1}(\cdot)(x_2 - f_{11}(\cdot) - f_{13}(\cdot,\theta)) \tag{4.40}$$

Derivative $\dot{x}_2$ can be easily found:

$$\begin{aligned}
\dot{x}_2 =& \tfrac{\partial f_{11}(\cdot)}{\partial x_1}x_2 + \tfrac{\partial f_{13}(x_1,\theta)}{\partial x_1}x_2 + \tfrac{\partial f_{13}(x_1,\theta)}{\partial \theta}\dot{\theta} + \tfrac{\partial (G_1(\cdot)\nu_2)}{\partial x_1}x_2 + G_1(\cdot)\dot{\nu}_2 \\
=& \tfrac{\partial f_{11}(\cdot)}{\partial x_1}x_2 + \tfrac{\partial f_{13}(x_1,\theta)}{\partial x_1}x_2 + \tfrac{\partial f_{13}(x_1,\theta)}{\partial \theta}\dot{\theta} + f(\cdot)\nu_2 + G_1(\cdot)(f_{21}(\cdot) + f_{22}\nu_2 + G_2(\cdot)u) \\
=& \tfrac{\partial f_{11}(\cdot)}{\partial x_1}x_2 + \tfrac{\partial f_{13}(x_1,\theta)}{\partial x_1}x_2 + \tfrac{\partial f_{13}(x_1,\theta)}{\partial \theta}\dot{\theta} \\
& + (f(\cdot) + G_1(\cdot)f_{22}(\cdot))G_1^{-1}(\cdot)(x_2 - f_{11}(\cdot) - f_{13}(\cdot,\theta)) + G_1(\cdot)f_{21}(\cdot) + G_1(\cdot)G_2(\cdot)u \\
=& \tfrac{\partial f_{11}(\cdot)}{\partial x_1}x_2 + (f(\cdot) + G_1(\cdot)f_{22}(\cdot))G_1^{-1}(\cdot)(x_2 - f_{11}(\cdot)) + G_1(\cdot)f_{21}(\cdot) \\
& + \tfrac{\partial f_{13}(x_1,\theta)}{\partial x_1}x_2 + \tfrac{\partial f_{13}(x_1,\theta)}{\partial \theta}\dot{\theta} - (f(\cdot) + G_1(\cdot)f_{22}(\cdot))G_1^{-1}(\cdot)f_{13}(\cdot,\theta) + G_1(\cdot)G_2(\cdot)u
\end{aligned}$$

where we note that the term $\frac{\partial (G_1(\cdot)\nu_2)}{\partial x_1}x_2$ can be transformed into $f(\cdot)\nu_2$ by a simple calculation, in which $f(\cdot)$ is function of x_1 and x_2.

We then rewrite (4.37) and (4.38) into:

$$\begin{cases} \dot{\theta} = \eta(x_1, x_2, \theta) & (4.41a) \\ \dot{x}_1 = x_2 & \\ \dot{x}_2 = Fs(\cdot) + Hs(\cdot, \theta) + Gs(\cdot)u & (4.41b) \end{cases}$$

where

$$\begin{cases} \eta(\cdot) & = \eta_0(\cdot)(G_1(\cdot))^{-1}(x_2 - f_{11}(x_1) - f_{13}(x_1, \theta)) \\ Fs(\cdot) & = \frac{\partial f_{11}(\cdot)}{\partial x_1} x_2 + (f(\cdot) + G_1(\cdot) f_{22}(\cdot)) G_1^{-1}(\cdot)(x_2 - f_{11}(\cdot)) + G_1(\cdot) f_{21}(\cdot) \\ Hs(\cdot, \theta) & = \frac{\partial f_{13}(x_1, \theta)}{\partial x_1} x_2 + \frac{\partial f_{13}(x_1, \theta)}{\partial \theta} \dot{\theta} - (f(\cdot) + G_1(\cdot) f_{22}(\cdot)) G_1^{-1}(\cdot) f_{13}(\cdot, \theta) \\ Gs(\cdot) & = G_1(\cdot) G_2(\cdot) \end{cases} \quad (4.42)$$

In (4.41), $Fs(\cdot)$ is function of x_1 and x_2. Function $Hs(\cdot)$ is function of x_1, x_2 and θ, $Hs(\cdot)$ can be expressed as:

$$\begin{aligned} Hs(\cdot) \quad = \quad & \frac{\partial f_{13}(x_1, \theta)}{\partial x_1} x_2 + \frac{\partial f_{13}(x_1, \theta)}{\partial \theta} \eta_0(x_1, x_2)(G_1(x_1))^{-1}(x_2 - f_{11}(x_1) - f_{13}(x_1, \theta)) \\ & - (f(x_1, x_2) + G_1(x_1) f_{22}(x_1)) G_1^{-1}(x_1) f_{13}(x_1, \theta) \end{aligned} \quad (4.43)$$

Remark 8 *We have some remarks:*

- η_0, f_{11}, G_1, $f_{13}(\cdot, \theta)$, f_{21}, f_{22} *and* G_2 *are function of aerodynamic coefficients under analytical forms by interpolation from wind tunnel test data.* $Fs(\cdot)$ *and* $Hs(\cdot)$*, formed from these functions, can be then bounded by a class* $\mathcal{K}$ *function and be a Lipschitz function in a flighting envelop. In the control design, we do not need a detail on these functions, we do not need to develop them then.*

- $Gs(\cdot)$ *is invertible in the flight domain, that means* $\alpha \in (-10°, 45°)$, $\theta \in (-90°, 90°)$, $\beta \in (-30°, 30°)$ *and* $\phi \in (-180°, 180°)$.

  As a consequence, they fulfill Assumptions 3.2.1 and 3.2.2.

Defining now the constant reference for the output $x_{1ref} = (\alpha_{ref}, \beta_{ref}, \phi_{ref})^T$ and the error vector $e_1 = x_1 - x_{1ref}$ and $e_2 = \dot{e}_1$. Equation (4.41b) can be transformed into:

$$\begin{cases} \dot{e}_1 = e_2 & (4.44a) \\ \dot{e}_2 = F(e_1, e_2) + H(e_1, e_2, \theta) + G(e_1, e_2)u & (4.44b) \end{cases}$$

- Function $F(e_1, e_2)$ is composed of aerodynamic coefficients, which analytical forms come from table look up wind tunnel tests, $F(e_1, e_2)$ satisfies then the assumption 3.2.1, which means $F(e_1, e_2)$ is bounded by a function of class $\mathcal{K}$ plus a constant F_0.

- Function $H(\cdot)$ depends on θ under cosines and sinus functions, it is easy to show that $H(\cdot,\theta)$ is bounded by a class $\mathcal{K}$ function $\gamma_1(\cdot)$ and a constant H_0.

$$|H(e_1,e_2,\theta)| \leq \gamma_1(|e_1|+|e_2|)+H_0 \tag{4.45}$$

- It is worth noticing that $G(e_1,e_2)$ is invertible for the entire domain of actuation of the system.

Control law

Applying the control algorithm presented in (3.31) for system (4.44) which in this case is a multi-input multi-output nonlinear system, gives the controller:

$$\begin{cases} u & = & -\Pi(e_1,e_2)sat(s/\mu) \\ \Pi(\cdot) & = & (G(\cdot))^{-1}(\Pi_0+(\gamma(\cdot)+\mu K_0+\Delta_0)I_3) \end{cases} \tag{4.46}$$

with

$$\begin{cases} s = K_0\sigma + K_1e_1 + e_2 \\ \dot{\sigma} = -K_0\sigma + \mu sat(s/\mu) \end{cases} \tag{4.47}$$

where Π_0, K_1 and K_0 are positive definite matrices and μ a positive constant.

◇

Stability Analysis

Theorem 4.3.1 *System (4.44) with $F(\cdot)$ satisfying Assumption 3.2.1, $G(\cdot)$ satisfying Assumption 3.2.2, and the control law (4.46-4.47), will globally reach an arbitrary error region in finite time, and there on will be stabilized towards its equilibrium point.*

□

Proof: We will consider the system in two regions: outside the boundary layer ($\|s\| \geq \mu$) and inside the boundary layer ($\|s\| \leq \mu$).

4.3.1.1 *In the region $\|s\| \geq \mu$, $sat(s/\mu) = s/\|s\|$.*

We differentiate the integral error measurement surface expressed in (4.47):

$$\begin{aligned} \dot{s} &= K_0\dot{\sigma} + K_1\dot{e}_1 + \dot{e}_2 \\ &= -K_0 s + \mu K_0 \text{sat}(s/\mu) + K_0(K_1e_1+e_2) + K_1e_2 + F(\cdot) + H(\cdot,\theta) + G(\cdot)u \end{aligned}$$

We define function Δ as:

$$\Delta(\cdot) = K_0(K_1e_1 + e_2) + K_1e_2 + F(\cdot) + H(\cdot, \theta)$$

The previous derivative becomes:

$$\dot{s}{=}-K_0s + \mu K_0\text{sat}(s/\mu) + \Delta(\cdot) + G(\cdot)u \tag{4.48}$$

Remark 9 *As previous remark, function $F(x_1, x_2)$ is bounded by a function $\gamma_2(\|e_1\| + \|e_2\|)$ outside the boundary region e.g. $\|s\| \geq \mu$ and a positive constant F_0, where $\gamma_2(\cdot)$ is a class $\mathcal{K}$ function.*

$$\|F(e_1, e_2)\| \leq \gamma_2(\|e_1\| + \|e_2\|) + F_0 \tag{4.49}$$

Function $H(\cdot)$ is also bounded in the same way (see (4.45)). Then $\Delta(\cdot)$ is bounded by a $\gamma(\cdot)$ class $\mathcal{K}$ function and a positive constant Δ_0:

$$\begin{array}{rcl} \|\Delta(e_1, e_2)\| & \leq & \gamma_1(\|e_1\| + \|e_2\|) + H_0 + \gamma_2(\|e_1\| + \|e_2\|) + F_0 \\ \|\Delta(e_1, e_2)\| & \leq & \gamma(\|e_1\| + \|e_2\|) + \Delta_0 \end{array} \tag{4.50}$$

where $\gamma(\cdot) = \gamma_1(\cdot) + \gamma_2(\cdot)$ and $\Delta_0 = H_0 + F_0$. $\gamma_1(\cdot)$ and $\gamma_2(\cdot)$ are chosen in the way that they are differentiable, then Lipschitz.
and as a consequence,

$$\|\Delta(e_1 = 0, e_2 = 0)\| = \|F(0, 0)\| \leq \Delta_0 \tag{4.51}$$

for $(e_1, e_2) \in \mathbb{R}^n \times \mathbb{R}^n$.

Consider the product $(s)^T\dot{s}$ inside the boundary layer.

$$\begin{array}{rcl} (s)^T\dot{s} & = & -(s)^TK_0s + \mu(s)^TK_0\text{sat}(s/\mu) + (s)^T\Delta(e_1, e_2) + (s)^Tg(e_1, e_2)u \\ & = & -(s)^TK_0s + \mu(s)^TK_0s/\|s\| + (s)^T\Delta(\cdot) - (s)^TG(\cdot)\Pi(\cdot)s/\|s\| \\ & \leq & -(s)^TK_0s + \mu(s)^TK_0s/\|s\| + \|\Delta(\cdot)\|\|s\| - (s)^TG(\cdot)\Pi(\cdot)s/\|s\| \\ & \leq & -(s)^TK_0s - (s)^T(G(\cdot)\Pi(\cdot) - \mu K_0 - (\gamma(\cdot) + \Delta_0)I_3)s/\|s\| \\ & \leq & -(s)^TK_0s - (s)^T\Pi_0s/\|s\| \\ & \leq & -\lambda_{min}(K_0)(s)^Ts - \lambda_{min}(\Pi_0)(s)^Ts/\|s\| \\ & \leq & \lambda_{min}(K_0)\|s\|^2 - \lambda_{min}(\Pi_0)\|s\| \end{array}$$

$(s)^T\dot{s}$ is then not positive and we also obtain

$$
\begin{aligned}
&(s)^T\dot{s} \leq -\lambda_{min}(K_0)\|s\|^2 - \lambda_{min}(\Pi_0)\|s\| \leq -\lambda_{min}(\Pi_0)\|s\| \\
&\therefore \quad \tfrac{d\|s\|^2}{dt} = 2\|s\|\tfrac{d(\|s\|)}{dt} = 2(s)^T\dot{s} \leq 2(-\lambda_{min}(\Pi_0)\|s\|) \\
&\therefore \quad \tfrac{d(\|s\|)}{dt} \leq -\lambda_{min}(\Pi_0) \\
&\therefore \quad \|s(t)\| \leq \|s(0)\| - \lambda_{min}(\Pi_0)t
\end{aligned}
$$

Then the integral error measurement surface $s(t)$ reaches the boundary layer μ in finite time.

.

4.3.1.2 *In the region* $\|s\| \leq \mu$, $sat(s/\mu) = s/\mu$.

Consider again (4.47) and (4.48), which inside the boundary layer may be rewritten as:

$$
\begin{cases}
\dot{\sigma} = -K_0\sigma + s & \text{(4.52a)} \\
\dot{e}_1 = -K_1 e_1 + s - K_0\sigma & \text{(4.52b)} \\
\dot{s} = \Delta(\cdot) - G(\cdot)\Pi(\cdot)s/\mu & \text{(4.52c)}
\end{cases}
$$

When $\dot{e}_1 = 0$, $\dot{\sigma} = 0$ and $\dot{s} = 0$ the system has an equilibrium point: $e_1 = e_2 = 0$, $s = \bar{s}$, $\sigma = \bar{\sigma}$ with $\bar{s} = K_0\bar{\sigma} = \mu\Pi^{-1}(0)G^{-1}(0)(F(0) + H(0,0,\theta))$,
where $F(0) = F(0,0)$, $g(0) = G(0,0)$ and $\Pi(0) = \Pi(0,0)$. $\Pi(0,0) = \Pi(e_1 = 0, e_2 = 0)$, $G(0,0) = G(e_1 = 0, e_2 = 0)$ and $F(0,0) = F(e_1 = 0, e_2 = 0)$.

System (4.52) may be rewritten with respect to $\bar{s}$ and $\bar{\sigma}$:

$$
\begin{cases}
\dot{\tilde{\sigma}} = -K_0\tilde{\sigma} + \tilde{s} & \text{(4.53a)} \\
\dot{e}_1 = -K_1 e_1 + \tilde{s} - K_0\tilde{\sigma} & \text{(4.53b)} \\
\dot{\tilde{s}} = \Delta(\cdot) - G(\cdot)\Pi(\cdot)\tilde{s}/\mu - G(\cdot)\Pi(\cdot)\bar{s}/\mu & \text{(4.53c)}
\end{cases}
$$

where $\tilde{\sigma} = \sigma - \bar{\sigma}$, $\tilde{s} = s - \bar{s}$.

Because $F(x_1, x_2)$ is a Lipschitz function inside the boundary region e.g. $\|s\| \leq \mu$ (see remark 8), one obtains:

$$
\|F(e_1, e_2) - F(0,0)\| \leq l_1\|K_1 e_1\| + l_2\|e_2\| \tag{4.54}
$$

where l_1 and $l_2 \in \mathbb{R}^+$.

Function $\gamma(\cdot)$ is a Lipschitz function in the boundary region e.g. $\|s\| \leq \mu$ (see remark 9), such that:

$$
\gamma(\cdot) \leq d_1\|K_1 e_1\| + d_2\|e_2\| \tag{4.55}
$$

where d_1 and $d_2 \in \mathbb{R}^+$.

We take again a Lyapunov candidate:

$$W = \frac{\lambda_1}{2}\tilde{\sigma}^T K_0 \tilde{\sigma} + \frac{\lambda_2}{2} e_1^T K_1 e_1 + \frac{1}{2}\tilde{s}^T \tilde{s}$$

where λ_1 and λ_2 are positive constants.

Its derivative can be easily developed as:

$$\begin{aligned}\dot{W}=&\lambda_1 \tilde{\sigma}^T K_0 \dot{\tilde{\sigma}} + \lambda_2 e_1^T K_1 \dot{e_1} + \tilde{s}^T \dot{\tilde{s}} \\ =&\lambda_1 \tilde{\sigma}^T K_0(-K_0\tilde{\sigma} + \tilde{s}) + \lambda_2 e_1^T K_1(-K_1 e_1 + \tilde{s} - K_0\tilde{\sigma}) \\ &+\tilde{s}^T(\Delta(\cdot) - G(\cdot)\Pi(\cdot)\tilde{s}/\mu - g(\cdot)\Pi(\cdot)\bar{s}/\mu)\end{aligned} \tag{4.56}$$

Since $\|s\| \leq \mu$, $\Delta(\cdot)$ can be expressed as:

$$\begin{aligned}\Delta(\cdot)=&K_0(s - K_0\sigma) + K_1(-K_1 e_1 + s - K_0\sigma) + F(\cdot) + H(\cdot,\theta) \\ =&(K_0 + K_1)\tilde{s} - (K_0 + K_1)K_0\tilde{\sigma} - K_1^2 e_1 + F(\cdot) + H(\cdot,\theta)\end{aligned}$$

In order to develop the derivative of the Lyapunov function candidate more clearly, we firstly consider the term using assumption 3.2.1:

$$\begin{aligned}&\|F(\cdot) - G(\cdot)\Pi(\cdot)\Pi^{-1}(0)g^{-1}(0)F(0)\| \\ &= \|F(\cdot) - (\Pi_0 + K_0\mu + (\gamma(\cdot) + \Delta_0)I_3)(\Pi_0 + K_0\mu + \Delta_0 I_3)^{-1}F(0)\| \\ &= \|F(\cdot) - F(0) - \gamma(\cdot)(\Pi_0 + K_0\mu + \Delta_0 I_3)^{-1}F(0)\| \\ &\leq \|F(\cdot) - F(0)\| + \|\gamma(\cdot)(\Pi_0 + K_0\mu + \Delta_0 I_3)^{-1}F(0)\| \\ &\leq \|F(\cdot) - F(0)\| + \gamma(\cdot) \leq (l_1 + d_1)\|K_1 e_1\| + (l_2 + d_2)\|e_2\|\end{aligned} \tag{4.57}$$

and then, using the relation in (3.3a) for term $(\tilde{s})^T(F(\cdot) - G(\cdot)\Pi(\cdot)\bar{s}/\mu)$:

$$\begin{aligned}&\tilde{s}^T(F(\cdot) - G(\cdot)\Pi(\cdot)\Pi^{-1}(0)g^{-1}(0)F(0)) \leq \|\tilde{s}\|\|F(\cdot) - G(\cdot)\Pi(\cdot)\Pi^{-1}(0)g^{-1}(0)F(0)\| \\ &\leq (l_1 + d_1)\|\tilde{s}\|\|K_1 e_1\| + (l_2 + d_2)\|\tilde{s}\|\|e_2\| \\ &\leq \tfrac{(l_1+d_1)}{2}(\tilde{s}^T\tilde{s} + e_1 K_1^2 e_1) + \tfrac{(l_2+d_2)}{2}(\tilde{s}^T\tilde{s} + e_2^T e_2) \\ &\leq \tfrac{(l_1+d_1)}{2}(\tilde{s}^T\tilde{s} + e_1 K_1^2 e_1) + \tfrac{(l_2+d_2)}{2}(\tilde{s}^T\tilde{s} + (\tilde{s} - K_0\tilde{\sigma} - K_1 e_1)^T(\tilde{s} - K_0\tilde{\sigma} - K_1 e_1)) \\ &\leq \tfrac{(l_1+d_1)}{2}(\tilde{s}^T\tilde{s} + e_1 K_1^2 e_1) + \tfrac{(l_2+d_2)}{2}(\tilde{s}^T\tilde{s} + 3(\tilde{s}^T\tilde{s} + \tilde{\sigma}^T K_0^2\tilde{\sigma} + e_1^T K_1^2 e_1)) \\ &\leq \tfrac{(l_1+d_1)+4(l_2+d_2)}{2}\tilde{s}^T\tilde{s} + \tfrac{3(l_2+d_2)}{2}\tilde{\sigma}^T K_0^2\tilde{\sigma} + \tfrac{(l_1+d_1)+3(l_2+d_2)}{2}e_1^T K_1^2 e_1 \\ &\leq c_1\tilde{\sigma}^T\tilde{\sigma} + c_2 e_1^T e_1 + c_3\tilde{s}^T\tilde{s}\end{aligned} \tag{4.58}$$

where $c_1 = 3/2(l_2 + d_2)\|K_0\|$, $c_2 = 1/2((l_1 + d_1) + 3/2(l_2 + d_2)\|K_1\|)$ and $c_3 = (1/2((l_1 + d_1) + 4(l_2 + d_2)) + (l_2 + d_2))$.

Because inside the boundary region e.g. $|s| \leq \mu$, functions $H(\cdot)$ and $\gamma(\cdot)$ are bounded, the following term is bounded by a positive constant:

$$\|H(\cdot,\theta) - H(0,\theta) - \gamma(\cdot)(\Pi_0 + \mu K_0 + \Delta_0 I_3)^{-1}H(0,0,\theta)\||\tilde{s}| \leq C\mu \tag{4.59}$$

where, as in the previous section, we allow the pitch θ to assume any value. Its derivative though will be shown to be stabilized.

We obtain then the derivative of Lyapunov function:

$$\begin{aligned}
\dot{W}=&-\lambda_1\tilde{\sigma}^T K_0^2\tilde{\sigma}+\lambda_1\tilde{\sigma}^T K_0\tilde{s}-\lambda_2 e_1^T K_1^2 e_1+\lambda_2 e_1^T K_1(\tilde{s}-K_0\tilde{\sigma})+(\tilde{s}^T(K_0+K_1)\tilde{s}\\
&-\tilde{s}^T(K_0+K_1)K_0\tilde{\sigma}-\tilde{s}^T K_1^2 e_1-\tilde{s}^T G(\cdot)\Pi(\cdot)\tilde{s}/\mu+\tilde{s}^T(F(\cdot)-G(\cdot)\Pi(\cdot)\bar{s}/\mu))\\
&+\tilde{s}^T(F(\cdot)+H(\cdot,\theta)-(\Pi_0+K_0\mu+(\gamma(\cdot)+\Delta_0)I_3)(\Pi_0+\mu K_0+\Delta_0 I_3)^{-1}(F(0)\\
&+H(0,0,\theta)))\\
=&-\lambda_1\tilde{\sigma}^T K_0^2\tilde{\sigma}+\lambda_1\tilde{\sigma}^T K_0\tilde{s}-\lambda_2 e_1^T K_1^2 e_1+\lambda_2 e_1^T K_1(\tilde{s}-K_0\tilde{\sigma})+(\tilde{s}^T(K_0+K_1)\tilde{s}\\
&-\tilde{s}^T(K_0+K_1)K_0\tilde{\sigma}-\tilde{s}^T K_1^2 e_1-\tilde{s}^T G(\cdot)\Pi(\cdot)\tilde{s}/\mu+\tilde{s}^T(F(\cdot)-G(\cdot)\Pi(\cdot)\bar{s}/\mu))\\
&+\tilde{s}^T(F(\cdot)-(\Pi_0+K_0\mu+(\gamma(\cdot)+\Delta_0)I_3)(\Pi_0+\mu K_0+\Delta_0 I_3)^{-1}F(0))\\
&+\tilde{s}^T(H(\cdot,\theta)-(\Pi_0+K_0\mu+(\gamma(\cdot)+\Delta_0)I_3)(\Pi_0+\mu K_0+\Delta_0 I_3)^{-1}H(0,0,\theta))
\end{aligned} \tag{4.60}$$

Using (4.58) and (4.59), the previous derivative continues to be developed:

$$\begin{aligned}
\dot{W}\leq&-\lambda_1\tilde{\sigma}^T K_0^2\tilde{\sigma}+\lambda_1/2(\tilde{s}^T\tilde{s}+\tilde{\sigma}^T K_0^2\tilde{\sigma})-\lambda_2 e_1^T K_1^2 e_1+\lambda_2/2(e_1^T K_1^2 e_1\\
&+(\tilde{s}-K_0\tilde{\sigma})^T(\tilde{s}-K_0\tilde{\sigma}))+(\tilde{s}^T(K_0+K_1)\tilde{s}+1/2(\tilde{s}^T(K_0+K_1)^2\tilde{s}+\lambda_1\tilde{\sigma}^T K_0^2\tilde{\sigma})\\
&+1/2(\tilde{s}^T K_1^2\tilde{s}+e_1^T K_1^2 e_1)-\tilde{s}^T G(\cdot)\Pi(\cdot)\tilde{s}/\mu+c_1\tilde{\sigma}^T K_0^2\tilde{\sigma}+c_2 e_1^T K_1^2 e_1+c_3\tilde{s}^T\tilde{s})\\
&+\tilde{s}^T(H(\cdot,\theta)-(\Pi_0+K_0\mu+(\gamma(\cdot)+\Delta_0)I_3)(\Pi_0+\mu K_0+\Delta_0 I_3)^{-1}H(0,0,\theta))\\
\leq&-\lambda_1\tilde{\sigma}^T K_0^2\tilde{\sigma}+\lambda_1/2(\tilde{s}^T\tilde{s}+\tilde{\sigma}^T K_0^2\tilde{\sigma})-\lambda_2 e_1^T K_1^2 e_1+\lambda_2/2(e_1^T K_1^2 e_1+2(\tilde{s}^T\tilde{s}+\tilde{\sigma}^T K_0^2\tilde{\sigma}))\\
&+(\tilde{s}^T(K_0+K_1)\tilde{s}+1/2(\tilde{s}^T(K_0+K_1)^2\tilde{s}+\tilde{\sigma}^T K_0^2\tilde{\sigma})+1/2(\tilde{s}^T K_1^2\tilde{s}+e_1^T K_1^2 e_1)\\
&-\tilde{s}^T G(\cdot)\Pi(\cdot)\tilde{s}/\mu+c_1\tilde{\sigma}^T K_0^2\tilde{\sigma}+c_2 e_1^T K_1^2 e_1+c_3\tilde{s}^T\tilde{s})\\
&+\|\tilde{s}\|\|H(\cdot,\theta)-H(0,\theta)-\gamma(\cdot)(\Pi_0+\mu K_0+\Delta_0 I_3)^{-1}H(0,0,\theta)\|\\
\leq&-\tilde{\sigma}^T(\lambda_1 K_0^2-\lambda_1/2K_0^2-\lambda_2 K_0^2-1/2K_0^2-c_1 K_0^2)\tilde{\sigma}\\
&-e_1^T(\lambda_2 K_1^2-\lambda_2/2K_1^2-1/2K_1^2-c_2 K_1^2)e_1\\
&-\tilde{s}^T((G(\cdot)\Pi(\cdot)/\mu-(K_0+K_1)-1/2(K_0+K_1)^2-1/2K_1^2-c_3 I_3)-\lambda_1/2I_3-\lambda_2 I_3)\tilde{s}\\
\leq&-(\lambda_1/2-\lambda_2-1/2-c_1)\tilde{\sigma}^T K_0^2\tilde{\sigma}-(\lambda_2/2-1/2-c_2)e_1^T K_1^2 e_1\\
&-\tilde{s}^T((\Pi_0+K_0\mu+(\gamma(\cdot)+\Delta_0)I_3)/\mu-(K_0+K_1)-1/2(K_0+K_1)^2-1/2K_1^2)\\
&-(\lambda_1/2+\lambda_2+c_3)I_3)\tilde{s}+C\mu
\end{aligned} \tag{4.61}$$

The control conditions imply that λ_1, λ_2 and $\Pi(\cdot)$ must be taken large enough and μ small enough to satisfy:

$$\begin{cases}
\lambda_1/2-\lambda_2-1/2-c_1 & >0\\
\lambda_2/2-1/2-c_2 & >0\\
(\Pi_0+\Delta_0 I_3)/\mu-K_1-1/2(K_0+K_1)^2-1/2K_1^2) & >(\lambda_1/2+\lambda_2+c_3)I_3
\end{cases}$$

Then $W(t)$ is converges to a neighborhood of zero when time tends to infinite independent of the pitch angle θ. As consequence, $e_1(t)$, σ and s tend to a region around

their equilibrium point as time tends to infinite and for every pitch angle θ. The system is ultimately bounded to a small region which is function of pitch angle θ.

4.3.2 Simulation Results

We continue now to apply the modified conditional servocompensator control technique presented in section 3.3 of chapter 3 to the airlaunch system. Unlike the modified Conditional Integrator control case where we designed two different modified Conditional Integrator controllers for two separated modes of the airlaunch system, in this case we will apply a mCS controller for the complete system.

As in the previous control application, we have considered the launch phase impact on the carrier as impulses on aerodynamic force and moments during a time interval T_{int}, and that the model following the launch phase is an F-16 which is a complete model with actuators dynamics and their limitations.

Baselines

We remind the objective of the controller designed for the airlaunch system during and after the launching phase

- the controller must return the airlaunch system to the equilibrium point of the second model which corresponds to angle of attack $\alpha_r = 4.6°$, sideslip $\beta_r = 0°$, and roll angle $\phi_r = 0°$ and all others variables to zero (at $V = 154m/s, h = 5000m$). The control surfaces at the equilibrium point are $\delta_a = 0°$, $\delta_e = -2.5°$ and $\delta_r = 0°$.
- There is no collision between airlaunch system and the rocket.
- ($\alpha_0 = 17.5°$, $\beta_0 = 4°$ and $\phi_0 = 10°$) are the initial conditions for the second model which represents the airlaunch system after the separation phase, all others variables are zero. This is the final state of the first model plus a small aleatory disturbance on the system output.

Numerical Applications

The control law is expressed as in 4.46:

$$\begin{cases} u & = & -\Pi(e_1, e_2)\text{sat}(s/\mu) \\ \Pi(\cdot) & = & G^{-1}(\cdot)(\Pi_0 + \gamma(\cdot)I_3) \end{cases}$$

where $\Pi(\cdot)$ is written in a simpler form, $\gamma(\cdot) = \gamma_1\|e_1\|^2 + \gamma_2\|e_2\|^2$, γ_1 and γ_2 positive constant and $G(\cdot)^{-1}$ defined in (4.42) (see in appendix A.5).

Π_0	μ	γ_1 and γ_2	K_0	K_1
$\begin{bmatrix} 7.0 & 0.0 & 0.0 \\ 0.0 & 9.0 & 0.0 \\ 0.0 & 0.0 & 8.0 \end{bmatrix}$	1.0	0.001 and 0.001	$\begin{bmatrix} 0.8 & 0.0 & 0.0 \\ 0.0 & 0.7 & 0.0 \\ 0.0 & 0.0 & 0.8 \end{bmatrix}$	$\begin{bmatrix} 1.3 & 0.0 & 0.0 \\ 0.0 & 1.3 & 0.0 \\ 0.0 & 0.0 & 1.5 \end{bmatrix}$

Table 4.3: Parameters for the modified conditional servocompensator controller

Π_0, γ_1, γ_2, μ, K_1 and K_0 are the set of parameters of the controller, which are determined in Table 4.3. Π_0, K_0 and K_1 are defined following the dynamic property of output variables *angle of attack*, *sideslip* and *roll angle*.

The second model is disturbed on its aerodynamic force and moments during an interval T_{int}.

- the perturbation $F_{w_p} = mg\cos\theta_0$ on the aerodynamic normal force, the perturbation on drag force is $F_{u_p} = -P\sin\theta_0 = -mg\sin\theta_0$, the perturbation $M_p = mgl_r\cos\theta_0/2$ on the aerodynamic pitch moment and a small perturbation on the aerodynamic roll force during T_{int}, where l_r is the rocket length.
- three sets of time interval are simulated:
  1. $T_{int} = 0.227s$ (corresponding to solid lines in Fig. 4.7 to Fig. 4.10), produces damped oscillations for constant inputs (Chapter 2).
  2. $T_{int} = 0.3s$ (corresponding to dashed lines in 4.7 to Fig. 4.10), the system is unstable for a simple LQR controller.
  3. $T_{int} = 0.43s$ (corresponding to dash dotted lines in 4.7 to Fig. 4.10), is stabilized by the mCS control.

We remind that the simple PI controller for the thrust to regulate airspeed is:

$$T = -k_P(V - V_{ref}) - k_I(\dot{V} - \dot{V}_{ref})$$

where V_{ref} is the airspeed reference, $k_P = 711.0$ and $k_I = 6.2$.

Results

Figs. 4.7, 4.9 and 4.10 show the output and the state variables of the system after the launching phase: angle of attack, sideslip and roll angle, three angular rates and three Euler's angles of the system. The system output return to their equilibrium value.

The angular rates return to zero, the pitch and yaw angles reach to a constant value. It illustrates the stabilization of the airlaunch system after the launching phase by the controller.

Fig. 4.12 shows the control surfaces of the system in three cases of the time interval T_{int}. When T_{int} is large, it means that the perturbation on aerodynamic forces and moments lasts, it needs a high control value for stabilizing the system. Because of the physical limit of the control surfaces, a saturation appears whenever T_{int} is large enough as we can see in the figures.

Collision Avoidance

Fig. 4.13 shows the altitude of the aircraft from 0 to 1s in the three previous cases of study $T_{int} = (0.227s, 0.3s, 0.43s)$ compared to the trajectory of the rocket that drop freely with the initial airspeed of the aircraft (the solid plot) as we did in the case of the modified Conditional Integrator control in Section 4.2. We obtain here the same result which means that there is no collision in the three sets of T_{int}.

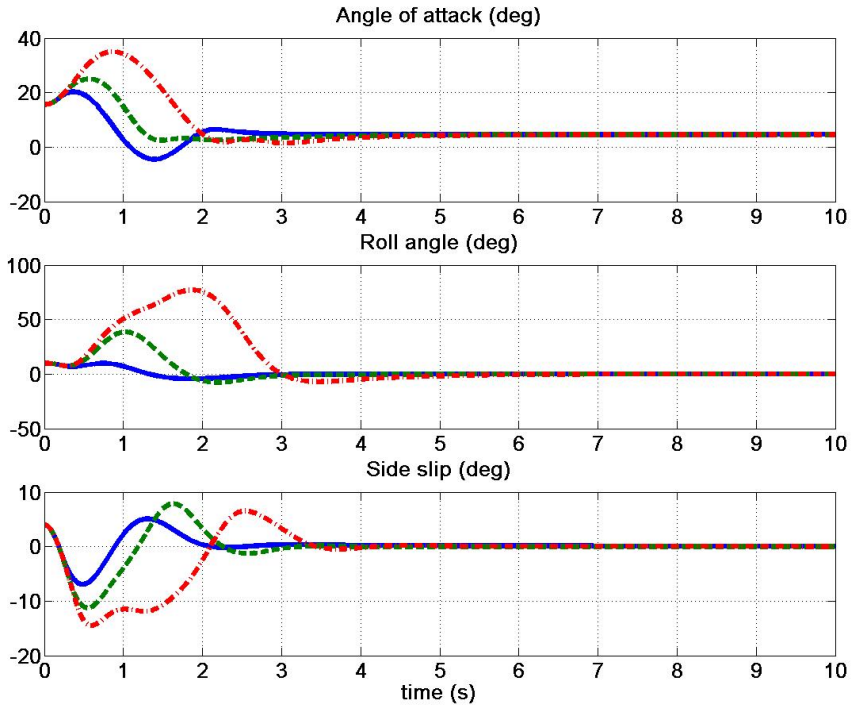

Figure 4.7: Angle of attack, Sideslip Angle and Roll angle correctly stabilized by SC controller

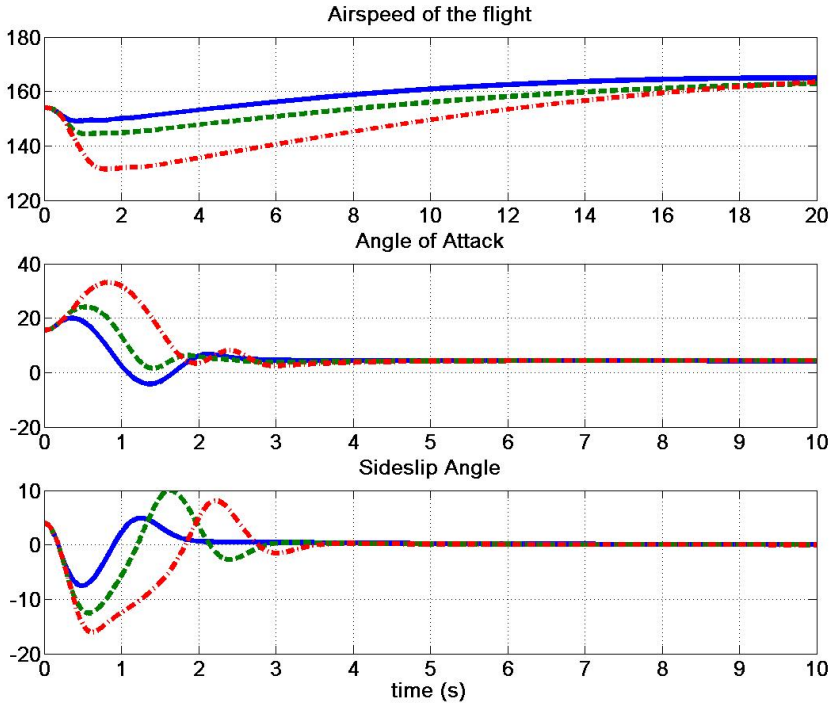

Figure 4.8: Airspeed, Angle of attack and Sideslip angle well stabilized by SC controller

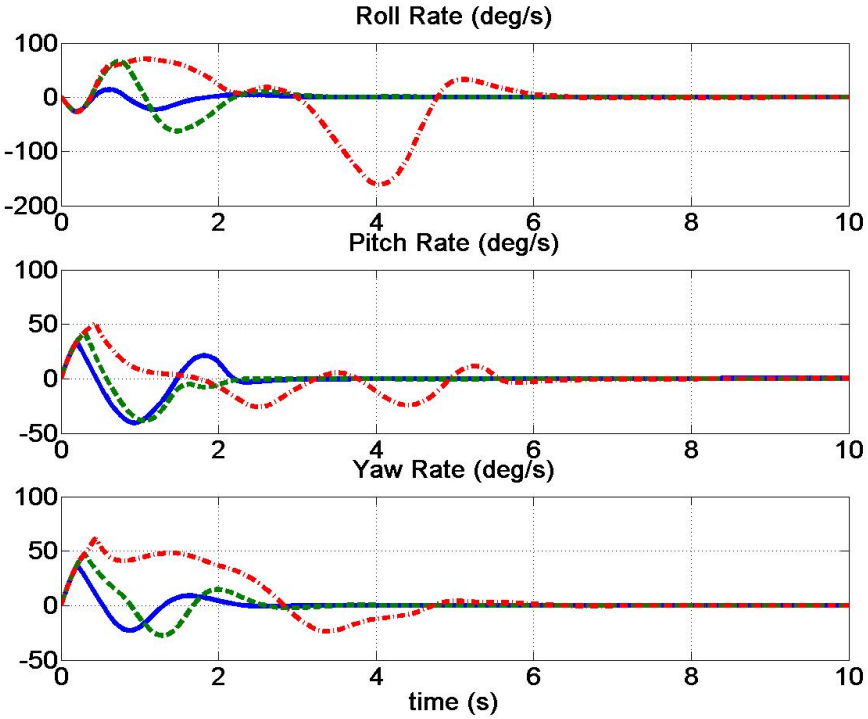

Figure 4.9: Roll rate, Pitch rate and Yaw rate correctly stabilized by SC controller

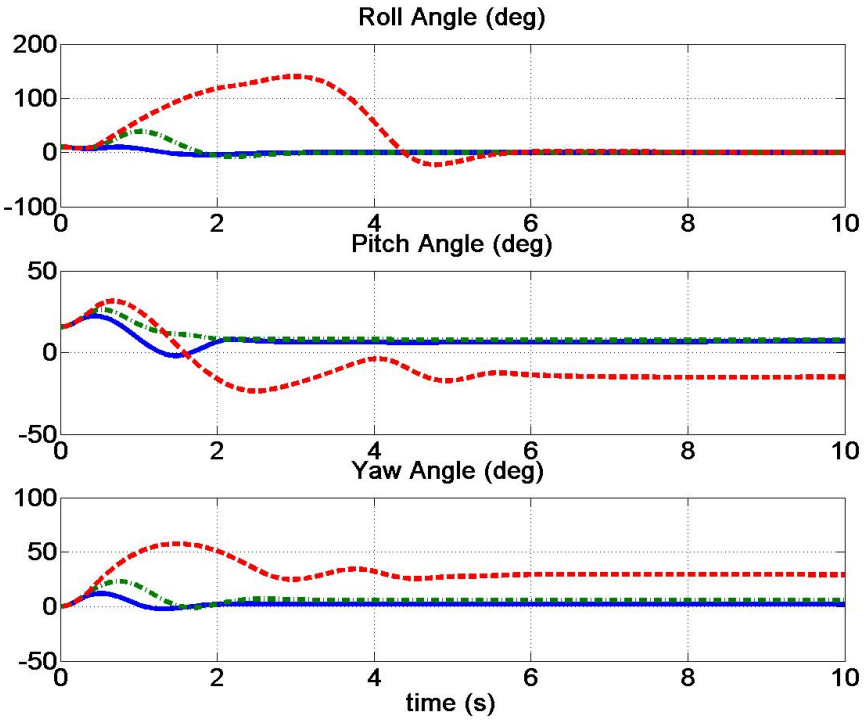

Figure 4.10: Roll angle, Pitch angle and Yaw angle stabilized by SC controller

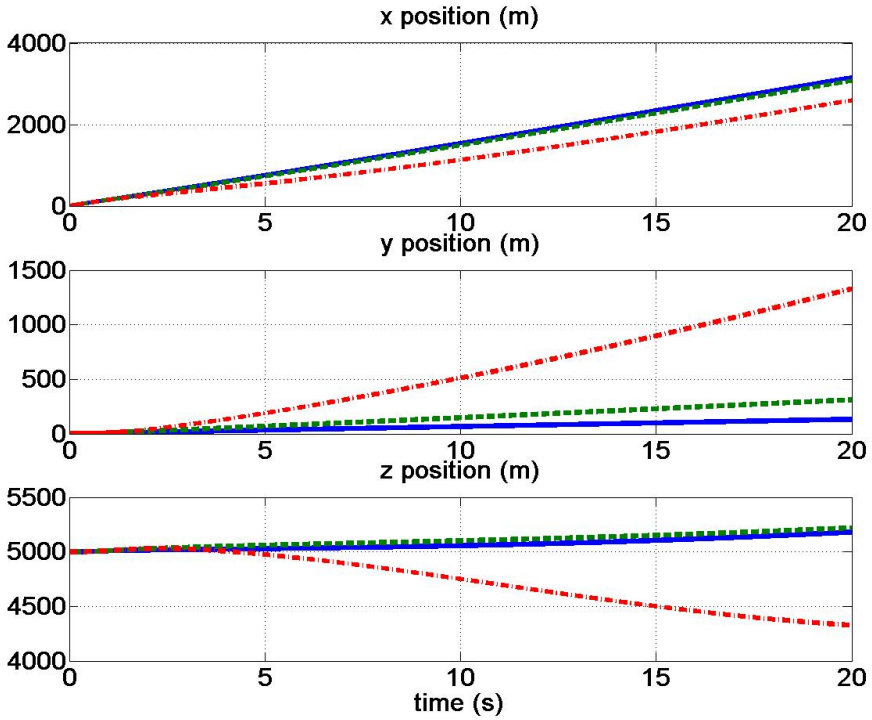

Figure 4.11: Three positions of the system with SC controller

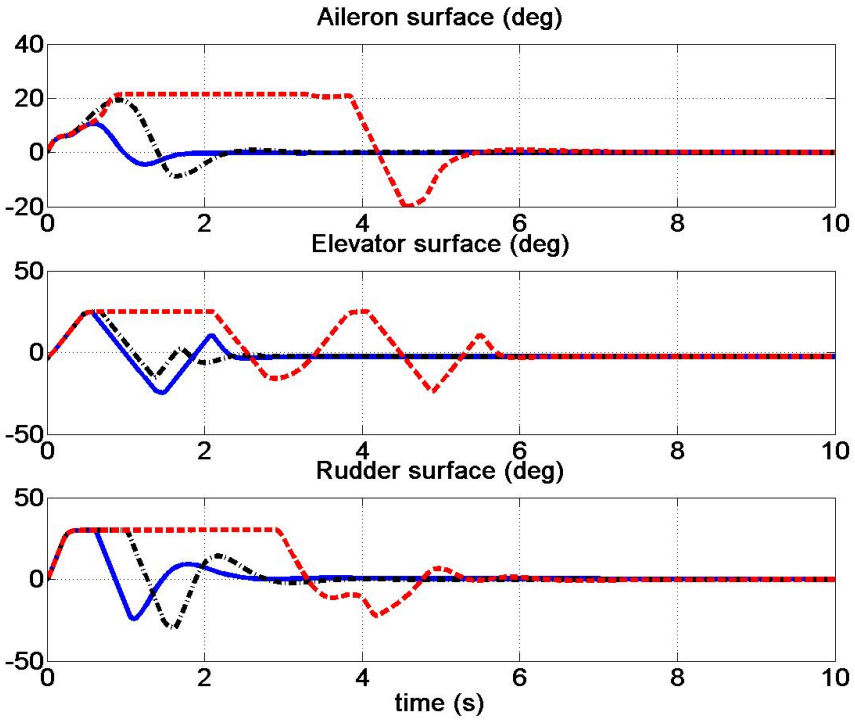

Figure 4.12: Aileron, Elevator and Rudder of SC controller

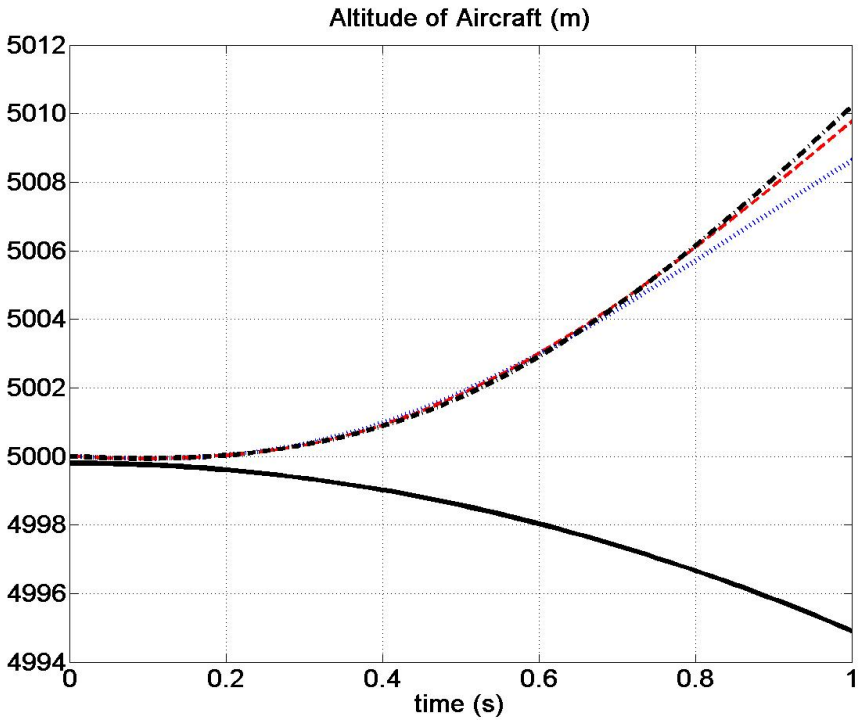

Figure 4.13: Altitude of the system in three cases of SC controller

4.4 Conclusion

In this chapter we have developed for the considered application, unmanned airlaunch, the theoretical results obtained in the previous Chapter 3. These results are the modified Conditional Integrator control and the modified conditional servocompensator control for the airlaunch system after the launching phase, modeled in Chapter 2 by impulses on aerodynamic forces and moments of the second model which represents the carrier after the separation stage, and in practice is an F-16 model. The results show the stabilization of the airlaunch system after the separation phase and collision avoidance.

The modified conditional servocompensator control is more promising if compared to the modified Conditional Integrator because it provides flexibility to adjust the parameters of the controller depending on the dynamics of each output. Although the two approaches have their limitations, the airspeed control in those approaches was still controlled by thrust through a separated PI control, that complicates the controller's parameters regulation task, and then is still an open topic for the next chapters.

Chapter 5

Full aircraft's Dynamic Feedback Linearization: Application to Airlaunch

5.1 Introduction

The works in Chapters 3 and 4 based on MIMO conditional integrator and conditional servocompensator developed gave good results on the stabilization of the airlaunch system. They have the fundamental advantage of being very robust to parameter's and model's uncertainties. In foot, those controllers only need bound functions for most system's dynamics. However the problem of full stabilization of an airlaunch system can still conveniently solved in those cases. In those results, at least one of airlaunch system's states remains uncontrolled. On the other hand the thrust force was not taken into account in the stabilization procedure. As a consequence, the available inputs are being underused while some states still need to be better controlled.

For all these reasons we suggest a new possibility of applying a dynamic feedback linearization controller for this problem. Many works have suggested feedback linearization for aircraft control when large state excursion is expected (see [51] and [7]).

Flight stabilization and control were widely studied in recent decades particularly in extreme flight conditions, such as high angle of attack or high angular rates. First there are the conventional linear design methods ([52], [53] and [54]). These methods are based on linearization that normally requires that a controller be designed for a large number of different points in the flight envelope. Other methods are based on the separation of

longitudinal control and lateral control in considering a small coupling between two motion modes (see [6] and [47]). In extreme flight conditions, their performance deteriorates due to unmodeled nonlinear effects or a strong coupling between lateral and longitudinal modes in the flight dynamics.

Nonlinear flight control offers several advantages over the conventional schemes in extreme flight conditions. This is due to the fact that the nonlinear flight control approach takes into account the nonlinearities of aerodynamic forces and moments, and the coupling of lateral and longitudinal motions. Nonlinear control schemes have also the advantage of clearly showing the interactions of states and control inputs, i.e. which states are directly controlled by which inputs.

A nonlinear flight control, based on inverse dynamics is presented in [7] and is improved as a probabilistic robust control of nonlinear uncertain flight system in [55]. The inverse dynamics control provided high performance for large angle of attack conditions. Other nonlinear approaches were based on backstepping control laws (see [56]) and backstepping and neural network control (see [9]) in the case of extreme flight conditions.

A different nonlinear approach from inverse dynamic is presented in [51] for the V/TOL aircraft and for a helicopter in [57] by using nonlinear feedback linearization. In order to be feedback linearizable, the system must satisfy necessary and sufficient conditions shown in [58] and [21]. The regulator is designed, following a system transformation, such that the system tracks the output of a reference model.

Based on the dynamic feedback linearization theory (see [18], [19] and [20]) it was proved that, given some assumptions, a simplified version of the considered system can be dynamic feedback linearizable using a first order integration of the thrust input.

These results have pointed some specific system characteristics that are further exploited in the thesis. Here it is used the dynamic feedback control strategy based on the nonlinear model to globally stabilize the full 12^{th} order airlaunch system in extreme situations after launch phase.

In this chapter, we describe in Section 5.2 the flight dynamics in the body fixed reference frame, and in Section 5.3 the dynamic feedback linearization control design, its application to the full nonlinear system model will be presented in Section 5.4. The chapter is completed by some computer simulations and conclusions.

5.2 Nonlinear control problem

In the previous chapter, we have described the flight dynamics in aerodynamic reference frame and have studied the conditional integrator and conditional servocompensator con-

trols for the airlaunch system. In order to facilitate the task of feedback linearization of the flight dynamics, the aircraft's dynamics of the airlaunch will be also described in the body fixed axes as (see [10] and [12]):

$$
\begin{cases}
\dot{x} = u\cos\psi\cos\theta + v(\cos\psi\sin\theta\sin\phi - \sin\psi\cos\phi) + w(\cos\psi\sin\theta\cos\phi + \sin\psi\sin\phi) & \text{(5.1a)}\\
\dot{y} = u\sin\psi\cos\theta + v(\sin\psi\sin\theta\sin\phi + \cos\psi\cos\phi) + w(\sin\psi\sin\theta\cos\phi - \cos\psi\sin\phi) & \text{(5.1b)}\\
\dot{z} = -u\sin\theta + v\cos\theta\sin\phi + w\cos\theta\cos\phi & \text{(5.1c)}\\
\dot{u} = rv - qw - g\sin\theta + \dfrac{1}{m}(F_u + T) & \text{(5.1d)}\\
\dot{v} = pw - ru + g\sin\phi\cos\theta + \dfrac{1}{m}F_v & \text{(5.1e)}\\
\dot{w} = qu - pv + g\cos\phi\cos\theta + \dfrac{1}{m}F_w & \text{(5.1f)}\\
\dot{\phi} = p + \tan\theta(q\sin\phi + r\cos\phi) & \text{(5.1g)}\\
\dot{\theta} = q\cos\phi - r\sin\phi & \text{(5.1h)}\\
\dot{\psi} = \dfrac{q\sin\phi + r\cos\phi}{\cos\theta} & \text{(5.1i)}\\
\dot{p} = \dfrac{1}{I_{xx}I_{zz} - I_{xz}^2}[(I_{yy}I_{zz} - I_{zz}^2 - I_{xz}^2)rq - I_{xz}(I_{xx} + I_{zz} - I_{yy})pq + I_{zz}L - I_{xz}N] & \text{(5.1j)}\\
\dot{q} = \dfrac{1}{I_{yy}}[(I_{zz} - I_{xx})pr + I_{xz}(p^2 - r^2) + M] & \text{(5.1k)}\\
\dot{r} = \dfrac{1}{I_{xx}I_{zz} - I_{xz}^2}[(-I_{xx}I_{yy} + I_{zz}^2 + I_{xz}^2)pq + I_{xz}(I_{xx} + I_{zz} - I_{yy})rq + I_{xx}N - I_{xz}L] & \text{(5.1l)}
\end{cases}
$$

where all parameters are defined in Section 2.3 of Chapter 2.

Before entering into the design of a Nonlinear Dynamic Feedback Linearization controller for stabilizing the airlaunch system after dropping phase, we state again the following standard assumption:

Assumption 5.2.1 *The control surface deflections only produce moments, not forces. Moreover, their dynamics are assumed to be fast enough to be disregarded.*

The aerodynamic forces depend only on linear velocities, not on angular rates.

The assumption means that the control surfaces deflection and angular rates have no effects on the aerodynamic forces (F_u, F_v and F_w) but only on moments L, M, N. These forces F_w, F_u and F_v depend then only on the linear velocities u, v, w. This assumption is used in the control design procedure. The stability analysis will then take in account the effects of control surfaces deflection and the dependence on angular rates.

Unlike Assumption 4.1.2, the dynamic feedback linearization control takes into account the airspeed of the airlaunch system, and it considers the thrust force as an input.

5.3 Dynamic Feedback Linearization Control for an Aircraft

5.3.1 Control Design

$$\begin{cases} \dot{x} = u\cos\psi\cos\theta + v(\cos\psi\sin\theta\sin\phi - \sin\psi\cos\phi) + w(\cos\psi\sin\theta\cos\phi + \sin\psi\sin\phi) \\ \dot{y} = u\sin\psi\cos\theta + v(\sin\psi\sin\theta\sin\phi + \cos\psi\cos\phi) + w(\sin\psi\sin\theta\cos\phi - \cos\psi\sin\phi) \\ \dot{z} = -u\sin\theta + v\cos\theta\sin\phi + w\cos\theta\cos\phi \\ \dot{u} = rv - qw - g\sin\theta + f_u + \eta \\ \dot{v} = pw - ru + g\sin\phi\cos\theta + f_v \\ \dot{w} = qu - pv + g\cos\phi\cos\theta + f_w \\ \dot{\phi} = p + \tan\theta(q\sin\phi + r\cos\phi) \\ \dot{\theta} = q\cos\phi - r\sin\phi \\ \dot{\psi} = \frac{q\sin\phi + r\cos\phi}{\cos\theta} \end{cases} \tag{5.2}$$

where $\eta = T/m$, $f_u = F_u/m$, $f_v = F_v/m$ and $f_w = F_w/m$.

As already mentioned in the introduction, previous works in dynamic feedback linearization theory have proven that, system (5.2) composed by the first nine differential equations from (5.1a) to (5.1i) which satisfies Assumption 5.2.1, can be dynamic feedback linearizable using (p, q, r) as control variables, as well as a first order integrator applied on the thrust (see [18], [19] and [20]).

We follow and make a step forward on this technique to demonstrate the dynamic feedback linearizability of the complete 12^{th} order flight dynamics. We will use a second order integration of thrust input and develop a nonlinear control algorithm in order to stabilize the aircraft and track a given trajectory.

Because (p, q, r) in (5.1) from (5.1j) to (5.1l) can be controlled by (L, M, N) and as a consequence controlled by $(\delta_a, \delta_e, \delta_r)$ contained in (L, M, N), we can, by a suitable choice of δ_a, δ_e and δ_r, simplify the angular motion of the last three equations in (5.1) as [1]:

$$\begin{cases} \dot{p} = \dot{p}_0 \\ \dot{q} = \dot{q}_0 \\ \dot{r} = \dot{r}_0 \end{cases} \tag{5.3}$$

where we consider $\dot{p}_0, \dot{q}_0, \dot{r}_0$ as the control inputs.

System (5.1) with a simplification of derivative p, q, r in (5.3) is then of the type:

[1] Remark that the three last equations in (5.1) are linear independent

$$\begin{cases} \dot{x} = u\cos\psi\cos\theta + v(\cos\psi\sin\theta\sin\phi - \sin\psi\cos\phi) + w(\cos\psi\sin\theta\cos\phi + \sin\psi\sin\phi) \\ \dot{y} = u\sin\psi\cos\theta + v(\sin\psi\sin\theta\sin\phi + \cos\psi\cos\phi) + w(\sin\psi\sin\theta\cos\phi - \cos\psi\sin\phi) \\ \dot{z} = -u\sin\theta + v\cos\theta\sin\phi + w\cos\theta\cos\phi \\ \dot{u} = rv - qw - g\sin\theta + f_u + \eta \\ \dot{v} = pw - ru + g\sin\phi\cos\theta + f_v \\ \dot{w} = qu - pv + g\cos\phi\cos\theta + f_w \\ \dot{\phi} = p + \tan\theta(q\sin\phi + r\cos\phi) \\ \dot{\theta} = q\cos\phi - r\sin\phi \\ \dot{\psi} = \frac{q\sin\phi + r\cos\phi}{\cos\theta} \\ \dot{p} = \dot{p}_0 \\ \dot{q} = \dot{q}_0 \\ \dot{r} = \dot{r}_0 \end{cases} \tag{5.4}$$

Or,

$$\dot{\xi}_s = f(\xi_s) + \dot{p}_0 g_1(\xi_s) + \dot{q}_0 g_2(\xi_s) + \dot{r}_0 g_3(\xi_s) + \eta g_4(\xi_s) \tag{5.5}$$

where f, g_1, g_2, g_3, g_4 are obtained from (5.4) respectively and $\eta = T/m$,

$$f(\xi_s) = \begin{bmatrix} u\cos\psi\cos\theta + v(\cos\psi\sin\theta\sin\phi - \sin\psi\cos\phi) + w(\cos\psi\sin\theta\cos\phi + \sin\psi\sin\phi) \\ u\sin\psi\cos\theta + v(\sin\psi\sin\theta\sin\phi + \cos\psi\cos\phi) + w(\sin\psi\sin\theta\cos\phi - \cos\psi\sin\phi) \\ -u\sin\theta + v\cos\theta\sin\phi + w\cos\theta\cos\phi \\ rv - qw - g\sin\theta + f_u + \eta \\ pw - ru + g\sin\phi\cos\theta + f_v \\ qu - pv + g\cos\phi\cos\theta + f_w \\ p + \tan\theta(q\sin\phi + r\cos\phi) \\ q\cos\phi - r\sin\phi \\ \frac{q\sin\phi + r\cos\phi}{\cos\theta} \\ 0 \\ 0 \\ 0 \end{bmatrix}$$

$$\xi_s = (x, y, z, u, v, w, \phi, \theta, \psi, p, q, r)^T$$

$$g_1 = (0,0,0,0,0,0,0,0,0,1,0,0)^T$$

$$g_2 = (0,0,0,0,0,0,0,0,0,0,1,0)^T$$

$$g_3 = (0,0,0,0,0,0,0,0,0,0,0,1)^T$$

$$g_4 = (0,0,0,1,0,0,0,0,0,0,0,0)^T$$

Or g_1, g_2, g_3 and g_4 can be displayed simply:

$$g_1 = \frac{\partial}{\partial p};\ g_2 = \frac{\partial}{\partial q};\ g_3 = \frac{\partial}{\partial r};\ g_4 = \frac{\partial}{\partial u}$$

Definition 2 *Let $\mathcal{G}$ be a distribution on a manifold M. The distribution $\mathcal{G}$ is called involutive if the Lie brackets $[X,Y] \in \mathcal{G}$ whenever X and Y are vectorfields in $\mathcal{G}$.*

▪

Theorem 5.3.1 *System (5.1) satisfying Assumption 5.2.1 is not statically linearizable, but it is dynamically linearizable with a second order of integration of the thrust force.*

◇

Proof:

System is not statically linearizable

We can compute the Lie brackets $ad_{g_i} g_j$ for $1 \leq i,j \leq 4$ and check that

- $\mathcal{G}_0 = span(g_1, g_2, g_3, g_4)$ is involutive
- $\mathcal{G}_1 = span(g_1, g_2, g_3, g_4, ad_f g_1, ad_f g_2, ad_f g_3, ad_f g_4)$ is not involutive

This result implies (see [21]) that system (5.1) is not static feedback linearizable (see Appendix B for the theorem of static feedback linearizability of a nonlinear system and the above verification).

□

System is dynamically linearizable

We have then considered the possibility of developing a dynamic feedback linearization. The first step is to acknowledge that g_4, which lies in the direction of thrust, plays an important role in the dynamics of the aircraft. For this reason, we augment the system by a second order integrator on the thrust (η,$\dot{\eta}$, $\ddot{\eta}$), and check the condition for dynamic feedback linearization.

$$\begin{cases} \Delta_0 = span(g_1, g_2, g_3) \\ \Delta_1 = \Delta_0 + ad_f \Delta_0 + span\{g_4\} \\ \Delta_2 = \Delta_1 + ad_f \Delta_1 + span\{g_4\} \\ \Delta_3 = \Delta_2 + ad_f \Delta_2 = \mathbb{R}^{12} \end{cases} \tag{5.6}$$

System (5.6) satisfies all sufficient conditions of the theory presented in [20] and [22], which means(see Appendix B):

- Δ_0 is involutive and has rank 3
- Δ_1 is involutive and has rank 7
- Δ_2 is involutive and has rank 10
- Δ_3 is involutive and has rank 12

The extended system in (5.1) with the simplified equations (5.3) and the second order integrator on thrust is dynamic feedback linearizable. This can be physically explained by the fact that engine dynamics of thrust are of second order type, as mentioned in [7].

□

The work in [22] has shown that the system composed by the nine first differential equations of (5.1), using $(p, q, r, \dot{\eta})$ as control variables, can be dynamically feedback linearized. There it is first defined $\zeta_1 = x$, $\zeta_2 = y$, $\zeta_3 = z$, $\sigma_1 = \eta$. Then, a change of coordinates from $\tilde{X} = (x, y, z, u, v, w, \phi, \theta, \psi, \eta)$ to $\tilde{\zeta} = (x, L_{\tilde{f}}x, L^2_{\tilde{f}}x, y, L_{\tilde{f}}y, L^2_{\tilde{f}}y, z, L_{\tilde{f}}z, L^2_{\tilde{f}}z, \sigma_1)$ makes the nine first differential equations in (5.1) feedback linearizable in respect to the control variables $(p, q, r, \dot{\eta})$. There, (5.2) with $v_4 = \dot{\eta} = \dot{T}/m$ is rewritten in the form $\dot{\tilde{X}} = \tilde{f} + \tilde{g}\tilde{u}$.

In this thesis, distinctly from [22], we will define σ_1 as another variable to avoid singularity of the matrix $\gamma_1(\cdot)$ that we will introduce later.

For this reason, now the nine first differential equations 5.2 and the first order integrator on the thrust can be transformed into a new feedback linearizable system as:

$$\begin{cases} \dot{\zeta}_1 = \zeta_4 = L_{\tilde{f}}x \\ \dot{\zeta}_2 = \zeta_5 = L_{\tilde{f}}y \\ \dot{\zeta}_3 = \zeta_6 = L_{\tilde{f}}z \\ \dot{\zeta}_4 = \zeta_7 = L^2_{\tilde{f}}x \\ \dot{\zeta}_5 = \zeta_8 = L^2_{\tilde{f}}y \\ \dot{\zeta}_6 = \zeta_9 = L^2_{\tilde{f}}z \\ \dot{\zeta}_7 = D^0_1 + D^1_1 p + D^2_1 q + D^3_1 r + D^4_1 v_4 \\ \dot{\zeta}_8 = D^0_2 + D^1_2 p + D^2_2 q + D^3_2 r + D^4_2 v_4 \\ \dot{\zeta}_9 = D^0_3 + D^1_3 p + D^2_3 q + D^3_3 r + D^4_3 v_4 \\ \dot{\sigma}_1 = D^0_4 + D^1_4 p + D^2_4 q + D^3_4 r + D^4_4 v_4 \end{cases} \tag{5.7}$$

where $v_4 = \dot{\eta}$ and D^i_j for $i = 1..4$, $j = 0..3$ are function of $\tilde{X}$ and can be computed:

$$\zeta_4 = u\cos\theta\cos\psi + v(\cos\psi\sin\theta\sin\phi - \cos\phi\sin\psi) + w(\sin\theta\cos\phi\cos\psi + \sin\phi\sin\psi)$$

$$\zeta_5 = u\cos\theta\sin\psi + v(\sin\psi\sin\theta\sin\phi + \cos\phi\cos\psi) + w(\sin\theta\cos\phi\sin\psi - \sin\phi\cos\psi)$$

$$\zeta_6 = -\sin\theta u + v\cos\theta\sin\phi + w\cos\theta\cos\phi$$

$$\begin{aligned}
\zeta_7 &= \cos\theta\cos\psi(-g\sin\theta + f_u + \eta) + (\cos\psi\sin\theta\sin\phi - \cos\phi\sin\psi)(g\cos\theta\sin\phi + f_v) \\
&\quad + (\sin\theta\cos\phi\cos\psi + \sin\phi\sin\psi)(g\cos\phi\cos\theta + f_w) \\
\zeta_8 &= \cos\theta\sin\psi(-g\sin\theta + f_u + \eta) + (\sin\psi\sin\theta\sin\phi + \cos\phi\cos\psi)(g\cos\theta\sin\phi + f_v) \\
&\quad + (\sin\theta\cos\phi\sin\psi - \sin\phi\cos\psi)(g\cos\phi\cos\theta + f_w) \\
\zeta_9 &= -\sin\theta(-g\sin\theta + f_u + \eta) + \cos\theta\sin\phi(g\cos\theta\sin\phi + f_v) \\
&\quad + \cos\theta\cos\phi(g\cos\phi\cos\theta + f_w)
\end{aligned}$$

$$\begin{aligned}
D_1^0 &= L_{\tilde{f}} f_u \cos\theta\cos\psi + L_{\tilde{f}} f_v(\cos\psi\sin\theta\sin\phi - \cos\phi\sin\psi) \\
&\quad + L_{\tilde{f}} f_w(\sin\theta\cos\phi\cos\psi + \sin\phi\sin\psi) \\
D_2^0 &= L_{\tilde{f}} f_u \cos\theta\sin\psi + L_{\tilde{f}} f_v(\sin\psi\sin\theta\sin\phi + \cos\phi\cos\psi) \\
&\quad + L_{\tilde{f}} f_w(\sin\theta\cos\phi\sin\psi - \sin\phi\cos\psi) \\
D_3^0 &= -L_{\tilde{f}} f_u \sin\theta + L_{\tilde{f}} f_v \cos\theta\sin\phi + L_{\tilde{f}} f_w \cos\theta\cos\phi
\end{aligned}$$

$$\begin{aligned}
D_1^1 &= f_v(\sin\theta\cos\phi\cos\psi + \sin\phi\sin\psi) - f_w(\cos\psi\sin\theta\sin\phi - \cos\phi\sin\psi) + d_1^1 \\
D_1^2 &= -(f_u + \eta)(\sin\theta\cos\phi\cos\psi + \sin\phi\sin\psi) + f_w\cos\theta\cos\psi + d_1^2 \\
D_1^3 &= (f_u + \eta)(\cos\psi\sin\theta\sin\phi - \cos\phi\sin\psi) - f_v\cos\theta\cos\psi + d_1^3 \\
D_1^4 &= \cos\theta\cos\psi
\end{aligned}$$

$$\begin{aligned}
D_2^1 &= f_v(\sin\theta\cos\phi\sin\psi - \sin\phi\cos\psi) - f_w(\sin\psi\sin\theta\sin\phi + \cos\phi\cos\psi) + d_2^1 \\
D_2^2 &= -(f_u + \eta)(\sin\theta\cos\phi\sin\psi - \sin\phi\cos\psi) + f_w\cos\theta\sin\psi + d_2^2 \\
D_2^3 &= (f_u + \eta)(\sin\psi\sin\theta\sin\phi + \cos\phi\cos\psi) - f_v\cos\theta\sin\psi + d_2^3 \\
D_2^4 &= \cos\theta\sin\psi
\end{aligned}$$

$$\begin{aligned}
D_3^1 &= f_v\cos\theta\cos\phi - f_w\cos\theta\sin\phi + d_3^1 \\
D_3^2 &= -(f_u + \eta)\cos\theta\cos\phi - f_w\sin\theta + d_3^2 \\
D_3^3 &= (f_u + \eta)\cos\theta\sin\phi + f_v\sin\theta + d_3^3 \\
D_3^4 &= -\sin\theta
\end{aligned}$$

D_4^0, D_4^1, D_4^2, D_4^3 and D_4^4 will depend on the choice of the last variable with

$$
\begin{aligned}
d_1^i &= L_{g_i} f_u \cos\theta\cos\psi + L_{g_i} f_v(\cos\psi\sin\theta\sin\phi - \cos\phi\sin\psi) \\
&\quad + L_{g_i} f_w(\sin\theta\cos\phi\cos\psi + \sin\phi\sin\psi) \quad \text{for } 1 \le i \le 3 \\
d_2^i &= L_{g_i} f_u \cos\theta\sin\psi + L_{g_i} f_v(\sin\psi\sin\theta\sin\phi + \cos\phi\cos\psi) \\
&\quad + L_{g_i} f_w((\sin\theta\cos\phi\sin\psi - \sin\phi\cos\psi) \quad \text{for } 1 \le i \le 3 \\
d_3^i &= -L_{g_i} f_u \sin\theta + L_{g_i} f_v \cos\theta\sin\phi + L_{g_i} f_w \cos\theta\cos\phi \qquad \text{for } 1 \le i \le 3
\end{aligned}
$$

and

$$
\begin{aligned}
L_{\tilde{f}} f_u &= \frac{\partial f_u}{\partial u}(-g\sin\theta + f_u) + \frac{\partial f_u}{\partial v}(g\sin\phi\cos\theta + f_v) + \frac{\partial f_u}{\partial w}(g\cos\phi\cos\theta + f_w) \\
L_{\tilde{f}} f_v &= \frac{\partial f_v}{\partial u}(-g\sin\theta + f_u) + \frac{\partial f_v}{\partial v}(g\sin\phi\cos\theta + f_v) + \frac{\partial f_v}{\partial w}(g\cos\phi\cos\theta + f_w) \\
L_{\tilde{f}} f_w &= \frac{\partial f_w}{\partial u}(-g\sin\theta + f_u) + \frac{\partial f_w}{\partial v}(g\sin\phi\cos\theta + f_v) + \frac{\partial f_w}{\partial w}(g\cos\phi\cos\theta + f_w)
\end{aligned}
$$

$$
\begin{aligned}
L_{g_1} f_u &= w\frac{\partial f_u}{\partial v} - v\frac{\partial f_u}{\partial w};\ L_{g_2} f_u = -w\frac{\partial f_u}{\partial u} + u\frac{\partial f_u}{\partial w};\ L_{g_3} f_u = v\frac{\partial f_u}{\partial u} - u\frac{\partial f_u}{\partial v} \\
L_{g_1} f_v &= w\frac{\partial f_v}{\partial v} - v\frac{\partial f_v}{\partial w};\ L_{g_2} f_v = -w\frac{\partial f_v}{\partial u} + u\frac{\partial f_v}{\partial w};\ L_{g_3} f_v = v\frac{\partial f_v}{\partial u} - u\frac{\partial f_v}{\partial v} \\
L_{g_1} f_w &= w\frac{\partial f_w}{\partial v} - v\frac{\partial f_w}{\partial w};\ L_{g_2} f_w = -w\frac{\partial f_w}{\partial u} + u\frac{\partial f_w}{\partial w};\ L_{g_3} f_w = v\frac{\partial f_w}{\partial u} - u\frac{\partial f_w}{\partial v}
\end{aligned}
$$

From (5.7), we define four new variables $\zeta_{10} = \dot{\zeta}_7$, $\zeta_{11} = \dot{\zeta}_8$, $\zeta_{12} = \dot{\zeta}_9$ and $\sigma_2 = \dot{\sigma}_1$.

$$
\begin{bmatrix} \zeta_{10} \\ \zeta_{11} \\ \zeta_{12} \\ \sigma_2 \end{bmatrix} = \chi_1(\tilde{X}) + \gamma_1(\tilde{X}) \begin{bmatrix} p \\ q \\ r \\ v_4 \end{bmatrix} \tag{5.8}
$$

where

$$
\chi_1(\tilde{X}) = \begin{bmatrix} D_0^1 \\ D_0^2 \\ D_0^3 \\ D_0^4 \end{bmatrix}; \gamma_1(\cdot) = \begin{bmatrix} D_1^1 & D_1^2 & D_1^3 & D_1^4 \\ D_2^1 & D_2^2 & D_2^3 & D_2^4 \\ D_3^1 & D_3^2 & D_3^3 & D_3^4 \\ D_4^1 & D_4^2 & D_4^3 & D_4^4 \end{bmatrix} \tag{5.9}
$$

D_4^i for $i = 1..4$ are function of $\tilde{X}$ and depend on the choice of variable σ_1 to avoid singularity of $\gamma_1(\cdot)$.

We return to the angular dynamics which was simplified in (5.3). Noticing in this time that L, M, N are function of system states and control surfaces:

$$
L = (C_l(\beta) + C_{l_p}(\alpha,\beta)p\bar{b}/(2V) + C_{l_r}(\alpha,\beta)r\bar{b}/(2V) + C_{l_{\delta_a}}(\alpha)\delta_a + C_{l_{\delta_r}}(\alpha)\delta_r)\bar{q}S\bar{b}
$$

$$M = (C_m(\alpha) + C_{m_q}(\alpha)q\bar{c}/(2V) + C_{m_{\delta_e}}(\alpha)\delta_e)\bar{q}S\bar{c}$$

$$N = (C_n(\beta) + C_{n_p}(\alpha,\beta)p\bar{b}/(2V) + C_{n_r}(\alpha,\beta)r\bar{b}/(2V) + C_{n_{\delta_a}}(\alpha)\delta_a + C_{n_{\delta_r}}(\alpha)\delta_r)\bar{q}S\bar{b}$$

Substituting L, M, N into the three last equations in 5.1, The angular dynamics are then rewritten as:

$$\begin{aligned}\begin{bmatrix}\dot{p}\\ \dot{q}\\ \dot{r}\end{bmatrix} &= \begin{bmatrix} I_2pq + I_1qr \\ I_5pr - I_6(p^2 - r^2) \\ I_2qr + I_8pq \end{bmatrix} + \begin{bmatrix} I_3C_l(\alpha,\beta)\bar{q}S\bar{b} + I_4C_n(\alpha,\beta)\bar{q}S\bar{b} \\ I_7C_m(\alpha)\bar{q}S\bar{c} \\ I_4C_l(\alpha,\beta)\bar{q}S\bar{b} + I_9C_n(\alpha,\beta)\bar{q}S\bar{b} \end{bmatrix} \\ &+\tfrac{\rho VS}{4}\begin{bmatrix} I_3C_{lp}(\alpha)\bar{b} + I_4C_{np}(\alpha)\bar{b} & 0 & I_3C_{lr}(\alpha)\bar{b} + I_4C_{nr}(\alpha)\bar{b} \\ 0 & I_7C_{mq}(\alpha)\bar{c} & 0 \\ I_4C_{lp}(\alpha)\bar{b} + I_9C_{np}(\alpha)\bar{b} & 0 & I_4C_{lr}(\alpha)\bar{b} + I_9C_{nr}(\alpha)\bar{b} \end{bmatrix}\begin{bmatrix}p\\q\\r\end{bmatrix} \\ &+\bar{q}S\begin{bmatrix} I_3C_{l\delta_a}(\alpha,\beta)\bar{b} + I_4C_{n\delta_a}(\alpha,\beta)\bar{b} & 0 & I_3C_{l\delta_r}(\alpha,\beta)\bar{b} + I_4C_{n\delta_r}(\alpha,\beta)\bar{b} \\ 0 & I_7C_{mq}(\alpha)\bar{c} & 0 \\ I_4C_{l\delta_a}(\alpha,\beta)\bar{b} + I_9C_{n\delta_a}(\alpha,\beta)\bar{b} & 0 & I_4C_{l\delta_r}(\alpha,\beta)\bar{b} + I_9C_{n\delta_r}(\alpha,\beta)\bar{b} \end{bmatrix}\begin{bmatrix}\delta_a\\\delta_e\\\delta_r\end{bmatrix}\end{aligned} \tag{5.10}$$

where $I_3 = \frac{I_{zz}}{(I_{xx}I_{zz} - I_{xz}^2)}$, $I_4 = \frac{I_{xz}}{(I_{xx}I_{zz} - I_{xz}^2)}$, $I_9 = \frac{I_{xx}}{(I_{xx}I_{zz} - I_{xz}^2)}$ and $I_7 = 1/I_{yy}$. $C_x(\alpha)$, $C_{x_q}(\alpha)$, $C_z(\alpha)$, $C_{z_q}(\alpha)$, $C_m(\alpha)$, $C_{m_q}(\alpha)$ $C_{m_{\delta_e}}(\alpha)$, $C_y(\alpha,\delta_e)$, $C_{y_p}(\alpha)$, $C_{y_r}(\alpha)$, $C_l(\alpha,\beta)$, $C_n(\alpha,\beta)$, $C_{l_p}(\alpha)$, $C_{n_p}(\alpha)$, $C_{l_r}(\alpha)$, $C_{n_r}(\alpha)$, $C_{l_{\delta_a}}(\alpha)$, $C_{n_{\delta_a}}(\alpha)$, $C_{l_{\delta_r}}(\alpha)$, $C_{n_{\delta_r}}(\alpha)$ are aerodynamic coefficients taken from [48].

We can rewrite more symbolically the previous expression,

$$\begin{bmatrix}\dot{p}\\\dot{q}\\\dot{r}\end{bmatrix} = \chi_r(u,v,w,p,q,r) + \gamma_r(u,v,w)\begin{bmatrix}\delta_a\\\delta_e\\\delta_r\end{bmatrix} \tag{5.11}$$

then,

$$\begin{bmatrix}\dot{p}\\\dot{q}\\\dot{r}\\\dot{v}_4\end{bmatrix} = \begin{bmatrix}\chi_r(\cdot)\\0\end{bmatrix} + \begin{bmatrix}\gamma_r(u,v,w) & 0\\0 & 1\end{bmatrix}\begin{bmatrix}\delta_a\\\delta_e\\\delta_r\\\dot{v}_4\end{bmatrix}$$

where $\chi_r(u,v,w,p,q,r) \in \mathbb{R}^{3\times 1}$, $\gamma_r(u,v,w) \in \mathbb{R}^{3\times 3}$ represent the terms in (5.10) respectively. It is important to remark that matrix $\gamma_r(u,v,w)$ is invertible in the required flight envelop.

The derivatives of (5.8) can be easily found using (5.11):

$$\begin{aligned}
\begin{bmatrix} \dot{\zeta}_{10} \\ \dot{\zeta}_{11} \\ \dot{\zeta}_{12} \\ \dot{\sigma}_2 \end{bmatrix} =& \dot{\chi}_1(\tilde{X}) + \dot{\gamma}_1(\tilde{X}) \begin{bmatrix} p \\ q \\ r \\ v_4 \end{bmatrix} + \gamma_1(\tilde{X}) \begin{bmatrix} \chi_r(\cdot) \\ 0 \end{bmatrix} + \gamma_1(\tilde{X}) \begin{bmatrix} \gamma_r(u,v,w)0 \\ 0 \quad 1 \end{bmatrix} \begin{bmatrix} \delta_a \\ \delta_e \\ \delta_r \\ \dot{v}_4 \end{bmatrix} \\
=& \chi_T(\tilde{X}, p, q, r, v_4) + \gamma_1(\tilde{X}) \begin{bmatrix} \gamma_r(u,v,w)0 \\ 0 \quad 1 \end{bmatrix} \begin{bmatrix} \delta_a \\ \delta_e \\ \delta_r \\ \dot{v}_4 \end{bmatrix} \\
=& \chi_T(\tilde{X}, p, q, r, v_4) + \gamma_T(\tilde{X}) \begin{bmatrix} \delta_a \\ \delta_e \\ \delta_r \\ \dot{v}_4 \end{bmatrix}
\end{aligned} \tag{5.12}$$

where

$$\chi_T(\tilde{X}) = \dot{\chi}_1(\tilde{X}) + \dot{\gamma}_1(\tilde{X}) \begin{bmatrix} p \\ q \\ r \\ v_4 \end{bmatrix} + \gamma_1(\tilde{X}) \begin{bmatrix} \chi_r(\cdot) \\ 0 \end{bmatrix} \tag{5.13}$$

$$\gamma_T(\tilde{X}) = \gamma_1(\tilde{X}) \begin{bmatrix} \gamma_r(u,v,w)0 \\ 0 \quad 1 \end{bmatrix} \tag{5.14}$$

By defining $v_4 = \dot{\nu} = \tau$ as a state variable, $\dot{v}_4$ as the input u_T, we have a feedback linearizable system in (5.7) and (5.12) with 14 states by the change of coordinates from $(x, y, z, u, v, w, \phi, \theta, \psi, p, q, r, \eta, \tau)$ to $(\zeta_1, \zeta_2, \zeta_3, \zeta_4, \zeta_5, \zeta_6, \zeta_7, \zeta_8, \zeta_9, \zeta_{10}, \zeta_{11}, \zeta_{12}, \sigma_1, \sigma_2)$.

$$
\begin{cases}
\dot{\zeta}_1 = \zeta_4 = L_{\tilde{f}} x \\
\dot{\zeta}_2 = \zeta_5 = L_{\tilde{f}} y \\
\dot{\zeta}_3 = \zeta_6 = L_{\tilde{f}} z \\
\dot{\zeta}_4 = \zeta_7 = L^2_{\tilde{f}} x \\
\dot{\zeta}_5 = \zeta_8 = L^2_{\tilde{f}} y \\
\dot{\zeta}_6 = \zeta_9 = L^2_{\tilde{f}} z \\
\dot{\zeta}_7 = \zeta_{10} = D^1_0 + D^1_1 p + D^2_1 q + D^3_1 r + D^4_1 \tau \\
\dot{\zeta}_8 = \zeta_{11} = D^2_0 + D^1_2 p + D^2_2 q + D^3_2 r + D^4_2 \tau \\
\dot{\zeta}_9 = \zeta_{12} = D^3_0 + D^1_3 p + D^2_3 q + D^3_3 r + D^4_3 \tau \\
\dot{\sigma}_1 = \sigma_2 = D^4_0 + D^1_4 p + D^2_4 q + D^3_4 r + D^4_4 \tau \\
\begin{bmatrix} \dot{\zeta}_{10} \\ \dot{\zeta}_{11} \\ \dot{\zeta}_{12} \\ \dot{\sigma}_2 \end{bmatrix} = \chi_T(\tilde{X}, p, q, r, \tau) + \gamma_1(\tilde{X}) \begin{bmatrix} \gamma_r(u, v, w) & 0 \\ 0 & 1 \end{bmatrix} \begin{bmatrix} \delta_a \\ \delta_e \\ \delta_r \\ u_T \end{bmatrix}
\end{cases} \tag{5.15}
$$

In (5.15), we have 12 physical states from the aircraft, and 2 states from the integration of thrust. We need now the nonsingularity of $\gamma_T(\cdot)$, that means the nonsingularity of matrix $\gamma_1(\cdot)$, since $\gamma_r(\cdot)$ is nonsingular by the physical characteristics of the aircraft in the required flying envelop.

Now we will define σ_1 as ϕ, which has the dynamics:

$$\dot{\phi} = p + q \tan\theta \sin\phi + r \tan\theta \cos\phi$$

Matrix $\gamma_1(\cdot)$ then becomes

$$
\gamma_1(\cdot) = \begin{bmatrix} D^1_1 & D^2_1 & D^3_1 & D^4_1 \\ D^1_2 & D^2_2 & D^3_2 & D^4_2 \\ D^1_3 & D^2_3 & D^3_3 & D^4_3 \\ 1 & \tan\theta \sin\phi & \tan\theta \cos\phi & 0 \end{bmatrix} \tag{5.16}
$$

The nonsingularity of matrix $\gamma_1(\cdot)$ in this case is guaranteed in the required flight envelop. It is physically explained by the fact that three control variables are used to control the trajectory of the aircraft, and the last control variable is used to control the roll motion.

The linearizing feedback can now be given as:

$$\begin{bmatrix}\delta_a\\ \delta_e\\ \delta_r\\ u_T\end{bmatrix}=\gamma_T^{-1}(\cdot)(-\chi_T(\cdot)+\begin{bmatrix}\dot{\zeta}_{10ref}\\ \dot{\zeta}_{11ref}\\ \dot{\zeta}_{12ref}\\ \dot{\sigma}_{2ref}\end{bmatrix}+\begin{bmatrix}-k_{11}(\zeta_1-\zeta_{1ref})-k_{12}(\zeta_4-\zeta_{4ref})\\ -k_{21}(\zeta_2-\zeta_{2ref})-k_{22}(\zeta_5-\zeta_{5ref})\\ -k_{31}(\zeta_3-\zeta_{3ref})-k_{32}(\zeta_6-\zeta_{6ref})\\ 0\end{bmatrix}+\begin{bmatrix}-k_{13}(\zeta_7-\zeta_{7ref})-k_{14}(\zeta_{10}-\zeta_{10ref})\\ -k_{23}(\zeta_8-\zeta_{8ref})-k_{24}(\zeta_{11}-\zeta_{11ref})\\ -k_{33}(\zeta_9-\zeta_{9ref})-k_{34}(\zeta_{12}-\zeta_{12ref})\\ -k_{33}(\sigma_1-\sigma_{1ref})-k_{44}(\sigma_2-\sigma_{2ref})\end{bmatrix}) \tag{5.17}$$

where the k_{ij} for $1\leq i,j\leq 4$ are positive parameters to be tunned, the output references are defined as:

$$\begin{cases}(x_{ref},y_{ref},z_{ref})^T=(\zeta_{1ref},\zeta_{2ref},\zeta_{3ref})^T\\ (\dot{x}_{ref},\dot{y}_{ref},\dot{z}_{ref})^T=(\zeta_{4ref},\zeta_{5ref},\zeta_{6ref})^T\\ (\ddot{x}_{ref},\ddot{y}_{ref},\ddot{z}_{ref})^T=(\zeta_{7ref},\zeta_{8ref},\zeta_{9ref})^T\\ (x^{(3)}_{ref},y^{(3)}_{ref},z^{(3)}_{ref})^T=(\zeta_{10ref},\zeta_{11ref},\zeta_{12ref})^T\\ (x^{(4)}_{ref},y^{(4)}_{ref},z^{(4)}_{ref})^T=(\dot{\zeta}_{10ref},\dot{\zeta}_{11ref},\dot{\zeta}_{12ref})^T\\ \phi_{ref}=\sigma_{1ref};\dot{\phi}_{ref}=\sigma_{2ref};\ddot{\phi}_{ref}=\dot{\sigma}_{2ref}\end{cases} \tag{5.18}$$

The system output will track the output reference when time tends to infinite.

$$\begin{cases}\dot{\zeta}_{10}-\dot{\zeta}_{10ref}+k_{11}(\zeta_1-\zeta_{1ref})+k_{12}(\zeta_4-\zeta_{4ref})+k_{13}(\zeta_7-\zeta_{7ref})+k_{14}(\zeta_{10}-\zeta_{10ref})=0\\ \dot{\zeta}_{11}-\dot{\zeta}_{11ref}+k_{21}(\zeta_2-\zeta_{2ref})+k_{22}(\zeta_5-\zeta_{5ref})+k_{23}(\zeta_8-\zeta_{8ref})+k_{24}(\zeta_{11}-\zeta_{11ref})=0\\ \dot{\zeta}_{12}-\dot{\zeta}_{12ref}+k_{31}(\zeta_3-\zeta_{3ref})+k_{32}(\zeta_6-\zeta_{6ref})+k_{33}(\zeta_9-\zeta_{9ref})+k_{34}(\zeta_{12}-\zeta_{12ref})=0\\ \dot{\sigma}_2-\dot{\sigma}_{2ref}+k_{31}(\zeta_3-\zeta_{3ref})+k_{33}(\sigma_1-\sigma_{1ref})+k_{44}(\sigma_2-\sigma_{2ref})=0\end{cases}$$

In summary, the linearizing feedback controller of the aircraft is determined as:

$$\begin{aligned}u_a(X)=\gamma_T^{-1}(X)(-\chi_T(X)-K_1(\xi_1-R_1)-K_2(\xi_2-R_2)-K_3(\begin{bmatrix}\xi_3\\ \xi_{1\phi}\end{bmatrix}-R_3)\\ -K_4(\begin{bmatrix}\xi_4\\ \xi_{2\phi}\end{bmatrix}-R_4)+R_5)\end{aligned} \tag{5.19}$$

where $\xi_1=(\zeta_1,\zeta_2,\zeta_3)^T$, $\xi_2=(\zeta_4,\zeta_5,\zeta_6)^T$, $\xi_3=(\zeta_7,\zeta_8,\zeta_9)^T$, $\xi_4=(\zeta_{10},\zeta_{11},\zeta_{12})^T$; $\xi_{1\phi}=\sigma_1=\phi$, $\xi_{2\phi}=\sigma_2=\dot{\phi}$;

$$R_1=\begin{bmatrix}\zeta_{1ref}\\ \zeta_{2ref}\\ \zeta_{3ref}\end{bmatrix};R_2=\begin{bmatrix}\zeta_{4ref}\\ \zeta_{5ref}\\ \zeta_{6ref}\end{bmatrix};R_3=\begin{bmatrix}\zeta_{7ref}\\ \zeta_{8ref}\\ \zeta_{9ref}\\ \sigma_{1ref}\end{bmatrix};R_4=\begin{bmatrix}\zeta_{10ref}\\ \zeta_{11ref}\\ \zeta_{12ref}\\ \sigma_{2ref}\end{bmatrix};R_5=\begin{bmatrix}\dot{\zeta}_{10ref}\\ \dot{\zeta}_{11ref}\\ \dot{\zeta}_{12ref}\\ \dot{\sigma}_{2ref}\end{bmatrix} \tag{5.20}$$

$$K_1 = \begin{bmatrix} k_{11} & 0 & 0 \\ 0 & k_{21} & 0 \\ 0 & 0 & k_{31} \\ 0 & 0 & 0 \end{bmatrix}; K_2 = \begin{bmatrix} k_{12} & 0 & 0 \\ 0 & k_{22} & 0 \\ 0 & 0 & k_{32} \\ 0 & 0 & 0 \end{bmatrix}; K_3 = \begin{bmatrix} k_{13} & 0 & 0 & 0 \\ 0 & k_{23} & 0 & 0 \\ 0 & 0 & k_{33} & 0 \\ 0 & 0 & 0 & k_{43} \end{bmatrix}; K_4 = \begin{bmatrix} k_{14} & 0 & 0 & 0 \\ 0 & k_{24} & 0 & 0 \\ 0 & 0 & k_{34} & 0 \\ 0 & 0 & 0 & k_{44} \end{bmatrix} \tag{5.21}$$

Remark 10 *The forth row of K_1 and K_2 is zero because they don't interfere the control of variable state ϕ.*

5.3.2 Stability Analysis

In the last section, through Assumption 5.2.1 we neglected the effect of moments and the effect of control surfaces on the aerodynamic force in considering that they are small. We designed the Feedback Linearization Control based on the approximate system. This subsection is to analyze the stability of the Feedback Linearization Control in the presence of these effects. We suppose that the effects of angular rates and of control surfaces on the aerodynamic forces by the following assumption:

Assumption 5.3.1 *The effect of angular rates (p, q, r) on the aerodynamic force F_u, F_v, F_w is defined by function $\psi_{1u}(X)$, $\psi_{1v}(X)$, $\psi_{1w}(X)$ with the factor ϵ_1, and the effect of control surfaces ($u_a = (\delta_a, \delta_e, \delta_r)^T$) is defined by functions $\psi_{2ue}(X)$, $\psi_{2va}(X)$, $\psi_{2vr}(X)$ and $\psi_{2we}(X)$. they can be then expressed as:*

$$\begin{bmatrix} F_u/m \\ F_v/m \\ F_w/m \end{bmatrix} = \begin{bmatrix} f_u \\ f_v \\ f_w \end{bmatrix} + \epsilon_1 \begin{bmatrix} \psi_{1u}(X) \\ \psi_{1v}(X) \\ \psi_{1w}(X) \end{bmatrix} + \epsilon_2 \begin{bmatrix} 0 & \psi_{2ue}(X) & 0 \\ \psi_{2va}(X) & 0 & \psi_{2vr}(X) \\ 0 & \psi_{2we}(X) & 0 \end{bmatrix} \begin{bmatrix} \delta_a \\ \delta_e \\ \delta_r \end{bmatrix} \tag{5.22}$$

where $X = (x, y, z, u, v, w, \phi, \theta, \psi, p, q, r, \eta, \tau)^T$, ϵ_1 and ϵ_2 are constant.

Taking in account the effects of angular rates and control surfaces, the true aircraft dynamics can be written as:

$$
\begin{cases}
\dot{x} & = u\cos\psi\cos\theta + v(\cos\psi\sin\theta\sin\phi - \sin\psi\cos\phi) + w(\cos\psi\sin\theta\cos\phi + \sin\psi\sin\phi) \\
\dot{y} & = u\sin\psi\cos\theta + v(\sin\psi\sin\theta\sin\phi + \cos\psi\cos\phi) + w(\sin\psi\sin\theta\cos\phi - \cos\psi\sin\phi) \\
\dot{z} & = -u\sin\theta + v\cos\theta\sin\phi + w\cos\theta\cos\phi \\
\begin{bmatrix}\dot{u}\\ \dot{v}\\ \dot{w}\end{bmatrix} & = \begin{bmatrix} rv - qw - g\sin\theta + f_u + \eta \\ pw - ru + g\sin\phi\cos\theta + f_v \\ qu - pv + g\cos\phi\cos\theta + f_w \end{bmatrix} + \epsilon_1 \begin{bmatrix}\psi_{1u}(X)\\ \psi_{1v}(X)\\ \psi_{1w}(X)\end{bmatrix} + \epsilon_2 \begin{bmatrix} 0 & \psi_{2ue}(X) & 0 \\ \psi_{2va}(X) & 0 & \psi_{2vr}(X) \\ 0 & \psi_{2we}(X) & 0 \end{bmatrix} \begin{bmatrix}\delta_a\\ \delta_e\\ \delta_r\end{bmatrix} \\
\dot{\phi} & = p + \tan\theta(q\sin\phi + r\cos\phi) \\
\dot{\theta} & = q\cos\phi - r\sin\phi \\
\dot{\psi} & = \frac{q\sin\phi + r\cos\phi}{\cos\theta} \\
\dot{p} & = \frac{1}{I_{xx}I_{zz} - I_{xz}^2}[(I_{yy}I_{zz} - I_{zz}^2 - I_{xz}^2)rq - I_{xz}(I_{xx} + I_{zz} - I_{yy})pq + I_{zz}L - I_{xz}N] \\
\dot{q} & = \frac{1}{I_{yy}}[(I_{zz} - I_{xx})pr + I_{xz}(p^2 - r^2) + M] \\
\dot{r} & = \frac{1}{I_{xx}I_{zz} - I_{xz}^2}[(-I_{xx}I_{yy} + I_{zz}^2 + I_{xz}^2)pq + I_{xz}(I_{xx} + I_{zz} - I_{yy})rq + I_{xx}N - I_{xz}L] \\
\dot{\eta} & = \tau \\
\dot{\tau} & = u_T
\end{cases}
\tag{5.23}
$$

or compactly,

$$
\dot{X} = f(X) + g(X)u_a + \epsilon_1\psi_1(X) + \epsilon_2\psi_2(X)u_a \tag{5.24}
$$

where

$$
\psi_1(X) = \begin{bmatrix} 0 \\ 0 \\ 0 \\ \psi_{1u}(X) \\ \psi_{1v}(X) \\ \psi_{1w}(X) \\ 0 \\ ... \\ 0 \end{bmatrix}; \quad \psi_2(X) = \begin{bmatrix} 0 & 0 & 0 & 0 \\ 0 & 0 & 0 & 0 \\ 0 & 0 & 0 & 0 \\ 0 & \psi_{2ue}(X) & 0 & 0 \\ \psi_{2va}(X) & 0 & \psi_{2vr}(X) & 0 \\ 0 & \psi_{2we}(X) & 0 & 0 \\ 0 & 0 & 0 & 0 \\ ... & ... & ... & ... \\ 0 & 0 & 0 & 0 \end{bmatrix}
$$

While the approximate system dynamics which is used to design the dynamic feedback linearization law, is expressed symbolically as:

$$
\dot{X} = f(X) + g(X)u_a \tag{5.25}
$$

This system is called slightly non - minimum phase system, a stability analysis for such systems can be seen in [51]. In the following, we demonstrate that an aircraft is

exponentially stabilized by the previously designed controller in considering the effect of moments and control surfaces on the aerodynamic force.

We define state vectors,

$$\begin{cases} \xi_1 =(x,y,z)^T = (\zeta_1,\zeta_2,\zeta_3)^T \\ \xi_2 =\dot{\xi_1} = (\dot{x},\dot{y},\dot{z})^T = (\zeta_4,\zeta_5,\zeta_6)^T \\ \xi_3 =\dot{\xi_2} = (\ddot{x},\ddot{y},\ddot{z})^T = (\zeta_7,\zeta_8,\zeta_9)^T \\ \xi_4 =\dot{\xi_3} = (x^{(3)},y^{(3)},z^{(3)})^T = (\zeta_{10},\zeta_{11},\zeta_{12})^T \\ \xi_{1\phi}=\phi = \sigma_1 \\ \xi_{2\phi}=\dot{\xi}_{1\phi} = \dot{\phi} = \sigma_2 \end{cases} \tag{5.26}$$

From (5.7), (5.12), (5.26) and (5.25), the approximate system can be described as:

$$\begin{cases} \dot{\xi}_1 =\frac{\partial \xi_1}{\partial X}\dot{X} = \frac{\partial \xi_1}{\partial X}(f(X)+g(X)u_a) = \xi_2 \\ \dot{\xi}_2 =\frac{\partial \xi_2}{\partial X}(f(X)+g(X)u_a) = \xi_3 \\ \dot{\xi}_3 =\frac{\partial \xi_3}{\partial X}(f(X)+g(X)u_a) = \xi_4 \\ \dot{\xi}_{1\phi}=\xi_{2\phi} \\ \dot{\xi}_4 =\frac{\partial \xi_4}{\partial X}(f(X)+g(X)u_a) = \chi_{T0}(X)+\gamma_{T0}(X)u_a \\ \dot{\xi}_{2\phi}=\chi_{T1}(X)+\gamma_{T1}(X)u_a \end{cases} \tag{5.27}$$

where the matrix $\gamma_T(X) = \begin{bmatrix} \gamma_{T0}(X) \\ \gamma_{T1}(X) \end{bmatrix}$ is nonsingular in the studied field of X and $\chi_T(X) = \begin{bmatrix} \chi_{T0}(X) \\ \chi_{T1}(X) \end{bmatrix}$, $\gamma_{T0}(X) \in \mathbb{R}^{3\times 4}$, $\gamma_{T1}(X) \in \mathbb{R}^{1\times 4}$, $\chi_{T0}(X) \in \mathbb{R}^{3\times 1}$ and $\chi_{T0}(X) \in \mathbb{R}$.

Computing the effects of moment and of control surfaces, we have the derivatives of transformation variables as:

$$\begin{cases} \dot{\xi}_1=\frac{\partial \xi_1}{\partial X}(f(X)+g(X)u_a+\epsilon_1\psi_1(X)+\epsilon_2\psi_2(X)u_a) = \xi_2 \\ \dot{\xi}_2=\frac{\partial \xi_2}{\partial X}(f(X)+g(X)u_a+\epsilon_1\psi_1(X)+\epsilon_2\psi_2(X)u_a) = \xi_3+\frac{\partial \xi_2}{\partial X}(\epsilon_1\psi_1(X)+\epsilon_2\psi_2(X)u_a(X)) \\ \dot{\xi}_3=\frac{\partial \xi_3}{\partial X}(f(X)+g(X)u_a+\epsilon_1\psi_1(X)+\epsilon_2\psi_2(X)u_a) = \xi_4+\frac{\partial \xi_3}{\partial X}(\epsilon_1\psi_2(X)+\epsilon_2\psi_2(X)u_a(X)) \\ \dot{\xi}_4=\chi_{T0}(X)+\gamma_{T0}(X)u_a+\frac{\partial \xi_4}{\partial X}(\epsilon_1\psi_1(X)+\epsilon_2\psi_2(X)u_a(X)) \end{cases}$$

It is worth noticing that ξ_1 does not depend on angular rates and control surfaces, then the effects of angular rates and control surfaces do not appear in the derivative of ξ_1. The true system dynamics can be then described as:

$$\begin{cases} \dot{\xi}_1 = \xi_2 \\ \dot{\xi}_2 = \xi_3 + \frac{\partial \xi_2}{\partial X}(\epsilon_1\psi_1(X) + \epsilon_2\psi_2(X)u_a(X)) \\ \dot{\xi}_3 = \xi_4 + \frac{\partial \xi_3}{\partial X}(\epsilon_1\psi_2(X) + \epsilon_2\psi_2(X)u_a(X)) \\ \dot{\xi}_{1\phi} = \xi_{2\phi} \\ \dot{\xi}_4 = \chi_{T0}(X) + \gamma_{T0}(X)u_a + \frac{\partial \xi_4}{\partial X}(\epsilon_1\psi_1(X) + \epsilon_2\psi_2(X)u_a(X)) \\ \dot{\xi}_{2\phi} = \chi_{T1}(X) + \gamma_{T1}(X)u_a \end{cases} \tag{5.28}$$

The approximate tracking controller that we designed in the last subsection is:

$$\begin{aligned} u_a(X) = &\begin{bmatrix} \gamma_{T0}(X) \\ \gamma_{T1}(X) \end{bmatrix}^{-1} (- \begin{bmatrix} \chi_{T0}(X) \\ \chi_{T1}(X) \end{bmatrix} - K_1(\xi_1 - R_1) - K_2(\xi_2 - R_2) - K_3(\begin{bmatrix} \xi_3 \\ \xi_{1\phi} \end{bmatrix} - R_3) \\ &-K_4(\begin{bmatrix} \xi_4 \\ \xi_{2\phi} \end{bmatrix} - R_4) + R_5) \end{aligned} \tag{5.29}$$

We define the trajectory error vector:

$$\begin{cases} e_1 = \xi_1 - R_1 \\ e_2 = \xi_2 - R_2 \\ \begin{bmatrix} e_3 \\ e_5 \end{bmatrix} = \begin{bmatrix} \xi_3 \\ \xi_{1\phi} \end{bmatrix} - R_3 \quad \text{or} \quad e = \xi - R \\ \begin{bmatrix} e_4 \\ e_6 \end{bmatrix} = \begin{bmatrix} \xi_4 \\ \xi_{2\phi} \end{bmatrix} - R_4 \end{cases} \tag{5.30}$$

Then the system (5.28) with the approximate tracking controller in (5.17) can be rewritten as:

$$\begin{bmatrix} \dot{e_1} \\ \dot{e_2} \\ \begin{bmatrix} \dot{e_3} \\ \dot{e_5} \end{bmatrix} \\ \begin{bmatrix} \dot{e_4} \\ \dot{e_6} \end{bmatrix} \end{bmatrix} = \begin{bmatrix} I_3 & 0 & 0 & 0 \\ 0 & I_3 & 0 & 0 \\ 0 & 0 & I_4 & 0 \\ -K_1 & -K_2 & -K_3 & -K_4 \end{bmatrix} \begin{bmatrix} e_1 \\ e_2 \\ \begin{bmatrix} e_3 \\ e_5 \end{bmatrix} \\ \begin{bmatrix} e_4 \\ e_6 \end{bmatrix} \end{bmatrix} + \begin{bmatrix} 0 \\ \frac{\partial \xi_2}{\partial X}\epsilon_1\psi_1(X) \\ \frac{\partial \xi_3}{\partial X}\epsilon_1\psi_1(X) \\ 0 \\ \frac{\partial \xi_4}{\partial X}\epsilon_1\psi_1(X) \\ 0 \end{bmatrix} + \begin{bmatrix} 0 \\ \frac{\partial \xi_2}{\partial X}\epsilon_2\psi_2(X)u_a(X) \\ \frac{\partial \xi_3}{\partial X}\epsilon_2\psi_2(X)u_a(X) \\ 0 \\ \frac{\partial \xi_4}{\partial X}\epsilon_2\psi_2(X)u_a(X) \\ 0 \end{bmatrix} \tag{5.31}$$

Or compactly,

$$\dot{e} = Ae + \epsilon_1\Psi_1(X) + \epsilon_2\Psi_2(X)u_a(X) \tag{5.32}$$

We will show now that e is bounded. To this end, we consider the Lyapunov candidate:

$$W = e^T P e \tag{5.33}$$

where matrix P is the solution of:

$$A^T P + PA = -I_{14} \tag{5.34}$$

By assuming that all output references are bounded, that means R_i for $1 \leq i \leq 5$ are bounded, or R bounded by a constant b_d, we have then:

$$\begin{aligned} &\xi = e + R \\ \Rightarrow \quad &\|\xi\| \leq \|e\| + \|R\| \\ \Rightarrow \quad &\|\xi\| \leq \|e\| + b_d \end{aligned} \tag{5.35}$$

Furthermore, we can check that $\Psi_1(X)$ and $\Psi_2(X)u_a(X)$ are locally Lipschitz, note that X is a local diffeomorphism of ξ, so $\|X\| \leq l_x\|\xi\|$.

$$\|P\Psi_1(X)\| \leq l_1\|X\| \leq l_1 l_x\|\xi\| \tag{5.36}$$

$$\|P\Psi_2(X)u_a(X)\| \leq l_2\|X\| \leq l_2 l_x\|\xi\| \tag{5.37}$$

Take the derivative of Lyapunov function (5.33), we find that:

$$\begin{aligned} \dot{W} =& -e^T e + 2e^T P(\epsilon_1\Psi_1(X) + \epsilon_2\Psi_2(X)u_a(X)) \\ \leq& -\|e\|^2 + 2\|e\|(\epsilon_1 l_1 l_x\|\xi\| + \epsilon_2 l_2 l_x\|\xi\|) \\ \leq& -\|e\|^2 + 2\|e\|(\epsilon_1 l_1 l_x(\|e\| + b_d) + \epsilon_2 l_2 l_x(\|e\| + b_d)) \\ \leq& -\|e\|^2 + 2(\epsilon_1 l_1 l_x + \epsilon_2 l_2 l_x)\|e\|^2 + 2(\epsilon_1 l_1 l_x + \epsilon_2 l_2 l_x)b_d\|e\| \\ \leq& -(3/4 - 2(\epsilon_1 l_1 l_x + \epsilon_2 l_2 l_x))\|e\|^2 - (\|e\|/2 - 2(\epsilon_1 l_1 l_x + \epsilon_2 l_2 l_x)b_d)^2 \\ &+(2(\epsilon_1 l_1 l_x + \epsilon_2 l_2 l_x)b_d)^2 \end{aligned} \tag{5.38}$$

Remark 11 *$\dot{W} \leq 0$ whenever e is large, then ξ and X are bounded. If the references are chosen neighborhood of initial conditions so that b_d is sufficiently small, all system states remain in a small neighborhood of the tracked values. For the purpose of aircraft stabilization after the launching phase, the references and their derivatives are zero, by (5.30) R is equal to zero, and then b_d is zero. The system is then exponentially stable if ϵ_1 and ϵ_2 are sufficiently small. We can see for the purpose of flight stabilization, the dynamic feedback linearization controller satisfies the performance requirement.*

5.4 Simulation Results

In Section 5.3, the design methodology of a dynamic feedback linearization controller to stabilize a flight system is proposed. The stability analysis has shown that the aircraft system is exponentially stabilized for the case of small effects of control surface and angular rates's deflections on the aerodynamic force. In this section will apply this control

to the air launch system after the launching phase. Then, it will be presented numerical simulation results for the controller to demonstrate the performance of the proposed feedback linearization control laws in the drop phase.

Similarly to the case of applying modified conditional integrator and conditional servocompensator controls to the airlaunch system, the launching phase is considered as a perturbation on aerodynamic force and moment during an interval T_{int}. This perturbation affects affects the aircraft model following the launch phase, which model is taken as an F-16 as we mentioned in Section 2.4 of Chapter 2. We then remind that the model used in the following simulations is even more complete than that used in the control design, for example it includes actuator dynamics and their limitations. As a consequence, simulations also illustrate some properties of robustness to unmodeled dynamics.

Baselines

We remind the objective of the controller designed for the airlaunch system after the launching phase

- ($\alpha_0 = 17.5°$, $\beta_0 = 4°$ and $\phi_0 = 10°$) is the initial condition of the second model which is the airlaunch system after the separation phase, all others variables start at zero. This is the final state of the first model added by a small disturbance on the system output.
- The controller must return the airlaunch system to the angle of attack $\alpha_r = 4.6°$, sideslip $\beta_r = 0°$, and roll angle $\phi_r = 0°$ and all others variables to zero, which corresponds to the equilibrium point of the second model following the launch phase (at $V = 154m/s, h = 5000m$). That corresponds to $u_{ref} = 150m/s$, $w_{ref} = 33m/s$, $v_{ref} = 0m/s$ and $\phi_{ref} = 0°$, all other variables are zero in body fixed reference frame. The control surfaces at the equilibrium point are $\delta_a = 0°$, $\delta_e = -2.5°$ and $\delta_r = 0°$.
- There is no collision between airlaunch system and the rocket.

Numerical Applications

The linearizing feedback controller of the airlaunch system is determined as in (5.19):

$$u_a(X) = \gamma_T^{-1}(X)(-\chi_T(X) - K_1(\xi_1 - R_1) - K_2(\xi_2 - R_2) - K_3(\begin{bmatrix} \xi_3 \\ \xi_{1\phi} \end{bmatrix} - R_3) - K_4(\begin{bmatrix} \xi_4 \\ \xi_{2\phi} \end{bmatrix} - R_4) + R_5)$$

where $\gamma_T(X)$ is defined in (5.13), $\chi_T(X)$ is defined in (5.14). R_1, R_2, R_3, R_4 and R_5 are defined in (5.20), and K_1, K_2, K_3, K_4 and K_5 are defined in (5.21).

Because the controller stabilizes the system to the equilibrium point of the second model at the altitude $6500m$, R_1, R_2, R_3, R_4 and R_5 are then determined as:

$$R_1 = \begin{bmatrix} \zeta_{1ref} = Vt = 150t \\ \zeta_{2ref} = 0 \\ \zeta_{3ref} = -6500 \end{bmatrix}; R_2 = \begin{bmatrix} \zeta_{4ref} = V \\ \zeta_{5ref} = 0 \\ \zeta_{6ref} = 0 \end{bmatrix}; R_3 = \begin{bmatrix} \zeta_{7ref} = 0 \\ \zeta_{8ref} = 0 \\ \zeta_{9ref} = 0 \\ \sigma_{1ref} = 0 \end{bmatrix};$$

$$R_4 = \begin{bmatrix} \zeta_{10ref} = 0 \\ \zeta_{11ref} = 0 \\ \zeta_{12ref} = 0 \\ \sigma_{2ref} = 0 \end{bmatrix}; R_5 = \begin{bmatrix} \dot{\zeta}_{10ref} = 0 \\ \dot{\zeta}_{11ref} = 0 \\ \dot{\zeta}_{12ref} = 0 \\ \dot{\sigma}_{2ref} = 0 \end{bmatrix}$$

Parameters K_1, K_2, K_3, K_4 and K_5 are found as:

$$K_1 = \begin{bmatrix} 0.10 & 0 & 0 \\ 0 & 0.10 & 0 \\ 0 & 0 & 0.20 \\ 0 & 0 & 0 \end{bmatrix}; K_2 = \begin{bmatrix} 100 & 0 & 0 \\ 0 & 100 & 0 \\ 0 & 0 & 300 \\ 0 & 0 & 0 \end{bmatrix}; K_3 = \begin{bmatrix} 100 & 0 & 0 & 0 \\ 0 & 400 & 0 & 0 \\ 0 & 0 & 400 & 0 \\ 0 & 0 & 0 & 200 \end{bmatrix}; K_4 = \begin{bmatrix} 200 & 0 & 0 & 0 \\ 0 & 500 & 0 & 0 \\ 0 & 0 & 400 & 0 \\ 0 & 0 & 0 & 30 \end{bmatrix}$$

The second model is disturbed on aerodynamic force and moment during an interval T_{int} as in Chapter 2.

- Perturbation $F_{w_p} = mg\cos\theta_0$ on the aerodynamic normal force, the perturbation on drag force is $F_{u_p} = -P\sin\theta_0 = -mg\sin\theta_0$ and the perturbation $M_p = mgl_r\cos\theta_0/2$ on the aerodynamic pitch moment during T_{int}, where l_r is the rocket length.
- three sets of time interval are simulated:
  1. $T_{int} = 0.227s$, the system is visually unstable for constant inputs as mentioned in the part of Modeling and Simulation of the airlaunch system (see Chapter 2). The simulation results correspond to solid lines in Fig. 5.1 to Fig. 5.6.
  2. $T_{int} = 0.3s$, the system is unstable for a simple LQR controller (see Chapter 2). The simulation results correspond to dashed lines in Fig. 5.1 to Fig. 5.6.
  3. $T_{int} = 0.43s$, this is a very long time interval for the perturbation on the aerodynamic force and moment. The simulation results correspond to dash dotted lines in Fig. 5.1 to Fig. 5.6.

Results

It is interesting to remind that the aircraft with constant inputs (trim conditions) is unstable for T_{int} greater than $0.227s$ (see [59]). The dynamic feedback linearization controller we designed in Section 5.3 will stabilize the system for much longer periods. Finally, we can verify that the system will be unstable for an interval T_{int} greater than $0.43s$. Nevertheless, in this case the control inputs are strongly saturated. As a consequence this time interval represents more likely the limitations of the aircraft itself than the limitations of the control algorithm.

Figs. 5.1 to 5.3 represent the convergence of the system states to the operating point of the aircraft at the end of 10s for three cases of $T_{int} = (0.227s, 0.3s, 0.43s)$. For $T_{int} = (0.227s, 0.3s)$ the system is well stabilized, while for T_{int} assuming larger values the system becomes more oscillatory and attains its limits of stability in case of $T_{int} = 0.43s$.

Fig. 5.5 shows how the control variables and thrust behave for the three cases of study. The control surfaces in the last case are saturated by their physical limitations due to a high perturbation on aerodynamic force and moment. It can be said that the performance of the Feedback Linearization Controller allows the system to keep stability even with large perturbation during a long time interval T_{int}.

Collision Avoidance

Airlaunch problem does not only require stability of system's states, but also to avoid the possibility of collision between the aircraft and the rocket after the drop phase. Fig. 5.7 shows the altitude of the aircraft from 0 to $1s$ in the three previous cases of study by using the Feedback Linearization Controller. They are compared with the trajectory of the rocket that drop freely with the initial airspeed of the aircraft (the thin solid plot).

In the three cases (dotted plot, dashed plot and dash dotted plot), the altitude of the aircraft satisfies the specification that requires there is no collision between the aircraft and the rocket in the airlaunch phase.

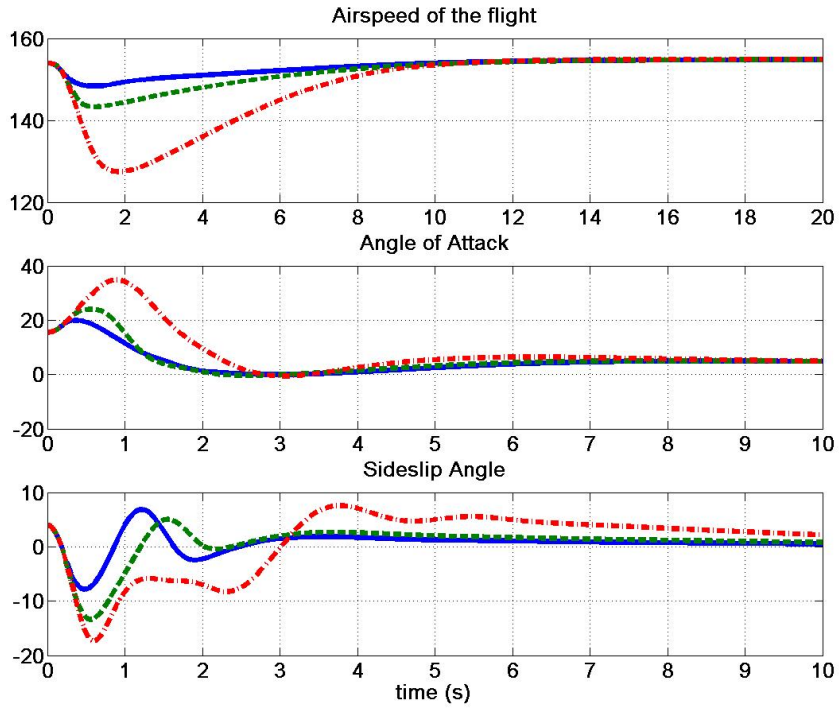

Figure 5.1: Airspeed, Angle of attack and sideslip angle stabilized by DFL Controller

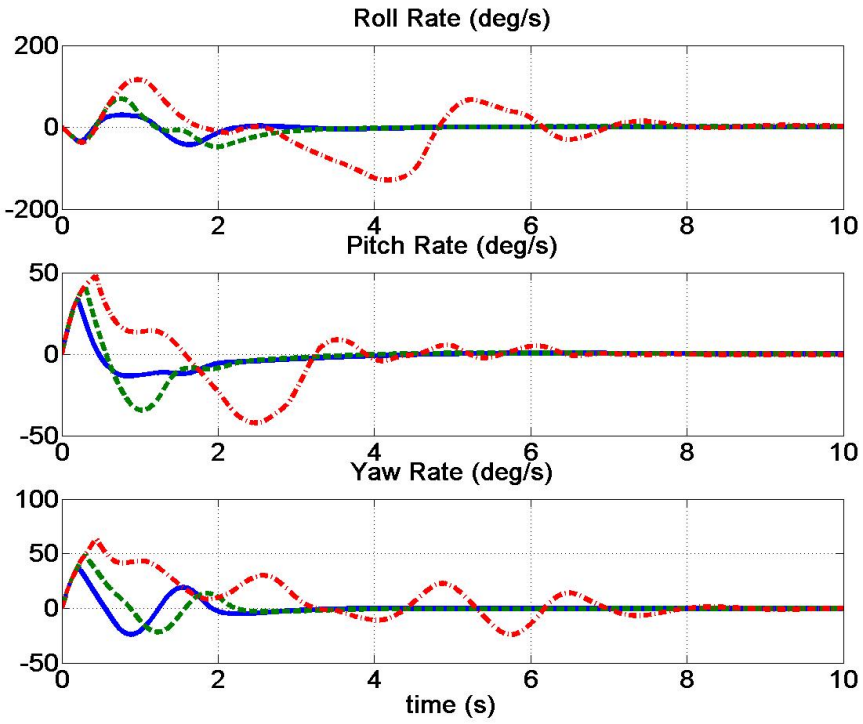

Figure 5.2: Angular rates stabilized by DFL Controller

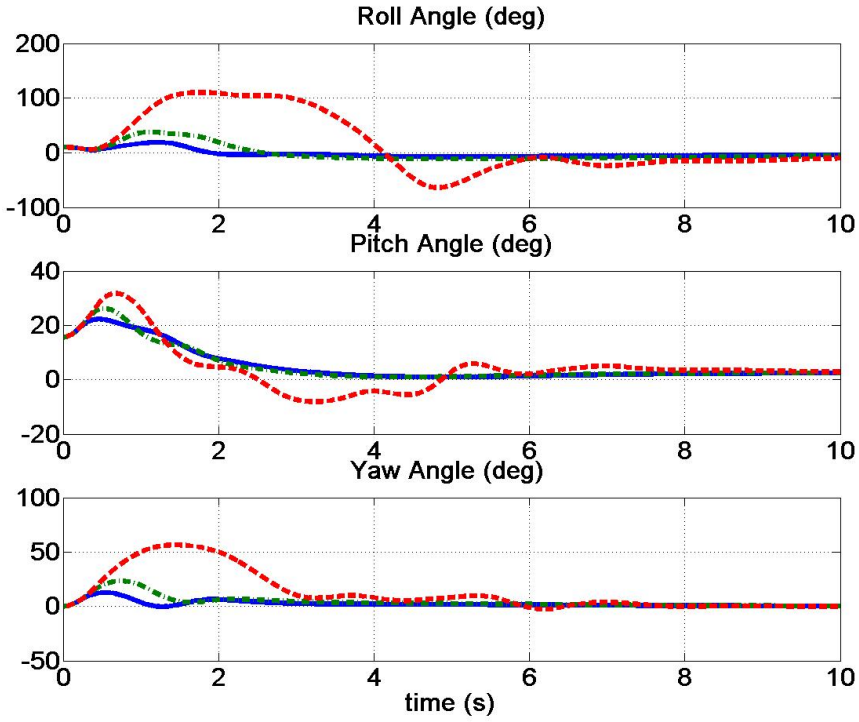

Figure 5.3: Euler's angles stabilized by DFL Controller

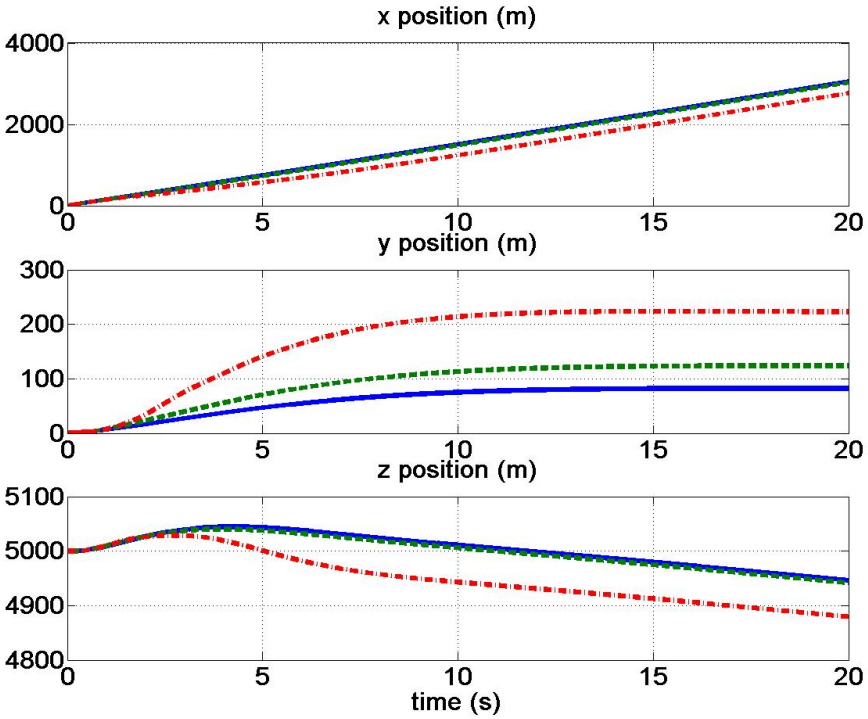

Figure 5.4: Three positions of the aircraft carrier after the launching phase

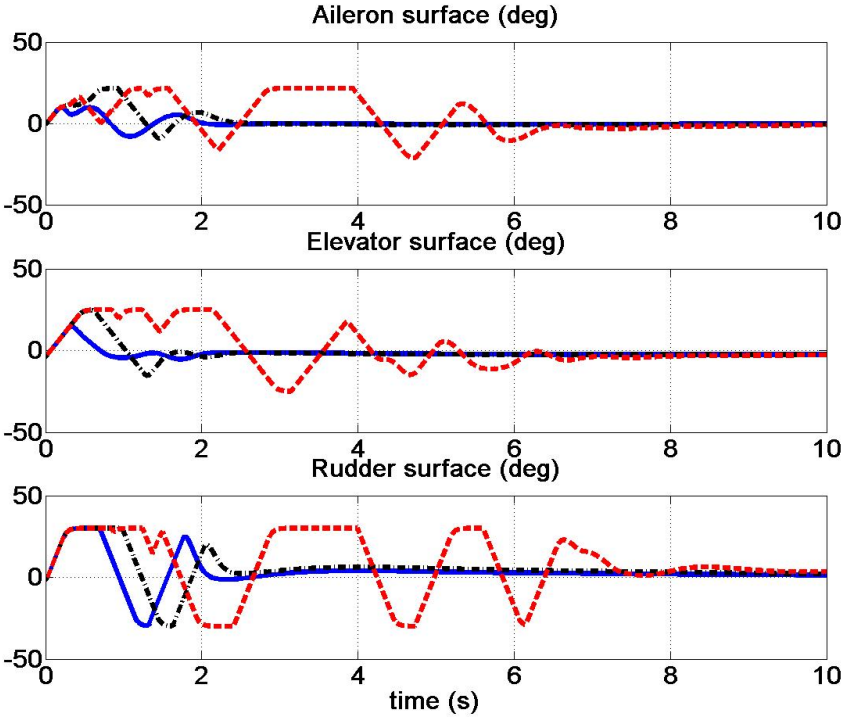

Figure 5.5: Aileron, elevator and Rudder of DFL Controller

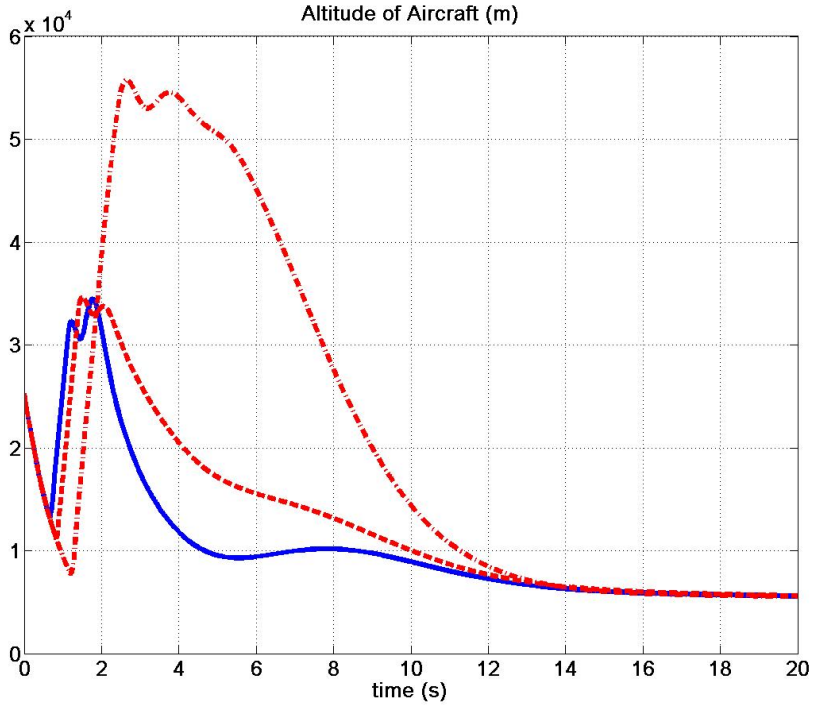

Figure 5.6: Thrust Force of DFL Controller

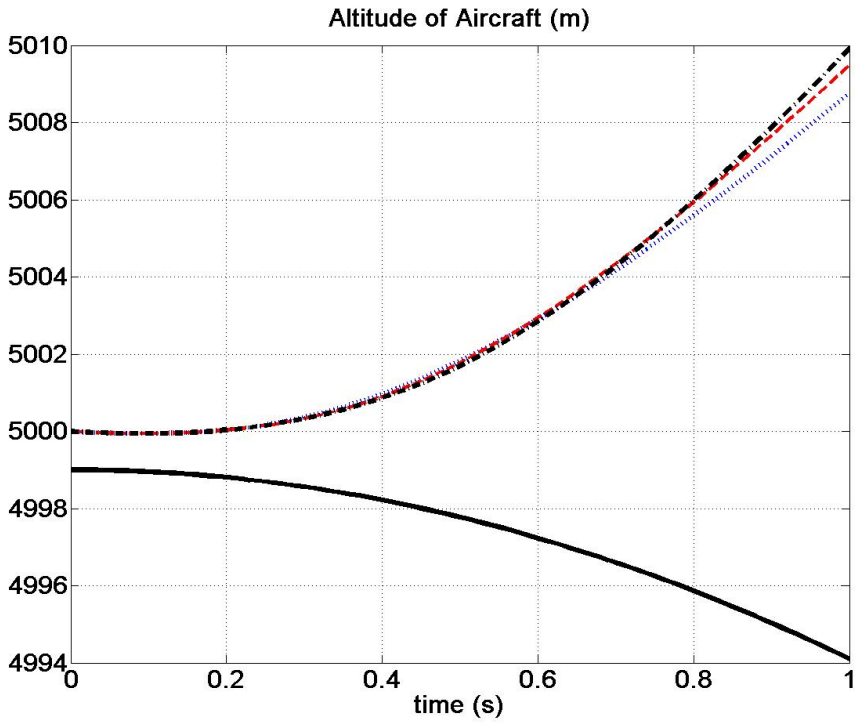

Figure 5.7: Altitude of the aircraft with DFL Controller

5.5 Conclusion

We have presented the design of Full Dynamic Feedback Linearization Controller aiming to control an aircraft. This chapter has its starting point in the work of [22] from the literature. This chapter shows that a flight system is not be static feedback linearizable, but by using a special class of dynamic compensator, a second order integration of thrust, the flight system becomes able to be dynamic feedback linearizable in a first step where it was neglected the derivatives of aerodynamic forces with respect to control surfaces and angular rates. In a second step, a deeper analysis shows that this dynamic feedback linearization controller exponentially stabilizes the aircraft towards a small residual set even when are taken into account the effects of the control surfaces and angular rates on the aerodynamic forces.

The proposed controller is then applied to the airlaunch system which has been modeled by an F-16 model disturbed by large impulses on forces and moments that may destabilize the system as explained in Section 2.4. The performance of the proposed controller is illustrated by computer simulations with initial conditions representing the final (stable) state before the launch phase. In three of the studied cases, the stability of the

system after the drop phase is assured, all states return to their equilibrium values, and there is no collision between the aircraft and the rocket, even if the the perturbation interval T_{int} becomes large. The controller satisfies then the requirement of flight stabilization and collision avoidance with the rocket.

Until now, this thesis has developed a modified conditional integrator control and conditional servocompensator control in Chapters 3 and 4 and dynamic feedback linearization control in Chapter 5, and applied them to our airlaunch problem. In the next chapter, there will be a comparison of these control techniques.

Chapter 6

Comparison of Control Approaches

Contents

6.1 Introduction

In the three last chapters we have presented the modified Conditional Integrator(mCI), modified Conditional Servocompensator(mCS) controls (Chapters 3 and 4) and dynamic feedback linearization control (Chapter 5) with their application to the air launch system. The simulation results have shown the stabilization of the air launch system after the launching phase with a certain performance both control methods. In this chapter we will compare these controls in particular the modified conditional servocompensator control and dynamic feedback linearization control. We illustrate also advantages and disadvantages of each control. We conclude by providing insights on the choice of each of these controls.

6.2 Comparison

The mCS control designed in Chapters 3 and 4 has the sliding mode properties outside the boundary layer and has the integral servo-compensation inside the boundary layer

which allows the system to avoid chattering effects. While dynamic feedback linearization control is designed in Chapter 5 based on the dynamic feedback linearizability of the system with double integration of the thrust force.

6.2.1 Baselines

We remind the objective of the controller designed for the airlaunch system after the launching phase

- ($\alpha_0 = 17.5°$, $\beta_0 = 4°$ and $\phi_0 = 10°$) is the initial conditions of the second model which is the airlaunch system after the separation phase, all others variables are initially taken as zero. This is the final state of the first model with a small disturbance on system output.

- The controller must return the airlaunch system to angle of attack $\alpha_r = 4.6°$, sideslip $\beta_r = 0°$, and roll angle $\phi_r = 0°$ and all others variables to zero, which corresponds to the equilibrium point of the second model following the launch phase ($V = 154m/s, h = 5000m$). The control surfaces at the equilibrium point are $\delta_a = 0°$, $\delta_e = -2.5°$ and $\delta_r = 0°$.

- There is no collision between airlaunch system and the rocket.

6.2.2 Numerical Applications

In order to avoid repetition(we consider the CI as an special case of CS), we take the modified conditional servocompensator control law expressed in 4.46 and dynamic feedback controller for (5.1) determined in (5.19).

The second model is disturbed on aerodynamic force and moment during an interval T_{int} as in Chapter 2 by:

- the perturbation $F_{w_p} = mg\cos\theta_0$ on the aerodynamic normal force, the perturbation on drag force is $F_{u_p} = -P\sin\theta_0 = -mg\sin\theta_0$ and the perturbation $M_p = mgl_r\cos\theta_0/2$ on the aerodynamic pitch moment and a negligible perturbation on the aerodynamic roll force during T_{int}, where l_r is the rocket length.

- Four sets of time interval are simulated:

  1. $T_{int} = 0.227s$, the system is visually unstable for constant inputs (see Chapter 2). The simulation results correspond to Fig. 6.1 to Fig. 6.6.

2. $T_{int} = 0.3s$, the system is unstable for a simple LQR controller (see chapter 2). The simulation results correspond to Fig. 6.7 to Fig. 6.12.

3. $T_{int} = 0.43s$, this is a large time interval for the perturbation on the aerodynamic force and moment. The simulation results correspond to Fig. 6.13 to Fig. 6.18.

6.2.3 Simulation Results

The simulation results of the modified conditional servocompensator control are illustrated by continuous lines in Figs. 6.1 to 6.18, while that of the dynamic feedback linearization control correspond to dashed lines. It is worth noticing that the dynamic feedback linearization control was designed for the set of state variables: linear velocities (u, v, w), angular rates (p, q, r), Euler's angles (ϕ, θ, ψ) and system's positions (x, y, z). In the results the set of airspeed (V), angle of attack (α) and sideslip angle (β) are illustrated instead of linear velocities (u, v, w) to compare with the results of the mCS control. The transformation from (u, v, w) to (V, α, β) can be effected as in (2.20):

$$\begin{array}{lcl} u = V\cos\alpha\cos\beta & & V = \sqrt{u^2+v^2+w^2} \\ v = V\sin\beta & \Leftrightarrow & \alpha = \arctan(w/u) \\ w = V\sin\alpha\cos\beta & & \beta = \arcsin(v/V) \end{array}$$

Time interval: $T_{int} = 0.227s$, which corresponds to the case where the system is visibly unstable with constant inputs. We have some remarks:

Stabilization of system's states

Fig. 6.1 to Fig. 6.4: The stabilization of the principal state variables are assured after 10s such as the angle of attack, sideslip, roll angle and angular rates.

In the case of the mCS control, the pitch angle and yaw angle are move freely. The yaw angle converges to a constant. The pitch angle and airspeed are stabilized slowly to a constant. As a consequence, the lateral position y is free, and the altitude is stabilized very slowly.

In the case of the dynamic feedback linearization control, a complete stabilization of the system is obtained but slower than the results of the mCS control. Because the control parameters for three positions are leak, three positions don't converge to the desired positions but with an error.

System's Control:

Fig. 6.5 and Fig. 6.6: The control surfaces are the same for two controllers with a small saturation on rudder. Inversely, the thrust forces on the two cases are different.

For the dynamic feedback linearization control, the thrust force converges fast, while it converges slowly in the case of CSC. It explains the difference of convergence on system's airspeed in the two cases.

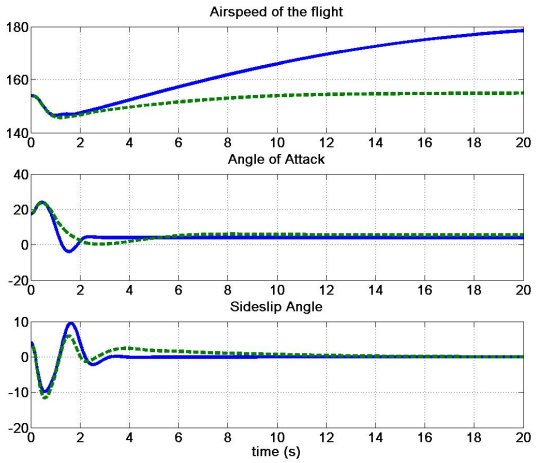

Figure 6.1: Airspeed, Angle of attack and sideslip angle for $T_{int} = 0.227s$

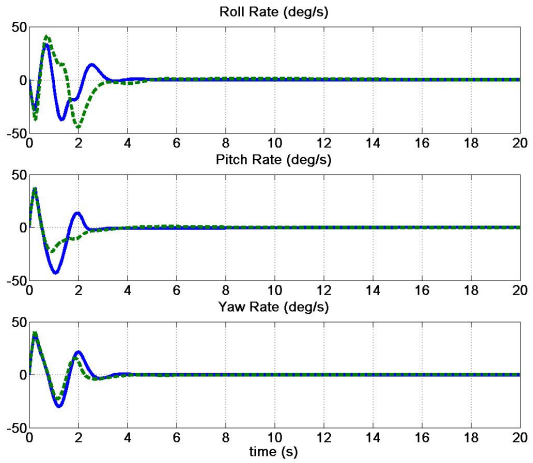

Figure 6.2: Angular Rates: roll, pitch and yaw rates for $T_{int} = 0.227s$

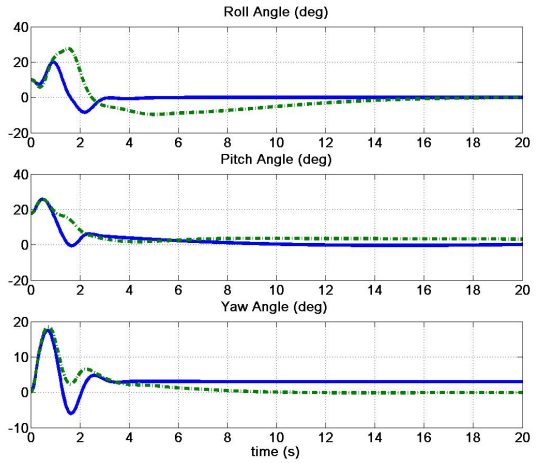

Figure 6.3: Euler's Angles for $T_{int} = 0.227s$

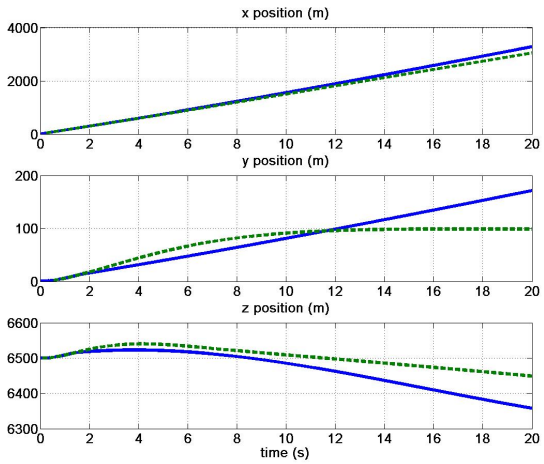

Figure 6.4: System's Position for $T_{int} = 0.227s$

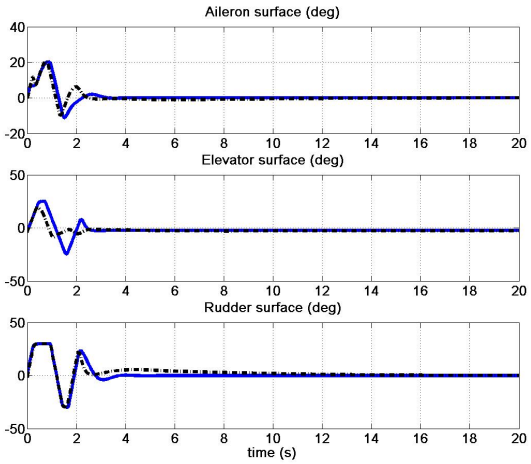

Figure 6.5: Control Surfaces for $T_{int} = 0.227s$

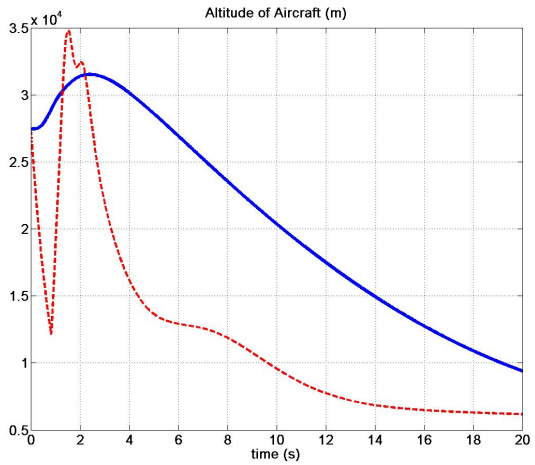

Figure 6.6: Thrust Force for $T_{int} = 0.227s$

Time interval $T_{int} = 0.3s$ which corresponds to the case where the system is visibly unstable with a simple LQR controller (see Chapter 2).

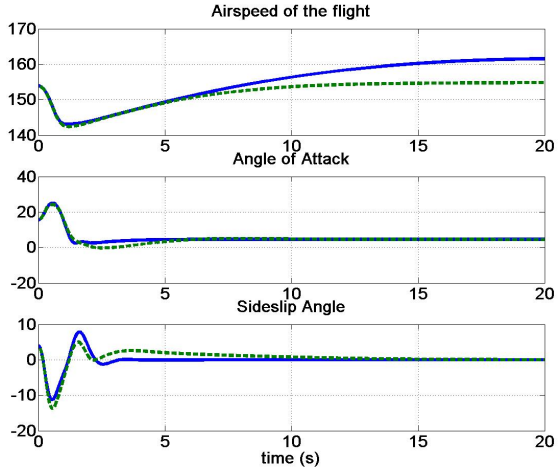

Figure 6.7: Airspeed, Angle of attack and sideslip angle for $T_{int} = 0.3s$

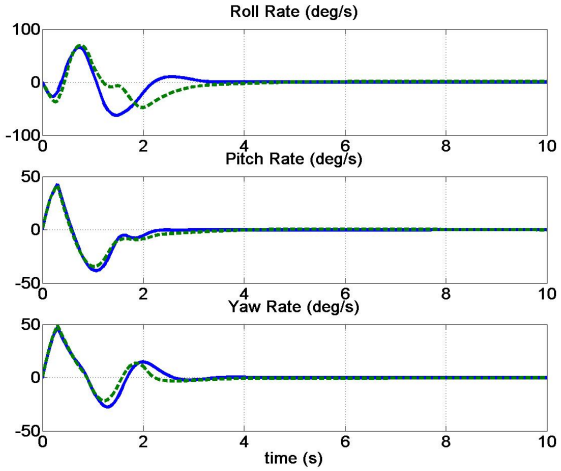

Figure 6.8: Angular Rates: roll, pitch and yaw rates for $T_{int} = 0.3s$

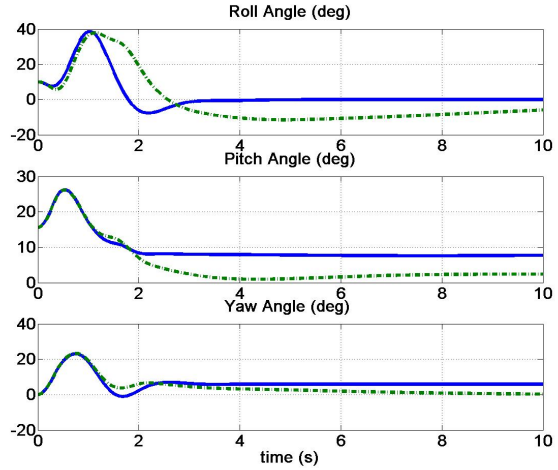

Figure 6.9: Euler's Angles for $T_{int} = 0.3s$

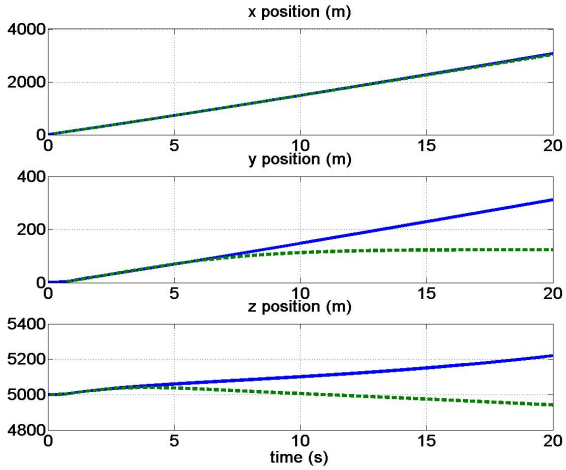

Figure 6.10: System's Position for $T_{int} = 0.3s$

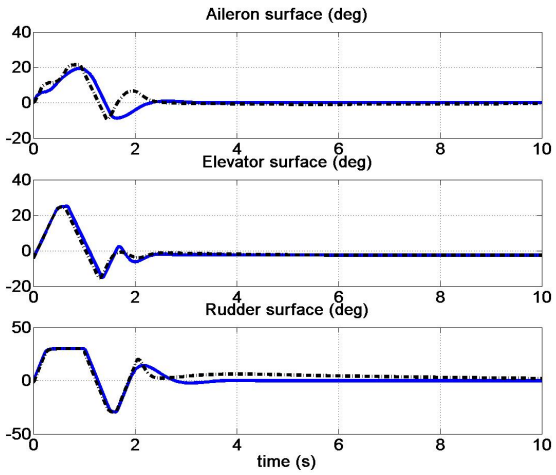

Figure 6.11: Control Surfaces for $T_{int} = 0.3s$

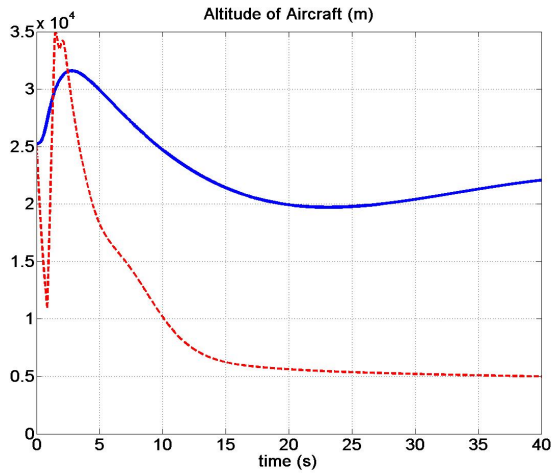

Figure 6.12: Thrust Force for $T_{int} = 0.3s$

It is worth noticing that:

Stabilization of system's states

Fig. 6.7 to Fig. 6.10: The stabilization of the airlaunch system is assured after the launching phase by the controller.

In the case of the mCS control, the convergence of the state variables is fast. But we obtain again a slow convergence of non controlled state variables like pitch angle, yaw angle, airspeed and positions of the air launch system after the separation phase.

In the case of the dynamic feedback linearization control, a complete stabilization of the system is obtained again but slower.

System's Control:

Fig. 6.11 and Fig. 6.12: For the two control methods, the control surfaces are much more saturated when the perturbation on aerodynamic forces moments lasts longer.

Time interval $T_{int} = 0.43s$ which corresponds to a large time interval where the system is still stable for both controllers as we can see in Chapters 4 and 5. Some remarks are:

Stabilization of system's states

Fig. 6.13 to Fig. 6.16: Even if the the stabilization of the airlaunch system is assured after the launching phase by both control methods, the system's state variables oscillate clearly, in particular the angular rates (Fig. 6.14) and Euler's angles (Fig. 6.15). The air launch system is at the limit of stability in this case.

Modified Conditional servocompensator control case: The convergence of the state variables is still fast to their equilibrium values. It is worth noticing that the pitch angle oscillates with a high amplitude (20°), it causes a risk of collision with the separated rocket. The yaw angle which is left free, causes the turn of the air launch system to the

left.

Dynamic feedback linearization control case: Also a complete stabilization of the system is obtained but much slower than the other control method. We note also that the state variables oscillate with a high amplitude, in particular the angle of attack and the sideslip angle which exceed the physical limit of these state variables.

System's Control:

Fig. 6.17 and Fig. 6.18: It is clear that the control surfaces are saturated for the two control methods. However, even with a slower convergence of the state variables for the case of the dynamic feedback linearization control, the control surfaces of this controller is more saturated than the other control method.

Using the dynamic feedback linearization control for the airlaunch system to stabilize the system, the thrust force varies strongly at the beginning of the simulation. It is not the case for the CSC where the thrust is used to control justly the airspeed of the system (see Fig. 6.18).

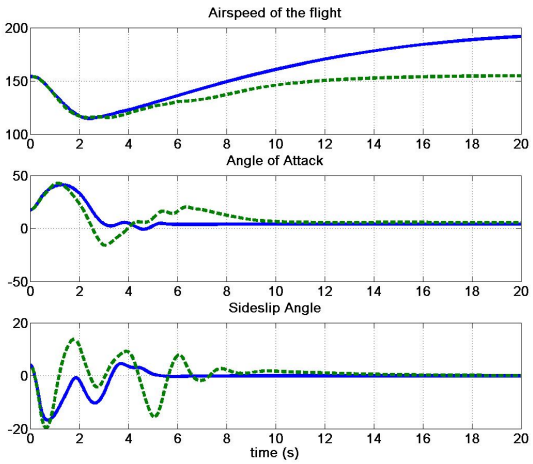

Figure 6.13: Airspeed, Angle of attack and sideslip angle for $T_{int} = 0.43s$

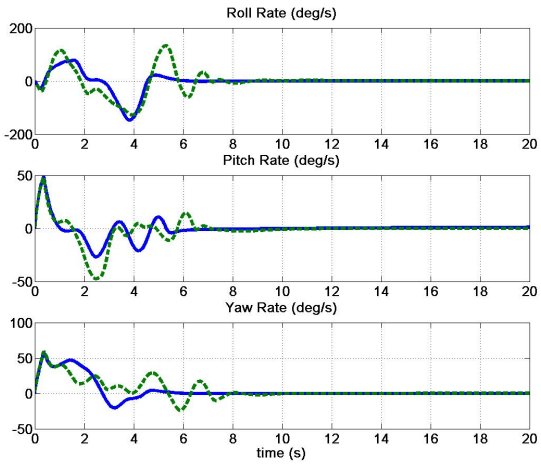

Figure 6.14: Angular Rates: roll, pitch and yaw rates for $T_{int} = 0.43s$

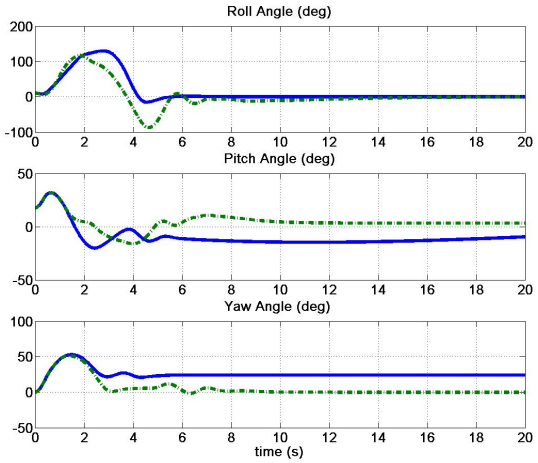

Figure 6.15: Euler's Angles for $T_{int} = 0.43s$

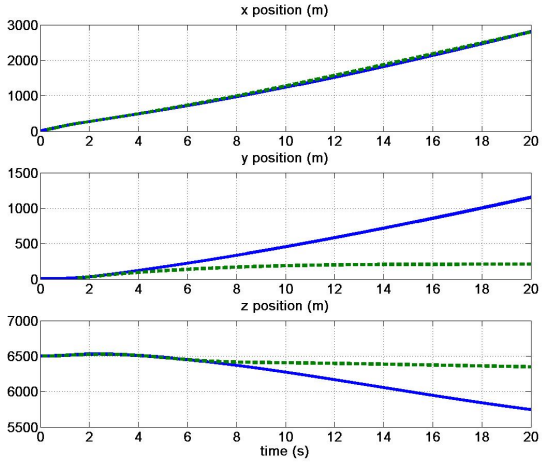

Figure 6.16: System's Position for $T_{int} = 0.43s$

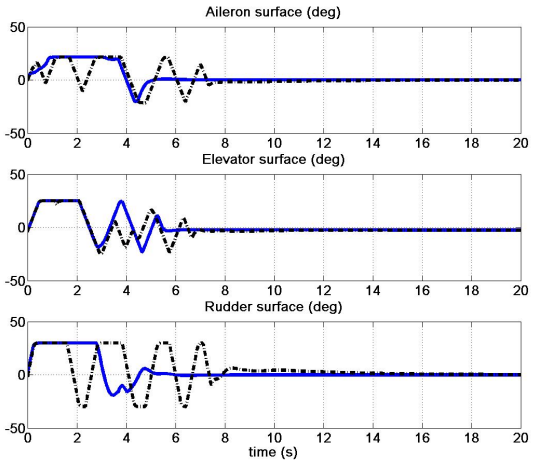

Figure 6.17: Control Surfaces for $T_{int} = 0.43s$

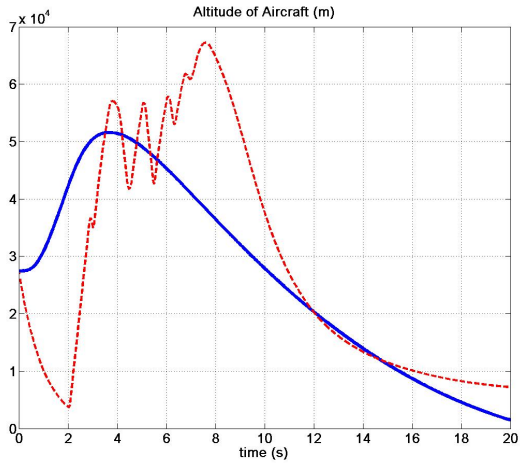

Figure 6.18: Thrust Force for $T_{int} = 0.43s$

System's Altitudes

Fig. 6.19: We are interested in the moment just after the launching phase and can see from the previous chapters that there are no collision between the airlaunch system and the rocket $1s$ after the separation phase. However, we also remark that when the rocket goes up to Earth orbit and the airlaunch system is still stabilizing, with large amplitude of oscillation on the pitch angle in the case of mCS control, it risks a possible collision with the rocket when the airlaunch system goes down.

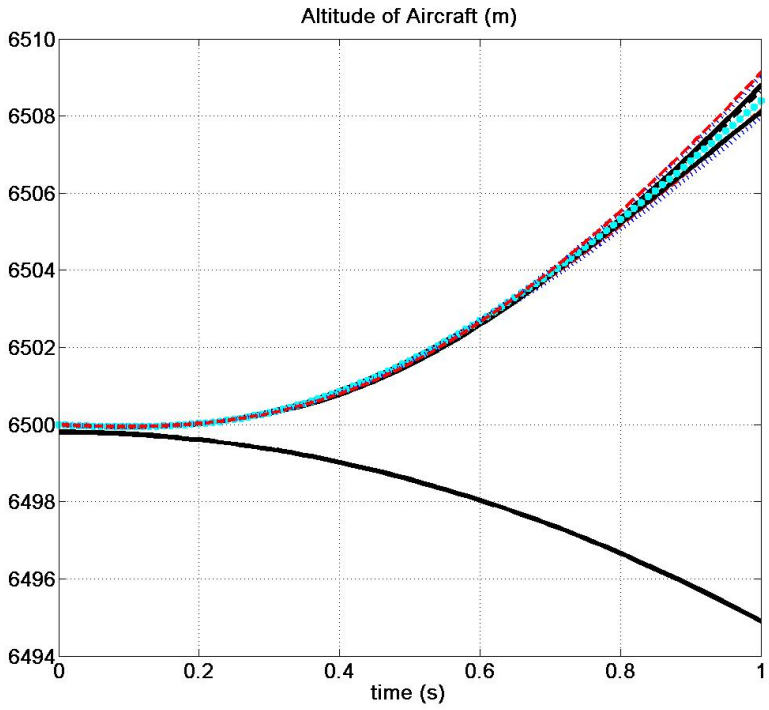

Figure 6.19: Altitude of the system for two control methods vs altitude of the rocket

6.3 Conclusion

The chapter can be concluded by some remarks:

- The modified Conditional Servocompensator control is applied to the airlaunch system through three system's outputs: angle of attack, sideslip and roll angle. The airspeed of the system is controlled by a PI controller through the thrust force. Because the controller is designed for the airlaunch system under a normal form with 6 state variables, the controller guarantees the stabilization of these state variables but not a complete stabilization of the system after the launching phase. For example, the pitch angle and yaw angle evolute freely. It may risk a collision between the airlaunch system and the rocket after the separation phase. Inversely, the dynamic feedback linearization control guarantees a complete stabilization of the airlaunch system after the separation phase as demonstrated in Chapter 5. However, it does not allow to guarantee that certain state variables remain in their physical limits such as angle of attack or sideslip angle.

- Two controls are designed under some assumptions previously mentioned. For the

modified conditional servocompensator control, it is assumed that the control surface deflections affect only aerodynamic moments and not aerodynamic forces, and that the airspeed of the system is much slower than other state variables. For the dynamic feedback linearization control, it is also assumed that the control surface deflections affect only aerodynamic moments and not aerodynamic forces and that the aerodynamic forces depend only on linear velocities but not on angular rates.

- The modified conditional servocompensator control is designed less based on the system model than the dynamic feedback linearization control, which requires a precision of aerodynamic coefficient data and their derivatives. It is an advantage of the conditional servocompensator control compared to the dynamic feedback linearization control.

The choice of the control methods depends on some criterion of the system. If the system has less information about the aerodynamic characteristics, the modified conditional servocompensator control will be a better solution. In the case where the system has information enough, the dynamic feedback linearization control is a better choice. In our case, it may be better to choose the dynamic feedback linearization control. It must be confirm by a test of two controls on the model of the real platform.

Chapter 7

Conclusion and Future works

Contents

7.1 Main Contributions

In this thesis, we have investigated and developed the airlaunch system model during and after the launching phase, a modified Conditional Integrator(mCI) control, a modified Conditional Servocompensator(mCS) control and a dynamic feedback linearization control as possible framework for stabilizing the airlaunch system and collision avoidance. The main contributions of the thesis are:

In term of modeling:

- Modeling the airlaunch system during and after the drop phase has been done using two approaches (see Chapter 2):
  - Initial conditions approach
  - Impulses on aerodynamic force and moment

In term of control methodologies:

- The design of a simple LQR control as a first standard approach to stabilize our airlaunch system after the separation phase. The controller allowed us to have a

first point of view on the stabilization of the system and can be considered as a standard to be compared to the new nonlinear controllers developed in this thesis.

- The development of a modified Conditional Integrator control for a class of multi-input multi-output nonlinear systems from conditional integrator control theory developed by Khalil and his co-workers, and in the following, its applications to airlaunch.

- An extended modified Conditional Servocompensator control from the modified Conditional Integrator one is developed for the same class of MIMO nonlinear systems. Its shows a better performance compared to LQR controller, sliding mode controller and also the conditional integrator control for the linearized air launch system around its equilibrium point.

- The demonstration of the possibility for an aircraft to be dynamic feedback linearizable is shown in Chapter 5. A dynamic feedback linearization control is then designed for the flight system. The interest of this control technique is that it is able to formally stabilize a complete flight system.

In term of applications and results

- The application of the LQR controller as the first approach gave us the stabilization of the air launch system, but only for small initial conditions in the first approach for air launch system modeling, and for a small time interval T_{int} of disturbances on the aerodynamic forces and moments, as we can see in Chapter 2.

- The modified Conditional Integrator control, and in particular the modified Conditional Servocompensator, have shown a better performance to stabilize the air launch system after the separation phase through a large time interval T_{int} corresponding to the duration of the separation phase. In addition, the moCI control and mCS control are developed for a class of MIMO nonlinear systems. In this thesis, they have been applied to other examples of this class of MIMO nonlinear systems as we have shown in Chapter 3.

- The dynamic feedback linearization control was more effective to fully stabilize the airlaunch system. As shown in Chapter 5, it stabilized the complete air launch system including Euler's angles, to linear velocities and angular rates.

- The three studied controllers were able to avoid collision between the air launch system and the rocket during and after the separation phase.

7.2 Future Works

This thesis has addressed a challenging new (and open) problem of stabilizing an unmanned airlaunch. Several good and important results were obtained, in the form of different control systems, each adducted for different situations. These results are (in our best knowledge) the first obtained in this field. As consequence of this originality, much field is still open for future works. Some of the most important ones are summarized in the following:

- Modeling the airlaunch system during and after the launching phase was a key point of the thesis, because of unavailability of a real model with real data in the literature. We have adopted two successive approaches. The first considers that the split was instantaneous, and has already finished. As a consequence of the split, the aircraft was brought to an initial condition, from where the controller must stabilize the system. The second consider the switch from one first model (with the launcher still attached to the carrier) to a second model corresponding to the carrier alone. This switch is not considered as instantaneous, and last a certain amount of time Tint. During this time impulses, representing a worst case, disturb the aircraft. The controller must guarantee the stability of the system during the longest as possible time interval, and bring all states back to their new equilibrium values. If we could obtain a better model for the airlaunch prior to the split phase, the strategy of switching among three phases could be enhanced, and taken more explicitly into account.

- A second result was the development of a mCI control and then a mCS control have been developed for a class of MIMO nonlinear systems. These two control strategies were considered to be applied for the airlaunch problem, but they were not able to address MIMO nonlinear systems. Nevertheless, these control theories present several advantages (in particular its robustness to unknown parameters) that make them very interesting to the control of aerial vehicles. For this reason we have extended this theory to a class of MIMO nonlinear system that includes aircrafts. In the following, there results were used to the airlaunch problem as shown in Section 3.4 of Chapter 3.

- The dynamic feedback linearization control allows us to obtain a better simulation results compared to the modified conditional integrator control or mCS control. It stabilizes completely the airlaunch system after the separation phase. However, the control depends on more detailed analytical models for aerodynamic coefficients

which in practice are under look up table from wind tunnel tests. As a consequence, the precision of analytical models and their parameters are not assured. Therefore, it is necessary to couple this theory to other estimation or adaptive schemes that can reduce its dependence on accurate models. Possibilities would be first to develop an adaptive version of DFL controller. Another would be to make this indirectly through signal processing . approaches to identify these parameters online, and use these estimations in the control algorithms.

- For all control design procedures, we have assumed that all state variables of the airlaunch system are measurable, but sometimes it is not the case. In those cases we would need an estimator to reconstruct these variables for the design procedure. The choice of observer's structure depends on the performance requirement and can be found in the literature (see for example [23] and [24]).

- It would be interesting to extend the simulation results in Chapters 4 and 5. Besides, a comparison with other control methods would be interesting to show the performance of the proposed methods: modified Conditional Integrator, modified Conditional Servocompensator control and dynamic feedback linearization control.

- Test of the proposed control methods on a real platform is needed.

References

[1] Hoa Vo and Sridhar Seshagiri. Robust control of f-16 lateral dynamics. *Industrial Electronics, 2008. IECON 2008. 34th Annual Conference of IEEE*, pages 343–348, 2008.

[2] Bandu N. Pamadi, Thomas A. Neirynck, Nathaniel J. Hotchko, Paul V. Tartabini, William I. Scallion, Kelly J. Murphy, and Peter F. Covell. Simulation and analyses of stage separation of two-stage reusable launch vehicles. *Journal of Spacecraft and Rockets*, 44:66–80, 2007.

[3] Bandu N. Pamadi, Thomas A. Neirynck, Peter F. Covell, Nathaniel Hotchko, and David Bose. Simulation and analyses of staging maneuvers of next generation reusable launch vehicles. *AIAA Atmospheric Flight Mechanics Conference and Exhibit; Providence, RI, USA*, August, 2004.

[4] Bandu N. Pamadi, Paul V. Tartabini, Mathew D. Toniolo, Carlos M. Roithmay, Christopher Karlgaard, and Jamshid Samareh. Application of cfe/post2 for simulation of launch vehicle stage separation. *AIAA Atmospheric Flight Mechanics Conference, Chicago, Illinois, USA*, August, 2009.

[5] Gary J. Balas, John C. Doyle, Keith Glover, , Andy Packard, and Roy Smith. μ - analysis and synthesis toolbox: Users guide version 3. *MUSYN Inc. and The MathWorks, Inc.*, 1993.

[6] Jacob Reiner, Gary J. Balas, and William L. Garrard. Flight control design using robust dynamic inversion and time-scale separation. *Automatica*, 32:1493–1504, 1996.

[7] Stephen H. Lane and Robert F. Stengel. Flight control design using non-linear inverse dynamics. *American Control Conference, Seattle, WA, USA*, pages 587–596, June 18-20, 1986.

[8] Ola Harkegard. *Flight Control Design Using Backstepping*. PhD thesis, Linkopings Universitet, Sweden, 2001.

[9] Taeyoung Lee and Youdan Kim. Nonlinear adaptive flight control using backstepping and neural networks controller. *Journal of guidance, control and dynamics*, 24:675–682, 2001.

[10] Thor I. Fossen. *Guidance and Control of Ocean Vehicles*. Wiley, 1994.

[11] Lars Sonneveldt. *Nonlinear F-16 Model Description*. Delft University of Technology, Netherlands, 2006.

[12] Peter H. Zipfel. *Modeling and Simulation of Aerospace Vehicle Dynamics, 2nd edition*. American Institute of Aeronautics and Astronautics, January, 2001.

[13] L. T. Nguyen, M.E. Ogburn, and P. Deal. Simulator study of fighter airplane with relaxed longitudinal static stability. *Technical report NASA*, 1979.

[14] Nazmi A. Mahmoud and Hassan K. Khalil. Robust control for a nonlinear servomechanism problem. *International Journal of Control*, 66:779–802, April 1, 1997.

[15] Hassan K. Khalil. On the design of robust servomechanisms for minimum phase nonlinear systems. *Robust Nonlinear Control 2000, John Wiley & Sons*, 10:339–361, 2000.

[16] Gilney Damm and Van Cuong Nguyen. Mimo conditional integrator control for a class of nonlinear systems. In *In proceedings of System Theory, Control, and Computing (ICSTCC), 2011 15th International Conference, Sinaia, Romania*, October 14-16, 2011.

[17] Sridhar Seshagiri and Hassan K. Khalil. Robust output feedback regulation of minimum-phase nonlinear systems using conditional integrators. *Automatica*, 41:43–54, January, 2005.

[18] B. Charlet, J. Levine, and R. Marino. On dynamic feedback linearization. *Systems & Control Letters*, 13:143–151, 1989.

[19] B. Charlet, J. Levine, and R. Marino. Dynamic feedback linearization with application to aircraft control. *In Proceedings of the 27th Conference on Decision and Control Austin, Texas, USA*, 1:701–705, December 7 - 9, 1988.

[20] B. Charlet, J. Levine, and Riccardo Marino. New sufficient conditions for dynamic feedback linearization. *IFAC Symposium Capri, Italy*, June 14-16, 1989.

[21] H. Nijmeijer and A.J. Van der Schaft. *Nonlinear dynamical control systems*. Springer, 1990.

[22] B. Charlet, J. Levine, and Marino R. Sufficient conditions for dynamic feedback linearization. *SIAM Journal of Control and Optimization*, 1991.

[23] Antonio Tornambé. High-gain observers for non-linear systems. *International Journal of Systems Science*, 23:1475–1489, 1992.

[24] E. Bullinger and F. Allgower. An adaptive high-gain observer for nonlinear systems. *Proceedings of the 36th IEEE Conference on Decision and Control, San Diego, CA, USA.*, 5:4348–4353, December, 1997.

[25] Marti Sarigul-Klijn and Nesrin Sarigul-Klijn. A study of air launch methods for rlvs. *American Institute of Aeronautics and Astronautics*, 2001.

[26] Encyclopedia astronautica at http://www.astronautix.com/lvs/saegerii.htm and http://www.astronautix.com/lvs/spil5050.htm.

[27] Airlaunch system at http://space.skyrocket.de/doc_lau/airlaunch.htm.

[28] Kelly space & technology, inc. at http://www.kellyspace.com/launchvehicle/.

[29] Alabama 35814 Stratolaunch Systems, Inc. P.O. Box 22132 Huntsville. Stratolaunch systems, inc. at http://www.stratolaunch.com/presskit.html.

[30] M.-M. Burlacu and J. Kohlenberg. An analysis of the nanosatellites launches between 2004 and 2007. *3rd International Conference on Systems and Networks Communications*, pages 292–297, 2008.

[31] Marti Sarigul-Klijn and Nesrin Sarigul-Klijn. Selection of a carrier aircraft and a launch method for air launching space vehicles. In *AIAA SPACE 2008 Conference and Exposition, San Diego, California, USA*, September 9 - 11, 2008.

[32] Gary C. Hudson. Quickreach responsive launch system. In *4th Responsive Space Conference, Los Angeles, CA, USA*, April 24-27, 2006.

[33] Colonel Dan Fritz and Chris Webber. Falcon quickreach - airdrop envelope expansion to enable low cost space acces. *Air Force Flight Test Center*, 2005.

[34] Debra Facktor Lepore and Dr. Ralph Ewig. Results of quickreach small launch vehicle propulsion testing and next steps to demonstration flights. *Utah State Small Satellite Conference*, August, 2008.

[35] Debra Facktor Lepore and Joseph Padavano. Progress toward first flight of the quickreach small launch vehicle. *Utah State Small Satellite Conference*, August, 2007.

[36] Debra Facktor Lepore and Joseph Padavano. Airlaunch's quickreach small launch vehicle: Operationally responsive access to space. *15th Annual AIAA/USU Conference on Small Satellites*, 2006.

[37] Jacob Lopata and Burt Rutan. Rascal - a demonstration of operationally responsive space launch. *2nd Responsive Space Conference, Los Angeles, CA*, April 19-22, 2004.

[38] J.-F. Magni, S. Bennani, and J.Terlouw. *Robust Flight Control : A Design Challenge*. Springer, 1997.

[39] Emmanuel Trélat. *Commande optimale*. Notes du cours A08, 2008.

[40] Sridhar Seshagiri and Hassan K. Khalil. Output feedback regulation of minumum-phase nonlinear systems using conditional integrators. *Automatica*, 41:43–54, 2005.

[41] Sridhar Seshagiri and Hassan K. Khalil. Robust output regulation of minimum phase nonlinear systems using conditional servocompensators. *International Journal of Robust and Nonlinear Control*, 22:83–102, January, 2005.

[42] Attaullah Y. Memona and Hassan K. Khalil. Output regulation of nonlinear systems using conditional servocompensators. *Automatica*, 46:1119–1128, July, 2010.

[43] Gilney Damm and Van Cuong Nguyen. Mimo conditional servo-compensator control for a class of nonlinear systems (accepted). *In Proceedings of the 51th Conference on Decision and Control, Maui - Hawaii, USA.*, December 10-13, 2012.

[44] Hassan K. Khalil. *Nonlinear Systems*. Prentice Hall, 2001.

[45] Riccardo Marino and Patrizio Tomei. *Nonlinear Control Design: Geometric, Adaptive and Robust*. Prentice Hall, 1st edition, 1995.

[46] Alberto Isidori. *Nonlinear Control Systems*. Springer Verlag, 1995.

[47] Sridhar Seshagiri and Ekprasit Promtun. Sliding mode control of f-16 longitudinal dynamics. *American Control Conference*, pages 1770–1775, 2008.

[48] Eugene Morelli. Global nonlinear parametric modeling with application to f-16 aerodynamics. *In Proceedings of the 1998 American Control Conference, Philadelphia, PA , USA*, 2:997–1001, Junuary 21-26, 1998.

[49] Amanda Young, Chengyu Cao, and Naira Hovakimyan. An adaptive approach to nonaffine control design for aircraft applications. In *AIAA Guidance, Navigation, and Control Conference and Exhibit, Keystone, Colorado*, 21-24 August, 2006.

[50] S. Seshagiri and H.-K. Khalil. On introducing integral action in sliding mode control. *Proceedings of the 41st IEEE Conference on Decision and Control, 2002*, 2:1473–1478, Dec, 2002.

[51] G. Meyer, R. Su, and L. R. Hunt. Application of nonlinear transformations to automatic flight control. *Automatica*, 20:103 – 107, January, 1984.

[52] Stevens Brian L. and Lewis Frank L. *Aircraft Control and Simulation*. John Wiley & Sons, 1992.

[53] Jan Roskam. *Airplane Flight Dynamic and Automatic Flight Controls, Part 1*. Design, Analysis and Research Corporation, 2001.

[54] J.-F. Magni, S. Bennani, and J.Terlouw. *Robust Flight Control : A Design Challenge*. Springer, 1997.

[55] Qian Wang and Robert F. Stengel. Robust nonlinear flight control of a high-performance aircraft. *IEEE Transaction on control systems technology*, 13:15–26, 2005.

[56] John W. C. Robinson. Block backstepping for nonlinear flight control law design. *Springer*, 365:231–257, 2007.

[57] John Hauser, Shankar Sastry, and George Meyer. Nonlinear control design for slightly non-minimum phase systems: Application to v/stol aircraft. *Automatica*, 28:665–679, July, 1992.

[58] L. R. Hunt, Renjeng Su, and George Meyer. Global transformations of nonlinear systems. *IEEE Transactions on Automatic Control*, 28:24–31, January, 1983.

[59] Van Cuong Nguyen and Gilney Damm. Modeling and conditional integrator control of an unmanned aerial vehicle for airlaunch. *in Proceedings of the 2012 American Control Conference (ACC), Montreal, Canada*, June 27-29, 2012.

Appendix A

Modified Conditional Integrator and Modified Conditional Servocompensator

A.1 Modified Conditional Servo-Compensator in the case of $f(\cdot)$ and $g(\cdot)$ unknown

Consider the system:

$$\begin{cases} \dot{e}_1 &= e_2 \\ \dot{e}_2 &= f(e_1, e_2) + g(e_1, e_2)u \end{cases} \tag{A.1}$$

Let us impose the sliding surface as:

$$s = K_0\sigma + K_1 e_1 + e_2 \tag{A.2}$$

where $\sigma \in \mathbb{R}^n$ is the output of the conditional servocompensator

$$\dot{\sigma} = -K_0\sigma + \mu sat(s/\mu) \tag{A.3}$$

in which μ is the boundary layer, K_0 is a positive definite matrix, $K_1 \in \mathbb{R}^{n\times n}$ is chosen such a way that $K_1 + sI_n$ is Hurwitz., I_n is the $n \times n$ identity matrix. The saturation function is determined as:

$$sat(s/\mu) = \begin{cases} s/\|s\| & \text{if } \|s\| \geq \mu \\ s/\mu & \text{if } \|s\| < \mu \end{cases} \tag{A.4}$$

where $\|\cdot\|$ is a L2 norm.

The derivative of the sliding surface can be expressed as:

$$\dot{s} \quad = \quad K_0\dot{\sigma} + K_1\dot{e_1} + \dot{e_2} \tag{A.5}$$

Equation (A.5) may be written again from (A.1) and (A.2)

$$\begin{aligned}\dot{s}=&K_0(-K_0\sigma + \mu sat(s/\mu)) + K_1e_2 + \dot{e}_2\\ =&-K_0s + K_0\mu sat(s/\mu) + K_1e_2 + \dot{e}_2 + K_0(K_1e_1 + e_2)\end{aligned} \tag{A.6}$$

Now by letting

$$\Delta(e_1, e_2) = K_0(K_1e_1 + e_2) + K_1e_2 + f(e_1, e_2) \tag{A.7}$$

Equation (A.6) becomes

$$\dot{s}=-K_0s + K_0\mu sat(s/\mu) + \Delta(e_1, e_2) + g(e_1, e_2)u \tag{A.8}$$

We can then define the controller:

$$u = -\Pi(e_1, e_2)sat(s/\mu) \tag{A.9}$$

This controller allows to robustly stabilize the system (A.1) in a semi-global manner.

We will now demonstrate that the control law defined in (A.9) can stabilize the class of nonlinear MIMO systems defined in (A.1). This demonstration is decomposed in two parts representing the internal and external regions of the boundary layer and will be later formally stated in the form of a theorem.

A.1.1 *In the region* $\|s\| \geq \mu$, $sat(s/\mu) = s/\|s\|$.

In this part, we demonstrate that the control law in (A.9) with $\Pi(\cdot)$ defined later in (A.18) will bring the sliding surface inside the boundary layer. Before proceeding further, we remind the assumption 3.2.1 and introduce a new assumption on $g(\cdot)$ function.

Assumption 3.2.1: $\Delta(e_1, e_2)$ defined in equation (3.9) is bounded by a class $\mathcal{K}$ function $\gamma(\|e_1\| + \|e_2\|)$ and a positive constant Δ_0 :

$$\|\Delta(e_1, e_2)\| \leq \gamma(\|e_1\| + \|e_2\|) + \Delta_0 \tag{A.10}$$

and as a consequence,

$$\|\Delta(e_1 = 0, e_2 = 0)\| = \|f(0, 0)\| \leq \Delta_0$$

for $(e_1, e_2) \in \mathbb{R}^n \times \mathbb{R}^n$.

Function $f(e_1, e_2)$ is required to be Lipschitz for $(e_1, e_2) \in \mathcal{O}_\mu$, as a consequence

$$\|f(e_1, e_2) - f(0,0)\| \leq L_1\|K_1 e_1\| + L_2\|e_2\| \tag{A.11}$$

$\gamma(\|e_1\| + \|e_2\|)$ is also required to be Lipschitz for $(e_1, e_2) \in \mathcal{O}_\mu$:

$$\gamma(\|e_1\| + \|e_2\|) \leq \gamma_1\|K_1 e_1\| + \gamma_2\|e_2\| \tag{A.12}$$

□

Assumption A.1.1 *Function $g(e_1, e_2)$ satisfies two hypothesis:*

Hypothesis 1: *for $(e_1, e_2) \in \mathbb{R}^n \times \mathbb{R}^n$*

$$g(e_1, e_2) + g^T(e_1, e_2) \geq 2\lambda I_n, \text{ for a constant } \lambda > 0 \tag{A.13}$$

Hypothesis 2: *with $(e_1, e_2) \in \mathcal{O}_\mu$, function $g(e_1, e_2)$ satisfies the Lipschitz-like condition:*

$$\|g(e_1, e_2)g^{-1}(0,0) - I_n\| \quad \leq \quad \upsilon(e_1, e_2) \tag{A.14}$$

in which, $\upsilon(e_1, e_2)$ is a suitable function satisfying (should remind that e_1 and e_2 are in the bounded region):

$$\upsilon(e_1, e_2) \quad = \quad \upsilon_1\|K_1 e_1\| + \upsilon_2\|e_2\| \leq K_\upsilon \tag{A.15}$$

where υ_1, υ_2 and K_υ are suitable positive constants.

□

Lets now consider the product $s^T\dot{s}$

$$s^T\dot{s} \quad = \quad -s^T K_0 s + \mu s^T K_0 sat(s/\mu) + s^T\Delta(e_1, e_2) + s^T g(e_1, e_2)u \tag{A.16}$$

This product $s^T\dot{s}$ can be developed with the previous assumption and the definition of saturation function (A.4):

$$\begin{aligned} s^T\dot{s} =& -s^T K_0 s + \mu s^T K_0 s/\|s\| + s^T\Delta(\cdot) - s^T g(\cdot)\Pi(\cdot)s/\|s\| \\ \leq& -s^T K_0 s + \mu s^T K_0 s/\|s\| + \|\Delta(\cdot)\|\|s\| - s^T g(\cdot)\Pi(\cdot)s/\|s\| \\ \leq& -s^T K_0 s - s^T(\lambda\Pi(\cdot) - \mu K_0 - (\gamma(\cdot) + \Delta_0)I_n)s/\|s\| \\ & -1/2 s^T(g(\cdot) + g^T(\cdot) - \lambda I_n)\Pi(\cdot)s/\|s\| \\ \leq& -s^T K_0 s - \lambda s^T\Pi_0 s/\|s\| \leq -\lambda_{min}(K_0)\|s\|^2 - \lambda\lambda_{min}(\Pi_0)\|s\| \end{aligned} \tag{A.17}$$

where we define

$$\Pi(\cdot) = \Pi_0 + (K_0\mu + (\gamma(\cdot) + \Delta_0)I_n)/\lambda \tag{A.18}$$

and Π_0 is a positive definite matrix.

The product $s^T\dot{s}$ is then not positive and

$$\begin{cases} s^T\dot{s} \leq -\lambda_{min}(K_0)\|s\|^2 - \lambda\lambda_{min}(\Pi_0)\|s\| \leq -\lambda\lambda_{min}(\Pi_0)\|s\| \\ \frac{d\|s\|^2}{dt} = 2\|s\|\frac{d(\|s\|)}{dt} = 2s^T\dot{s} \leq 2(-\lambda\lambda_{min}(\Pi_0)\|s\|) \\ \Rightarrow \frac{d(\|s\|)}{dt} \leq -\lambda\lambda_{min}(\Pi_0) \\ \Rightarrow \|s(t)\| \leq \|s(0)\| - \lambda\lambda_{min}(\Pi_0)t \end{cases} \tag{A.19}$$

Then the sliding surface $s(t)$ reaches the set $\|s(t)\| \leq \mu$ in finite time.

□

A.1.2 *In the region* $\|s\| \leq \mu$, $sat(s/\mu) = s/\mu$.

Consider again (A.2), (A.19), (A.8) and control law (A.9), which inside the boundary layer may be rewritten as (A.20) (remind that $\dot{e}_1 = e_2$).

$$\begin{cases} \dot{\sigma} = -K_0\sigma + s \\ \dot{e}_1 = -K_1e_1 + s - K_0\sigma \\ \dot{s} = \Delta(\cdot) - g(\cdot)\Pi(\cdot)s/\mu \end{cases} \tag{A.20}$$

It can be shown that system (A.20) has an equilibrium point: $e_1 = e_2 = 0$, $s = \bar{s}$, $\sigma = \bar{\sigma}$ with $\bar{s} = K_0\bar{\sigma} = \mu\Pi^{-1}(0)g^{-1}(0)f(0)$.

System (A.20) may be rewritten with respect to $\bar{s}$ and $\bar{\sigma}$:

$$\begin{cases} \dot{\tilde{\sigma}} = -K_0\tilde{\sigma} + \tilde{s} \\ \dot{e}_1 = -K_1e_1 + \tilde{s} - K_0\tilde{\sigma} \\ \dot{\tilde{s}} = \Delta(\cdot) - \Pi(\cdot)g(\cdot)\tilde{s}/\mu - \Pi(\cdot)g(\cdot)\bar{s}/\mu \end{cases} \tag{A.21}$$

where $\tilde{\sigma} = \sigma - \bar{\sigma}$, $\tilde{s} = s - \bar{s}$.

In the following we will show that the state variables of the system (A.21) are driven to the equilibrium point when the control law (A.9) is applied, with $\Pi(\cdot)$ defined in (A.18), when the system is inside the boundary layer.

We would like to demonstrate that every trajectory starting inside the boundary layer, will approach the equilibrium point as time tends to infinity. Toward that end, we take

$$W = \frac{\lambda_1}{2}\tilde{\sigma}^TK_0\tilde{\sigma} + \frac{\lambda_2}{2}e_1^TK_1e_1 + \frac{\lambda_3}{2}\tilde{s}^T\tilde{s} \tag{A.22}$$

as a Lyapunov candidate, where λ_1 and λ_2 are positive constants.

Its derivative can be easily calculated as:

$$\begin{aligned}\dot{W}=&\lambda_1\tilde{\sigma}^T K_0\dot{\tilde{\sigma}}+\lambda_2 e_1^T K_1\dot{e_1}+\lambda_3\tilde{s}^T\dot{\tilde{s}}\\ =&\lambda_1\tilde{\sigma}^T K_0(-K_0\tilde{\sigma}+\tilde{s})+\lambda_2 e_1^T K_1(-K_1e_1+\tilde{s}-K_0\tilde{\sigma})\\ &+\lambda_3\tilde{s}^T(\Delta(\cdot)-g(\cdot)\Pi(\cdot)\tilde{s}/\mu-g(\cdot)\Pi(\cdot)\bar{s}/\mu)\end{aligned} \tag{A.23}$$

Since $(e_1,e_2)\in\mathcal{O}_\mu$, $\Delta(\cdot)$ can be expressed:

$$\begin{aligned}\Delta(\cdot)=&K_0(s-K_0\sigma)+K_1(-K_1e_1+s-K_0\sigma)+f(\cdot)\\ =&(K_0+K_1)\tilde{s}-(K_0+K_1)K_0\tilde{\sigma}-K_1^2e_1+f(\cdot)\end{aligned} \tag{A.24}$$

then,

$$\begin{aligned}\dot{W}=&-\lambda_1\tilde{\sigma}^T K_0^2\tilde{\sigma}+\lambda_1\tilde{\sigma}^T K_0\tilde{s}-\lambda_2 e_1^T K_1^2e_1+\lambda_2 e_1^T K_1(\tilde{s}-K_0\tilde{\sigma})\\ &+\lambda_3\tilde{s}^T((K_0+K_1)\tilde{s}-(K_0+K_1)K_0\tilde{\sigma}-K_1^2e_1-g(\cdot)\Pi(\cdot)\tilde{s}/\mu)\\ &+\lambda_3\tilde{s}^T(f(\cdot)-g(\cdot)\Pi(\cdot)\bar{s}/\mu)\end{aligned} \tag{A.25}$$

We denote $f(0)=f(0,0)$, $g(0)=g(0,0)$ and $\Pi(0)=\Pi(0,0)$. In order to express the derivative of the Lyapunov function candidate more clearly, we consider firstly the term using assumptions 3.2.1 and A.1.1:

$$\begin{aligned}f(\cdot)-g(\cdot)\Pi(\cdot)\bar{s}/\mu \quad &=f(\cdot)-g(\cdot)\Pi(\cdot)\Pi^{-1}(0)g^{-1}(0)f(0)\|\\ &=f(\cdot)-f(0)-(g(\cdot)g^{-1}(0)-I_n)f(0)\\ &\quad-(g(\cdot)g^{-1}(0)-I_n)g(0)(\Pi(\cdot)-\Pi(0))\Pi^{-1}(0)g^{-1}(0)f(0)\\ &\quad-g(0)(\Pi(\cdot)-\Pi(0))\Pi^{-1}(0)g^{-1}(0)f(0)\\ \Rightarrow\|f(\cdot)-g(\cdot)\Pi(\cdot)\bar{s}/\mu\|\leq&\|f(\cdot)-f(0)\|+\|(g(\cdot)g^{-1}(0)-I_n)\|\|f(0)\|\\ &\quad+\gamma(\cdot)/\lambda\|(g(\cdot)g^{-1}(0)-I_n)\|\|g(0)\|\|\Pi^{-1}(0)\|\|g^{-1}(0)\|\|f(0)\|\\ &\quad+\gamma(\cdot)/\lambda\|g(0)\|\|\Pi^{-1}(0)\|\|g^{-1}(0)\|\|f(0)\|\\ \Rightarrow\|f(\cdot)-g(\cdot)\Pi(\cdot)\bar{s}/\mu\|\leq&L_1\|K_1e_1\|+L_2\|e_2\|+\Delta_0(\upsilon_1\|K_1e_1\|+\upsilon_2\|e_2\|)\\ &\quad+G_0K_\upsilon(\gamma_1\|K_1e_1\|+\gamma_2\|e_2\|)+G_0(\gamma_1\|K_1e_1\|+\gamma_2\|e_2\|)\\ \Rightarrow\|f(\cdot)-g(\cdot)\Pi(\cdot)\bar{s}/\mu\|\leq&(L_1+\Delta_0\upsilon_1+G_0K_\upsilon\gamma_1+G_0\gamma_1)\|K_1e_1\|\\ &\quad+(L_2+\Delta_0\upsilon_2+G_0K_\upsilon\gamma_2+G_0\gamma_2)\|e_2\|\\ \Rightarrow\|f(\cdot)-g(\cdot)\Pi(\cdot)\bar{s}/\mu\|\leq&a_1\|K_1e_1\|+a_2\|e_2\|\end{aligned} \tag{A.26}$$

where $G_0=\|g(0,0)\|\|g^{-1}(0,0)\|$ is a constant, $a_1=L_1+\Delta_0\upsilon_1+G_0K_\upsilon\gamma_1+G_0\gamma_1$, $a_2=L_2+\Delta_0\upsilon_2+G_0K_\upsilon\gamma_2+G_0\gamma_2$ and remark that $\|\Pi^{-1}(0)\|\|f(0)\|\leq 1$.

Using the relation in (A.1), the previous equation can be expressed as:

$$\begin{aligned}
&\tilde{s}^T(f(\cdot)-g(\cdot)\Pi(\cdot)\bar{s}/\mu) \leq \|\tilde{s}\|\|f(\cdot)-g(\cdot)\Pi(\cdot)\bar{s}/\mu\| \\
&\leq a_1\|\tilde{s}\|\|K_1e_1\|+a_2\|\tilde{s}\|\|e_2\| \\
&\leq \tfrac{a_1}{2}(\tilde{s}^T\tilde{s}+e_1K_1^2e_1)+\tfrac{a_2}{2}(\tilde{s}^T\tilde{s}+e_2^Te_2) \\
&\leq \tfrac{a_1}{2}(\tilde{s}^T\tilde{s}+e_1K_1^2e_1)+\tfrac{a_2}{2}(\tilde{s}^T\tilde{s}+(\tilde{s}-K_0\tilde{\sigma}-K_1e_1)^T(\tilde{s}-K_0\tilde{\sigma}-K_1e_1)) \\
&\leq \tfrac{a_1}{2}(\tilde{s}^T\tilde{s}+e_1K_1^2e_1)+\tfrac{a_2}{2}(\tilde{s}^T\tilde{s}+3(\tilde{s}^T\tilde{s}+\tilde{\sigma}^TK_0^2\tilde{\sigma}+e_1^TK_1^2e_1)) \\
&\leq \tfrac{a_1+4a_2}{2}\tilde{s}^T\tilde{s}+\tfrac{3a_2}{2}\tilde{\sigma}^TK_0^2\tilde{\sigma}+\tfrac{a_1+3a_2}{2}e_1^TK_1^2e_1 \\
&\leq c_1\tilde{\sigma}^T\tilde{\sigma}+c_2e_1^Te_1+c_3\tilde{s}^T\tilde{s}
\end{aligned} \tag{A.27}$$

where we define $c_1 = 3/2a_2$, $c_2 = 1/2a_1 + 3/2a_2$ and $c_3 = 1/2(a_1 + 4a_2)$.

From (A.21) and (A.27) the derivative of W can be developed:

$$\begin{aligned}
\dot{W}=&-\lambda_1\tilde{\sigma}^TK_0^2\tilde{\sigma}+\lambda_1\tilde{\sigma}^TK_0\tilde{s}-\lambda_2e_1^TK_1^2e_1+\lambda_2e_1^TK_1(\tilde{s}-K_0\tilde{\sigma})+\lambda_3(\tilde{s}^T(K_0+K_1)\tilde{s} \\
&-\tilde{s}^T(K_0+K_1)K_0\tilde{\sigma}-\tilde{s}^TK_1^2e_1-\tilde{s}^Tg(\cdot)\Pi(\cdot)\tilde{s}/\mu+\tilde{s}^T(f(\cdot)-g(\cdot)\Pi(\cdot)\bar{s}/\mu)) \\
\leq&-\lambda_1\tilde{\sigma}^TK_0^2\tilde{\sigma}+\lambda_1/2(\tilde{s}^T\tilde{s}+\tilde{\sigma}^TK_0^2\tilde{\sigma})-\lambda_2e_1^TK_1^2e_1+\lambda_2/2(e_1^TK_1^2e_1 \\
&+(\tilde{s}-K_0\tilde{\sigma})^T(\tilde{s}-K_0\tilde{\sigma}))+\lambda_3(\tilde{s}^T(K_0+K_1)\tilde{s}+1/2(\tilde{s}^T(K_0+K_1)^2\tilde{s}+\lambda_1\tilde{\sigma}^TK_0^2\tilde{\sigma}) \\
&+1/2(\tilde{s}^TK_1^2\tilde{s}+e_1^TK_1^2e_1)-\lambda\tilde{s}^T\Pi(\cdot)\tilde{s}/\mu-1/2\tilde{s}^T(g(\cdot)+g^T(\cdot)-2\lambda)\Pi(\cdot)\tilde{s}/\mu \\
&+c_1\tilde{\sigma}^TK_0^2\tilde{\sigma}+c_2e_1^TK_1^2e_1+c_3\tilde{s}^T\tilde{s}) \\
\leq&-\lambda_1\tilde{\sigma}^TK_0^2\tilde{\sigma}+\lambda_1/2(\tilde{s}^T\tilde{s}+\tilde{\sigma}^TK_0^2\tilde{\sigma})-\lambda_2e_1^TK_1^2e_1+\lambda_2/2(e_1^TK_1^2e_1+2(\tilde{s}^T\tilde{s}+\tilde{\sigma}^TK_0^2\tilde{\sigma})) \\
&+\lambda_3(\tilde{s}^T(K_0+K_1)\tilde{s}+1/2(\tilde{s}^T(K_0+K_1)^2\tilde{s}+\tilde{\sigma}^TK_0^2\tilde{\sigma})+1/2(\tilde{s}^TK_1^2\tilde{s}+e_1^TK_1^2e_1) \\
&-\lambda\tilde{s}^T\Pi(\cdot)\tilde{s}/\mu-1/2\tilde{s}^T(g(\cdot)+g^T(\cdot)-2\lambda)\Pi(\cdot)\tilde{s}/\mu+c_1\tilde{\sigma}^TK_0^2\tilde{\sigma}+c_2e_1^TK_1^2e_1+c_3\tilde{s}^T\tilde{s}) \\
\leq&-\tilde{\sigma}^T(\lambda_1K_0^2-\lambda_1/2K_0^2-\lambda_2K_0^2-\lambda_3/2K_0^2-\lambda_3c_1K_0^2)\tilde{\sigma} \\
&-e_1^T(\lambda_2K_1^2-\lambda_2/2K_1^2-\lambda_3/2K_1^2-\lambda_3c_2K_1^2)e_1 \\
&-\tilde{s}^T(\lambda_3(\lambda\Pi(\cdot)/\mu-(K_0+K_1)-1/2(K_0+K_1)^2-1/2K_1^2-c_3I_n)-\lambda_1/2I_n-\lambda_2I_n)\tilde{s} \\
&-\lambda_3/2\tilde{s}^T(g(\cdot)+g^T(\cdot)-2\lambda)\Pi(\cdot)\tilde{s}/\mu \\
\leq&-(\lambda_1/2-\lambda_2-\lambda_3/2-\lambda_3c_1)\tilde{\sigma}^TK_0^2\tilde{\sigma}-(\lambda_2/2-\lambda_3/2-\lambda_3c_2)e_1^TK_1^2e_1 \\
&-\tilde{s}^T(\lambda_3(\lambda\Pi(\cdot)/\mu-(K_0+K_1)-1/2(K_0+K_1)^2-1/2K_1^2)-(\lambda_1/2+\lambda_2+\lambda_3c_3)I_n)\tilde{s} \\
&-\lambda_3/2\tilde{s}^T(g(\cdot)+g^T(\cdot)-2\lambda)\Pi(\cdot)\tilde{s}/\mu
\end{aligned} \tag{A.28}$$

It can be verified that by taking λ_1, λ_2 large enough, $\|\Pi(\cdot)\|$ large enough with respect to control dynamics or μ small enough, the following conditions are satisfied:

$$\begin{cases}
\lambda_1/2-\lambda_2-\lambda_3/2-\lambda_3c_1 & >0 \\
\lambda_2/2-\lambda_3/2-\lambda_3c_2 & >0 \\
\lambda_3(\lambda\Pi(\cdot)/\mu-(K_0+K_1)-1/2(K_0+K_1)^2-1/2K_1^2) & >(\lambda_1/2+\lambda_2+\lambda_3c_3)I_n \\
g(\cdot)+g^T(\cdot)-2\lambda>0 & \text{ from assumption A.1.1}
\end{cases}$$

In this way, $W(t)$ satisfies $W(t) > 0$ and $\dot{W} < -w_0 W$ (where w_0 is a positive constant) for all $\sigma \neq \bar{\sigma}$, $e_1 \neq 0$ and $s \neq \bar{s}$. Then $W(t)$ reaches exponentially zero when time tends to infinite. As consequence, the output error $e_1(t)$ tends to zero and σ and s tend to their equilibrium values as time tends to infinite. We may assure the stability of the system in the region of $\|s\| \leq \mu$.

We can then state the results developed above in the form of the theorem:

Theorem A.1.1 *A class of Multi-Input Multi-Output nonlinear systems described by (A.1), and satisfying assumptions (3.2.1 and A.1.1) can be stabilized globally to their constant reference by the controller (A.9-A.2-A.3-A.18) with tunning parameters (Π_0, K_0, μ and K_1 defined in the previous section) and function $\gamma(\cdot)$ conveniently set.*

■

A.2 Functions of lateral and longitudinal modes for the control design

- Functions defined in the lateral mode:

$$f_{11}^{\beta}(\cdot) = \begin{bmatrix} \frac{1}{mV}(-\cos(\alpha_0)\sin(\beta)(T + C_x(\alpha_0)\bar{q}S) + \cos(\beta)C_y(\beta)\bar{q}S - \sin(\alpha_0)\sin(\beta)C_z(\alpha_0,\beta)\bar{q}S) \\ 0 \\ +\frac{g}{V}(\cos(\alpha_0)\sin(\beta)\sin(\theta_0) + \cos(\beta)\cos(\theta_0)\sin(\phi) - \sin(\alpha_0)\sin(\beta)\cos(\phi)) \end{bmatrix}$$

$$f_{12}^{\beta}(\cdot) = \begin{bmatrix} \sin(\alpha_0) + \frac{\rho S}{4m}\cos(\beta)C_{y_p}(\alpha_0)\bar{b} & -\cos(\alpha_0) + \frac{\rho S}{4m}\cos(\beta)C_{y_r}(\alpha_0)\bar{b} \\ 1 & \cos(\phi)\tan(\theta_0) \end{bmatrix}$$

$$f_{21}^{\beta}(\cdot) = \begin{bmatrix} I_3 C_l(\alpha_0,\beta)\bar{q}S\bar{b} + I_4 C_n(\alpha_0,\beta)\bar{q}S\bar{b} \\ I_4 C_l(\alpha_0,\beta)\bar{q}S\bar{b} + I_9 C_n(\alpha_0,\beta)\bar{q}S\bar{b} \end{bmatrix}$$

$$f_{22}^{\beta}(\cdot) = \frac{\rho V S\bar{b}}{4}\begin{bmatrix} (I_3 C_{l_p}(\alpha_0) + I_4 C_{n_p}(\alpha_0)) & (I_3 C_{l_r}(\alpha_0) + I_4 C_{n_r}(\alpha_0)) \\ (I_4 C_{l_p}(\alpha_0) + I_9 C_{n_p}(\alpha_0)) & (I_4 C_{l_r}(\alpha_0) + I_9 C_{n_r}(\alpha_0)) \end{bmatrix}$$

$$g_2^{\beta}(\cdot) = \bar{q}S\begin{bmatrix} (I_3 C_{l_{\delta_a}}(\alpha_0) + I_4 C_{n_{\delta_a}}(\alpha_0)) & (I_3 C_{l_{\delta_r}}(\alpha_0) + I_4 C_{n_{\delta_r}}(\alpha_0)) \\ (I_4 C_{l_{\delta_a}}(\alpha_0) + I_9 C_{n_{\delta_a}}(\alpha_0)) & (I_4 C_{l_{\delta_r}}(\alpha_0) + I_9 C_{n_{\delta_r}}(\alpha_0)) \end{bmatrix}$$

$$G^{\beta}(\beta,\phi) = \bar{q}S\begin{bmatrix} (\sin(\alpha_0) + \frac{\rho S}{4m}\cos(\beta)C_{y_p}(\alpha_0)\bar{b}) & (-\cos(\alpha_0) + \frac{\rho S}{4m}\cos(\beta)C_{y_r}(\alpha_0)\bar{b}) \\ 1 & \cos(\phi)\tan(\theta_0) \end{bmatrix} \times$$
$$\begin{bmatrix} (I_3 C_{l_{\delta_a}}(\alpha_0) + I_4 C_{n_{\delta_a}}(\alpha_0)) & (I_3 C_{l_{\delta_r}}(\alpha_0) + I_4 C_{n_{\delta_r}}(\alpha_0)) \\ (I_4 C_{l_{\delta_a}}(\alpha_0) + I_9 C_{n_{\delta_a}}(\alpha_0)) & (I_4 C_{l_{\delta_r}}(\alpha_0) + I_9 C_{n_{\delta_r}}(\alpha_0)) \end{bmatrix}$$

- Functions defined in the longitudinal mode:

$$
\begin{aligned}
f_{11}^{\alpha}(\alpha) &= \frac{1}{mV}[-\sin\alpha(T + C_x(\alpha)\bar{q}S) + \cos\alpha C_z(\alpha)\bar{q}S] \\
f_{12}^{\alpha}(\alpha) &= \frac{\rho S}{4m}(-\sin\alpha C_{x_q}(\alpha)\bar{c} + \cos\alpha C_{z_q}(\alpha)\bar{c}) \\
f_{13}^{\alpha}(\alpha,\theta) &= \frac{g}{V}\cos(\theta_0 - \alpha); \quad f_{21}^{\alpha}(\alpha) = I_7\bar{q}S(C_m(\alpha)\bar{c} \\
f_{22}^{\alpha}(\alpha) &= C_{m_q}(\alpha)\bar{c}; \quad g_2^{\alpha}(\alpha) = C_{m_{\delta_e}}(\alpha)\bar{c} \\
G^{\alpha}(\alpha) &= (1 + \frac{\rho S}{4m}(-\sin\alpha C_{x_q}(\alpha)\bar{c} + \cos\alpha C_{z_q}(\alpha)\bar{c}))C_{m_{\delta_e}}(\alpha)\bar{c}
\end{aligned}
$$

A.3 Functions and parameters of the linearized system

In section 3.4 we remind some terms concerning the lateral mode dynamics in the stability reference frame. This appendix serves to define these terms. Y_β,Y_p,Y_r, L_β, L_r, δ_l, L_{δ_a}, L_{δ_r} and N_β, N_r, δ_n, N_{δ_a}, N_{δ_r}, $\delta_l(p_s, r_s)$ and $\delta_n(p_s, r_s)$ are determined in Appendix A.

$$
\left\{
\begin{aligned}
\dot{\beta} =& \tfrac{1}{mV}(-\cos\alpha_0\sin\beta(T + C_x(\alpha_0)\bar{q}S) + \cos\beta C_y(\beta)\bar{q}S - \sin\alpha_0\sin\beta C_z(\alpha_0,\beta)\bar{q}S) \\
& -r_s + \tfrac{\rho S}{4m}(\cos(\beta)\bar{b}(C_{y_p}(\alpha_0)\cos\alpha_0 + C_{y_r}(\alpha_0)\sin\alpha_0)p_s) \\
& + \tfrac{\rho S}{4m}(\cos\beta\bar{b}(-C_{y_p}(\alpha_0)\sin\alpha_0 + C_{y_r}(\alpha_0)\cos\alpha_0)r_s) \\
& + \tfrac{g}{V}(\cos\alpha_0\sin\beta\sin\theta_0 + \cos\beta\cos\theta_0\sin\phi - \sin\alpha_0\sin\beta\cos\phi\cos\theta_0) \\
\dot{\phi} =& \tfrac{\cos\gamma_0}{\cos\theta_0}p_s + \tfrac{\sin\gamma_0}{\cos\theta_0}r_s \\
\dot{p}_s =& \bar{q}S\bar{b}[(I_3C_l(\alpha_0,\beta) + I_4C_n(\alpha_0,\beta))\cos\alpha_0 + (I_4C_l(\alpha_0,\beta) + I_9C_n(\alpha_0,\beta))\sin\alpha_0] \\
& + \tfrac{\rho VS\bar{b}}{4}[(I_3C_{l_p}(\alpha_0) + I_4C_{n_p}(\alpha_0))\cos^2\alpha_0 + (I_3C_{l_r}(\alpha_0) + I_4C_{n_r}(\alpha_0))\cos\alpha_0\sin\alpha_0 \\
& + (I_4C_{l_p}(\alpha_0) + I_9C_{n_p}(\alpha_0))\cos\alpha_0\sin\alpha_0 + (I_4C_{l_r}(\alpha_0) + I_9C_{n_r}(\alpha_0))\sin^2\alpha_0]p_s \\
& + \tfrac{\rho VS\bar{b}}{4}[-(I_3C_{l_p}(\alpha_0) + I_4C_{n_p}(\alpha_0))\cos\alpha_0\sin\alpha_0 - (I_3C_{l_r}(\alpha_0) + I_4C_{n_r}(\alpha_0))\cos^2\alpha_0 \\
& - (I_4C_{l_p}(\alpha_0) + I_9C_{n_p}(\alpha_0))\sin^2\alpha_0 + (I_4C_{l_r}(\alpha_0) + I_9C_{n_r}(\alpha_0))\cos\alpha_0\sin\alpha_0]r_s \\
& + \bar{q}S[(I_3C_{l_{\delta_a}}(\alpha_0) + I_4C_{n_{\delta_a}}(\alpha_0))\cos\alpha_0 + (I_4C_{l_{\delta_a}}(\alpha_0) + I_9C_{n_{\delta_a}}(\alpha_0))\sin\alpha_0]\delta_a \\
& + \bar{q}S[(I_3C_{l_{\delta_r}}(\alpha_0) + I_4C_{n_{\delta_r}}(\alpha_0))\cos\alpha_0 + (I_4C_{l_{\delta_r}}(\alpha_0) + I_9C_{n_{\delta_r}}(\alpha_0))\sin\alpha_0]\delta_r \\
\dot{r}_s =& \bar{q}\bar{b}S[-(I_3C_l(\alpha_0,\beta) + I_4C_n(\alpha_0,\beta))\sin\alpha_0 + (I_4C_l(\alpha_0,\beta) + I_9C_n(\alpha_0,\beta))\cos\alpha_0] \\
& + \tfrac{\rho VS\bar{b}}{4}[-(I_3C_{l_p}(\alpha_0) + I_4C_{n_p}(\alpha_0))\cos\alpha_0\sin\alpha_0 - (I_3C_{l_r}(\alpha_0) + I_4C_{n_r}(\alpha_0))\sin^2\alpha_0 \\
& + (I_4C_{l_p}(\alpha_0) + I_9C_{n_p}(\alpha_0))\cos^2\alpha_0 + (I_4C_{l_r}(\alpha_0) + I_9C_{n_r}(\alpha_0))\cos\alpha_0\sin\alpha_0]p_s \\
& + \tfrac{\rho VS\bar{b}}{4}[(I_3C_{l_p}(\alpha_0) + I_4C_{n_p}(\alpha_0))\sin^2\alpha_0 - (I_3C_{l_r}(\alpha_0) + I_4C_{n_r}(\alpha_0))\cos\alpha_0\sin\alpha_0 \\
& - (I_4C_{l_p}(\alpha_0) + I_9C_{n_p}(\alpha_0))\cos\alpha_0\sin\alpha_0 + (I_4C_{l_r}(\alpha_0) + I_9C_{n_r}(\alpha_0))\cos^2\alpha_0]r_s \\
& + \bar{q}S[-(I_3C_{l_{\delta_a}}(\alpha_0) + I_4C_{n_{\delta_a}}(\alpha_0))\sin\alpha_0 + (I_4C_{l_{\delta_a}}(\alpha_0) + I_9C_{n_{\delta_a}}(\alpha_0))\cos\alpha_0]\delta_a \\
& + \bar{q}S[-(I_3C_{l_{\delta_r}}(\alpha_0) + I_4C_{n_{\delta_r}}(\alpha_0))\sin\alpha_0 + (I_4C_{l_{\delta_r}}(\alpha_0) + I_9C_{n_{\delta_r}}(\alpha_0))\cos\alpha_0]\delta_r
\end{aligned}
\right. \tag{A.29}
$$

The lateral force components need to be defined in (3.73):

$$
\begin{aligned}
Y_\beta &= \frac{1}{m}(-\cos(\alpha_0)(T + C_x(\alpha_0)\bar{q}S) + (\frac{\partial C_y(\beta)}{\partial \beta} - \sin(\alpha_0)C_z(\alpha_0,\beta))\bar{q}S) \\
Y_p &= \frac{\rho S V \bar{b}}{4m}(C_{y_p}(\alpha_0)\cos(\alpha_0) + C_{y_r}(\alpha_0)\sin(\alpha_0)) \\
Y_r &= \frac{\rho S V \bar{b}}{4m}(-C_{y_p}(\alpha_0)\sin(\alpha_0) + C_{y_r}(\alpha_0)\cos(\alpha_0))
\end{aligned}
$$

$$
\begin{aligned}
L_\beta &= \bar{q}S\bar{b}\frac{\partial[(I_3C_l(\alpha_0,\beta) + I_4C_n(\alpha_0,\beta))\cos\alpha_0 + (I_4C_l(\alpha_0,\beta) + I_9C_n(\alpha_0,\beta))\sin\alpha_0]}{\partial\beta}_{\beta=0} \\
L_p &= \frac{\rho V S\bar{b}}{4}[(I_3C_{l_p}(\alpha_0) + I_4C_{n_p}(\alpha_0))\cos^2\alpha_0 + (I_3C_{l_r}(\alpha_0) + I_4C_{n_r}(\alpha_0))\cos\alpha_0\sin\alpha_0 \\
&\quad + (I_4C_{l_p}(\alpha_0) + I_9C_{n_p}(\alpha_0))\cos\alpha_0\sin\alpha_0 + (I_4C_{l_r}(\alpha_0) + I_9C_{n_r}(\alpha_0))\sin^2\alpha_0] \\
L_r &= \frac{\rho V S\bar{b}}{4}[-(I_3C_{l_p}(\alpha_0) + I_4C_{n_p}(\alpha_0))\cos\alpha_0\sin\alpha_0 - (I_3C_{l_r}(\alpha_0) + I_4C_{n_r}(\alpha_0))\cos^2\alpha_0 \\
&\quad - (I_4C_{l_p}(\alpha_0) + I_9C_{n_p}(\alpha_0))\sin^2\alpha_0 + (I_4C_{l_r}(\alpha_0) + I_9C_{n_r}(\alpha_0))\cos\alpha_0\sin\alpha_0]
\end{aligned}
$$

$$
\begin{aligned}
N_\beta &= \bar{q}S\bar{b}\frac{\partial[-(I_3C_l(\alpha_0,\beta) + I_4C_n(\alpha_0,\beta))\sin\alpha_0 + (I_4C_l(\alpha_0,\beta) + I_9C_n(\alpha_0,\beta))\cos\alpha_0]}{\partial\beta}_{\beta=0} \\
N_p &= \frac{\rho V S\bar{b}}{4}[-(I_3C_{l_p}(\alpha_0) + I_4C_{n_p}(\alpha_0))\cos\alpha_0\sin\alpha_0 - (I_3C_{l_r}(\alpha_0) + I_4C_{n_r}(\alpha_0))\sin^2\alpha_0 \\
&\quad + (I_4C_{l_p}(\alpha_0) + I_9C_{n_p}(\alpha_0))\cos^2\alpha_0 + (I_4C_{l_r}(\alpha_0) + I_9C_{n_r}(\alpha_0))\cos\alpha_0\sin\alpha_0] \\
N_r &= \frac{\rho V S\bar{b}}{4}[(I_3C_{l_p}(\alpha_0) + I_4C_{n_p}(\alpha_0))\sin^2\alpha_0 - (I_3C_{l_r}(\alpha_0) + I_4C_{n_r}(\alpha_0))\cos\alpha_0\sin\alpha_0 \\
&\quad - (I_4C_{l_p}(\alpha_0) + I_9C_{n_p}(\alpha_0))\cos\alpha_0\sin\alpha_0 + (I_4C_{l_r}(\alpha_0) + I_9C_{n_r}(\alpha_0))\cos^2\alpha_0]
\end{aligned}
$$

$$
\begin{aligned}
L_{\delta_a} &= \bar{q}S[(I_3C_{l_{\delta_a}}(\alpha_0) + I_4C_{n_{\delta_a}}(\alpha_0))\cos\alpha_0 + (I_4C_{l_{\delta_a}}(\alpha_0) + I_9C_{n_{\delta_a}}(\alpha_0))\sin\alpha_0] \\
L_{\delta_r} &= \bar{q}S[(I_3C_{l_{\delta_r}}(\alpha_0) + I_4C_{n_{\delta_r}}(\alpha_0))\cos\alpha_0 + (I_4C_{l_{\delta_r}}(\alpha_0) + I_9C_{n_{\delta_r}}(\alpha_0))\sin\alpha_0] \\
N_{\delta_a} &= \bar{q}S[-(I_3C_{l_{\delta_a}}(\alpha_0) + I_4C_{n_{\delta_a}}(\alpha_0))\sin\alpha_0 + (I_4C_{l_{\delta_a}}(\alpha_0) + I_9C_{n_{\delta_a}}(\alpha_0))\cos\alpha_0] \\
N_{\delta_r} &= \bar{q}S[-(I_3C_{l_{\delta_r}}(\alpha_0) + I_4C_{n_{\delta_r}}(\alpha_0))\sin\alpha_0 + (I_4C_{l_{\delta_r}}(\alpha_0) + I_9C_{n_{\delta_r}}(\alpha_0))\cos\alpha_0] \\
\delta_l(p_s,r_s) &= \bar{q}S\bar{b}[(I_3C_l(\alpha_0,\beta) + I_4C_n(\alpha_0,\beta))\cos\alpha_0 + (I_4C_l(\alpha_0,\beta) + I_9C_n(\alpha_0,\beta))\sin\alpha_0] - L_\beta \\
\delta_n(p_s,r_s) &= \bar{q}S\bar{b}[-(I_3C_l(\alpha_0,\beta) + I_4C_n(\alpha_0,\beta))\sin\alpha_0 + (I_4C_l(\alpha_0,\beta) + I_9C_n(\alpha_0,\beta))\cos\alpha_0] - N_\beta
\end{aligned}
$$

A.4 Application of Modified Conditional Integrator Control to Airlaunch System

The modified Conditional Integrator controller for the lateral motion has the form (see section 3.3):

$$\begin{cases} u^\beta & = & -\Pi^\beta(e_1^\beta, e_2^\beta) sat(s^\beta/\mu^\beta) \\ \Pi^\beta(\cdot) & = & (\pi_0^\beta + \gamma^\beta(\cdot) + k_0^\beta \mu^\beta + \Delta_0^\beta)(G^\beta(\cdot))^{-1} \end{cases} \tag{A.30}$$

with

$$\begin{cases} s^\beta = k_0^\beta \sigma^\beta + K_1^\beta e_1^\beta + e_2^\beta \\ \dot{\sigma}^\beta = -k_0^\beta \sigma^\beta + \mu^\beta sat(s^\beta/\mu^\beta) \end{cases} \tag{A.31}$$

where Π_0^β is a constant large enough, k_0^β is a positive parameter, μ^β is the boundary layer and K_1^β is a positive definite matrix chosen such a way that $K_1^\beta + sI_2$ is Hurwitz.

$\diamond$

Theorem A.4.1 *System (3.55) with $F^\beta(\cdot)$ satisfying Assumption 3.2.1, $G^\beta(\cdot)$ satisfying Assumption 3.2.2, and applying the control law (A.30- A.31), will globally reach an arbitrary error region in finite time, and there on will be exponentially stabilized towards its equilibrium point.*

$\square$

Proof: In order to demonstrate the exponential stability of designed controller (A.30) and (A.31) for the lateral mode in (3.55) which is a nonlinear MIMO system where sideslip and roll angles are the outputs and aileron and rudder are the inputs, we will consider two regions: outside the boundary layer ($\|s^\beta\| \geq \mu^\beta$) and inside the boundary layer ($\|s^\beta\| \leq \mu^\beta$).

A.4.0.1 *In the region $\|s^\beta\| \geq \mu^\beta$, $sat(s^\beta/\mu^\beta) = s^\beta/\|s^\beta\|$.*

The derivative of s^β can be expressed as:

$$\begin{aligned} \dot{s}^\beta &= k_0^\beta \dot{\sigma}^\beta + K_1^\beta \dot{e}_1^\beta + \dot{e}_2^\beta \\ &= -k_0^\beta s^\beta + k_0^\beta \mu^\beta sat(s^\beta/\mu^\beta) + k_0^\beta (K_1^\beta e_1^\beta + e_2^\beta) + K_1^\beta e_2^\beta + F^\beta(\cdot) + G^\beta(\cdot) u^\beta \end{aligned}$$

Now by letting

$$\Delta^\beta(\cdot) = k_0^\beta (K_1^\beta e_1^\beta + e_2^\beta) + K_1^\beta e_2^\beta + F^\beta(\cdot)$$

It becomes:

$$\dot{s}^\beta = -k_0^\beta s^\beta + k_0^\beta \mu^\beta sat(s^\beta/\mu^\beta) + \Delta^\beta(\cdot) + G^\beta(\cdot)u^\beta \tag{A.32}$$

Because of boundedness of $F^\beta(x_1^\beta, x_2^\beta, \theta)$, $\Delta^\beta(\cdot)$ is bounded by a function of $\gamma^\beta(\|e_1^\beta\| + \|e_2^\beta\|)$ (where $\gamma^\beta(\cdot)$ is a class $\mathcal{K}$ function) and a positive constant Δ_0^β (assumption 3.2.1):

$$\|\Delta^\beta(e_1^\beta, e_2^\beta)\| \leq \gamma^\beta(\|e_1^\beta\| + \|e_2^\beta\|) + \Delta_0^\beta \tag{A.33}$$

and as a consequence,

$$\|\Delta^\beta(e_1^\beta = 0, e_2^\beta = 0)\| = \|F^\beta(0,0)\| \leq \Delta_0^\beta \tag{A.34}$$

for $(e_1^\beta, e_2^\beta) \in \mathbb{R}^n \times \mathbb{R}^n$.

Let's consider the product $(s^\beta)^T \dot{s}^\beta$

$$(s^\beta)^T \dot{s}^\beta = -(s^\beta)^T k_0^\beta s^\beta + k_0^\beta \mu^\beta (s^\beta)^T sat(s^\beta/\mu^\beta) + (s^\beta)^T \Delta^\beta(e_1^\beta, e_2^\beta) + (s^\beta)^T G^\beta(e_1^\beta, e_2^\beta)u^\beta$$

This product $(s^\beta)^T \dot{s}^\beta$ can be developed:

$$\begin{aligned}
(s^\beta)^T \dot{s}^\beta &= -(s^\beta)^T k_0^\beta s^\beta + \mu^\beta (s^\beta)^T k_0^\beta s^\beta/\|s^\beta\| + (s^\beta)^T \Delta^\beta(\cdot) - (s^\beta)^T G^\beta(\cdot)\Pi^\beta(\cdot)s^\beta/\|s^\beta\| \\
&\leq -(s^\beta)^T k_0^\beta s^\beta + \mu^\beta (s^\beta)^T k_0^\beta s^\beta/\|s^\beta\| + \|\Delta^\beta(\cdot)\|\|s^\beta\| - (s^\beta)^T G^\beta(\cdot)\Pi^\beta(\cdot)s^\beta/\|s^\beta\| \\
&\leq -(s^\beta)^T k_0^\beta s^\beta + \mu^\beta (s^\beta)^T k_0^\beta s^\beta/\|s^\beta\| + (\gamma^\beta(\cdot) + \Delta_0^\beta)\|s^\beta\| - (s^\beta)^T G^\beta(\cdot)\Pi^\beta(\cdot)s^\beta/\|s^\beta\| \\
&\leq -(s^\beta)^T k_0^\beta s^\beta - (s^\beta)^T (G^\beta(\cdot)\Pi^\beta(\cdot) - (\mu^\beta k_0^\beta + \gamma^\beta(\cdot) + \Delta_0^\beta) I_n) s^\beta/\|s^\beta\|
\end{aligned}$$

Replacing the control law in (A.30) and (A.31), the term $(s^\beta)^T \dot{s}^\beta$ can be expressed as:

$$\begin{aligned}
(s^\beta)^T \dot{s}^\beta &\leq -(s^\beta)^T k_0^\beta s^\beta - (s^\beta)^T (G^\beta(\cdot)\Pi^\beta(\cdot) - (\mu^\beta k_0^\beta + \gamma^\beta(\cdot) + \Delta_0^\beta) I_n) s^\beta/\|s^\beta\| \\
&\leq -(s^\beta)^T k_0^\beta s^\beta - (s^\beta)^T \pi_0^\beta s^\beta/\|s^\beta\| \\
&\leq -k_0^\beta \|s^\beta\|^2 - \pi_0^\beta \|s^\beta\|
\end{aligned}$$

The product $(s^\beta)^T \dot{s}^\beta$ is then not positive and we have also

$$\begin{aligned}
\tfrac{d(\|s^\beta\|^2)}{dt} &= 2\|s^\beta\| \tfrac{d(\|s^\beta\|)}{dt} = 2\tfrac{(s^\beta)^T \dot{s}^\beta}{dt} \leq 2(-\pi_0^\beta \|s^\beta\| - k_0^\beta \|s^\beta\|^2) \\
\therefore \ \tfrac{d(\|s^\beta\|)}{dt} &\leq -\pi_0^\beta - k_0^\beta \|s^\beta\| \\
\therefore \ \|s^\beta(t)\| &\leq \|s^\beta(0)\| - \pi_0^\beta t - \|s^\beta(0)\|(e^\beta)^{-k_0^\beta t} - 1)
\end{aligned}$$

Then the sliding surface $s^\beta(t)$ reaches the boundary layer μ^β in finite time.

.

A.4.0.2 *In the region* $\|s\| \leq \mu^\beta$*],* $sat(s/\mu^\beta) = s/\mu^\beta$*.*

Consider again (A.31) and (A.32), which inside the boundary layer may be rewritten as:

$$\begin{cases} \dot{\sigma}^\beta = -k_0^\beta \sigma^\beta + s^\beta & \text{(A.35a)} \\ \dot{e}_1^\beta = -K_1^\beta e_1^\beta + s^\beta - k_0^\beta \sigma^\beta & \text{(A.35b)} \\ \dot{s}^\beta = \Delta^\beta(\cdot) - G^\beta(\cdot)\Pi^\beta(\cdot)s^\beta/\mu^\beta & \text{(A.35c)} \end{cases}$$

It can be shown that this system has an equilibrium point: $\bar{e}_1^\beta = \bar{e}_2^\beta = 0$, $s^\beta = \bar{s}^\beta$, $\sigma^\beta = \bar{\sigma}^\beta$ with $\bar{s}^\beta = k_0^\beta \bar{\sigma}^\beta = \mu^\beta(\Pi^\beta(0,0))^{-1}(G^\beta(0,0))^{-1}F^\beta(0,0) = \mu^\beta F^\beta(0,0)/(\pi_0^\beta + k_0^\beta\mu^\beta + \Delta_0^\beta)$.

System (A.35) may be rewritten with respect to $\bar{s}^\beta$ and $\bar{\sigma}^\beta$:

$$\begin{cases} \dot{\tilde{\sigma}}^\beta = -k_0^\beta \tilde{\sigma}^\beta + \tilde{s}^\beta & \text{(A.36a)} \\ \dot{e}_1^\beta = -K_1^\beta e_1^\beta + \tilde{s}^\beta - k_0^\beta \tilde{\sigma}^\beta & \text{(A.36b)} \\ \dot{\tilde{s}}^\beta = \Delta^\beta(\cdot) - G^\beta(\cdot)\Pi^\beta(\cdot)\tilde{s}^\beta/\mu^\beta - G^\beta(\cdot)\Pi^\beta(\cdot)\bar{s}^\beta/\mu^\beta & \text{(A.36c)} \end{cases}$$

where $\tilde{\sigma}^\beta = \sigma^\beta - \bar{\sigma}^\beta$, $\tilde{s}^\beta = s^\beta - \bar{s}^\beta$.

$F^\beta(x_1^\beta, x_2^\beta)$ is a Lipschitz function inside the boundary region e.g. $\|s^\beta\| \leq \mu^\beta$, such that:

$$\|F^\beta(e_1^\beta, e_2^\beta) - F^\beta(0,0)\| \leq l_1^\beta \|e_1^\beta\| + l_2^\beta \|e_2^\beta\| \tag{A.37}$$

where l_1^β and $l_2^\beta \in \mathbb{R}^+$.

Following assumption 3.2.1 and (A.34), $\gamma^\beta(\cdot)$ is also a Lipschitz function, such that:

$$\gamma^\beta(\cdot)\|F^\beta(0,0)\| \leq (\pi_0^\beta + k_0^\beta\mu^\beta + \Delta_0^\beta)(\gamma_1^\beta\|e_1^\beta\| + \gamma_2^\beta\|e_2^\beta\|) \tag{A.38}$$

where γ_1^β and $\gamma_2^\beta \in \mathbb{R}^+$.

We would like to demonstrate that every trajectory of system (A.36) starting inside the boundary layer, will approach the equilibrium point as time tends to infinity when the control law (A.30) is applied. Toward that end, we take:

$$W^\beta = \frac{\lambda_1^\beta}{2}(\tilde{\sigma}^\beta)^T\tilde{\sigma}^\beta + \frac{\lambda_2^\beta}{2}e_1^T e_1^\beta + \frac{(\tilde{s}^\beta)^T\tilde{s}^\beta}{2}$$

as a Lyapunov candidate, where λ_1^β and λ_2^β are positive constants.

Its derivative can be easily developed as:

$$\begin{aligned} \dot{W}^\beta =& \lambda_1 k_0^\beta(\tilde{\sigma}^\beta)^T\dot{\tilde{\sigma}}^\beta + \lambda_2(e_1^\beta)^T K_1^\beta \dot{e}_1^\beta + (\tilde{s}^\beta)^T\dot{\tilde{s}}^\beta \\ =& \lambda_1 k_0^\beta(\tilde{\sigma}^\beta)^T(-k_0^\beta\tilde{\sigma}^\beta + \tilde{s}^\beta) + \lambda_2(e_1^\beta)^T K_1^\beta(-K_1^\beta e_1^\beta + \tilde{s}^\beta - k_0^\beta\tilde{\sigma}^\beta) \\ &+(\tilde{s}^\beta)^T(\Delta^\beta(\cdot) - G^\beta(\cdot)\Pi^\beta(\cdot)\tilde{s}^\beta/\mu^\beta - G^\beta(\cdot)\Pi^\beta(\cdot)\bar{s}/\mu^\beta) \end{aligned} \tag{A.39}$$

Since $\|s^\beta\| \leq \mu^\beta$, $\Delta^\beta(\cdot)$ can be expressed as:

$$\Delta^\beta(\cdot) = k_0^\beta\tilde{s}^\beta - (k_0^\beta)^2\tilde{\sigma}^\beta - (K_1^\beta)^2 e_1^\beta + K_1^\beta\tilde{s}^\beta - k_0^\beta K_1^\beta\tilde{\sigma}^\beta + F^\beta(\cdot)$$

Replacing system (A.36) and $\Delta^\beta(\cdot)$ into the derivative of the Lyapunov function, we have then (reminding that $\bar{s}^\beta = \mu^\beta(\Pi^\beta(0,0))^{-1}(G^\beta(0,0))^{-1}F^\beta(0,0)$ and $\Pi^\beta(0,0) = (\Pi_0^\beta + k_0^\beta\mu^\beta + \Delta_0^\beta)(G^\beta(0,0))^{-1}$):

$$
\begin{aligned}
\dot{W}^\beta =& \lambda_1 k_0^\beta(\tilde{\sigma}^\beta)^T(-k_0^\beta\tilde{\sigma}^\beta + \tilde{s}^\beta) + \lambda_2(e_1^\beta)^T K_1^\beta(-K_1^\beta e_1^\beta + \tilde{s}^\beta - k_0^\beta\tilde{\sigma}^\beta)\\
&+(\tilde{s}^\beta)^T(k_0^\beta\tilde{s}^\beta - (k_0^\beta)^2\tilde{\sigma}^\beta - (K_1^\beta)^2 e_1^\beta + K_1^\beta\tilde{s}^\beta - k_0^\beta K_1^\beta\tilde{\sigma}^\beta - G^\beta(\cdot)\Pi^\beta(\cdot)\tilde{s}^\beta/\mu^\beta)\\
&+(\tilde{s}^\beta)^T(F^\beta(\cdot) - G^\beta(\cdot)\Pi^\beta(\cdot)\bar{s}^\beta/\mu^\beta)\\
=&-\lambda_1(k_0^\beta)^2(\tilde{\sigma}^\beta)^T\tilde{\sigma}^\beta + \lambda_1 k_0^\beta(\tilde{\sigma}^\beta)^T\tilde{s}^\beta - \lambda_2(e_1^\beta)^T(K_1^\beta)^2 e_1^\beta + \lambda_2(e_1^\beta)^T K_1^\beta(\tilde{s}^\beta - k_0^\beta\tilde{\sigma}^\beta)\\
&+((\tilde{s}^\beta)^T(k_0^\beta I_n + K_1^\beta)\tilde{s}^\beta + (\tilde{s}^\beta)^T(k_0^\beta + K_1^\beta)k_0^\beta\tilde{\sigma}^\beta - (\tilde{s}^\beta)^T(K_1^\beta)^2 e_1^\beta - (\tilde{s}^\beta)^T G^\beta(\cdot)\Pi^\beta(\cdot)\tilde{s}^\beta/\mu^\beta)\\
&+(\tilde{s}^\beta)^T(F^\beta(\cdot) - F^\beta(0,0) - \tfrac{\gamma^\beta(\cdot)}{\Pi_0^\beta + k_0^\beta\mu^\beta + \Delta_0^\beta}F^\beta(0,0))
\end{aligned}
$$

Using equations (3.55a) and (A.36b), equation (A.37) can be expressed as:

$$
\begin{aligned}
&(\tilde{s}^\beta)^T(F^\beta(\cdot) - F^\beta(0,0) - \tfrac{\gamma^\beta(\cdot)}{\Pi_0^\beta + k_0^\beta\mu^\beta + \Delta_0^\beta}F^\beta(0,0))\\
&\le \|\tilde{s}\|(l_1^\beta\|K_1^\beta e_1^\beta\| + l_2^\beta\|e_2\|) + \tfrac{\gamma^\beta(\cdot)}{\Pi_0^\beta + k_0^\beta\mu^\beta + \Delta_0^\beta}\|\tilde{s}\|\|F^\beta(0,0)\|\\
&\le \|\tilde{s}\|(l_1^\beta\|K_1^\beta e_1^\beta\| + l_2^\beta\|e_2\|) + \tfrac{\Delta_0^\beta}{\Pi_0^\beta + k_0^\beta\mu^\beta + \Delta_0^\beta}\|\tilde{s}\|(\gamma_1^\beta\|K_1^\beta e_1^\beta\| + \gamma_2^\beta\|e_2\|)\\
&\le \|\tilde{s}\|(l_1^\beta\|K_1^\beta e_1^\beta\| + l_2^\beta\|e_2\|) + \|\tilde{s}\|(\gamma_1^\beta\|K_1^\beta e_1^\beta\| + \gamma_2^\beta\|e_2\|)\\
&\le (l_1^\beta + \gamma_1^\beta)\|\tilde{s}\|\|K_1^\beta e_1^\beta\| + (l_2^\beta + \gamma_2^\beta)\|\tilde{s}\|\|e_2\|\\
&\le \tfrac{(l_1^\beta+\gamma_1^\beta)}{2}((\tilde{s}^\beta)^T\tilde{s} + (e_1^\beta)^T(K_1^\beta)^2 e_1^\beta) + \tfrac{(l_2^\beta+\gamma_2^\beta)}{2}((\tilde{s}^\beta)^T\tilde{s} + e_2^T e_2)\\
&\le \tfrac{(l_1^\beta+\gamma_1^\beta)}{2}((\tilde{s}^\beta)^T\tilde{s} + (e_1^\beta)^T(K_1^\beta)^2 e_1^\beta) + \tfrac{(l_2^\beta+\gamma_2^\beta)}{2}((\tilde{s}^\beta)^T\tilde{s}\\
&+(\tilde{s} - k_0^\beta\tilde{\sigma}^\beta - K_1^\beta e_1^\beta)^T(\tilde{s} - k_0^\beta\tilde{\sigma}^\beta - K_1^\beta e_1^\beta))\\
&\le \tfrac{(l_1^\beta+\gamma_1^\beta)}{2}((\tilde{s}^\beta)^T\tilde{s} + (e_1^\beta)^T(K_1^\beta)^2 e_1^\beta) + \tfrac{(l_2^\beta+\gamma_2^\beta)}{2}((\tilde{s}^\beta)^T\tilde{s}\\
&+3((\tilde{s}^\beta)^T\tilde{s} + (k_0^\beta)^2(\tilde{\sigma}^\beta)^T\tilde{\sigma}^\beta + e_1^\beta(K_1^\beta)^2 e_1^\beta))\\
&\le \tfrac{3(l_2^\beta+\gamma_2^\beta)}{2}(k_0^\beta)^2(\tilde{\sigma}^\beta)^T\tilde{\sigma}^\beta + \tfrac{(l_1^\beta+\gamma_1^\beta)+3(l_2^\beta+\gamma_2^\beta)}{2}((e_1^\beta)^T(K_1^\beta)^2 e_1^\beta)\\
&+\tfrac{(l_1^\beta+\gamma_1^\beta)+4(l_2^\beta+\gamma_2^\beta)}{2}((\tilde{s}^\beta)^T\tilde{s})\\
&\le c_1(k_0^\beta)^2(\tilde{\sigma}^\beta)^T\tilde{\sigma}^\beta + c_2(\tilde{s}^\beta)^T\tilde{s} + c_3(e_1^\beta)^T(K_1^\beta)^2 e_1^\beta
\end{aligned}
\tag{A.40}
$$

Using (A.36) and (A.40), the derivative of the Lyapunov function is developed:

$$
\begin{aligned}
\dot{W}^{\beta}=&-\lambda_1(k_0^{\beta})^2(\tilde{\sigma}^{\beta})^T\tilde{\sigma}^{\beta}+\lambda_1(\tilde{\sigma}^{\beta})^Tk_0^{\beta}\tilde{s}-\lambda_2(e_1^{\beta})^T(K_1^{\beta})^2e_1^{\beta}+\lambda_2(e_1^{\beta})^TK_1^{\beta}(\tilde{s}-k_0^{\beta}\tilde{\sigma}^{\beta})\\
&+((\tilde{s}^{\beta})^T(k_0^{\beta}I_n+K_1^{\beta})\tilde{s}-(\tilde{s}^{\beta})^T(k_0^{\beta}+K_1^{\beta})k_0^{\beta}\tilde{\sigma}^{\beta}-(\tilde{s}^{\beta})^T(K_1^{\beta})^2e_1^{\beta}-(\tilde{s}^{\beta})^TG^{\beta}(\cdot)\Pi^{\beta}(\cdot)\tilde{s}^{\beta}/\mu^{\beta}\\
&+(\tilde{s}^{\beta})^T(F^{\beta}(\cdot)-G^{\beta}(\cdot)\Pi^{\beta}(\cdot)\bar{s}/\mu^{\beta}))\\
\leq&-\lambda_1(k_0^{\beta})^2(\tilde{\sigma}^{\beta})^T\tilde{\sigma}^{\beta}+\lambda_1/2((\tilde{s}^{\beta})^T\tilde{s}^{\beta}+(k_0^{\beta})^2(\tilde{\sigma}^{\beta})^T\tilde{\sigma}^{\beta})-\lambda_2(e_1^{\beta})^T(K_1^{\beta})^2e_1^{\beta}\\
&+\lambda_2/2((e_1^{\beta})^T(K_1^{\beta})^2e_1^{\beta}+(\tilde{s}^{\beta}-k_0^{\beta}\tilde{\sigma}^{\beta})^T(\tilde{s}^{\beta}-k_0^{\beta}\tilde{\sigma}^{\beta}))+((\tilde{s}^{\beta})^T(k_0^{\beta}I_n+K_1^{\beta})\tilde{s}^{\beta}\\
&+1/2((\tilde{s}^{\beta})^T(k_0^{\beta}I_n+K_1^{\beta})^2\tilde{s}^{\beta}+\lambda_1(k_0^{\beta})^2(\tilde{\sigma}^{\beta})^T\tilde{\sigma}^{\beta})+1/2((\tilde{s}^{\beta})^T(K_1^{\beta})^2\tilde{s}^{\beta}+(e_1^{\beta})^T(K_1^{\beta})^2e_1^{\beta})\\
&-(\tilde{s}^{\beta})^TG^{\beta}(\cdot)\Pi^{\beta}(\cdot)\tilde{s}^{\beta}/\mu^{\beta}+c_1(k_0^{\beta})^2(\tilde{\sigma}^{\beta})^T\tilde{\sigma}^{\beta}+c_2(e_1^{\beta})^T(K_1^{\beta})^2e_1^{\beta}+c_3(\tilde{s}^{\beta})^T\tilde{s}^{\beta})\\
\leq&-\lambda_1(k_0^{\beta})^2(\tilde{\sigma}^{\beta})^T\tilde{\sigma}^{\beta}+\lambda_1/2((\tilde{s}^{\beta})^T\tilde{s}^{\beta}+(k_0^{\beta})^2(\tilde{\sigma}^{\beta})^T\tilde{\sigma}^{\beta})-\lambda_2(e_1^{\beta})^T(K_1^{\beta})^2e_1^{\beta}\\
&+\lambda_2/2((e_1^{\beta})^T(K_1^{\beta})^2e_1^{\beta}+2((\tilde{s}^{\beta})^T\tilde{s}^{\beta}+(k_0^{\beta})^2(\tilde{\sigma}^{\beta})^T\tilde{\sigma}^{\beta}))+((\tilde{s}^{\beta})^T(k_0^{\beta}I_n+K_1^{\beta})\tilde{s}^{\beta}\\
&+1/2((\tilde{s}^{\beta})^T(k_0^{\beta}I_n+K_1^{\beta})^2\tilde{s}^{\beta}+(k_0^{\beta})^2(\tilde{\sigma}^{\beta})^T\tilde{\sigma}^{\beta})+1/2((\tilde{s}^{\beta})^T(K_1^{\beta})^2\tilde{s}^{\beta}+(e_1^{\beta})^T(K_1^{\beta})^2e_1^{\beta})\\
&-(\tilde{s}^{\beta})^TG^{\beta}(\cdot)\Pi^{\beta}(\cdot)\tilde{s}^{\beta}/\mu^{\beta}+c_1(k_0^{\beta})^2(\tilde{\sigma}^{\beta})^T\tilde{\sigma}^{\beta}+c_2(e_1^{\beta})^T(K_1^{\beta})^2e_1^{\beta}+c_3(\tilde{s}^{\beta})^T\tilde{s}^{\beta})\\
\leq&-(\lambda_1(k_0^{\beta})^2-\lambda_1/2(k_0^{\beta})^2-\lambda_2(k_0^{\beta})^2-1/2(k_0^{\beta})^2-c_1(k_0^{\beta})^2)(\tilde{\sigma}^{\beta})^T\tilde{\sigma}^{\beta}\\
&-(e_1^{\beta})^T(\lambda_2(K_1^{\beta})^2-\lambda_2/2(K_1^{\beta})^2-1/2(K_1^{\beta})^2-c_2(K_1^{\beta})^2)e_1^{\beta}\\
&-(\tilde{s}^{\beta})^T((G^{\beta}(\cdot)\Pi^{\beta}(\cdot)/\mu^{\beta}-(k_0^{\beta}I_n+K_1^{\beta})-\lambda_1/2I_n-\lambda_2I_n\\
&-1/2(k_0^{\beta}I_n+K_1^{\beta})^2-1/2(K_1^{\beta})^2-c_3I_n))\tilde{s}^{\beta}\\
\leq&-(\lambda_1/2-\lambda_2-1/2-c_1)(k_0^{\beta})^2(\tilde{\sigma}^{\beta})^T\tilde{\sigma}^{\beta}-(\lambda_2/2-1/2-c_2)(e_1^{\beta})^T(K_1^{\beta})^2e_1^{\beta}\\
&-(\tilde{s}^{\beta})^T((\Pi_0^{\beta}+k_0^{\beta}\mu^{\beta}+\gamma^{\beta}(\cdot)+\Delta_0^{\beta})/\mu^{\beta}-(k_0^{\beta}I_n+K_1^{\beta})-1/2(k_0^{\beta}I_n+K_1^{\beta})^2\\
&-1/2(K_1^{\beta})^2-(\lambda_1/2+\lambda_2+c_3)I_n)\tilde{s}^{\beta}
\end{aligned}
\tag{A.41}
$$

It can be verified that by taking $\lambda_1^{\beta}, \lambda_2^{\beta}$ and $\Pi^{\beta}(\cdot)$ large enough and μ^{β} small enough, the derivative of Lyapunov function is negative. We establish the additional design parameter's condition:

$$
\begin{cases}
\lambda_1/2-\lambda_2-1/2 & >c_1\\
\lambda_2/2-1/2 & >c_2\\
(\frac{(\Pi_0^{\beta}+k_0^{\beta}\mu^{\beta}+\gamma^{\beta}(\cdot)+\Delta_0^{\beta})}{\mu^{\beta}})I_n & >((k_0^{\beta}I_n+K_1^{\beta})-1/2(k_0^{\beta}I_n+K_1^{\beta})^2-1/2(K_1^{\beta})^2)\\
& \quad +(\lambda_1/2+\lambda_2+c_3)I_n
\end{cases}
$$

This inequality implies that the design condition of parameter k_0^{β} and matrix K_1^{β} must satisfy:

$$
\begin{cases}
\lambda_1-2\lambda_2 & >1+2c_1\\
\lambda_2 & >1+2c_2\\
\frac{(\Pi_0^{\beta}+\Delta_0^{\beta})}{\mu^{\beta}}I_n-K_1^{\beta}-1/2(k_0^{\beta}I_n+K_1^{\beta})^2-1/2(K_1^{\beta})^2 & >(\frac{\lambda_1}{2}+\lambda_2+c_3)I_n
\end{cases}
$$

In this way, $W^{\beta}(t)$ satisfies $W^{\beta}(t)>0$ and $\dot{W}^{\beta}<0$ for all $\sigma^{\beta}\neq\bar{\sigma^{\beta}}$, $e_1^{\beta}\neq 0$ and $s^{\beta}\neq\bar{s}^{\beta}$. Then $W^{\beta}(t)$ reaches zero when time tends to infinite. As consequence, the output error $e_1^{\beta}(t)$ tends to zero while σ^{β} and s^{β} tend to their equilibrium values as time tends to infinite. We may then assure the stability of the system in the region of $\|s^{\beta}\|\leq\mu^{\beta}$.

□

A.5 Functions used for Conditional Servocompensator Control Design

The functions defined in (4.39) are expressed as:

$$\eta_0 = \begin{bmatrix} 0 & \cos\phi & -\sin\phi \end{bmatrix}$$

$$f_{11}(\cdot) = \frac{1}{mV}\begin{bmatrix} -\frac{1}{\cos\beta}((T + C_x\bar{q}S)\sin\alpha + C_z\bar{q}S\cos\alpha) \\ -\sin\beta((T + C_x\bar{q}S)\cos\alpha + C_z\bar{q}S\sin\alpha) + C_y\bar{q}S\cos\beta \\ 0 \end{bmatrix}$$

$$G_1(\cdot) = \frac{\rho S}{4m}\begin{bmatrix} 0 & \frac{\bar{c}S}{\cos\beta}(C_{z_q}\cos\alpha - C_{x_q}\sin\alpha) & 0 \\ C_{y_p}\bar{b}\cos\beta & -\sin\beta(C_{x_q}\cos\alpha + C_{z_q}\sin\alpha)\bar{c} & C_{y_r}\bar{b}\cos\beta \\ 0 & 0 & 0 \end{bmatrix} + \begin{bmatrix} -\cos\alpha\tan\beta & 1 & -\sin\alpha\tan\beta \\ \sin\alpha & 0 & -\cos\alpha \\ 1 & \sin\phi\tan\theta & \cos\phi\tan\theta \end{bmatrix}$$

$$f_{13}(\cdot,\theta) = \frac{g}{V}\begin{bmatrix} \frac{1}{\cos\beta}(\sin\alpha\sin\theta + \cos\alpha\cos\phi\cos\theta) \\ \cos\alpha\sin\beta\sin\theta + \cos\beta\cos\theta\sin\phi - \sin\alpha\sin\beta\cos\theta\cos\phi \\ 0 \end{bmatrix}$$

$$f_{21}(\cdot) = \begin{bmatrix} I_2pq + I_1qr \\ I_5pr - I_6(p^2 - r^2) \\ I_2qr + I_8pq \end{bmatrix} + \begin{bmatrix} I_3C_l(\alpha,\beta)\bar{q}S\bar{b} + I_4C_n(\alpha,\beta)\bar{q}S\bar{b} \\ I_7C_m\bar{q}S\bar{c} \\ I_4C_l(\alpha,\beta)\bar{q}S\bar{b} + I_9C_n(\alpha,\beta)\bar{q}S\bar{b} \end{bmatrix}$$

$$f_{22}(\cdot) = +\frac{\rho VS}{4}\begin{bmatrix} I_3C_{lp}\bar{b} + I_4C_{np}\bar{b} & 0 & I_3C_{lr}\bar{b} + I_4C_{nr}\bar{b} \\ 0 & I_7C_{mq}\bar{c} & 0 \\ I_4C_{lp}\bar{b} + I_9C_{np}\bar{b} & 0 & I_4C_{lr}\bar{b} + I_9C_{nr}\bar{b} \end{bmatrix}$$

$$G_2(\cdot) = \bar{q}S\begin{bmatrix} I_3C_{l\delta_a}(\alpha,\beta)\bar{b} + I_4C_{n\delta_a}(\alpha,\beta)\bar{b} & 0 & I_3C_{l\delta_r}(\alpha,\beta)\bar{b} + I_4C_{n\delta_r}(\alpha,\beta)\bar{b} \\ 0 & I_7C_{mq}\bar{c} & 0 \\ I_4C_{l\delta_a}(\alpha,\beta)\bar{b} + I_9C_{n\delta_a}(\alpha,\beta)\bar{b} & 0 & I_4C_{l\delta_r}(\alpha,\beta)\bar{b} + I_9C_{n\delta_r}(\alpha,\beta)\bar{b} \end{bmatrix}$$

$$G(\cdot)^{-1} = G_1(\cdot)G_2(\cdot)$$

It is reminded that C_i, Cij are aerodynamic coefficients of the F-16 model under analytical forms found in [48].

Appendix B

Static and dynamic feedback linearization of a nonlinear system

Consider a nonlinear control system:

$$\dot{z} = f(z) + \sum_{i=1}^{m}(g_i(z)u(t)) = f(z) + G(z)u \quad z \in \mathbb{R}^n, \quad u \in \mathbb{R}^m \tag{B.1}$$

and a linear controllable system. The previous one is wanted to be transformed to:

$$\dot{x} = Ax + Bv \quad x \in \mathbb{R}^n, \quad v \in \mathbb{R}^m \tag{B.2}$$

Through the state space diffeomorphism:

$$x = \varphi(z) \;\; \varphi(0) = 0 \;\; x \in \mathbb{R}^n, \quad v \in \mathbb{R}^m \tag{B.3}$$

and the state feedback transformations:

$$u = \alpha(z) + \beta(z)v \;\; v \in \mathbb{R}^m \tag{B.4}$$

where $\alpha(0) = 0$ and $\beta(z) \in \mathbb{R}^{m\times m}$ a nonsingular matrix.

or the dynamic state feedback transformations

$$\begin{aligned} \dot{w} &= a(z,w) + b(z,w)v \quad w \in \mathbb{R}^q \\ u &= \alpha(z,w) + \beta(z,w)v \;\; v \in \mathbb{R}^m \end{aligned} \tag{B.5}$$

where $\alpha(0,0) = 0$ and $\beta(z,w) \in \mathbb{R}^{m\times m}$ a nonsingular matrix.

A special class of dynamic compensators, which is studied in this thesis, are defined as (see [22]):

$$\begin{bmatrix} u_1^{(\mu_1)} \\ . \\ . \\ . \\ u_m^{(\mu_m)} \end{bmatrix} = \alpha(z,w) + \beta(z,w) \begin{bmatrix} v_1 \\ . \\ . \\ . \\ v_m \end{bmatrix} \tag{B.6}$$

where $u^{(\mu)} = d^\mu u/dt^\mu$, $w = (u_1, \dot{u}_1, ...u_1^{(\mu_1)}, u_m, \dot{u}_m, ...u_m^{\mu_m})$ with $\mu_i \geq 0$, $1 \leq i \leq m$, $\mu = \sum_{i=1}^m \mu_i$, $\alpha(0,0) = 0$, $\beta(z,w)$ is nonsingular in V_0, a neighborhood of the origin in $\mathcal{R}^{n+\mu}$. It can be constructed as

$$\begin{aligned} \dot{w}_i^j &= w_{i+1}^j \quad 1 \leq j \leq \mu_j - 1 \quad 1 \leq j \leq m \quad \mu_j > 1 \\ \dot{w}_{\mu_j}^j &= \alpha_j(z,w) + \textstyle\sum_{l=1}^m \beta_{j,l}(z,w) v_l \quad 1 \leq j \leq m \quad \mu_j > 0 \end{aligned}$$

$$\begin{aligned} u_j &= w_1^j \quad \mu_j > 0 \\ u_j &= \alpha_j(z,w) + \textstyle\sum_{l=1}^m \beta_{j,l}(z,w) v_l \quad 1 \leq j \leq m \quad \mu_j = 0 \end{aligned}$$

When system (B.1) is transformable into (B.2) by (B.3) and (B.4) it is then called static feedback linearizable respectively.

We now recall the basic definition and results on the conditions for a nonlinear system to be static feedback linearizable. Define the distributions:

$$\begin{aligned} \mathcal{G}_0 &= span\{g_j,\ 1 \leq j \leq m\} \\ \mathcal{G}_i &= span\{ad_f^l g_j,\ 0 \leq l \leq i,\ 1 \leq j \leq m\},\quad i > 0 \end{aligned} \tag{B.7}$$

We denote by $ad_f g = [f,g]$ the Lie bracket of the smooth vector fields f and g. We have

$$[f,g] = \textstyle\sum_{i=1}^n \sum_{j=1}^n (f_j(\frac{\partial g_i}{\partial x_j}) - g_j(\frac{\partial f_i}{\partial x_j}))\frac{\partial}{\partial x_i}$$

It notes that $ad_f^0 g = g$ and $ad_f^k g = [f, ad_f^{k-1} g]$.

We remind the definition of an involutive distribution $\mathcal{G}$.

Definition 3 *Let $\mathcal{G}$ be a distribution on a manifold M. The distribution $\mathcal{G}$ is called involutive if $[X,Y] \in \mathcal{G}$ whenever X and Y are vectorfields in $\mathcal{G}$.*

▪

Theorem B.0.1 *System (B.1) is locally static feedback linearizable if and only if in U_0, a neighborhood of the origin in $\mathbb{R}^n$:*

- *$\mathcal{G}_i$ in an involutive distribution of constant rank for every $i \geq 0$*

- *rank* $\mathcal{G}_{n-1} = n$

Theorem B.0.2 *If for a set of integers* $\{\mu_1, ..., \mu_m,\ 0 \leq \mu_1 \leq ... \leq \mu_m,\ \mu = \sum_{i=1}^{m} \mu_i$, *the distributions, up to input reordering,*

- $\Delta_0 = span\{g_k,\ \mu_k = 0\}$
- $\Delta_{i+1} = \Delta_i + ad_f\Delta_i + span\{g_k;\ \mu_k = i+1\},\ i \geq 0$

are such that in U_0, *a neighborhood of the origin*

- Δ_i *is involutive and of constant rank for* $0 \leq i \leq n + \mu_m - 1$
- $\text{rank}\Delta_{n+\mu_m-1} = n$
- $[g_j, \Delta_i] \in \Delta_{i+1}$ *for all* $0 \leq i \leq m$, *such that* $\mu_j \geq 1$ *and all* i, $0 \leq i \leq n+\mu_m-1$; *then the system (B.1) is locally dynamic feedback linearizable by a dynamic compensator (B.6) with indexes* $\mu_1, ..., \mu_m$ *and a local diffeomorphism in* V_0, *a neighborhood of the origin in the extended state space* $\mathbb{R}^{n+\mu}$.

B.1 Proof of the non static feedback linearizability of the system

As mentioned in section 5.3.1, we will check that

- $\mathcal{G}_0 = span(g_1, g_2, g_3, g_4)$ is involutive
- $\mathcal{G}_1 = span(g_1, g_2, g_3, g_4, ad_fg_1, ad_fg_2, ad_fg_3, ad_fg_4)$ is not involutive

Proof:

$\mathcal{G}_0 = span(g_1, g_2, g_3, g_4)$ *is involutive*

We have $ad_{g_i}g_j = 0$ then $ad_{g_i}g_j \in \mathcal{G}_0$ for $1 \leq i \leq 4$, $1 \leq j \leq 4$ and $i \neq j$. $\mathcal{G}_0$ is involutive and $rank\mathcal{G}_0 = 4$.

$\mathcal{G}_1 = span(g_1, g_2, g_3, g_4, ad_fg_1, ad_fg_2, ad_fg_3, ad_fg_4)$ *is not involutive*

We recall that

$$g_1 = \frac{\partial}{\partial p}$$
$$g_2 = \frac{\partial}{\partial q}$$
$$g_3 = \frac{\partial}{\partial r}$$
$$g_4 = \frac{\partial}{\partial u}$$

We compute all vectors of the distribution $\mathcal{G}_1$.

$$
\begin{aligned}
ad_f g_1 = [f, g_1] &= w\frac{\partial}{\partial v} - v\frac{\partial}{\partial w} + \frac{\partial}{\partial \phi} \\
ad_f g_2 = [f, g_2] &= -w\frac{\partial}{\partial u} + u\frac{\partial}{\partial w} + \tan\theta \sin\phi \frac{\partial}{\partial \phi} + \cos\phi \frac{\partial}{\partial \theta} + \frac{\sin\phi}{\cos\theta}\frac{\partial}{\partial \psi} \\
ad_f g_3 = [f, g_3] &= v\frac{\partial}{\partial u} - u\frac{\partial}{\partial v} + \tan\theta \cos\phi \frac{\partial}{\partial \phi} - \sin\phi \frac{\partial}{\partial \theta} + \frac{\cos\phi}{\cos\theta}\frac{\partial}{\partial \psi} \\
ad_f g_4 = [f, g_4] &= \cos\psi\cos\theta\frac{\partial}{\partial x} + \sin\psi\cos\theta\frac{\partial}{\partial y} - \sin\theta\frac{\partial}{\partial z} + \frac{\partial f_u}{\partial u}\frac{\partial}{\partial u} + (-r + \frac{\partial f_v}{\partial u})\frac{\partial}{\partial v} \\
&\quad + (q + \frac{\partial f_w}{\partial u})\frac{\partial}{\partial w}
\end{aligned}
$$

It is easy to check that $[g_4, ad_f g_3] = -\frac{\partial}{\partial v}$ does not belong to $\mathcal{G}_1$, and as a consequence, $\mathcal{G}_1$ is not involutive. In another words, we can check that rank $\mathcal{G}_1 = 7$, and rank$\{\mathcal{G}_1, [g_4, ad_f g_3]\}$ 8.

We can then conclude that the conditions are not satisfied for Theorem B.0.1, and then system (5.1) is not static feedback linearizable.

B.2 Proof of the dynamic feedback linearizability of the system

This section is meant to demonstrate that the aircraft defined in (5.1) with a second order of thrust force is dynamic feedback linearizable as mentioned in section 5.3.1 of chapter 5. It means that Δ_i for $1 \leq i \leq 3$ satisfies Theorem B.0.2. We remind the definition of Δ_i for $1 \leq i \leq 3$ in (5.6)

$$
\begin{cases}
\Delta_0 = span\{g_1, g_2, g_3\} \\
\Delta_1 = \Delta_0 + ad_{f_s}\Delta_0 + span\{g_4\} \\
\Delta_2 = \Delta_1 + ad_{f_s}\Delta_1 + span\{g_4\} \\
\Delta_3 = \Delta_2 + ad_{f_s}\Delta_2
\end{cases}
$$

Proof:

$\Delta_0 = span\{g_1, g_2, g_3\}$, then Δ_0 is involutive.

$\Delta_1 = \Delta_0 + ad_{f_s}\Delta_0 + span\{g_4\} = span\{g_1, g_2, g_3, ad_f g_1, ad_f g_2, ad_f g_3, g_4\}$, Δ_1 is then involutive.

$\Delta_2 = span\{g_1, g_2, g_3, g_4, ad_f g_1, ad_f g_2, ad_f g_3, ad_f g_4, ad_f^2 g_1, ad_f^2 g_2, ad_f^2 g_3\}$, where $ad_f^2 g_1$, $ad_f^2 g_2$, $ad_f^2 g_3$ are computed below. It is easy to check that rank $\Delta_2 = 10$ and Δ_2 is involutive.

$$\begin{aligned} ad_f^2 g_1 = [f, ad_f g_1] = &((r + \tfrac{\partial f_u}{\partial u})w + (-q + \tfrac{\partial f_u}{\partial w})v)\tfrac{\partial}{\partial u} \\ &+((\tfrac{\partial f_v}{\partial v})w - (p + \tfrac{\partial f_v}{\partial w})v - qu + pv - f_w)\tfrac{\partial}{\partial v} \\ &+((-p + \tfrac{\partial f_w}{\partial v})w + (\tfrac{\partial f_w}{\partial w})v + pw - ru + f_v)\tfrac{\partial}{\partial w} + \tan\theta(q\cos\phi - r\sin\phi)\tfrac{\partial}{\partial \phi} \\ &+(-q\sin\phi - r\cos\phi)\tfrac{\partial}{\partial \theta} + (\tfrac{(q\cos\phi - r\sin\phi)}{\cos\theta})\tfrac{\partial}{\partial \psi} \end{aligned} \tag{B.8}$$

$$\begin{aligned} ad_f^2 g_2 = [f, ad_f g_2] = &(-(\tfrac{\partial f_u}{\partial u})w + (-q + \tfrac{\partial f_u}{\partial w})u + qu - pv + f_w)\tfrac{\partial}{\partial u} \\ &+(-(-r + \tfrac{\partial f_v}{\partial u})w + (p + \tfrac{\partial f_v}{\partial w})u)\tfrac{\partial}{\partial v} + (-(\tfrac{\partial f_w}{\partial u})w + (\tfrac{\partial f_w}{\partial w})u - rv - f_u)\tfrac{\partial}{\partial w} \\ &+(-p\tan\theta\cos\phi + r)\tfrac{\partial}{\partial \phi} + (p\sin\phi)\tfrac{\partial}{\partial \theta} - p\tfrac{\cos\phi}{\cos\theta}\tfrac{\partial}{\partial \psi} \end{aligned} \tag{B.9}$$

$$\begin{aligned} ad_f^2 g_3 = [f, ad_f g_3] = &((\tfrac{\partial f_u}{\partial u})v - (r + \tfrac{\partial f_u}{\partial v})u - pw + ru - f_v)\tfrac{\partial}{\partial u} \\ &+((\tfrac{\partial f_v}{\partial u})v - (\tfrac{\partial f_v}{\partial v})u - qw + f_u)\tfrac{\partial}{\partial v} + ((\tfrac{\partial f_w}{\partial u})v - (\tfrac{\partial f_w}{\partial v})u + vq + up)\tfrac{\partial}{\partial w} \\ &+(-q + p\tan\theta\cos\phi)\tfrac{\partial}{\partial \phi} + p\cos\phi\tfrac{\partial}{\partial \theta} + p\tfrac{\sin\phi}{\cos\theta}\tfrac{\partial}{\partial \psi} \end{aligned} \tag{B.10}$$

$\Delta_3 = \Delta_2 + span\{ad_f^2 g_4, ad_f^3 g_1, ad_f^3 g_2, ad_f^3 g_3\}$, rank $\Delta_3 = 12$. We have then Δ_3 involutive and $\Delta_3 = \mathbb{R}^{12}$.

Therefore, the sufficient conditions of Theorem B.0.2 are satisfied, which leads to the conclusion that system (5.1) is dynamic feedback linearizable.